UV Completion of Composite Higgs Models

Shahram Vatani

N° National de Thèse : 2021LYSE1155

THÈSE DE DOCTORAT DE L'UNIVERSITÉ DE LYON

opéré au sein de

l'Université Claude Bernard Lyon 1

École Doctorale ED52

De Physique et d'Astrophysique

Spécialité du doctorat: Physique Théorique

Soutenue publiquement le 28/07/2021 par

Shahram Vatani

UV Completion of Composite Higgs Models

Devant le jury composé de:

Mme.	Aoife BHARUCHA	*CNRS*	Examiatrice
M.	Giacomo CACCIAPAGLIA	*CNRS*	Directeur
M.	Aldo DEANDREA	*Université de Lyon*	Examinateur
Mme	Stefania DE CURTIS	*INFN*	Rapporteur
M.	Jérémie QUEVILLON	*CNRS*	Examinateur
M.	Francesco SANNINO	*CP3-Origins*	Rapporteur

Remerciements

Durant ces années de thèse j'ai eu la chance incroyable de recevoir un soutien de toutes parts. Aussi divers soit il, mon entourage a toujours été synonyme d'encouragement et cela m'a naturellement motivé et aidé dans mon travail. Pour tous ces moment, ces bonnes choses, je saurais vous remercier de vive voix.

Il y a cependant deux personnes que mes mots ne peuvent atteindre, et à qui je voudrais dédier ce manuscrit, mes deux grand-pères, Mahmoud Vatani et Achille Bottin. Que ce soit dans les instants les plus insolites, couper une pizza en six ou négocier le prix de mon vélo, je sais qui agit en moi. Pour tout ce que j'ai appris de vous, pour toute l'assurance à laquelle j'aspire, pour tout ce que vous m'avez offert, pour tout, je souhaite vous remercier de tout mon coeur.

Contents

Résumé

Le modèle standard (MS) est la théorie la plus aboutie décrivant les interactions fortes et électrofaibles. Ses prédictions, d'une incroyable précision, concordent très bien avec les résultats expérimentaux. Preuve en est la récente découverte du boson de Higgs en 2012 qui est indispensable à la théorie car c'est par son intermédiaire que toutes les particules acquièrent une masse. Cependant le MS n'explique pas tout:

- Des expériences ont confirmé le caractère massif des neutrinos, alors que le MS est incapable de leur attribuer une masse sans introduire des neutrinos d'hélicité droite, qui n'ont jamais été observés, ou des opérateurs non-renormalisables
- Le MS ne modélise toujours pas l'interaction gravitationnelle.
- La matière noire, hypothétique matière nécessaire à l'explication des observations astrophysiques, n'est pas décrite dans le MS.
- Le mécanisme de Higgs, qui confère une masse aux particules, se fait via l'ajout d'un potentiel *ad hoc* pour le boson de Higgs et des problèmes de fine-tuning apparaissent avec la masse de ce dernier.

Tout cela porte à croire que le MS est la manifestation à basse énergie d'une théorie plus fondamentale.

Cette thèse est axée sur l'étude des modèles Higgs Composite, qui tentent principalement de résoudre le dernier point. Cette classe de modèles propose de remplacer le boson de Higgs, et ses intéractions, par un nouveau secteur fermionique très semblable à la ChromoDynamique Quantique (QCD). Pour cela on suppose l'existence de nouveaux fermions, appelés technifermions, et chargés sous une nouvelle interaction, la technicouleur. Comme la couleur en QCD, la technicouleur confine à basse energie en formant un condensat qui brise ses symétries globales. Il en découle l'apparition à basse énergie de bosons de Goldstone pouvant jouer le rôle du boson de Higgs. Ainsi le boson de Higgs apparait comme un état lié de technifermions, supprimant ainsi les problèmes de fine-tuning. La nouvelle interaction forte permet d'obtenir une origine dynamique au potentiel du Higgs. Néanmoins, de nouvelles difficultés apparaissent si l'on veut générer une masse pour les fermions du MS. Le paradigme "Partial Compositness" tente de pallier cela en supposant

que la technicouleur forme des technibaryons à basse énergie, à l'instar du proton formé de quarks. Un mélange entre les technibaryons et les fermions du MS permettrait à ses derniers d'obtenir une masse.

Cette classe de modèles n'offre cependant pas une description complète des hautes énergies (au delà du TeV). Bien qu'elle permette de résoudre les problèmes liés au Higgs, la théorie doit pour cela entrer dans une dynamique presque conforme au dessus de l'échelle de confinement. De plus, le couplage nécessaire entre les technifermions et les fermions du MS, pour être dans le cadre de la "Partial Compositness", se font au moyen d'opérateurs non renormalisables à 4 fermions. Enfin, seulement l'origine de la masse du quark top est considéré, car phénoménologiquement c'est lui qui contribue le plus aux différentes interactions.

Ainsi l'objectif principal de cette thèse a été de faire face au prolongement nécessaire des modèles Higgs Composite aux hautes énergies, processus appelé UV Completion. Cette étape est cruciale et permettra de remettre en question tout ce qui a été obtenu depuis des approches effectives en les comparant avec un cadre solide, cela peut mener par exemple à une compréhension de l'origine de la saveur. Les projets effectués avaient donc à l'esprit de proposer des théories qui reproduisent à basse énergie les modèles existants, tout en étant complètes et fondamentales, i.e. défini jusqu'à l'échelle de Planck. Idéallement ces théories contiennent un nombre fini de couplages bien définis sous le groupe de renormalisation.

Le premier essai a permis l'élaboration du modèle Techni-Pati-Salam [ref]: le groupe de jauge du MS et de la technicouleur y sont partiellement unifiés en une théorie valable jusqu'à l'échelle de Planck, où les effets de gravité quantiques rentrent en jeu. Avec l'aide de nouvelles particules scalaires, le groupe de jauge total subit plusieurs brisures jusqu'à ce que l'on retrouve un modèle Higgs Composite. Les bosons de jauges massifs générés ainsi, en compagnie de certaines composantes scalaires, vont alors être les médiateurs de l'interaction recherchée entre les fermions et les technibaryons. Tous les outils analytiques à notre dispostion tendent à penser que ce modèle peut être réalisé. Cependant, ce sont surtout des résultats numériques via des calculs sur réseau qui pourront fixer le sort de cette théorie.

Dans un second projet, nous avons voulu prendre à notre avantage un problème connu dans les modèles Higgs Composites: beaucoup de nouveaux technifermions sont nécessaires pour expliquer la masse de toutes les particules du MS. En général cela implique l'apparition d'un pôle de Landau dans le running de cette interaction, autrement dit, la constante de couplage diverge aux hautes énergies. Le formalisme dit Large N permet de sonder autrement l'évolution de la constante de couplage, traditionnellement fait en théorie des perturbations. Un premier travail a consisté à se réapprorier ce formalisme pour l'appliquer au cadre des théories avec différentes représentations du groupe de jauge. Enfin il est apparu qu'avec cette approche le couplage ne diverge plus, au contraire il converge vers une valeur fixe non nulle. L'utilisation de ce formalisme a aussi permis de générer les interactions fermions / technibaryons au moyen de nouveaux scalaires dont les couplages vont aussi bien se comporter aux hautes énergies.

Ces deux approches semblent permettre de bien définir les modèles Higgs Composites, mais il est important de noter que ces tentatives ont été faites sur des choix particuliers

de modèles. Il serait très intéressant de voir si de telles extensions peuvent être réaliser avec d'autres modèles. Enfin, ce sont les résultats numériques, seules méthodes capables d'analyser le comportement de la théorie lorsque l'expansion perturbative n'est plus valable, qui permettront de fixer le sort de ces extensions.

Summary

The Standard Model (SM) is the most successful theory describing the interactions of elementary particles. Its predictions agree to a remarkably high degree of precision with experimental data. The last confirmation of the Standard Model has been the discovery of the Higgs boson in 2012, which is at the origin of the mass of the other particles and is thus essential to the theory. However, the SM is unable explain everything:

- Experiments have confirmed a mass for neutrinos, which the SM does not provide.
- Gravitational interactions are not a part of the SM.
- Dark Matter, hypothetical particle which could explain astrophysics observations, is not present in the SM
- The Higgs Mechanism that generates a mass for the $W^{\pm}$ and Z bosons, is ad-hoc via the introduction of the Higgs potential. The Higgs mass also suffers from quadratic sensitivity to the mass scales of new physics, which is required by the previous points.

These reasons motivate us to believe that the SM is just the low energy manifestation of a more fundamental theoy.

The main subject of this thesis is Composite Higgs Models, which principally try to solve the last issue of the above list. In this class of models, the Higgs boson, and all its interactions, are replaced by a new fermionic sector very similar to Quantum ChromoDynamics (QCD). For this purpose, new fermions called technifermions are introduced and charged under a new color dubbed technicolor. Like color in QCD, the technicolor theory confines at low energy and a condensate breaks its global symmetries. This generates Goldstone bosons, one of which can play the role of the SM Higgs boson. By its bound state nature, the new Higgs boson no longer has issues with the quantum corrections of its mass. In this scenario the new strong interaction gives a dynamical origin to the Higgs potential. Nonetheless, challenges appear if we want to generate a mass for the SM fermions. The paradigm of Partial Compositness tries to overcome this issue by postulating a linear mixing between the SM fermions and technibaryons, which are fermionic bound state of three technifermions, like the quarks forming the proton.

These models, however, do not offer a complete picture of the UV physics: on the one hand, they nicely describe the low energy spectrum but need to be extended in order to enter a near-conformal dynamics above the condensation scale (Walking); on the other hand, the couplings of the elementary top fields are introduced as non-renormalizable four-fermion interactions, which may come together with other relevant and omitted operators. Furthermore, the origin of light quark and lepton masses is not addressed.

In this thesis, we want to face the daring need for an Ultra-Violet completion for composite Higgs models: this step is crucial in order to base all we have learned from Effective Field Theory studies on more solid foundations and to truly understand the origin of flavor physics. What we aim at is to define a UV theory that reduces to a viable composite Higgs theory at low energies, around the TeV scale, while being complete and fundamental, i.e. defined up to the Planck scale. Ideally, this should be a theory containing a finite set of couplings closed under the renormalisation group equations, in the absence of quantum gravity effects (which are beyond our scope).

In a first attempt, Composite Higgs models have been extended to the Planck scale by means of the partially unified partial compositeness framework, that I originally proposed in this thesis work, with my collaborators. It is a partial unification of the confining technicolor gauge group with the Standard Model color group, where couplings of the Standard Model fermions are mediated by both gauge and scalar bosons. We present in detail the Techni-Pati-Salam model, based on a renormalizable gauge theory $SU(8)_{PS} \times SU(2)_L \times SU(2)_R$. We demonstrate that masses and mixings for all generations of Standard Model fermions can be obtained via partial compositeness at low energy, with four-fermion operators mediated by either heavy gauge bosons or scalars. The strong dynamics is predicted to be that of a confining $Sp(4)_{HC}$ gauge group, with technifermions in the fundamental and two-index anti-symmetric representations, with fixed multiplicities. This motivates the need for Lattice studies of the Infra-Red near-conformal walking phase, with results that may validate or rule out the model. This is the first complete and realistic attempt at providing an Ultra-Violet completion for composite Higgs models with top partial compositeness. In the baryon-number conserving vacuum, the theory also predicts a Dark Matter candidate, with mass in the few TeV range, protected by semi-integer baryon number.

Next, we present a novel paradigm that allows for the definition of a composite theory at the electroweak scale that is well defined all the way up to any energy by means of safety in the UV. The theory flows from a complete UV fixed point to an IR fixed point for strong dynamics (which gives the desired walking) before generating a mass gap at the TeV scale. This has been realized by using the Large N technique, that we had generalized earlier for the case of multiple representations, in which enter Composite Higgs. Indeed, a draw-back of Composite Higgs Model is the need for numerous new fields to generate mass for the Standard Model fields. We used this to our advantage by the used of the Large N_f formula, which enables to have a perfectly well defined theory. We discuss two models featuring a composite Higgs, Dark Matter and partial compositeness for all SM fermions. The UV theories can also be embedded in a Pati–Salam partial unification, thus removing the instability generated by the $U(1)$ running. Finally, we find a Dark Matter candidate still allowed at masses of 260 GeV, or 1.5–2 TeV, where the latter mass range

will be covered by next generation direct detection experiments.

The results presented in this work are stepping stones towards complete composite Higgs models, where the origin of the standard fermion masses can be finally addressed. Some crucial ingredients, like the presence of an IR window where large anomalous dimensions are generated, need input from lattice calculations.

Further studies could investigate the baryogenesis or even a leptogenesis scenario in the Techni-Pati-Salam project. The electroweak phase transition as well as the confinement might be strong first order, and thus generate gravitational waves. The future detector could be sensitive too such signals. Another follow up is to verify the nature of the large N_f fixed point, perhaps from higher order terms in the expansion.

List of Publications

During my thesis I have been given the chance to collaborate with amazing scientist and people. This has been concretized in the following publications. For this manuscript I will focus on the work presented in [1] , [2] , [3] , [4].

[1] G. Cacciapaglia, T. Ma, S. Vatani and Y. Wu, "Towards a fundamental safe theory of composite Higgs and Dark Matter," Published in : Eur.Phys.J.C 80 11
[Eur.Phys.J.C 80 (2020) 11, 1088[hep-ph]]

[2] G. Cacciapaglia and S. Vatani, "Large N_f for multiple representations,"
[arXiv :2005.07540[hep-ph], accepted in EPJC]

[3] G. Cacciapaglia, S. Vatani and C. Zhang, "Composite Higgs Meets Planck Scale : Partial Compositeness from Partial Unification,"
[Phys.Lett.B 815 (2021) 136177]

[4] G. Cacciapaglia, S. Vatani and C. Zhang, "The Techni-Pati-Salam Composite Higgs,"
[Phys.Rev.D 103 (2021) 055001[hep-ph]]

[5] G. Cacciapaglia, S. Vatani and Z. W. Wang, "Tumbling to the Top,"
[arXiv :1909.08628[hep-ph]]

[6] G.Cacciapaglia, C.Cot, M.Della Morte, S. Hohenegger, F.Sannino, S.Vatani,"The field theoretical ABC of epidemic dynamics," [arXiv:2101.11399 [q-bio.PE][hep-th][hep-la]], under review at Physics Reports

[7] G.Cacciapaglia, C.Cot, A. De Hoffer S. Hohenegger, F.Sannino, S.Vatani,"Epidemiological theory of virus variants," To be submitted in the coming days...

[8] G.Cacciapaglia, F.Conventi, C.Cot, A. De Hoffer, A. Giannini, S. Hohenegger, F.Sannino, S.Vatani,"Evolutionary model of COVID-19 diffusion via mutations applying Machine Learning to spike protein sequencing," To be submitted in the coming days...

Glossary

- **CH** : Composite Higgs
- **CHM** : Composite Higgs Model
- **EFT** : Effective Field Theory
- **EW** : Electro Weak
- **GB** : Goldstone Boson
- **HC** : HyperColor
- **IR** : Infra Red
- **PC** : Partial Compositness
- **pNGB**: pseudo-Nambu-Goldstone-Boson
- **QCD** : Quantum ChromoDynamics
- **SM** : Standard Model
- **TC** : TechniColor
- **UV** : Ultra Violet
- **4-F** : 4-Fermion

Chapter 1

Introduction

History is Philosophy teaching by examples.

Thucydid

The Standard Model (SM) of particle physics [1–3] has withstood all the attempts at discovering signs of New Physics, with most recently the null results from the LHC experiments. The discovery of a Higgs-like boson [4, 5] has further confirmed the validity of the SM. The main experimental confirmation has come from precise measurements in the electroweak (EW) sector of the theory, with most prominent results obtained at LEP [6]. What we know with a precision at the level of per-mille, is that there exist three Goldstone bosons, i.e. the longitudinal polarizations of the $W^{\pm}$ and Z gauge bosons, that complement the gauge principle in the SM and provide mass to the weak gauge bosons [7–10]. While all experimental results seem to point towards a SM-like Higgs boson, our knowledge of its properties is still far from the precision achieved in the gauge sector: the couplings of the Higgs boson are only known at best at the level of 10% [11], and the precision will not improve greatly at the end of the LHC programme [12]. This experimental status leaves open the question of the true nature of the discovered Higgs boson. As we will see, the extreme economy of the SM Higgs sector precludes a deeper understanding of how the electroweak scale is stabilized against radiative corrections and how fermion masses and flavor mixing are generated. A time honored alternative are the Composite Higgs Models (CHM) that rely on the dynamic of Quantum ChromoDynamics(QCD). In this class of theories the SM Higgs boson is replaced by a Pseudo-Nambu-Goldstone boson emerging from broken symmetries of a new interactive sector very similar to QCD. For these reasons it is important to fully appreciate the origin of both QCD and the electroweak symmetry. A drawback of this class of extension is that they are not fundamental theories, in the sens that they cannot be trusted up to an arbitrarly large scale. The origin of the mass of the SM fermions comes through non renormalizable 4-Fermions operators and the generation of flavor is not well understood. Those are the maint motivation behind this thesis, where we are looking for a well defined underlying theory, or UV completion.

Usually, to present such a study we should first start with the model at hand and

motivate why one should look beyond. The reader should be familiar with such an introduction, some of which are exceptionally well written and offer an enlightened point of view. Here we would like to take a different approach and to focus on historic journey and the path taken by the previous physicists. This could help to order the statements of the SM as well as establishing some of its issues. Obviously, the following examples are chosen to better illustrate our future intentions and much more could be said. This could maybe stand alone as a thesis subject by itself. Following this road will naturally lead us to the specific extension of the SM that are CHMs. In chapter 1 we will review the main features of such an approach, the assumptions and the context necessary to make it realistic. In particular we want to question the Ultra Violet (UV) behaviour, the main purpose of this manuscript. The organization of the next chapters will begin with a specific attempt to extend and well define CHM up to the planck scale by partially unifying the SM gauge groups and the new strong sector. In chapter 3 the formal results of the Large N expansion are presented in order to be used in another attempt of UV completion (chapter 4).

1 The Particle World of the last century

We will start our journey in 1932, just after the discovery of the neutron by James Chadwick. The particle world is rather small, the atom is explained as being composed of a nucleus with its nucleons, which are the proton and the neutron. Of course the electron is also here and ensures the electromagnetic neutrality of the atom. However, pieces were known to be missing:

- What keeps the protons together, against the charge repulsion? What is responsible for the stability of the nucleus? What interaction is binding the nucleons together? The answer has been found in two steps, through the strong nuclear interaction at first, which was itself then explained later by the theory of Quantum ChromoDynamics (QCD).

- What was at the origin of the β-decays ? It is known to be the weak force that allows such a transition. The interpretation of this phenomenon is a key part in our journey towards the SM.

1 .1 4-Fermion Interactions

Since its discovery at the end of the 19th century, the β-decay was puzzling the scientific community. There was no explanation for this process, which was violating energy-momentum conservation as well as the spin. To solve this issue, Pauli proposed, out of desperation, in 1930 the existence of what will be later called the neutrino. This hypothesis was written in the famous letter addressed to participants of a nuclear conference in Tubinge, and lead to the first effective description of this process by Enrico Fermi. In 1933 Fermi proposed his theory [13] where the 4 particles participating in the decay (proton,

neutron, electron and neutrino) interact directly from a single operator. It is a point-like interaction between the 4 particles, or contact interaction. An effective operator like the one proposed by Fermi is nowadays called a 4-Fermion Interaction (4-F) and we are going to make use of them, a lot! As mentioned, these operators are effective, thus they need to be generated by the help of a mediator (see Figure 1.1). This is a challenging task as well as a tool to be used in favor of the prediction of a new particle. In 1983, many years after the proposition of 4-F interactions, the $W^{\pm}$ and Z bosons, mediators of the fermi operator, were discovered at CERN [14].

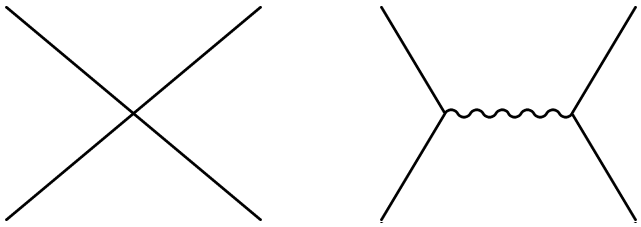

Figure 1.1: The point-like 4-F interaction (left) and the generated 4-F interaction (right).

Fermi's description of this interaction, even at the effective level, was very powerful, and it has a remarkable feature: it connects the nucleon sector to the lepton sector. At that time the nucleon sector (which will become the quark sector) was composed of the proton and the neutron. The electron was the only representant of its family but the muon would come few years later followed by the neutrinos. This particularity of "sectors mixing" is absent in the other great description of the photon interaction, Quantum ElectroDynamics (QED). However, it was known that a more fundamental interaction had to be hidden somewhere. Indeed the stability of the nucleus could not be explained by the interactions energy coming from the 4-F theory. What keeps the proton and neutron inside the nucleus is the next step in our historical quest.

1 .2 The Yukawa Interaction

Hideki Yukawa postulated in 1935 the existence of new spin 0 particles [15], called mesons, connected to a proton and a neutron (what we will call now 'à la Yukawa'). This generates a potential between the nucleons with a characteristic length that has to be around 200 MeV in order to bind the nucleons together. Because its mass was predicted to lie between those of the proton and the electron, Yukawa named the particle mesons, since in ancient Greek " mesos " means "in the middle" .

This meson is of course different to the mediator at the origin of the β-decay. It took more than 10 years for an experimental confirmation, but in 1947 and 1948 the mesons now called the pions $\pi^{\pm}$ were respectively discovered in cosmic rays and produced at the Berkeley Cyclotron. Cosmic rays, particles coming from outer space, leave traces in photographic plates. In Figure 1.2 we can follow the course of a Kaon decaying into 3 pions, and one of them producing a muon. This discovery was quickly followed by the Kaons, and then in the 50's practically one particle every year appeared. This was considered to be a real particle zoo, leaving the community overwhelmed. Some logic had to be found.

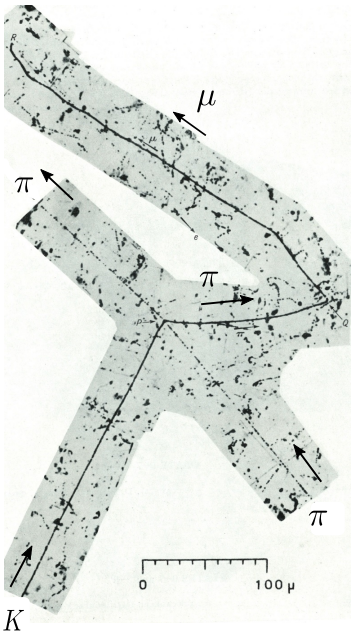

Figure 1.2: Example of a cosmic rays decay shower. Charged particles leave traces (emulsion) into photographic plates. These plates were placed at very high altitude to capture cosmic ray particles.

1 .3 Status during the 50's

Let us recap the world of hadrons discovered up to the begining of the 60's. By hadron we mean everything that is related to the strong nuclear interaction. We have the nucleons, and following Dirac equations the anti-nucleons which were at that time discovered. The pions $\pi^{\pm}$ are also part of this group. Using the technique of cosmic ray tracking, followed by particle collisions, a whole tower of new particles were detected in the following years. They were classified in two groups, the bosonic states (eg mesons) and the fermionic states (eg baryons).

First came the charged meson dubbed "Kaon" ($K^{\pm}$). Then the neutral pion π^0 and Kaon K^0 were spotted, quickly followed by the baryon Λ^0. The Kaon and Λ have a "strange" property. They were being created in proton collisions almost instantaneously, but they decayed much more slowly. Murray Gell-Mann and Kazuhiko Nishijima [16] proposed that the behaviour of the "strange" new particles could be explained if they were carrying a new type of charge that is conserved in strong interactions but not conserved in weak interactions. This property leads to the "strangeness" quantum number. The particle interactions creating Kaons were involving the strong force. However the decay will be through the weak channel, because of the energy and mass of the Kaon, thus it will take longer and will violate the "strangeness".

To introduce order, Sakata proposed in 1956 a model [17] in which the proton p, the neutron n and Λ are elementary and building blocks of all the other resonances. It is a way to extend the $SU(2)$ Isospin between the proton and the neutron with an $SU(3)$

symmetry. This generalized Isospin embeds now the "strange" quantum number by the intermediate of Λ. The baryons are either p,n, Λ, or composite states made of 3 of them. Mesons are simply baryon-antibaryon states. It is worth noting that the idea of compositness was proposed some years before by C.N. Yang and Fermi in an attempt to describe the pions as nucleon-antinucleon. The Sakata model had some drawbacks. Too many resonances are predicted and yet weren't being seen, and their masses had to be higher than observed. To cure those issues, simultaneusly Ne'emann and Gell-Mann proposed in 1964 the Eightfold-Way [18].

1 .4 From the Eightfold-Way to the Quark Model

The periodic table classifying the atoms in terms of their properties (atomic mass and number of charges) revolutionized our vision of the chemical specificies by aranging them in groups. The work of Ne'emann and Gell-Mann is in the footsteps of the success of Mendeleiev. In 1961 they proposed [18] aranging the spin 0 mesons and the spin 1/2 baryons according to the 8 representation of $SU(3)$ (octet). This is the same $SU(3)$ as the one considered by Sakata. For any representation of $SU(3)$ the elements can be cast in terms of their eigenvalues for 2 specific generators. Here Gell-Mann and Ne'emann chose the I_3 from the Isospin and S the strangeness. In figure 1.3 we plotted the visual representations for the mesons and the baryons.

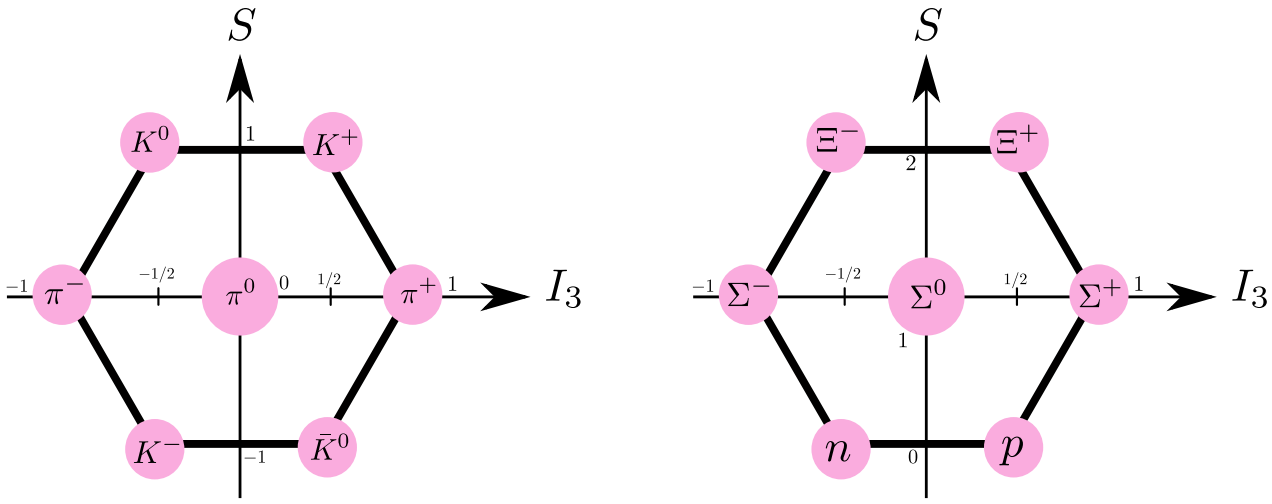

(a) Meson Octet (b) Baryon Octet

Figure 1.3: The Eightfold-Way. The 8 states of the octet representation have specific quantum numbers under I_3 and S. The particles perfectly fit those numbers and are represented on the edge and center of an hexagon.

This is an immediate success. Adding an explicit breaking of $SU(3)$ that conserves the Isospin results in the famous Gell-Mann–Okubo formula relating the masses of the particles, for example:

$$2\left(m_N + m_\Xi\right) = 3m_\Lambda + m_\Sigma \tag{1.1}$$

Quark	Isospin	Strangeness	Electric Charge
u	1/2	0	2/3
d	-1/2	0	-1/3
s	0	-1	-1/3

Table 1.1: Properties of the quarks

Plugging the known measured masses into Eq. (1.1) we found 4514 MeV for the left term and 4544 MeV for the right one, in other words a difference of 0.005% !

A year later Gell-Mann found that the 9 baryons observed with spin 3/2 could easily fit a 10 or decuplet representation of $SU(3)$. This implies the existence of a new particle named Ω^-, and following the Gell-Mann–Okubo formula its mass should be around 1.67 GeV.

At the end of 1963, an experiment at Brookhaven led by Nick Samios [19] detected this particle as predicted by Gell-Mann. The Eightfold-Way was in triumph.

We are now very close to introducing quarks as elementary constituants of the hadronic world. There were different hints to get there. The hadrons were represented as an octet and a singlet (the η) for the pseudoscalar mesons we described earlier and also for the pseudovector mesons Fig.1.3. The baryons were organised as a singlet, an octet and a decuplet. What about the fundamental representation of $SU(3)$? It is mathematically very clean to use it as the elementary blocks. Indeed we have:

$$3 \times 3 \times 3 = 1 \oplus 8 \oplus 8 \oplus 10 \qquad \rightarrow \textbf{Baryons} \tag{1.2}$$

$$3 \times \bar{3} = 1 \oplus 8 \qquad \rightarrow \textbf{Mesons} \tag{1.3}$$

This is exactly what Gell-Mann used when he proposed the quark model. Quarks come in three flavor: up u, down d and strange s. They are spin 1/2 fermions and their quantum numbers are summarized in Table 1.1. Pairs of quark-antiquark form spin 0 and spin 1 Mesons while triplets of quarks constitute Baryons. Their arangement, giving rise to Baryons of spin 1/2 (the octet + singlet) and spin 3/2 is displayed in figure 1.4 along the spin 0 Mesons (octet + singlet).

It is important to note that George Zweig came up with the idea of aces as fundamental constituant of the hadrons at the same periode when Gell-Mann proposed the Quark Model. However Zweig had a slighty different motivation. At that time there was something weird in the decay of the ϕ meson ($s\bar{s}$ bound state). It seemed that the channel $\phi \rightarrow K\ \bar{K}$ was favored against the $\phi \rightarrow \pi + \rho$. As the pions are much lighter than the Kaons an explanation has to be found. To overcome this issue, George Zweig proposed that baryons and mesons are composed of elementary particles, the aces. A process involving hadrons could be viewed as the interaction between aces. If the aces dynamics had some rules, the hadrons should obey them. Hence it was possible to explain the absence of the $\phi \rightarrow \pi + \rho$ channel if the dynamics disfavored the creation of aces-antiaces. This is known as the Zweig rule, also called the OZI rule. Figure 1.5 illustrates the case of the ϕ decay. For the reader interested in the elaboration of the aces, George Zweig wrote a nice review [20].

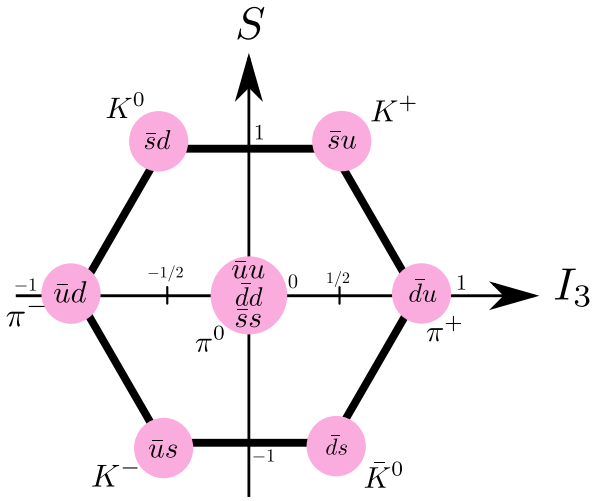

(a) Meson Octet

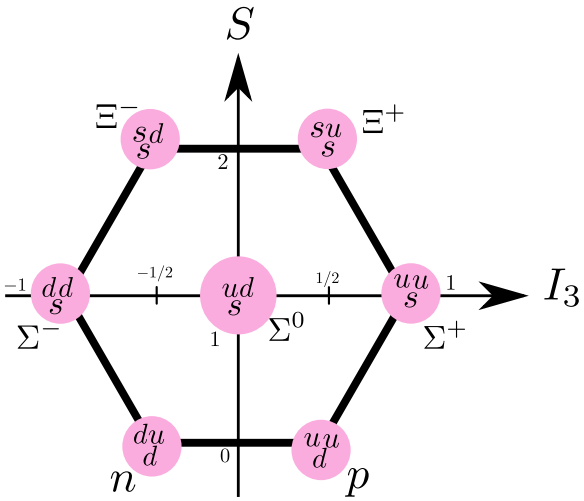

(b) Baryon Octet

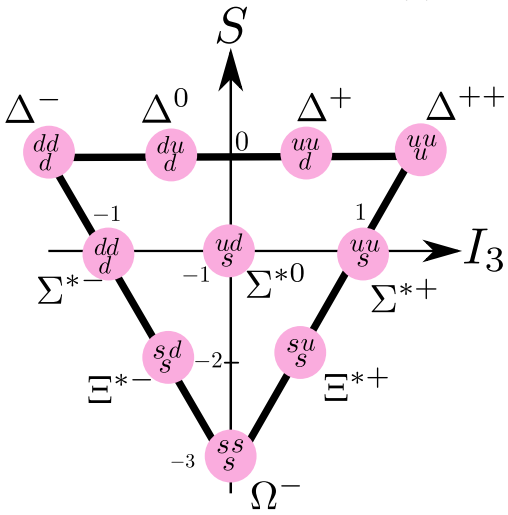

(c) Baryon Decuplet

Figure 1.4: The Eightfold-Way in terms of the quarks constituents. We have now the decuplet representation with the missing Ω^-

In 1968 evidence of the existence of quarks was found at Stanford Linear Accelerator Center (SLAC) by deep inelastic scattering experiments in which they bombarded protons with high speed electrons. The electron in motion behaves like a wave whose wavelength varies inversely to its energy. A spectrometer could therefore distinguish between high energy short wavelength electrons and lower energy long wavelength electrons.

If a proton was a solid singlular particle, the electrons would bounce off the massive proton losing little energy in making the proton recoil, and its remaining energy could be monitored in the spectrometer. If the proton however consisted of a quark triplet in a random orientation with each quark having its own inherent energy, field, and motion, the energy of the recoiling electrons would be spread over a range of wavelengths depending

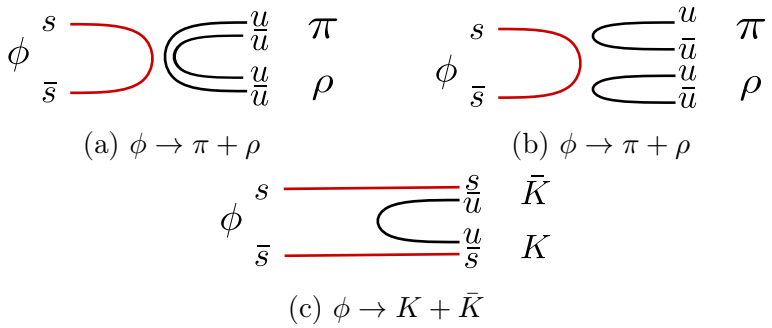

(a) $\phi \to \pi + \rho$ (b) $\phi \to \pi + \rho$

(c) $\phi \to K + \bar{K}$

Figure 1.5: The 3 processes contributing to the ϕ decay. The first 2 decays into pions are suppressed because there are 3 creations of quark-antiquark, whereas only one for the decay into Kaons.

on its impact with the quark, indicating that the proton had a substructure. This spread of energy could be measured by the spectrometers providing evidence of the scattering effect of the quarks as well as an indication of their energies.

1 .5 QCD

The Quark Model was a success, nevertheless a particular implication was left unexplained. Oscar W. Greenberg pointed out that the identical quarks in the $\Omega^- = sss$ violated Pauli's exclusion principle. He suggested that quarks should have three new degrees of freedom to allow such states. The notion of a quantum color charge with three possible values (red, green, blue) on the quarks was introduced and Yoichiro Nambu suggested a gauge symmetry. This is the birth of QCD. The massless gauge boson is dubbed gluon (chosen by Gell-Mann, another of his names that stuck into the community). Few years later in 1973, D. Gross and F. Wilczek and H. Politzer proposed the concept of asymptotic freedom [21, 22], a property that QCD should exhibit. It tells us that pulling away quarks will increase the binding energy coming from the exchange of gluons. On the contrary, the closer quarks are, the weaker is the force between them. This explains why we have never been able to observe colored particles, as they are confined in colorless states. As a consequence, very high energy electron-positron collisions should create hadronic jets, particles linked by the strong interaction and flying in the same spatial direction (usually visualized as a cone). In particular J. Ellis, G. Ross and M. Gaillard put forward the idea that 3 co-planar jets should be produced [23].

In 1979 these events were detected (figure 1.6) by the TASSO collaboration at DESY in Hamburg. They provided the first direct experimental evidence for the existence of gluons.

It is worth noting that in Table 1.1, the three quarks are not exactly the same, their quantum numbers are different. Yet we said before that there are three flavors, and based on this symmetry we are able to classify the bound states of quarks. The reason why we are allowed to do that is because from the point of view of the strong dynamic of QCD, which is responsible for the bound states, u, d and s are the same. Indeed they are linked in the same way to the gluons, in other words they are in the same representation of the

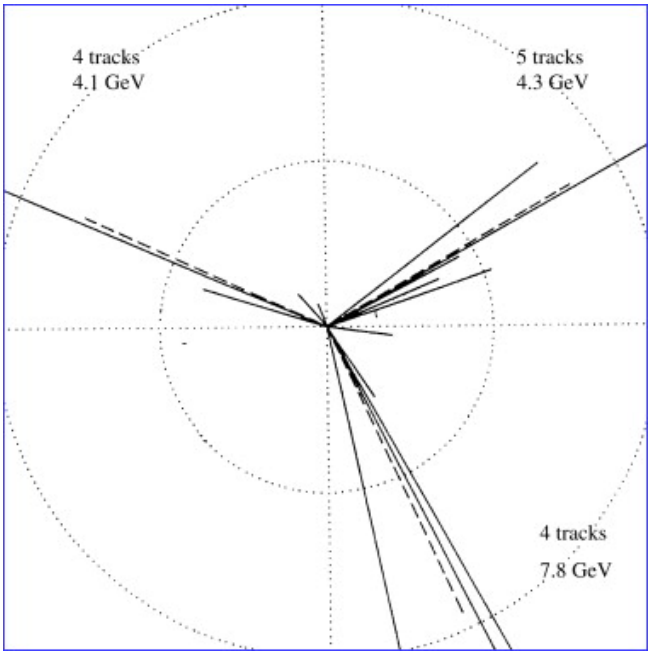

Figure 1.6: The 3 detected jets from the TASSO collaboration, 1979

color symmetry $SU(3)_c$ (for the 3 colors), this representation being the fundamental. The $SU(3)$ flavor symmetry, elementary block of the Baryons and Mesons representations, is an approximate symmetry. In fact, because the mass of the strange is higher than the up and down quark, we can use this difference to generate a mass splitting between the bound states with strange quarks and the ones without. This is exactly the strategy of the Gell-Mann Okubo mass formula (see appendix). The same logic of approximate symmetries is used to describe the bound states of the new strong sector in Composite Higgs Models that we will explore along this manuscript.

1 .6 The embedding of Electroweak Symmetry

In the previous two subsections we described the progress in the strong sector. Along the same years major breakthroughs were found to explain the weak interactions.

First E.Sudarshan and R.Marshak [24] followed by R.Feynman and M.Gell-Mann [25] proposed the V-A theory in 1958. Now only left handed fermions are present in the 4-F operators of the weak interactions. The quarks and the leptons were only described with Dirac spinors, which contain left and right handed Weyl spinors. We did not specify this before and were implicitly talking about Dirac fermions Ψ containing the left handed chirality Ψ_L and the right handed Ψ_R. Until the proposition of the V-A theory there were no distinctions between left and right fermions. Both were present and nature was symmetric under the inversion between right and left spinors. This symmetry is really profound as it is linked to Parity Transformations which modify the space and time coordinates from $(t, x, y, z) \to (t, -x, -y, -z)$. It is like looking at the world in a mirror, and there is no reason for the law of physics to be different. Where it becomes intriguing is how spinors transform under Parity, left handed spinors become right handed

and vice versa. Defining a theory with Dirac spinors makes it symmetric under Parity transformations, but the idea that the weak force is only linked to left handed spinors is revolutionary and highly non-intuitive. This is an explicit breaking of Parity: the mirror world does not behave like ours! More extraordinary, this has experimentally been confirmed, where Parity was observed not to be conserved after the incredible experiment of C. Wu in 1956 [26].

More than 20 years after Fermi proposed his theory of the weak interaction there was no explanation for the origin of the 4-F operators. At this time J.Schwinger and his former student Sheldon Glashow were trying to explain the weak force with a gauge symmetry and massive gauge bosons, of which two of them have to be charged and a third one neutral. They were on the hunt for the $W^{\pm}$ and Z bosons. S.Glashow, in his famous paper [1], was able to unify electromagnetism and the weak force within the $SU(2)_{EW} \times U(1)_Y$ gauge groups, where $SU(2)_{EW}$ is the weak group and $U(1)_Y$ the hypercharge. The electric charge and QED will come out of this unification as a part of $SU(2)_{EW}$ and $U(1)_Y$. At that time, the origin of the mass of the gauge boson was mysterious, and will be discussed in the next section.

Focusing on this embedding, we note that it requires some sensitivity from the quarks u, d and s to the weak force. Each of them is already a multiplet of QCD, but here the situation seems a little different. The weak force in the β-decays links proton to neutron, which are made of up and down quarks. To consistently embed quarks the only possibility is to see the up and down as components of a doublet of $SU(2)_{EW}$. And as we saw above, only the left handed quarks need to be sensitive to the electroweak sector. Hence $q_L = (u_L, d_L)$ is a doublet where u_R and d_R remain singlets.

A similar strategy is adopted for the lepton. The electron and neutrino are part of a weak doublet $L_L = (\nu_L, e_L)$ whereas e_R and ν_R are singlets. In fact the presence of ν_R is still under research. What about the strange quark and the muon? Their quantum numbers make them cousins of d_R and μ_R, respectively. But in 1962 a new neutrino ν_μ was found, which was different from the past one. To explain its interaction it has to be embedded in a new doublet $L_{\mu_L} = (\nu_{\mu_L}, \mu_L)$. By analogy with the quark sector could it be that a new quark was hiding and could it be associated with the strange quark forming a new doublet?

The fourth quark was named charm (c). A few years later, this quark was found to be a important ingredient of the GIM mechanism [27]. In this scenario the presence of the charm quark and its coupling to $SU(2)_{EW}$ magically suppresses some unwanted theoretical processes that have never been observed, where the down quark becomes a strange quark. This is called Flavor Neutral Changing Current (FCNC). The term Flavor originates with identical particles that have exactly the same quantum numbers but differ in their masses like s and d or e and μ. It was in 1974 at SLAC that the famous J/Ψ resonance was observed, corresponding to a meson with the charm quark [28] [29].

We have reviewed the road taken by physicists in the last century and how with incredible experiments this lead to the actual content of the Standard Model particles with its symmetries. We are now ready to write the SM Lagrangian with explicit mass terms for the quarks and leptons. It is the origin of their mass that will drive us down a new road.

2 The Massive SM Lagrangian

The fermions of the Standard Model are all charged under the gauge group $SU(3)_c \times SU(2)_{EW} \times U(1)_Y$. In table 1.2 we listed the fermion content. Note that we put a family index (i) to indicate the flavor or generation. We already saw why there are at least two flavors, but in reality there are 3. The reason will be explained later, once the Higgs boson has been introduced. For now we will use a generic value for the number of flavors, indexed by (i), and write a generic Lagrangian for those particles. To get to the SM formulation we will, step by step, build and add new structures until we obtain a construction consistent theoretically and experimentally. As we will see, the problems are in the electroweak sector, because it treats differently the left handed fermions from the right handed.

	Field	$SU(3)$	$SU(2)_{EW}$	$U(1)_Y$
Quarks	$q_L{}^{(i)} = \begin{pmatrix} u_L{}^{(i)} \\ d_L{}^{(i)} \end{pmatrix}$	3	2	1/6
	$u_R{}^{(i)}$	3	1	2/3
	$d_R{}^{(i)}$	3	1	$-1/3$
Leptons	$L_L{}^{(i)} = \begin{pmatrix} \nu_L{}^{(i)} \\ e_L{}^{(i)} \end{pmatrix}$	1	2	$-1/2$
	$e_R{}^{(i)}$	1	1	-1

Table 1.2: The fermions fields and their quantum numbers under the SM gauge group.

2 .1 What is wrong with the electroweak sector?

First we need to account for the kinetic terms of the gauge bosons and fermions:

$$\begin{aligned}\mathcal{L}_{\mathcal{K}} = &-\frac{1}{4}G^a_{\mu\nu}G^{a\,\mu\nu} \quad -\frac{1}{4}W^i_{\mu\nu}W^{i\,\mu\nu} \quad -\frac{1}{4}B_{\mu\nu}B^{\,\mu\nu} \\ &+ q_L{}^{(i)\dagger}\not{D}q_L{}^{(i)} + u_R{}^{(i)\dagger}\not{D}u_R{}^{(i)} + d_R{}^{(i)\dagger}\not{D}q_R{}^{(i)} + \text{Leptons}\end{aligned} \tag{1.4}$$

$G_{\mu,\nu}, W_{\mu\nu}$ and $B_{\mu\nu}$ are the tensor fields of $SU(3)_c$, $SU(2)_{EW}$ and $U(1)_Y$, respectively. The explicit definition of $\not{D}$ is:

$$\not{D} = \begin{cases} \sigma_\mu \text{ for right handed} \\ \\ \bar{\sigma}_\mu \text{ for left handed} \end{cases} \times \left(\partial_\mu + \sum_x g_x A^{x,r}_\mu T^{x,r}\right) \tag{1.5}$$

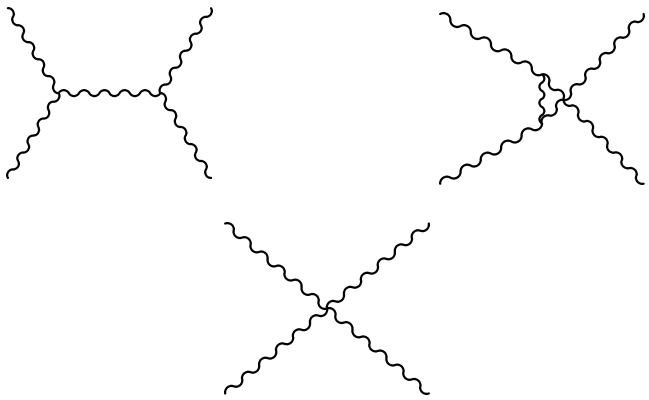

Figure 1.7: The 3 diagrams of the $W_L\ Z_L \longrightarrow W_L Z_L$ scattering

With $\sigma_\mu = (1, \vec{\sigma})\,, \quad \bar{\sigma}_\mu = (1, -\vec{\sigma})$ and $\vec{\sigma}$ are the usual Pauli matrices. The sum is over the gauge groups x under a certain representation with the associated generators $T^{x,r}$, the gauge fields $A_\mu^{x,r}$, and the coupling constant g_x. On purpose, we omitted the lepton's kinetic terms as they play no role in the following arguments.

The Lagrangian $\mathcal{L}_\mathcal{K}$ is by definition gauge invariant under the SM local symmetries. However, it does not account for the mass of the particles that have been experimentally observed and measured. Therefore we need to add mass term operators :

$$\mathcal{L}_{\text{mass}} = {m^2}_W {W^+}_\mu W^{-\mu} + \frac{1}{2} {m_Z}^2 Z_\mu Z^\mu - \sum_i {m^u}_i \bar{q}_L^{(i)} {u_R}^{(i)} + m_i^d \bar{q}_L^{(i)} {d_R}^{(i)} \tag{1.6}$$

Mixing flavors is not important at this point and we will come to that later. The important point is that even if $\mathcal{L}_{\text{mass}}$ can explain the mass spectrum, it explicitly breaks $SU(2)_{EW} \times U(1)_Y$. Is this an issue?

Well, in one part this Lagrangian can be very predictive, but this is up to a limited range of energy. This limitation is due to the mass of the $SU(2)_{EW}$ gauge bosons. Massive vector bosons, of mass m, have longitudinal polarizations ϵ_μ^L that grow like the energy: $\epsilon_\mu^L \sim E$ for $E \gg m$. Studying the $2-2$ scattering of the longitudinal components could lead to high divergences up to E^4. An explicit example is the $W_L\ Z_L \longrightarrow W_L Z_L$ scattering, where there are three tree level diagrams from $\mathcal{L}_\mathcal{K} + \mathcal{L}_{\text{mass}}$ that contributes, as shown in Fig. **??**:

The interested reader can find details of the computation in [30]. The total amplitude of the process yelds:

$$\mathcal{M}_{\text{tot}}\left(W_L\ Z_L \longrightarrow W_L Z_L\right) = \frac{g^2}{4m_W^2} t + \mathcal{O}(1) \tag{1.7}$$

with g the $SU(2)_{EW}$ coupling constant and where t is the Mandelstam variable, at high energy $t \sim E_{CM}^2$. The total amplitude of Eq. (1.7) grows like E^2, whereas the E^4 terms have been cancelled between the 3 diagrams. This is a special property of gauge theory relating the 3-point vertices to the 4-point vertex of gauge bosons. The growth will violate the unitarity bounds that a consistent theory should have. Indeed the Optical

Theorem [30] tells us that every coefficient a_j in the partial wave decomposition of an amplitude:

$$\mathcal{M} \underbrace{(\theta)}_{\text{scattering angle}} = 16\pi^2 \sum_j a_j \ (2j+1) \underbrace{P_j(\cos\theta)}_{\text{Legendre Polynomials}} \tag{1.8}$$

should satisfy:

$$Im(a_j) \geq \|a_j\|^2 . \tag{1.9}$$

In order to have a unitary theory, the optical theorem [30] impose $|a_i| \leq 1$. Moving to the center of mass frame (CM) we have in the limit $E_{CM} \gg m_W, m_Z$:

$$\mathcal{M}_{\text{tot}}(\theta) = \frac{-g^2}{8m_W^2} E_{CM}(1-\cos\theta) \tag{1.10}$$

The bound on a_0 imposes the restricition $E_{CM} \leq 2.5\text{TeV}$, on the center of mass energy. Thus above this energy unitarity is lost. It is not per se because the Lagrangian (1.6) breaks the gauge symmetry but because of the longitudinal polarization. In fact, to understand more profoundly where the inconsistency lies, we can slighty modify (1.6) to restore gauge invariance. For that purpose we introduce the sigma matrix:

$$\Sigma(x) = \exp\left[i\sqrt{2}/f \begin{pmatrix} \frac{z}{\sqrt{2}} & w^- \\ w^+ & -\frac{z}{\sqrt{2}} \end{pmatrix} \right] \tag{1.11}$$

Where $w^{\pm}, z$ are elementary scalar fields. They are often called Goldstone Bosons but that requires the knowledge of an underlying theory and its symmetries. To restore gauge invariance we can charge Σ under $SU(2)_{EW} \times U(1)_Y$ so that it transforms as:

$$SU(2)_{EW} : \Sigma(x) \longrightarrow U\Sigma(x) , \quad \text{for } U \in SU(2)_{EW} \tag{1.12}$$

$$U(1)_Y : \Sigma(x) \longrightarrow \Sigma(x)\ exp\left[-\frac{i}{2}\sigma_3 \right] \tag{1.13}$$

The covariant derivative is simply:

$$D_\mu \Sigma = \partial_\mu \Sigma - ig\frac{\sigma^a}{2} W_\mu^a \Sigma + ig'\Sigma\frac{\sigma^3}{2} B_\mu \tag{1.14}$$

Now we can write a new massive Lagrangian:

$$\mathcal{L}'_{\text{mass}} = \frac{f^2}{4}\text{Tr}\left[(D_\mu\Sigma)^\dagger (D^\mu\Sigma) \right] - f\sum_i \left(\bar{u}_L^{(i)}, \bar{d}_L^{(i)} \right) \Sigma(x) \begin{pmatrix} m_i^u u_R^{(i)} \\ m_i^d \bar{q}_L^{(i)} d_R^{(i)} \end{pmatrix} \tag{1.15}$$

$\mathcal{L}'_{\text{mass}}$ is now manifestly gauge invariant. To recover our previous massive Lagrangian we should fix $\langle\Sigma\rangle = \mathbb{1}$ and have the condition $f = \frac{2m_W}{g}$. This gauge fixing condition is called 'unitary gauge' and it is an explicit breaking of the gauge symmetry. One should

be able to go to the unitary gauge only once the symmetry is broken. We have now linked $\mathcal{L'}_{\text{mass}}$ to $\mathcal{L}_{\text{mass}}$.

Even if we no longer have the longitudinal polarizations for W and Z, there are new diagrams that diverge $\sim E^2$. In the expansion of first term in Eq. (1.15) we find:

$$\mathcal{L'}_{\text{mass}} \supset -\frac{1}{3f^2}\left[z\partial_\mu w^- - w^-\partial_\mu z\right]\left[z\partial_\mu w^+ - w^+\partial_\mu z\right] \tag{1.16}$$

Which results in $z, w^+ \longrightarrow z, w^+$ scattering with an amplitude:

$$\mathcal{M}\left(z, w^+ \longrightarrow z, w^+\right) = \frac{t}{f^2} \tag{1.17}$$

With $f = \frac{2m_W}{g}$ we recover exactly the $W_L, Z_L \longrightarrow W_L, Z_L$ amplitude. This is not at all a suprise, since when we go to the unitary gauge, the w and z scalars are eaten by the gauge bosons and become their longitudinal polarizations. This observation follows from a general result called "Goldstone Equivalence Theorem", stating that any physical process involving the longitudinal polarization is, at leading order in $1/f^2$, equal to the same process with the scalar fields instead of the gauge boson [30].

Let us recap what we have found. Initially asking for a fermion mass term breaks the electroweak symmetry. However, we knew at some level that the symmetry has to be broken, as massive vector are needed to describe the weak force. As an aside, we could have massive vector boson with a global symmetry instead of a local one, and we did not explain why $SU(2)_{EW}$ needs to be local. If the symmetry is global, the vector boson can have a mass, and we just observed that this puts a limited scale on the theory. Having the symmetry be local forbids mass terms for the gauge bosons, thus the theory is valid up to any scale. In the case of QCD, as gluons are massless, the theory is always well defined. But for the electroweak sector, to define it properly at high energy it needs to be unbroken. Thus a mechanism has to be found to break the symmetry. In the SM this is done through the Higgs mechanism [9] as we will see.

We have reformulated the issue of the $W_L, Z_L \longrightarrow W_L, Z_L$ scattering with the help of the $\Sigma(x)$ field, and at the same time rendering the gauge symmetry manifest. To UV complete the electroweak sector we need to find a way to cure the divergent scattering like $z, w^+ \longrightarrow z, w^+$ and to find an explicit origin of the electroweak symmetry breaking (EWSB). The Higgs boson is the way chosen in the SM to account for the above issues. In the next subsection we will see how the Higgs is a very economical way to solve the above points. Finally we will be able to present the SM before discussing how the dynamic of QCD itself shows us an alternative path to EWSB.

2 .2 The Higgs Boson, final piece of the SM

In the kinetic and modified mass Lagrangian , $\mathcal{L}_{\mathcal{K}} + \mathcal{L'}_{\text{mass}}$, a global symmetry $SU(2)_L \times SU(2)_R$ was hidden, in which we identify $SU(2)_L$ to $SU(2)_{EW}$. For U_L, U_R in $SU(2)_L \times SU(2)_R$ the fields transform as:

$$\begin{aligned} q_L = \begin{pmatrix} u_L \\ d_L \end{pmatrix} &\longrightarrow U_L q_L \\ \begin{pmatrix} u_R \\ d_R \end{pmatrix} &\longrightarrow U_R \begin{pmatrix} u_R \\ d_R \end{pmatrix} \\ \Sigma(x) &\longrightarrow U_L \Sigma(x) U_R^\dagger \end{aligned} \tag{1.18}$$

They will leave $\mathcal{L}_\mathcal{K} + \mathcal{L}'_{\text{mass}}$ invariant in the limit $g' = 0$ (i.e. not gauging $U(1)_Y$) and identical mass terms for the quarks ($m_i^u = m_i^d$) . To quantify by how much this symmetry is broken, we can use the Weinberg angle θ_W :

$$\tan\theta_W = \frac{g'}{g} \tag{1.19}$$

In the limit where $g' \to 0$ and (and with equal fermion masses) the symmetry $SU(2)_L \times SU(2)_R$ is conserved and one will find in the unitary gauge $m_W = m_Z$. However, by keeping the $U(1)_Y$ gauge symmetry, the latter relation becomes:

$${m_Z}^2 = {m_W}^2 \left(1 + \frac{{g'}^2}{g^2}\right) = {m_W}^2 \frac{1}{\cos{\theta_W}^2} \tag{1.20}$$

Leading to the definition of the "rho" parameter ρ:

$$\rho = \frac{{m_W}^2}{{m_Z}^2 \cos{\theta_W}^2} \tag{1.21}$$

In the SM thre tree level value of ρ is 1, and experimentally it is measured to be very close to 1. The important point is that it stays close to 1 because it is protected by a residual symmetry, named custodial symmetry. Indeed , going to the unitary gauge only breaks $SU(2)_L \times SU(2)_R$ to a diagonal $SU(2)_c$ where $U_R = U_L$ in Eq. (1.18). $SU(2)_c$ is called the custodial symmetry, and it is only broken by the gauging of $U(1)_y$. A realistic theory should keep this ρ relatively close to 1, and having a custodial symmetry can help achieving that. This is the way chosen by the SM by adding one new degree of freedom to the theory: a singlet h under $SU(2)_c$. This will not modify the action of $SU(2)_L \times SU(2)_R$ on our Lagrangians, which become:

$$\mathcal{L}_\mathcal{K} \to \quad \mathcal{L}_\mathcal{K} + \frac{1}{2}\left(\partial_\mu h\right)^2 \tag{1.22}$$

$$\begin{aligned} \mathcal{L}'_{\text{mass}} \to \quad & V(h) + \frac{f^2}{4}\text{Tr}\left[\left(D_\mu \Sigma\right)^\dagger \left(D^\mu \Sigma\right)\right]\left(1 + 2a\frac{h}{f} + b\frac{h^2}{f^2} + \dots\right) \\ & - f\sum_i \left(\bar{u}_L^{(i)}, \bar{d}_L^{(i)}\right)\Sigma(x)\begin{pmatrix} m_i^u u_R^{(i)} \\ m_i^d \bar{q}_L^{(i)} d_R^{(i)} \end{pmatrix}\left(1 + 2c\frac{h}{f} + \dots\right) \end{aligned} \tag{1.23}$$

with $V(h)$ a possible potential for h. The goal is to determine the coefficients a, b and c that cancel the previous divergences. The scattering studied above (Figure 1.7) can

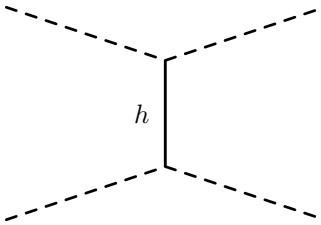

Figure 1.8: The $z, w^+ \longrightarrow z, w^+$ scattering mediated by h.

now be mediated by h following only in the t-channel (see Figure 1.8). This leads to an amplitude $\mathcal{M}$:

$$\mathcal{M} = \frac{-a^2 t}{f^2} + \mathcal{O}\left(\frac{\text{mass}_h}{E_{CM}}\right) \tag{1.24}$$

Choosing $a = 1$ perfectly cancels the previous divergence. Doing the same exercise for other divergences (and also new ones involving h as asymptotic states) gives $a = b = c = 1$. For details of the calcultion we refer to [31]. Now the unitarity of the theory is ensured! Few steps are required before obtaining the SM. First we notice that the previous condition $a = b = c = 1$ enables us to represent the $\Sigma(x)$ field and the h fields in an unified and compact way by defining H as:

$$H(x) = \frac{1}{\sqrt{2}} \exp\left[i\sqrt{2}/f \begin{pmatrix} \frac{z}{\sqrt{2}} & w^- \\ w^+ & -\frac{z}{\sqrt{2}} \end{pmatrix}\right] \begin{pmatrix} 0 \\ f + h(x) \end{pmatrix} = \begin{pmatrix} h_1 + ih_2 \\ h_3 + ih_4 \end{pmatrix} \tag{1.25}$$

Following the transformations rules of $\Sigma(x)$, $H(x)$ transforms simply as a doublet of $SU(2)_L$ (or $SU(2)_{EW}$, which are used interchangeably). H is called the Higgs doublet and h, the Higgs boson. Under $U(1)_Y$, H also inherits the Σ transformation thus it is charged with hypercharge $Y = -1/2$.

Now we need to justify how the electroweak symmetry is broken. We saw that going to the unitary gauge results in mass terms for our fields, but to do so we need to be allowed to fix the gauge, in other words, we need to be sure that the symmetry is broken. This is where our new field $H(x)$ comes to the rescue. It is possible to choose a potential that spontaneously breaks the symmetry, This is exactly what happens in the SM with the Higgs potential:

$$V(H) = \lambda(H^\dagger H - v^2)^2 \tag{1.26}$$

The potential Eq. (1.26) is clearly invariant under $SU(2)_L \times U(1)_Y$, and the ground state of the potential is reached when $H^\dagger H = v^2$. There are an infinite number of equivalent vacua (see Figure 1.9) which are all related to each other, but nature can only be fixed to one. Usually the convention is to choose:

$$H_{\text{vacuum}} = \begin{pmatrix} 0 \\ v \end{pmatrix} \tag{1.27}$$

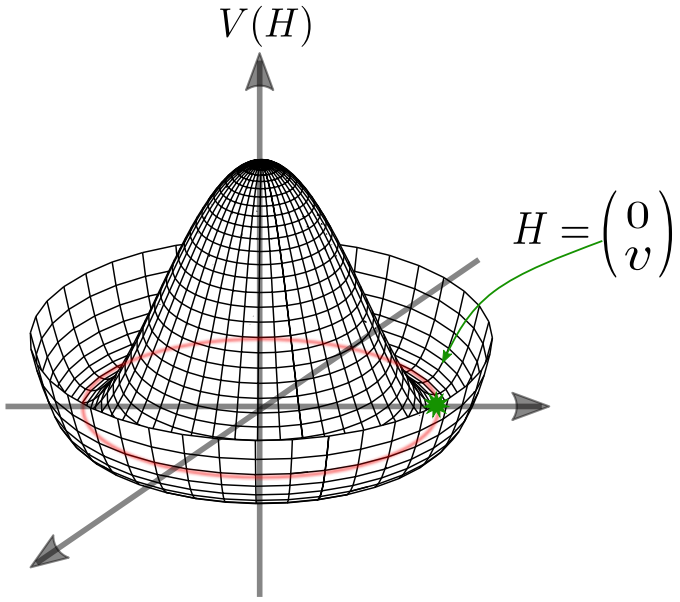

Figure 1.9: Sketch of the Higgs Potential, often called "Mexican Hat". The possible vacua are highlighted in red, and the chosen ground state has been positionned in green.

Which breaks the symmetry $SU(2)_{EW} \times U(1)_Y \longrightarrow U(1)_Q$, with $U(1)_Q$ the electromagnetic gauge group. The electric charge Q is defined by the combination of the generators of $SU(2)_{EW} \times U(1)_Y$ that leaves the vacuum (1.27) invariant:

$$Q = Y + \sigma_3 \tag{1.28}$$

To study the excitations around the vacuum we expand $H(x)$ around it, exactly like in Eq. (1.25), but with now $f = v$. Going into the unitary gauge will give a mass to the gauge boson, this is the Higgs mechanism! An illustration of the potential and the vacuum is proposed in Figure 1.9 .

Finally we are able to write our complete SM Lagrangian:

$$\begin{aligned}\mathcal{L}_{\text{SM}} = &-\frac{1}{4} G_{\mu\nu}{}^a G^{a\,\mu\nu} \quad -\frac{1}{4} W_{\mu\nu}{}^i W^{i\,\mu\nu} \quad -\frac{1}{4} B_{\mu\nu} B^{\mu\nu} \\ &+ q_L{}^{(i)\dagger} \not{D} q_L{}^{(i)} + u_R{}^{(i)\dagger} \not{D} u_R{}^{(i)} + d_R{}^{(i)\dagger} \not{D} d_R^{(i)} + \text{Leptons} \\ &+ (D_\mu H)^\dagger (D^\mu \Sigma) + V(H) \\ &- Y^u{}_{i,j} \bar{q}_L^{(i)} i\sigma_2 H^* u_R{}^{(j)} - Y^d{}_{i,j} \bar{q}_L^{(i)} H d_R{}^{(j)}\end{aligned} \tag{1.29}$$

Here Y^u and Y^d are the Yukawa matrices, and the interactions generated are the Yukawa couplings. Equation (1.29) is the most general Lagrangian that can be written with the fermion fields of Table 1.2, and including the Higgs doublet. The Yukawa matrices can also be non diagonal, facilitating mixing between families. We now have all the

ingredients needed to explain why there are 3 families. To be more accurate, the complete SM Lagrangian also includes the leptons. The charged leptons (electron, muon, tau) acquire a mass through the Higgs vev, exactly like the quarks. We know that neutrinos have a mass however, we still don't know if it is a Dirac mass from the Higgs or a Majorana mass.

2 .3 CKM matrix, CP violation and the SM families

Once the Higgs gets its vaccum expection value (v.e.v.), the Yukawa operators of Eq. (1.29) generate mass terms mixing for the SM fermions. Using the degrees of freedom present between the families and the phases of the fermions yields to the quarks masses:

$$\mathcal{L}_{\text{mass,SM}} = -m_i^d \bar{d}_L^{(i)} d_R - m_i^u \bar{u}_L^{(i)} u_R + h.c. \tag{1.30}$$

with m^d and m^u real. This is done by unitary redefinitions of the quarks field, according to the above degrees of freedom. For more details we refer the reader to [30]. However, this "diagonalisation" of the Yukawa matrices is only apparent in the mass terms. Indeed for the electroweak gauge bosons which link u_L and d_L, the consequences of the above tranformations lead to the Lagrangian:

$$\mathcal{L}_{EW} \supset \frac{g}{\sqrt{2}} \left[{W_\mu}^+ \bar{u}_L^{(i)} \gamma^\mu V^{ij} {d_L}^{(j)} + {W^-}_\mu \bar{d}_L^{(i)} \gamma^\mu {V^\dagger}^{ij} {u_L}^{(i)} \right] \tag{1.31}$$

The matrix V is called the Cabibbo-Kobayashi-Maskawa (CKM) matrix and is unitary. From the above equation we see that going to the fermion mass basis generates mixing between families through the $W^\pm$ massive gauge bosons. The same is not true for the Z current (also named neutral current), as it does not mix the upper and lower component of the fermions left handed doublet. However if there were only one doublet q_L and singlet s_L (left handed strange quark), which were the only quarks known in the begining of the 60's, then we could have mixing between d_L and s_L from the Yukawa operators. The neutral current will be connected to this mixing and we will get unwanted FCNC. The GIM mechanism, postulating a second doublet, compensates exactly the FCNC!

It is the CP violation in the charged current sector that motivates a third family. Indeed, performing a CP transformation on Equation (1.31) will leave the Lagrangian invariant only if $V = V^*$. In other words, to avoid CP violation no phase should be present in V. However, CP violation has been measured in the Kaon sector and is consistent with a phase in the CKM matrix. In the case of only two families, counting the degrees of freedom we have to construct the CKM matrix will leave no phase, as they can all be asborbed into redefinition of the quarks fields. Doing the exercise with 3 families allows for a single phase, completely in balance with the experiments [32]. This is the motivation for the third generation $q_L^3 = \begin{pmatrix} t_L \\ b_L \end{pmatrix}$ comprised of the top and the bottom quarks.

Could it be possible to have a fourth generation? The experimental results relating the Higgs coupling to gluons indicated that this is not the case. The diagram in Figure 1.10 is the dominant contribution. The curious fact about this diagram is that fermions heavier than the Higgs contribute equally in the loop, and in the SM only the top quark is

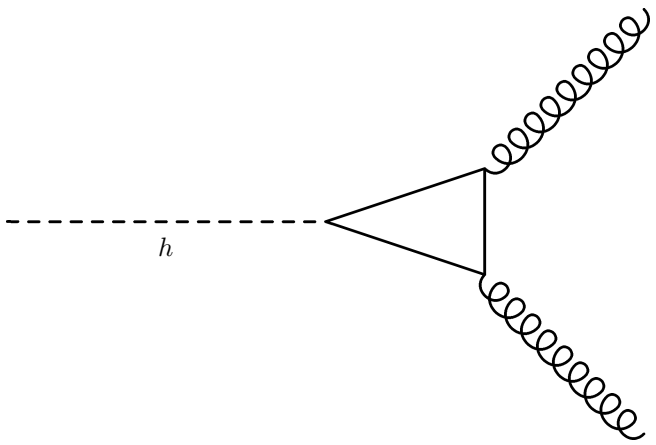

Figure 1.10: The process yielding gluon production through the Higgs.

heavier. A fourth generation will necessarily be heavier than the top, and will thus blow up the Higgs coupling to gluons. This is experimentally not possible in the SM.

To recap our approach, we have started with minimum ingredients and we have found some inconsitencies. The Higgs boson turned on to be a very efficient way to overcome those issues, but is it the only way?

We ask the question, but we should justify the quest for another mechanism of EWSB. The issue with the SM Higgs comes with the scalar nature of this particle. Spin 0 fields suffer from quadratic correction to their mass: $\delta m^2 \sim \Lambda^2$, with Λ the scale of new physics. There are two reasons why such scale exists and is physical. First, there is the Planck scale $\sim 10^{19}$ GeV, around which strong gravity effects kick in, and we have no idea of their impact. The other scale comes from the Landau pole of $U(1)_Y$, this happens at higher energy than the Planck scale. This correction can be removed via fine tuning, a cancellation with the bare mass, to match with the observed mass of the Higgs boson. However this requires an incredible precision due to the very high scale of new physics. Physicists were pushed in the chase of a new source of EWSB, and the CHM offers a very rich alternative which rely on a mechanism already at work in the SM. As we will see in the next section how the SM itself, and especially the QCD sector, provide a natural way to achieve the EWSB.

2 .4 From QCD to the Quark Model

In section 1 .4 we saw how the Baryons and Mesons were formed by smaller structure, the quarks. We will now do the reverse process, and look specifically how the pions arise from the underlying theory of quarks.

The force acting on the quarks is, for one part the electroweak group $SU(2)_{EW} \times U(1)_Y$, and the color from $SU(3)_c$. However, the color interaction gets very strong at low energy so that we can neglect the other forces. This happens around a scale of 150MeV (called Λ_{QCD}), below which the binding energy between quarks is so high that they become colorless bound states of QCD. Because of the strong coupling pertubation theory

breaks down and it is very hard to describe the physics around that scale. Nonetheless, symmetries through the language of effective field theory is a very efficient tool to define the low energy dynamic.

We know that around Λ_{QCD} only the up and down quarks are relevant, because their mass is way below it. As also the other interactions are negligeable, from the QCD point of view there is a $SU(2)_L \times SU(2)_R$ symmetry. This symmetry acts on the quarks fields exactly as defined in Equation 1.18. This is natural considering only the up and down quarks, as the Lagrangian becomes:

$$\mathcal{L} = {u_L}^{(i)^\dagger} \not{D} {u_L}^{(i)} + {d_L}^{(i)^\dagger} \not{D} {d_L}^{(i)} + {u_R}^{(i)^\dagger} \not{D} {u_R}^{(i)} + {d_R}^{(i)^\dagger} \not{D} {d_R}^{(i)} \tag{1.32}$$

However the dynamic of the strong interaction generate a ground state resulting in a non-zero expectation value for the quark bilinears:

$$\langle \bar{u_L} u_R \rangle = \langle \bar{d_L} d_R \rangle \neq 0 \tag{1.33}$$

The vacuum breaks spontaneously and dynamically $SU(2)_L \times SU(2)_R$ down to $SU(2)_D$ exactly like we observed in the previous section.

The Goldstone Theorem tells us that if a global symmetry G is broken down to a subgroup H, this should generated in the low energy spectrum $N_{\text{Goldstone}}$ massless bosons called Goldstone bosons. The number of Goldstone bosons (GB) is simply determined by:

$$N_{\text{Goldstone}} = \dim(G) - \dim(H) \tag{1.34}$$

In our case we find 3 GB that correspond to the $\pi^\pm, \pi^0$ pions . To get the 8 pions of the octet we should also consider the strange quark in the dynamic, even if it is heavier than u and d. In fact in the low energy description, the use of an explicit distinction between s compare to u and d is at the origin of the Gell-Mann Okubo mass formula (see Appendix). In the next section we will present in more details how to use the symmetries and to write an effective Lagrangian. Before let us study how the vaccum of QCD generates a mass for the $W^\pm$.

(a) The QCD correction. (b) The pions correction.

Figure 1.11: The total propagator's correction (left) and specifically the pions correction (right).

The $W^\pm$ acquire a mass because of the dynamics of QCD. Indeed, when computing the full propagator of the W we should take into acount the QCD correction (see Figure 1.11). The propagator of $W^\pm$, $G_{\mu\nu}$, is given by:

$$iG^{\mu\nu} = -i\left(g^{\mu\nu} - \frac{p^\mu p^\nu}{p^2}\right)\frac{1}{p^2\left(1+\Pi\left(p^2\right)\right)} \tag{1.35}$$

where $\Pi\left(p^2\right)$ comes from the QCD correction (see Figure 1.11 (a)):

$$(\mathrm{a}) = -i\left(p^2 g^{\mu\nu} - p^\mu p^\nu\right)\Pi\left(p^2\right) \tag{1.36}$$

A particular part of this correction is given by the pion $\pi^\pm$ exchange (Figure 1.11 (b)) . As the pions are Goldstone boson they verify:

$$\langle 0|{J_\mu}^\pm(x)|\pi^\pm(p)\rangle = i f_\pi p_\mu e^{-ip.x} \tag{1.37}$$

with f_π the pion decay constant and ${J_\mu}^\pm$ is the conserved current. It follows that the pions contribution to Π is:

$$\Pi\left(p^2\right) \supset \frac{g^2 f_\pi^2}{2p^2} \tag{1.38}$$

With $f_\pi = 93MeV$ and $g \sim 0.42$, the $W^\pm$ pick up a mass of ~ 41 MeV, unfortunately way below its actual observed mass (80GeV). Here we have considered that the current couples to the gauge bosons following the term in the largangian: $\mathcal{L} \supset \frac{g}{\sqrt{2}} W^\mu J_\mu$. Thus $\Pi\left(p^2\right)$ has a pole in p^2, in other words, the propagator has a mass term. This comes from the massless nature of the pions which induces a pole in p^2. In Eq. (1.37) the presence of p_μ implies that the pions appear only through derivative coupling, thus they cannot have a mass neither a potential. This last point will be also captures by the effective field approach. All the other resonnances due to QCD interactions being massive, it assures the presence of this pole in the complete form factor $\Pi(p^2)$.

We found that the dynamic of QCD naturally leads to the EWSB. However, the scale of this breaking linked to the pion decay constant is too small to explain the mass of the observed $W^\pm$ and Z bosons.

The idea behind Composite Higgs Models is to postulate a new strong sector, very similar to QCD, with its new fermion. It is dubbed technicolor (or hypercolor) and the particles technifermion (or hyperfermion). The dynamic will generate non zero expectation value on the technifermion condensate, breaking the desire symmetry. In the next chapter we will take a deeper look in this class of models.

Chapter 2

Composite Higgs Models

I must break you.

Rocky IV.

In the previous section we have discussed the importance of explaining the origin of the EWSB. The SM with the Higgs doublet and its potential raises the question of Naturalness and the hierarchy problem. To overcome this issue we want to explore an alternative in wich the Higgs sector, the scalar field and its interactions, is replaced by a new strongly interacting dynamics like QCD. As we saw QCD is already able to trigger the EWSB, unfortunately at a scale which is too low, leading to the idea of Technicolor (TC).

Historically the idea of TC, which is essentially a scaled up version of QCD has been proposed in [33] and [34], where the equivalent of color is called here HyperColor (HC) ($SU(3)_c \sim \mathcal{G}_{HC}$). We said "scaled up" as indeed we can relate the scale of confinement Λ to the decay constant f by $\Lambda = 4\pi f$, which as we saw in the previous section needs to be much higher than the QCD value to explain the mass of the EW gauge bosons. The breaking of the global symmetry by the condensate will generate a tower of resonances in which the SM Higgs boson is identified as a light spin 0, making it composite. But things are not so simple and a first challenge appears to explain the small mass of the Higgs compared to the scale of confinement. Furthermore, in these theories it is hard to explain the origin of the SM fermion mass, leading to extension of the HC group [35], as we will see in the next subsection. Trying to accomodate those issues is a very rich subject, but beyond the scope of this thesis, where we are interested in a slightly different scenario and in another mechanism achieving a mass for the SM fermions.

A few years after the the TC proposal, a variation was introduced [36] in which the HC interactions no longer break the EW gauge group. The theory still confines leading to the breaking of the global symmetry. This process delivers Goldstone Bosons in the low energy spectrum, which are charged under the unbroken subgroup, chosen to contain the EW sector. Depending on EW embedding in the unbroken group, the Higgs doublet can now arise as a GB. Like in the TC scenario, the GB are also bound states of the new fermions, hence this class of models has been named Composite Higgs Model (CHM).

However, GB are known to be massless which is not the case of the Higgs! Moreover, the CHM as it is described above cannot account for the breaking of the EW group. Indeed, the emergence of a potential for the GB is not generated by the strong dynamics alone, and in this approach the condensate is EW preserving.

To overcome these two issues at once, explicit sources of breaking can be added to the theory. This would transform the so-called GB into pseudo-Nambu-Goldstone Bosons (pNGB) which can have a mass (small in comparison to Λ) and a potential, exactly like the pions of QCD. We remark that in this scenario the true vacuum of the strong sector must also break the EW gauge group. In this sense Technicolor and Composite Higgs are related, as both condensates break the EW group. However, what differentiate CHM to purely TC is the identification of the Higgs. In CHM, some of the GB have the quantum numbers of the SM Higgs doublet, and their approximate Goldstone nature makes them very light. This last features also allows us to push the condensation scale higher, delaying at the same time signs of new physics, which have not been seen yet. In the effective analysis we will point out the parameter that enables us to go from the Techincolor vacuum to the Composite Higgs vacuum, preserving the EW group, making clear how they are related.

Several reviews [31, 37–39], which complete each other, give an in-depth presentation of Composite Higgs and Technicolor. Reproducing that work here will be extremely challenging and far away from the main goal of the thesis which, as we recall, consists of studying the UV behaviour of CHM. Nonetheless, having in mind how the machinery works will help us to establish the underlying theory.

For this purpose we will start to present the different symmetry patterns allowed by the strong dynamics, where in fact not every choice can be realized. Then we will introduce the general low energy description. A particular example will be chosen to illustrate the mechanism giving a mass to the $W^{\pm}$, Z and Higgs bosons. We will see how an explicit breaking can generate a mass for the top quark. Finally, the interaction at the origin of such breaking will be question in the last section, where we will examine the necessary ingredients to explain the mass of the SM fermions, especially through the paradigm of Partial Compositness (PC). In this paradigm, the SM fermions acquire a mass by a linear mixing with fermionic bound states of the new strong sector. Some hypotheses have to be made in order to generate such mixing, and this is exactly what we aim to provide in this thesis.

1 Dear Symmetry

The global symmetry depends on the choice of the underlying dynamics; here we consider some new fermions Ψ charged under a HC group $\mathcal{G}_{HC}$ exhibiting a global symmetry G. Upon confinement and condensation, the strong interaction will generate a non-zero value for the fermion condensate $\langle \Psi\Psi \rangle \neq 0$ leading to the spontaneous breaking of G to a subgroup H. In TC or CHM the EW group is a part of the global symmetry. Understanding the possible choices for G/H will enable us to consider the possible embedding of the EW sector in it.

To establish the different symmetry patterns possible we need to notice first that

the structure of the technifermion condensate (Lorentz and gauge invariant) is the same as a Dirac mass term. Thus Ψ can be considered as Dirac fermions, at the same time suppressing gauge anomalies. So let us consider N_f Dirac fermions $\Psi^i = \begin{pmatrix} \Psi^i_L \\ \Psi^i_R \end{pmatrix}$ under a representation $\mathcal{R}$ of the HC group (the superscript i denotes the flavor index). According to this representation we are upon three choices:

- If $\mathcal{R}$ is real, the right handed components of Ψ can be recasted by charge conjugation into left handed Weyl fermions. At the end we can consider the N_f Dirac fermions as $2N_f$ left handed Weyl fermions in the same representation $\mathcal{R}$, leading to an overall $SU(2N_f)$ global symmetry. The unbroken symmetry will lean on the properties of the condensate, $\langle \Psi^i_L \Psi^j_L \rangle = \Sigma_0^{ij}$, which can be symmetric or antisymmetric depending on the the contraction of the non-written indices, color and spin. Here, Lorentz invariance and the reality of the representation impose that the flavor indices be symmetric. This symmetric structure of the condensate will break $SU(2N_f)$ to $SO(2N_f)$. It is worth detailing this last point, where the global symmetry $SU(2N_f)$ acts on the condensate following its action on the technifermions. For a global transformation, let $U \in SU(2N_f)$ such as: $\Psi^i_L \to U^i_k \Psi^k_L$, then:

  $$\Sigma_0^{i,j} \to U^i_k U^j_l \Sigma_0^{k,l} \quad \textbf{i.e.} \quad \Sigma_0 \to U \Sigma_0 U^{\mathrm{T}} \tag{2.1}$$

  Σ_0 which is symmetric can be diagonalised, i.e. there exists $U' \in SU(2N_F)$ such as $\Sigma_0 = U' D U^{\mathrm{T}}$ with D diagonal. Here we assume that $D \sim \mathbb{1}_{2N_f \times 2N_f}$. In other words, the expectation value of the vacuum is the same for all the technifermions. Now we see that the unbroken group is easy to identify as it represents the elements that leave invariant D following the law of transformation (2.1).

- For $\mathcal{R}$ pseudo-real the same argument as above imposes an antisymmetric structure of flavor indices, implying the breaking pattern $SU(2N_f) \to Sp(2N_f)$.

- $\mathcal{R}$ is a complex representation. Then we are really in a QCD like theory with $SU(N_f)_L \times SU(N_f)_R$ global symmetry, acting respectively on the left and right chirality of the Dirac fermion. The condensate $\langle {\Psi^i_L}^\dagger \Psi^i_R \rangle$ will break it to the diagonal $SU(N_f)_{L+R}$.

We have determined the general pattern of symmetry breaking, but there are two last important requirements. First we recall that the theory needs to be outside the conformal window. In practice neither N_f, nor the dimension of the representation, can be too large. In the set of GB, which transforms under the unbroken group, at least one needs to be a doublet of $SU(2)_L \times SU(2)_R$. We ask specifically for the custodial symmetry in order to protect the ρ parameter from tree level correction. The Goldstone Theorem tells us that the GB π^a are created from the non-conserved currents:

$$\langle 0 | J^a_\mu(x) | \pi^a(p) \rangle = i f_\pi p_\mu e^{-ip.x} \tag{2.2}$$

Thus to determine how the GB π^a transforms we simply need to know the law of transformation of the current, i.e. the broken generators. In the real or pseudo-real representation cases, the unbroken generators T^a of $SU(2N_f)$ are the ones leaving the vacuum invariant under the transformation (2.1). With a generic expectation value of the condensate Σ_0 they must verify:

$$T^a\Sigma_0 + \Sigma_0 \left(T^a\right)^{\mathrm{T}} = 0 \tag{2.3}$$

From this we obtain a set of $\dim\left(SO(2N_f)\right)$ unbroken generators in the real case (or $\dim\left(Sp(2N_f)\right)$ in the pseudo-real case). This set can be completed with the remaining generators of $SU(2N_f)$, setting the broken generators X^a. The usual convention is to choose the broken generators orthogonal to the unbroken set, i.e. $\mathrm{Tr}\left(T^aX^b\right) = 0$. This will imply:

$$X^a\Sigma_0 - \Sigma_0(X^a)^{\mathrm{T}} = 0 \tag{2.4}$$

Once again we stress that this is a convention, nevertheless it simplifies the computations in the effective field approach. Finally this yields to the broken current:

$$j^a_\mu = \Psi^\dagger_{Li} X^{ai}{}_j \bar{\sigma}_\mu \Psi^j_L \tag{2.5}$$

with i and j the flavor indices. Naturally from what we obtained, the current must transform in the adjoint representation of the global symmetry.

The above argument can also be employed in the case of complex TC representation. The logic is the same and the only difference comes from the global symmetry, which here is $SU(N_f)_L \times SU(N_f)_R$ and the transformation law of the fermion condensate:

$$\Sigma_0 \to U^*{}_L \Sigma_0 U^{\mathrm{T}}_R \tag{2.6}$$

Now that we captured the symmetry properties of the GB, the next step is to write an effective Lagrangian to describe the theory below the condensation scale. In other words, we want to use effective scalar fields π^a to construct the low energy interactions. Other resonances like the vectors could play an important role. We could add also in our low energy Lagrangian the scalar singlet which is indentified as the Higgs in the TC alternative. However we want to take things simple and we will only consider the pions in the effective field description. To do so we recall that symmetries are key and it is the unbroken group H that links the theory above and below confinement. Thus the embedding of the π^a must respect the transformation properties of the broken current under H, i.e. being in the adjoint of H. Up to this point, the properties that we have deduced for the GB come from the underlying field, which will not be the case once we go in an effective field approach. There is a last point we should remember; that Eq (2.2) implies the massless nature of the GB and it forbids them to have a potential.

2 The Chiral Lagrangian

In most of the CH papers, the chiral Lagrangian describing the pions will be written according to:

$$\mathcal{L}_{eff} = \frac{f^2}{8}\mathrm{Tr}\left[(D_\mu\Sigma)^\dagger (D^\mu\Sigma)\right] \tag{2.7}$$

with $\Sigma = \exp\left(2\sqrt{2}\frac{\pi^a}{f}X^a\right)\Sigma_0$. Here $\exp\left(2\sqrt{2}\frac{\pi^a}{f}X^a\right) = U(\pi)$ is called the pion matrix and Σ_0 is the vacuum of the theory, as we have defined it with the condensate. This is the so called "chiral Lagrangian", from which as we will see, we can explain the origin of the mass of the broken gauge bosons and the coupling of the GB Higgs to the $W^\pm$ and Z. However, to fully appreciate this choice and the symmetry properties we would like to take a step back and explain very briefly their origin, the CCWZ formalism [40, 41]. We note that the above Lagrangian is only at order 2 in the momentum (derivative) expansion. We could go to the next leading order in the effective description, however this is not our goal, and the phenomenology of the first order is already quite rich and have interesting features.

2 .1 The CCWZ Formalism

The CCWZ approach allows the possibility to describe the dynamics of the GB, following symmetry principles. To present it, we can be very general, so we consider a group G spontaneously broken down to a subgroup H with T^a and X^a the respective generators of G and H. The general way to parametrize the excitation from the GB $\pi^a(x)$ around the vaccum ϕ_0 is chosen to arrives through the mean of multiplet scalar field:

$$\phi(x) = U\left[\pi(x)\right]\phi_0, \quad U\left[\pi(x)\right] = \exp\left(\sqrt{2}\frac{\pi^a}{f}X^a\right) \tag{2.8}$$

Again $U[\pi]$ is called the pion matrix and is part of the coset G/H. Now performing a global transformation from G should imply:

$$G: \ \phi(x) \to \phi'(x) = g\phi(x) = gU[\pi]\phi_0 \ , \quad g \in G \tag{2.9}$$

where the action of g on $\phi(x)$ is the action of G on the vacuum. What appears here is that $gU[\pi]$ can be outside of the G/H coset. However it can be expressed with a new pion configuration π' such as it stays in the coset. In that sense we use the property that each element g of G can be uniquely written $g = g_{G/H}.h$, with $g_{G/H}$ in the coset G/H and h in H. Thus there exist h such as $g.U[\pi] = U[\pi'].h$. Plugged into the last equation we obtain:

$$G : \phi(x) \to \phi'(x) = g\phi(x) = U[\pi']\phi_0 \tag{2.10}$$

$$\text{with } U[\pi'] = g.U[\pi].h^{-1} \tag{2.11}$$

where we used the fact that h leaves ϕ_0 invariant. Hence, the pions are transformed through a global transformation of G with $\pi \to \pi'$. This is a non-linear transformation which depends on G and H, however if we act on the pion matrix with H things are different. Indeed as we wrote it before $h = h[\pi, g]$ depends on pions and on the element g. But if we act only with h from H:

$$H:\ \phi(x) \to \phi'(x) = h\phi(x) = hU[\pi]h^{-1}h\phi_0 \tag{2.12}$$

In this particular case $U[\pi] \to hU[\pi]h^{-1} = U[h\pi h^{-1}] \in G/H$. So $\pi' = h\pi h^{-1}$, here the pions transforms in the adjoint of H following the underlying theory! The other special case is the action of a G/H element $\kappa = \exp(i\alpha^a X^a)$. It results in a shift in the pion fields configuration: $\pi \to \pi' = \pi + \alpha + \mathcal{O}(\alpha)$. To prove it in the general case is technical and not essential for the rest. However, this so called "shift symmetry" forbids mass and potential terms for the GB, which again, we already understood from the derivative coupling of the pions to the current Eq (2.2).

Now that we have obtained a law of transformation for the pion matrix, we can try to write a G-invariant Lagrangian for the pions. For this purpose we follow the logic of [42] and try a Lorentz-invariant operator:

$$\mathcal{L}_{\text{try}} = \frac{f^2}{8}\text{Tr}\left[\left(\partial_\mu U(x)^{-1}\right)\left(\partial^\mu U(x)\right)\right] \tag{2.13}$$

Unfortunately, under a G transformation we get:

$$G:\ \mathcal{L}_{\text{try}} \to \frac{f^2}{8}\text{Tr}\left[\left(\partial_\mu h(x)U(x)^{-1}g\right)\left(\partial^\mu gU(x)h^{-1}(x)\right)\right] \tag{2.14}$$

The element $h(x)$, being x-dependent, does not commute with the derivative, and $\mathcal{L}_{\text{try}}$ is thus not invariant. To point out where the shoe pinches we can observe that $\mathcal{L}_{\text{try}}$ can be rewritten as:

$$\mathcal{L}_{\text{try}} = \frac{f^2}{8}\text{Tr}\left[\left(-U^{-1}\partial_\mu U\right)\left(-U^{-1}\partial^\mu U\right)\right] \tag{2.15}$$

The object used is called the Maureer-Cartan form, $a_\mu[U]$, and can be decomposed uniquely as:

$$a_\mu[U] = iU^{-1}\partial^\mu U \tag{2.16}$$
$$= d_\mu[U]^a X^a + e_\mu[U]^a T^a \tag{2.17}$$

Using how $U[\pi]$ transforms we can deduce how d_μ and e_μ do under G, respectively:

$$d_\mu[U] \to h(x)d_\mu[U]h^{-1}(x) \tag{2.18}$$
$$e_\mu[U] \to h(x)e_\mu[U]h^{-1}(x) + h(x)\partial_\mu h^{-1}(x) \tag{2.19}$$

This points out that the non invariance under G comes from e_μ. Writing our Lagrangian only with d_μ ensures a complete invariance under the global symmetry. Thus our lagrangian for the GB is:

$$\mathcal{L} = \frac{f^2}{8}\text{Tr}\left[d_\mu[U]d^\mu[U]\right] \tag{2.20}$$

Up to this point we have only considered gobal symmetries, but as we know, the EW group must be embedded inside G. To deal with gauge fields is very simple, as we only need to change our definition of the Maureer-Cartan form:

$$a_\mu[U] = iU^{-1}\partial^\mu U \to \tilde{a}_\mu[U] = iU^{-1}D^\mu U \tag{2.21}$$
$$= iU^{-1}\left(\partial^\mu + igA^\mu\right)U \tag{2.22}$$

with gA^μ the gauge fields (part of algebra of G) and its coupling constant. From the above definition we can also decompose the broken and unbroken generators:

$$\tilde{a}_\mu[U] = \tilde{d}_\mu[U]^a X^a + \tilde{e}_\mu[U]^a T^a \tag{2.23}$$

The transformations rules of d_μ and e_μ will hence be the same for $\tilde{d}_\mu$ and $\tilde{e}_\mu$. Thus the CCWZ formalism enables us to describe the GB with gauge fields according to:

$$\mathcal{L} = \frac{f^2}{8}\mathrm{Tr}\left[\tilde{d}_\mu[U]\tilde{d}^\mu[U]\right] - \frac{1}{4}F^{\mu\nu}F_{\mu\nu} \tag{2.24}$$

The reader might wonder why we are going through these details of the formalism, and we are actually pretty close to jump to the usual way CH are described as in (2.7). In the CCWZ approach, we decided to describe the pion fields according to the logic (2.8), which has imposed the pions fields to transform non-linearly under the complete group G. We are still able to write down a complete Lagrangian invariant G; however, the form of $d_\mu[U]$ is very hard to determine and to handle. But in a special case of coset, in which CH enters, things can be simplified. This happens when G/H has the property of a symmetric coset. In that case the broken and unbroken generators verify:

$$[T^a, T^b] = f^{ab}{}_c T^c \qquad (a) \tag{2.25}$$
$$[T^a, X^b] = f^{ab}{}_c X^c \qquad (b) \tag{2.26}$$
$$[X^a, X^b] = f^{ab}{}_c T^c \qquad (c) \tag{2.27}$$

with f the antisymmetric tensor structure. Condition (a) characterizes the property of H to be a subalgebra. Condition (b) corresponds to the action of H over G/H. It generates an easy-to-use representation of the unbroken group over the broken generator because we chose the broken generators orthogonal to the unbroken set. Finally (c) is the property of a symmetric coset, where the commutator is only proportional to unbroken generators. It is called symmetric as we can define a transformation τ acting on X^a:

$$\tau : \; X^a \to -X^a \tag{2.28}$$

One can easily check that $-X^a$ also satisfies the condition (a), (b) and (c). τ transforms U according to:

$$\tau : \; U[\pi] \to U[-\pi] = U^{-1} \tag{2.29}$$

Thus,

$$\tau : \; a_\mu[U] \to a_\mu[U^{-1}] = -d_\mu[U]_a X^a + e_\mu[U]_a T^a \tag{2.30}$$

and:

$$d_\mu[U] = \frac{1}{2}\left(a_\mu[U] - a_\mu[U^{-1}]\right) \tag{2.31}$$

one obtains that:

$$\mathcal{L} = \frac{f^2}{8}\mathrm{Tr}\left[\partial_\mu\left(U^{-1}U^{-1}\right)\partial^\mu\left(UU\right)\right] \tag{2.32}$$

such that we finally get $\mathcal{L}_{eff} = \mathcal{L}$ and we can work with the Σ field;

$$\Sigma(x) = \exp\left(2\sqrt{2}\frac{\pi(x)^a}{f}X^a\right)\Sigma_0 \tag{2.33}$$

By knowing the structure of the vacuum Σ_0 we can determine the broken generators X^a and the effective field used will be simply given by (2.33).

It is time now to apply this approach to a CH model.

3 Composite Higgs Template

We now have at hand all the tools to tackle the description below the confinement scale of a CHM. To illustrate it we could be very general in the coset G/H, but it is better to use a concrete example. For this purpose we define the underlying theory to be a $SU(2)_{HC}$ gauge group with 2 Dirac fermions (or 4 Weyl spinors F_i) in its fundamental representation (pseudo-real):

$$\mathcal{L} = -\frac{1}{4}F^{\mu\nu}F_{\mu\nu} + F_i^\dagger \not{D} F^i - M^{ij}F_i F_j \tag{2.34}$$

From the symmetry pattern discussion, we know that the global symmetry is $SU(4)$ and the mass term M^{ij} (or a condensate) breaks it downto $Sp(4)$. First principle lattice simulations have shown that these dynamics indeed generate a non-zero condensate at low energy [43–45].

3 .1 The different vacua

To embed the EW gauge group inside the global $SU(4)$, we consider that 2 of the Weyl spinors (or one Dirac) are an EW doublet, while the other two F's are singlets. In the complete set of the $SU(4)$ generators, we then identify :

$$T^{1,2,3} = \frac{1}{2}\begin{pmatrix}\sigma_i & 0\\ 0 & 0\end{pmatrix}, \quad T^{4,5,6} = \frac{1}{2}\begin{pmatrix}0 & 0\\ 0 & -\sigma^{i\,\mathrm{T}}\end{pmatrix} \tag{2.35}$$

to be the $SU(2)_L \times SU(2)_R$ generators. They can be seen as $SU(2)_L$ acting on F^1, F^2 while $SU(2)_R$ only deals with F^3, F^4. A CH scenario implies that the condensate is electroweak

invariant. Here, as the representation of the HC group is pseudo-real, the condensate Σ_0 transforms as a 2-index antisymmetric of $SU(4)$: $\Sigma_0 \to u\Sigma_0 u^{\mathrm{T}},\ u \in SU(4)$, leaving two possible EW conserving vacua:

$$\Sigma_A = \frac{1}{2}\begin{pmatrix} i\sigma_2 & 0 \\ 0 & i\sigma_2 \end{pmatrix}, \quad \Sigma_B = \frac{1}{2}\begin{pmatrix} i\sigma_2 & 0 \\ 0 & -i\sigma_2 \end{pmatrix} \tag{2.36}$$

They are related to each other by an $U(4)$ transformation, or equivalently by a phase redefinition of the techni fermions. For now, we choose to work with Σ_B as it has been regulary used in the recent litterature.

Having fixed the vacuum we can now clearly identify the other unbroken generators. We recall that the unbroken group is $Sp(4)$ and has dimension 10, so we are only missing 4 generators:

$$T^{7,8,9} = \frac{1}{2\sqrt{2}}\begin{pmatrix} 0 & i\sigma_i \\ -i\sigma_i & 0 \end{pmatrix}, \quad T^{10} = \frac{1}{2\sqrt{2}}\begin{pmatrix} 0 & 1 \\ 1 & 0 \end{pmatrix} \tag{2.37}$$

while the $5 = \dim(SU(4)) - \dim(Sp(4))$ unbroken generators are:

$$X^1 = \frac{1}{2\sqrt{2}}\begin{pmatrix} 0 & \sigma_3 \\ \sigma_3 & 0 \end{pmatrix}, \quad X^2 = \frac{1}{2\sqrt{2}}\begin{pmatrix} 0 & i \\ -i & 0 \end{pmatrix}, \quad X^3 = \frac{1}{2\sqrt{2}}\begin{pmatrix} 0 & \sigma_1 \\ \sigma_1 & 0 \end{pmatrix} \tag{2.38}$$

$$X^4 = \frac{1}{2\sqrt{2}}\begin{pmatrix} 0 & \sigma_2 \\ \sigma_2 & 0 \end{pmatrix}, \quad X^5 = \frac{1}{2\sqrt{2}}\begin{pmatrix} 1 & 0 \\ 0 & -1 \end{pmatrix} \tag{2.39}$$

Thus we can write or $\Sigma(x)$ field as:

$$\Sigma(x) = \exp\left(2\sqrt{2}i\frac{\pi^a}{f}X^a\right)\Sigma_B \tag{2.40}$$

$$= \Sigma_B + \frac{2\sqrt{2}}{f}\begin{pmatrix} 0 & i\pi^5 & \pi^4 + i\pi^3 & \pi^2 - i\pi^1 \\ -i\pi^5 & 0 & -\pi^2 - i\pi^1 & \pi^4 - i\pi^3 \\ -i\pi^4 - i\pi^3 & \pi^2 + i\pi^1 & 0 & i\pi^5 \\ -\pi^2 + i\pi^1 & -\pi^4 + i\pi^3 & -i\pi^5 & 0 \end{pmatrix} + \mathcal{O}\left(\left(\frac{\pi^a}{f}\right)^2\right) \tag{2.41}$$

In which we can identify the Higgs doublet $H \sim \{\pi^1, \pi^2, \pi^3, \pi^4\}$. As we already discussed, the Higgs being a Goldstone boson in this scenario, it cannot acquire a mass, and an explicit breaking of the EW group is necessary.

We now introduce the electroweak breaking vacuum:

$$\Sigma_H = \begin{pmatrix} 0 & 1 \\ -1 & 0 \end{pmatrix} \tag{2.42}$$

We should emphasize two important points. First, indeed Σ_H breaks $SU(2)_L$, however $Q = T^3 + T^6 \sim T^3 + Y$ corresponds to the electromagnetic charge and is conserved through this new vacuum. Secondly, there exists a transformation $\Sigma_H = e^{\pi\sqrt{2}iX^4}\Sigma_B$, where a

rotation using the X^4 generators links the two vacua. Hence, a non-zero expectation value for $\langle \pi^4 \rangle$ will break $SU(2)_L$ while keeping the electromagnetic group safe.

Having this in mind, we can now write the most general vaccum Σ_0 by adding a new parameter θ:

$$\Sigma_0 = e^{2\sqrt{2}i\theta X^4}\Sigma_B = \cos\theta\Sigma_B + \sin\theta\Sigma_H \tag{2.43}$$

The dynamics that generates the breaking of $SU(2)_L$ is now fully encoded in θ, and we will see from the use of explicit breaking in addition to the chiral Lagrangian, how we can determine the value of θ. The link between TC and CH is now manifest: if the effective theory indicates $\theta = \pi/2$ then it is a purely TC model, whereas in the limit where $\theta \to 0$ we converge to a CH model. An important point is that finding $\theta = 0$ will not be realistic, as we need to break the EW group!

3 .2 Mass and Couplings

We have determined the correct vacua to work with, but unfortunately this changes the broken generators. The 5 new ones are:

$$Y^1 = c_\theta X^1 - s_\theta \frac{T^1 - T^4}{\sqrt{2}}\,, \quad Y^2 = c_\theta X^2 - s_\theta \frac{T^2 - T^5}{\sqrt{2}}\,, \quad Y^3 = c_\theta X^3 - s_\theta \frac{T^3 - T^6}{\sqrt{2}} \tag{2.44}$$

$$Y^4 = X^4\,, \quad Y^5 = c_\theta X^5 - s_\theta T^8 \tag{2.45}$$

with $c_\theta = \cos\theta$ and $s_\theta = \sin\theta$. We could work with the field $\Sigma(x) = \exp\left(2\sqrt{2}i\frac{\pi^a}{f}Y^a\right).\Sigma_0$, but we should use it to advantage that the vacuum breaks the EW gauge symmetry. Thus by going to the unitary gauge we could absorb some degrees of freedom in $\Sigma(x)$. A quick look in Eq (2.44) shows that the $SU(2)_L$ generators appears in Y^1,Y^2 and Y^3, which can then be removed. We are left with:

$$\Sigma(x) = \exp\left(2\sqrt{2}i\left(\frac{h}{f}Y^4 + \frac{\eta}{f}Y^5\right)\right).\Sigma_0 = \left[\cos\frac{x}{f}\mathbb{1} + \frac{2\sqrt{2}i}{x}\sin\frac{x}{f}\left(hY^4 + \eta Y^5\right)\right]\Sigma_0 \tag{2.46}$$

with $x = \sqrt{h^2 + \eta^2}$. The physical Goldstone boson h can be identified with the Higgs boson, and further results will enforce this idea. Note that we also get an additional GB, η. By expanding the chiral Lagrangian we find:

$$\begin{aligned}\mathcal{L}_{eff} =& \frac{f^2}{8}\mathrm{Tr}\left[\left(D_\mu\Sigma\right)^\dagger\left(D^\mu\Sigma\right)\right] \\ &= \frac{1}{2}\left(\partial_\mu h\right)^2 + \frac{1}{2}\left(\partial_\mu\eta\right)^2 - \frac{1}{6f^2}\left[h\partial_\mu\eta - \eta\partial_\mu h\right]^2 + \mathcal{O}\left(\frac{1}{f^3}\right) \\ &+ \left(\frac{g^2}{4}{W_\mu}^+W^{\mu-} + \frac{g^2+g'2}{8}Z_\mu Z^\mu\right)\left[f^2{s^2}_\theta + s_{2\theta}fh\left(1 - \frac{2}{3f^2}\left(h^2+\eta^2\right)\right)\right. \\ &\left. + c_{2\theta}h^2 - {s_\theta}^2\eta^2\left(1 - \frac{1}{3f^2}\left(h^2+\eta^2\right)\right)\right] \end{aligned} \tag{2.47}$$

From the above equation we can extract the mass of the W and Z boson:

$${m^2}_W = \frac{g^2}{4}f^2{s^2}_\theta\ , \quad {m^2}_Z = \frac{g^2+{g'}^2}{4}f^2{s^2}_\theta = \frac{{m^2}_W}{{c^2}_W} \tag{2.48}$$

Thus we identify the weak scale $v = f\sin\theta$. The smaller θ is, the larger the hierarchy will be between the TC scale and the scale of the EW symmetry breaking, which is exactly what we were looking for. We also observed the correct relation between the mass of the Z and W, confirming the presence of the custodial symmetry. The coupling between the Higgs and the gauge bosons reads:

$$g_{hWW} = gm_W c_\theta = {g_{hWW}}^{SM}c_\theta \tag{2.49}$$

$$g_{hZZ} = \sqrt{g^2{g'}^2}m_Z c_\theta = {g_{hZZ}}^{SM}c_\theta \tag{2.50}$$

$$g_{hhWW} = \frac{g^2}{4}c_{2\theta} = {g_{hhWW}}^{SM}c_{2\theta} \tag{2.51}$$

$$g_{hhZZ} = \frac{g_{hhWW}}{{c^2}_W} \tag{2.52}$$

The supscript SM indicate the SM tree values, thus h couples much like the Higgs does in the SM, reinforcing the idea that it could play the role of the Higgs boson.

We can now turn to the determination of θ, which is crucial as it is now a parameter that impacts SM masses and couplings.

3 .3 Loop Induced Potential

As we already discussed, to go through the Σ_0 vaccum we need explicit breaking of the flavor $SU(4)$ symmetry. The Chiral Lagrangian only takes into account the symmetries from the dynamics of the TC group. But the gauging of the EW group inside its global flavor symmetry or the coupling to the Higgs to the top will explicitly break the global symmetry. This will destabilize the vaccuum from Σ_B to Σ_0. Here we want to take that into account in the effective field approach. It will yield a potential for the h field that will enable us to fix the value of θ.

Gauge Contributions

Keeping in mind the transformation law of the gauge bosons related to the generators T^1, T^2, T^3 for $SU(2)_L$ and T^6 for $U(1)_Y$, the lowest effective operators that can be written are:

$$V_{\text{gauge}} = -C_g f^4 \text{Tr} \sum_i g^2{}_i \left[T^i \Sigma \left(T^i \Sigma \right)^* \right] \tag{2.53}$$

$$\sim C_g \frac{3g + g'^2}{2} \left(-f^4 c^2{}_\theta + f^3 s_{2\theta} h + f^2 \left(c_{2\theta} h^2 - s^2{}_\theta \eta^2 \right) + \dots \right) \tag{2.54}$$

with C_g an unknown low energy constant. We stress again that Σ_0 is already the correct vaccum and thus θ has already been taken into account in the effective description, through the vacuum definition. To determine the correct value of θ we simply have to suppress the tadpole that appears in the induced potential. This implies the condition:

$$\frac{1}{f} \frac{\partial V_{\text{gauge}}(0,0,\theta)}{\partial \theta} = \left. \frac{\partial V_{\text{gauge}}(h,\eta,\theta)}{\partial h} \right|_{h=\eta=0} \tag{2.55}$$

In the case of V_{gauge} the minimum seems to prefer $\theta = 0$

Top Contribution

In the SM the top is the fermion with the largest coupling to the Higgs, the top yukawa $y_t \sim 1$. Up to now, the TC sector we have introduced is not related to the SM fermions, but a coupling could appear through 4-Fermion interactions like:

$$\frac{Y_t}{\Lambda} (q_L t^c{}_R)^\dagger{}_\alpha F^{\text{T}} P^\alpha F \tag{2.56}$$

Λ corresponds to the scale where this operator is generated, α corresponds to the $SU(2)_L$ index while P^α is a projector selecting the α component. The operator (2.56) will translate at low energy to:

$$y'_t f \left(q_L t^c{}_R \right)_\alpha \text{Tr} \left[P^\alpha \Sigma \right] \sim y'_t \left(f s_\theta + c_\theta h - \frac{1}{2f} s_\theta (h^2 + \eta^3) + \dots \right) t_L t^c{}_R \tag{2.57}$$

We can thus identify a mass for the top, $m_{top} = y'_t f s_\theta$
This also induces a potential:

$$V_{top} = -C_t y'^2{}_t f^4 \sum_\alpha \left[\text{Tr} \left[P^\alpha \Sigma \right]^2 \right] \tag{2.58}$$

$$\sim -C_t y'^2{}_t \left[f^4 s^2{}_\theta + f^3 s_{2\theta} h + f^2 \left(c_{2\theta} h^2 - s^2{}_\theta \eta^2 \right) + \dots \right] \tag{2.59}$$

with C_t also a low energy constant. This potential prefers $\theta \to \pi/2$.

Explicit Breaking

A last feature which can induce a potential and also explicitly break the symmetry is a mass term for the TC fermions M. It induces a potential:

$$V_{\text{mass}} = C_m f^4 \text{Tr}\left[M\Sigma(x)\right] \tag{2.60}$$

with $M = \Sigma_B$ we get:

$$V_{\text{mass}} \sim 4C_m \left[-f^4 c_\theta + f^3 s_\theta h + \frac{1}{2} f^2 c_\theta (h^2 + \eta^2) + \dots\right] \tag{2.61}$$

which also tends to select the $\theta = \pi/2$ configuration.

Complete contributions

We can now sum the different contributions to find the resulting θ. In [39] only the top and mass contributions were considered, as the gauge loops are weaker, yielding to:

$$V(\theta) = -4C_m - f^4 c_\theta - C_t {y'^2}_t f^4 s^2{}_\theta \tag{2.62}$$

This leads to a minimum in θ_{min}:

$$\cos\theta_{\text{min}} = \frac{2C_m}{C_t {y'^2}_t} \tag{2.63}$$

Thus a small θ is achieved if $2C_m \sim C_t {y'^2}_t$. The constant C_t and C_m are expected to be close to one.

Here we have observed a key feature of the Chiral Lagrangian. Even at first order from the kinetic term, we were able to understand the origin of the mass of the gauge bosons as well as the couplings of the Higgs. Another extension that could impact the phenomenology is to take into account the other resonances, like the vector. The important point was to show how the Higgs can arise from the composite dynamics. For that we connected the top quark to the pions in the low energy description. Such coupling needs to originate from the underlying dynamics where in particular we need to couple the SM fermions to the TC dynamics. This has been achieved through 4-F operators. We will turn now to them and how they modify the underlying dynamics.

4 Partial Compositness

In the SM, the origin of the fermion mass takes place via their couplings to the Higgs. The mass results in the product of the Yukawa coupling to the Higgs vacuum expectation value. This structure has been tested experimentally, and small deviations are allowed [11]. Nevertheless, achieving this structure schematically could lead to a realitisc scenario. For these reasons, CHM try to recreate the SM Yukawa operator, for which UV assumptions have to be made. After reviewing the traditional approach, we will focus on the mechanism of Partial Compositness.

4 .1 Historic Attempt

Traditionally, the origin of fermion mass has been implemented by requiring 4-Fermions operators between two technifermions or hyperfermions and two SM fermions:

$$\mathcal{O}_{\text{mass}} \sim \frac{\Psi_{SM}\Psi_{SM}\Psi_{HC}\Psi_{HC}}{\Lambda^2_{ETC}} \tag{2.64}$$

where Λ_{ETC} is the scale at which the 4-F is generated. The two hyperfermions are linked by the HC interactions to the condensate, which itself is connected to the Higgs. This results in an effective interaction betwen two SM fields and the Higgs, exactly like in the SM.

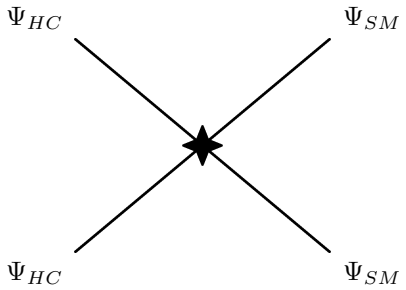

(a) The 4-F operator $\mathcal{O}_{\text{mass}}$.

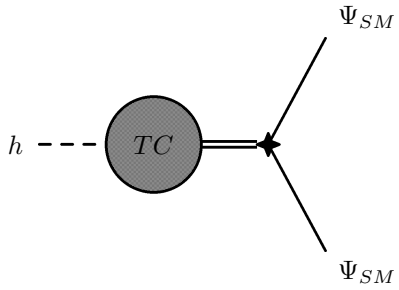

(b) Sketch of the low energy interaction between the Higgs and the SM fermions.

As we already discussed, the presence of 4-F operators calls for an underlying theory to explain them. This is generally done through an extension of the HC groups called Extended TechniColor (ETC) at a higher scale Λ_{ETC}. But there is a cost to pay , which usually comes from dangerous 4-F interactions with only SM fields induced by the extension:

$$\mathcal{O}_{\text{mixing}} \sim \frac{\Psi_{SM}\Psi_{SM}\Psi_{SM}\Psi_{SM}}{\Lambda^2_{ETC}} \tag{2.65}$$

These operators could lead to unwanted FCNC and need to be highly suppressed by pushing Λ_{ETC} to very high scale ($\sim 10^5$ TeV). Unfortunately this will also supress the mass operator for the SM fields, leading to an unsolvable tension in the theory scale.

However, this estimation is done by treating the strong interactions like QCD, and that might not be the case. Indeed, it has been shown that the scaling of the operator according to the energy could change if the theory is conformal or near conformal. In Conformal Field Theory, the scaling of an operator depends on its anomalous dimension γ. For this scenario to occur the coupling constant must reach a plateau at low energy, simulating an IR fixed point. Then, at lower energy the theory exits the conformal regime and the coupling blows up. In figure 2.2 we propose a sketch of this behaviour called Walking.

How will this change the picture? First, this should not change the estimation of $\mathcal{O}_{\text{mixing}}$ as it has only SM fields, the HC interactions don't play a role. The same is not

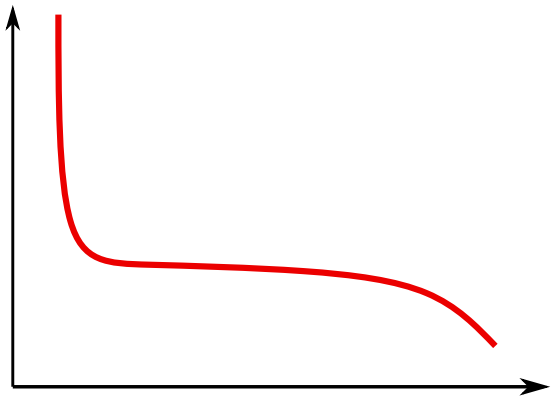

Figure 2.2: Sketch of the gauge coupling evolution in the walking scenario. The plateau corresponds to the conformal regime, below the coupling explodes and above it decreases following asymptotic freedom.

true for $\mathcal{O}_{\text{mass}}$ which relies on the HC dynamics, and should generate a mass m for the SM fermions:

$$m \sim \frac{\langle \Psi_{HC}\Psi_{HC}\rangle_{ETC}}{\Lambda^2_{ETC}} \tag{2.66}$$

where $\langle \Psi_{TC}\Psi_{TC}\rangle_{ETC}$ is the condensate evaluated at the ETC scale. In a QCD like theory this condensate is related to the TC scale following:

$$\langle \Psi_{HC}\Psi_{HC}\rangle_{ETC} = \left(\ln \frac{\Lambda_{ETC}}{\Lambda_{HC}}\right)^{\gamma} \langle \Psi_{HC}\Psi_{HC}\rangle_{TC} \tag{2.67}$$

Thus logarithmic scaling of equation (2.67) will be dominated by the power of law from equation (2.66) as mentioned before. But in a walking regime the ETC and TC condensates are linked by:

$$\langle \Psi_{HC}\Psi_{HC}\rangle_{ETC} = \left(\frac{\Lambda_{ETC}}{\Lambda_{TC}}\right)^{\gamma} \langle \Psi_{HC}\Psi_{HC}\rangle_{TC} \tag{2.68}$$

Here the power law given by the anomalous dimension γ can enhance the resulting mass of equation (2.66). This leads to two questions:

- Is it possible to obtain a walking scenario?
- What values of γ are reachable?

Unfortunately a concrete answer can only come from Lattice simulations, the ultimate way to probe these regimes which are highly non perturbative. We can now turn to the very promising approach of Partial Compositeness.

4 .2 The Partial Compositeness paradigm

In this manuscript we aim to study an alternative mechanism called Partial Compositness [46] in which the mass generation of the SM fermions comes from a mixing with

baryonic operators of the HC sector, avoiding the dangerous issues related to flavor. This mechanism relies also on 4-F interactions but now with three technifermions and one SM field:

$$\mathcal{O}_{PC} \sim \frac{\Psi_{SM}\Psi_{THC}\Psi_{HC}\Psi_{HC}}{\Lambda^2_{ETC}} \tag{2.69}$$

Here the three technifermions have to be seen as spin 1/2 resonances of the TC interactions. In other words, it represents a techni baryon $\mathcal{B}$ of the new strong sector, $\mathcal{B} = \Psi_{HC}\Psi_{HC}\Psi_{HC}$. As the elementary Ψ_{HC} are vector-like so will be the techni baryons, which can have a Dirac mass term. Such mass is generated dynamically provided by the TC interactions, exactly like the proton mass in QCD. The mixing caused by $\mathcal{O}_{PC}$ will allow the SM fields to absorb a part of their mass. The next figure illustrate this mechanism:

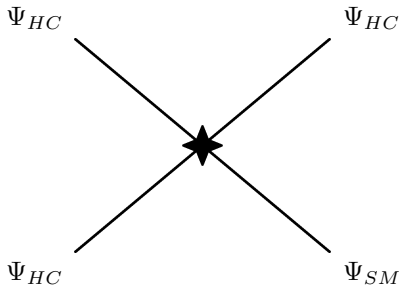

(a) The 4-F operator $\mathcal{O}_{PC}$.

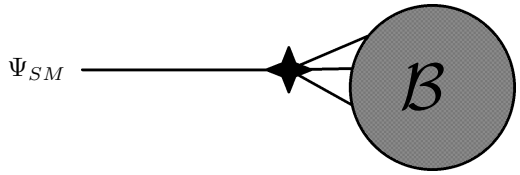

(b) The resulting interaction between the SM fermions and the techni baryon.

We can illustrate this process with an effective lagrangian, implementing the simple case of baryon partners mixing with the top quark field. For this purpose, let us consider the Dirac fields $\mathcal{B}_L$ and $\mathcal{B}_R$, the technibaryons that couple respectively to the elementary quark doublet q_L and the right handed top t_R. The effective lagrangian should now contain:

$$\mathcal{L}_{\text{EFF}} \supset m_L\bar{\mathcal{B}}_L B_L + m_R\bar{\mathcal{B}}_R B_R + \lambda_L\mathcal{B}_L P_L q_L + \lambda_R\mathcal{B}_R P_R t_R + y\bar{\mathcal{B}}_R H\mathcal{B}_L \tag{2.70}$$

with $m_{L/R}$ the mass of the techni baryons, $\lambda_{L/R}$ the mixing coupling whose origin relies on the 4-F interactions, and finally y is the coupling of the techni baryons to the Higgs field. The latter being also composite, this coupling is completely generated by the strong dynamic. Getting the physical states requires to find the mass eigenstates. We thus identify by Q_L and T_R the lightest quark states from the mixing in (2.70), they correspond to the SM fields observed. Formaly we have:

$$Q_L = \sin\theta_L q_L + \cos\theta_L \mathcal{B}_L \tag{2.71}$$

$$T_R = \sin\theta_R t_R + \cos\theta_R \mathcal{B}_R \tag{2.72}$$

$$\sin\theta_{L/R} = \frac{\lambda^2_{L/R}}{\sqrt{\lambda^2_{L/R} + m^2_{L/R}}} \tag{2.73}$$

The larger the coupling of the 4-F interaction is, the larger the the mixing of the SM fields will be. The name Partial Compositness makes sense as the observed SM fields are a superposition of the composite states and the elementary fields. From the above formula we can deduce the effective SM like top Yukawa coupling y':

$$y' = y \sin\theta_L \sin\theta_R \tag{2.74}$$

To pursue the idea that fermionic bound states of the strong dynamic mix with the SM fields will require some modifications in the underlying theory which, as we will see, will leave us with limited possibilities. It is worth noting that the PC paradigm still needs to enhance the scaling of operators like the baryonic bound state. This enables us to push the TC scale while keeping a large enough top mass and top Yukawa coupling. For this reason we will still consider the Walking scenario.

4 .3 Extension of the Global Symmetries

Partial Compositness depends upon the presence of partner to the SM fields. The low energy spectrum now needs to provide for fermionic states with quantum numbers matching the SM ones. This can only be done if some technifermions are also charged under QCD.

The simplest way to account for this is to consider a new species of technifermions χ charged under a different representation of the TC group and under the color group. They need to be carefully chosen such as technibaryons made of $\Psi\Psi\chi$ or $\Psi\chi\chi$ can form the desired SM partners. The TC group now has two distinct representations, each of them exhibiting its own global symmetry:

- First, the Ψ fermions are exactly as we described earlier, their global symmetry should generate the pNGB Higgs.
- The χ will also provide a spontaneous symmetry breaking, delivering Goldstone bosons charged under QCD, leading to promising phenomenology [47].

The addition of the χ fields also plays a role in the TC dynamics, which is required to confine at low energy. A tension appears as we want to obtain a theory near conformal to generate large anomalous dimension, which at some point needs to be broken to get outside the conformal window. To be or not to be, in the conformal window, is very tricky because we cannot rely on perturbation theory. We will discuss this point more precisely in the next chapter. To continue with the CH scenario, a way to break conformal invariance, called Ideal Walking, makes use of the 4-F interactions whose couplings can

break the chiral symmetry [48]. Here we take another approach, where the conformal invariance can be broken if some hyperfermions have a heavy mass, thus they disappear from the running and the theory can be outside the conformal window. The scale around which this happens can be viewed as the TC scale we had formerly in mind.

Within those constraint we are left with three minimal cosets G/H in the Ψ sector that are: $SU(5)/SO(5), SU(4)/Sp(4)$ and finally $SU(4) \times SU(4)/SU(4)$. The different possibilites for the multiplicities of the fermions Ψ and χ (respectively N_Ψ and N_χ) associated to their representation (respectively R_Ψ, R_χ) are displayed in Table 2.4 from [47]. The column "Restriction" indicates when asymptotic freedom is realized and the column "Non Conformal" specifies the subrange when the model is likely outside the conformal window. Finally the column "q_χ/q_Ψ" relates the charge of the gloabl anomalous $U(1) \times G_{HC}^2$ in the Ψ and the sector. Having two sectors allows for a combination of those $U(1)$ to be non-anomalous and this depends on the ratio of the charges.

These models, however, do not offer a complete picture of the UV physics: on the one hand, these models nicely describe the low energy spectrum but need to be extended in order to enter a near-conformal dynamics above the condensation scale; on the other hand, the couplings of the elementary top fields are introduced as non-renormalizable 4-Fermion interactions, which may come together with other relevant and omitted operators. Furthermore, the origin of light quark and lepton masses is not addressed. Lattice studies of the low energy properties for some of these theories are also available [49–54]. Alternatively, (light) scalar fields charged under the confining gauge symmetry have been introduced in Refs [55, 56]: at the price of giving up naturalness, one potentially obtains a complete and fundamental theory of flavor [57]. We should also mention the possibility of bosonic Technicolor [58], where an elementary Higgs doublet is re-introduced [59, 60].

Trying to achieve a complete composite theory of flavor based on gauge and fermion fields alone is a much more daring task: this would be similar to the quest for extended Technicolor theories [35, 61] that, despite intense efforts [62–65], have not produced any fully realistic model so far. The next chapter proposes a fundamental way to accomplish the last points, where the theory can naturally be defined up to the Planck scale.

$G_{\rm HC}$	ψ	χ	Restrictions	$-q_\chi/q_\psi$	Y_χ	Non Conformal	Model Name
	Real	Real	SU(5)/SO(5) × SU(6)/SO(6)				
$SO(N_{\rm HC})$	$5\times\mathbf{S}_2$	$6\times\mathbf{F}$	$N_{\rm HC}\geq 55$	$\frac{5(N_{\rm HC}+2)}{6}$	1/3	/	
$SO(N_{\rm HC})$	$5\times\mathbf{Ad}$	$6\times\mathbf{F}$	$N_{\rm HC}\geq 15$	$\frac{5(N_{\rm HC}-2)}{6}$	1/3	/	
$SO(N_{\rm HC})$	$5\times\mathbf{F}$	$6\times\mathbf{Spin}$	$N_{\rm HC}=7,9$	$\frac{5}{6}$, $\frac{5}{12}$	1/3	$N_{\rm HC}=7,9$	M1, M2
$SO(N_{\rm HC})$	$5\times\mathbf{Spin}$	$6\times\mathbf{F}$	$N_{\rm HC}=7,9$	$\frac{5}{6}$, $\frac{5}{3}$	2/3	$N_{\rm HC}=7,9$	M3, M4
	Real	Pseudo-Real	SU(5)/SO(5) × SU(6)/Sp(6)				
$Sp(2N_{\rm HC})$	$5\times\mathbf{Ad}$	$6\times\mathbf{F}$	$2N_{\rm HC}\geq 12$	$\frac{5(N_{\rm HC}+1)}{3}$	1/3	/	
$Sp(2N_{\rm HC})$	$5\times\mathbf{A}_2$	$6\times\mathbf{F}$	$2N_{\rm HC}\geq 4$	$\frac{5(N_{\rm HC}-1)}{3}$	1/3	$2N_{\rm HC}=4$	M5
$SO(N_{\rm HC})$	$5\times\mathbf{F}$	$6\times\mathbf{Spin}$	$N_{\rm HC}=11,13$	$\frac{5}{24}$, $\frac{5}{48}$	1/3	/	
	Real	Complex	SU(5)/SO(5) × SU(3)²/SU(3)				
$SU(N_{\rm HC})$	$5\times\mathbf{A}_2$	$3\times(\mathbf{F},\overline{\mathbf{F}})$	$N_{\rm HC}=4$	$\frac{5}{3}$	1/3	$N_{\rm HC}=4$	M6
$SO(N_{\rm HC})$	$5\times\mathbf{F}$	$3\times(\mathbf{Spin},\overline{\mathbf{Spin}})$	$N_{\rm HC}=10,14$	$\frac{5}{12}$, $\frac{5}{48}$	1/3	$N_{\rm HC}=10$	M7
	Pseudo-Real	Real	SU(4)/Sp(4) × SU(6)/SO(6)				
$Sp(2N_{\rm HC})$	$4\times\mathbf{F}$	$6\times\mathbf{A}_2$	$2N_{\rm HC}\leq 36$	$\frac{1}{3(N_{\rm HC}-1)}$	2/3	$2N_{\rm HC}=4$	M8
$SO(N_{\rm HC})$	$4\times\mathbf{Spin}$	$6\times\mathbf{F}$	$N_{\rm HC}=11,13$	$\frac{8}{3}$, $\frac{16}{3}$	2/3	$N_{\rm HC}=11$	M9
	Complex	Real	SU(4)²/SU(4) × SU(6)/SO(6)				
$SO(N_{\rm HC})$	$4\times(\mathbf{Spin},\overline{\mathbf{Spin}})$	$6\times\mathbf{F}$	$N_{\rm HC}=10$	$\frac{8}{3}$	2/3	$N_{\rm HC}=10$	M10
$SU(N_{\rm HC})$	$4\times(\mathbf{F},\overline{\mathbf{F}})$	$6\times\mathbf{A}_2$	$N_{\rm HC}=4$	$\frac{2}{3}$	2/3	$N_{\rm HC}=4$	M11
	Complex	Complex	SU(4)²/SU(4) × SU(3)²/SU(3)				
$SU(N_{\rm HC})$	$4\times(\mathbf{F},\overline{\mathbf{F}})$	$3\times(\mathbf{A}_2,\overline{\mathbf{A}}_2)$	$N_{\rm HC}\geq 5$	$\frac{4}{3(N_{\rm HC}-2)}$	2/3	$N_{\rm HC}=5$	M12
$SU(N_{\rm HC})$	$4\times(\mathbf{F},\overline{\mathbf{F}})$	$3\times(\mathbf{S}_2,\overline{\mathbf{S}}_2)$	$N_{\rm HC}\geq 5$	$\frac{4}{3(N_{\rm HC}+2)}$	2/3	/	
$SU(N_{\rm HC})$	$4\times(\mathbf{A}_2,\overline{\mathbf{A}}_2)$	$3\times(\mathbf{F},\overline{\mathbf{F}})$	$N_{\rm HC}=5$	4	2/3	/	

Figure 2.4: List of the minimal models. The notations $\mathbb{F}, \mathbb{A}_2, \mathbb{S}_2, \mathbb{Ad}$ and $\mathbb{Spin}$ denote the fundamental, two-index antisymmetric, two-index symmetric, adjoint and spinorial irreps respectively. A bar denotes the conjugate irrep

Chapter 3

The Techni-Pati-Salam Model

We are only as strong as we are
united, as weak as we are divided.

J.K. Rowling, Harry Potter and the Goblet of Fire

1 Introduction

In this chapter, we want to face the daring need for an Ultra-Violet completion for composite Higgs models: this step is crucial in order to base all we learned from EFT studies on more solid foundations and to truly understand the origin of flavor physics. What we aim at is to define a UV theory that reduces to a viable composite Higgs theory at low energies, around the TeV scale, while being complete and fundamental, i.e. defined up to the Planck scale. Ideally, this should be a theory containing a finite set of couplings closed under the renormalisation group equations, in absence of quantum gravity effects (which are beyond our scope).

In the present work, we follow the route opened in Ref. [66] within the partially unified partial compositeness (PUPC) framework: the confining gauge symmetry is partially unified with the SM ones, with the gauge symmetry breaking due to high-scale scalars. In this sense, this approach lies in between the early extended Technicolor approaches and theories with scalars, while retaining the ambition of achieving a complete theory of flavor in a natural way, i.e. without large hierarchies between scalar masses and the Planck scale. Our main goal will be to give a proof-of-principle that such a theory can be constructed, while leaving its final validation to lattice results in the conformal window lying between the compositeness scale and the Planck scale. While we show how flavorful couplings for all SM quarks and leptons can be generated as a combination of gauge and scalar mediation, we will not attempt to prove that the theory can survive the severe flavor bounds from experiments. In fact, without the input of lattice on the anomalous dimensions of the composite operators that couple to the SM fermions, an analysis based on the EFT approach would be similar to results already present in the literature [67–70].

Our construction offers the benefit of providing a complete set of operators that couple to the SM fields, and the properties of the strongly-coupled gauge interactions that can be studied via first-principle lattice calculations.

The general idea is described in Ref. [66]: here we focus specifically on the Techni-Pati-Salam (TPS) model based on a partially unified gauge symmetry

$$\mathcal{G}_{\rm TPS} = SU(8)_{\rm PS} \times SU(2)_L \times SU(2)_R \,.$$

We will show how to construct a minimal model, which also helps predicting the properties of the microscopic theory underlying the low energy composite dynamics (that can be studied on the lattice), and the dynamics of the walking phase. Analysing how flavor structures arise can help better understand the low energy properties of composite models: for instance, we can show that the multi-scale scenario of Ref. [69] cannot be achieved in this framework and only top partners, i.e. light-ish spin-1/2 resonances associated to the third generation, are possible.

The chapter is organised as follows. In Section 2 we present the general features of the PUPC framework, and the characteristics that lead us to focus on the TPS model and its symmetry breaking pattern. In Section 3 we discuss in detail how the masses for the third generation of SM fermions can be generated, starting from a fundamental gauge-Yukawa theory at high scale. In particular, we will show how the mass hierarchy between top, bottom, tau and neutrino can be achieved. In Section 4 we investigate the possibility of extending the construction to the first and second families: we identify the necessary and minimal ingredients needed to generating all masses and non-trivial Cabibbo-Kobayashi-Maskawa (CKM) [32, 71] and Pontecorvo-Maki-Nakagawa-Sakata (PMNS) [72] mixing matrices. We also establish how baryon number conservation can be imposed to avoid proton decay, thus leading to the existence of a potential Dark Matter candidate. We offer our conclusion and the perspectives in Section 5 .

2 General considerations

2 .1 The PUPC proposal

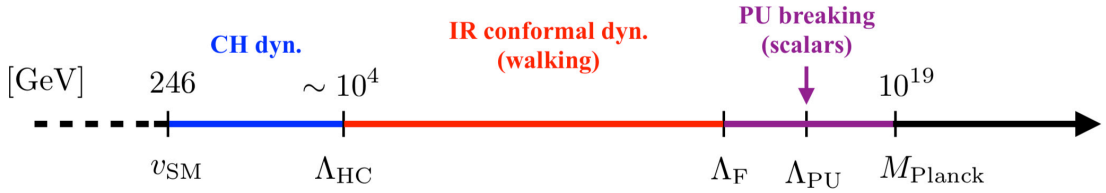

Figure 3.1: Schematic representation of the dynamical phases of PUPC models.

The main goal of our PUPC approach [66] is to provide a genuine UV completion for composite Higgs models with top partial compositeness, which could explain the origin of

the partial compositeness couplings and flavor physics. The theory also needs to be valid all the way up to the Planck scale, where quantum gravity effects become relevant. To achieve this goal, we require that the theory in the UV consists of a renormalizable gauge-Yukawa theory. Scalars, therefore, are added with a "natural" potential, in the sense that all the dimension-of-mass parameters are not too far from the Planck scale. We remind the reader that this "naturalness" principle does not apply to fermion masses. The low energy target is a composite Higgs model with, at least, top partial compositeness. This implies that the UV theory needs to provide both the couplings to achieve top PC, and an intermediate walking phase to enhance them at low energy: the PUPC model, therefore, needs to pass through several different dynamical phases at various scales, as schematically depicted in Fig. 3.1. Here, we expect the low energy dynamics, above the EW scale, to be that of a confining theory with a typical scale $\Lambda_{\rm HC} \approx 10$ TeV (implying a Higgs pNGB decay constant $f \approx \frac{\Lambda_{\rm HC}}{4\pi} \approx 1$ TeV). An IR walking phase thus occurs, separating the confinement scale from the scale where flavor physics is generated, $\Lambda_{\rm F}$. How large this scale needs to be depends on the flavor bounds in a specific model, however we expect it to be close to the scale of gauge symmetry breaking of the UV theory. The latter is achieved by giving vacuum expectation values (VEVs) to the scalars in the theory, at a scale $\Lambda_{\rm PU}$, which is allowed to be roughly one loop-factor below $M_{\rm Planck}$. Thus, typically, $\Lambda_{\rm F} \approx \Lambda_{\rm PU} \approx 10^{16\div 19}$ GeV.

In this section, we will present some general features of PUPC models. The first issue is about choosing the gauge groups. Then, we will show how the SM fermions can be embedded into the PUPC theory, and the scalar sector needed for the symmetry breaking. Finally, we will discuss the conditions under which a walking dynamics can be achieved. In the following two sections we will discuss more gory details about the generation of masses for the third generation first, and then how to extend the theory to the light generations and full flavor structures.

We will start this exploration from the IR end of the spectrum. It has been shown that only a finite number of gauge-fermion theories can lead to the desired low energy phase [73–75], where both a pNGB Higgs and top PC are achieved. The 12 minimal models have been identified, M1-M12, each characterized by its own gauge group and hyper-fermion representations. As mentioned, such theories lie outside of the conformal window: in order to enter the needed walking phase between $\Lambda_{\rm HC}$ and $\Lambda_{\rm F}$, additional hyper-fermions can be added, with a mass $\sim \Lambda_{\rm HC}$. This IR theory, then, needs to be embedded in the UV PUPC theory, where the HC gauge group is partially unified with the SM one. We will shortly see that this step is non-trivial, and it has consequences for the low energy dynamics, as it can be used to further select the gauge theories in the confined phase. This selection is crucial in particular for Lattice studies.

The models that achieve the low energy dynamics with top PC resort to HC groups $SO(N)_{\rm HC}$, $SU(N)_{\rm HC}$ and $Sp(N)_{\rm HC}$, with hyper-fermions in the fundamental, spinorial and two-index antisymmetric representations. Following minimality, we decided to unify QCD and HC groups: this is due to the fact that mediators for top PC typically carry QCD charges. As a consequence, we need to embed the hyper-fermion representation and $SU(3)_c$ fundamentals in the same representation of the extended-HC (EHC) group: this is easiest to do for models based on $Sp(N)_{\rm HC}$, like model M8 [47, 73]. The reason is that

$SO(N)_{\rm HC}$ models always contain the spinorial representation, which is hard to embed together with a fundamental of QCD, while $SU(N)_{\rm HC}$ theories with fundamental tend to inherit the chiral spectrum of the SM in the hyper-fermion sector. While this analysis certainly does not exclude other possibilities, we decided for simplicity to focus on M8, as a template IR model for the first PUPC construction.

The low energy model, therefore, will consist on $Sp(4)_{\rm HC}$ with four hyper-fermions in the fundamental representation: one pair forms a doublet of the gauged $SU(2)_L$ while the other a doublet of the custodial $SU(2)_R$ (the hypercharge corresponds to the diagonal generator). This sector ensures that the pNGB Higgs arises at low energy, and its effect preserves the custodial relation between the W and Z masses. Furthermore, the model needs to include hyper-fermions in the two-index antisymmetric representation in order to obtain top partners in the form of hyper-baryons. The HC and QCD gauge groups are unified as diagonal-subgroups of a $SU(7)_{\rm EHC}$. It is then possible to show that quarks and hyper-fermions in the fundamental can be embedded in fundamentals of $SU(7)_{\rm EHC}$, by suitably choosing the charges under a $U(1)_{\rm E}$, in order to fit the correct hypercharges and cancel gauge anomalies. Leptons here remain as singlets of $SU(7)_{\rm EHC}$, thus they will not receive any contribution to their coupling to hyper-fermions from gauge mediation. This feature, plus the cancellation of anomalies, points towards a unification of quarks–hyper-fermions with leptons, *à la* Pati-Salam [76]. Finally, the PUPC gauge group we choose to work with is

$$\mathcal{G}_{\rm TPS} = SU(8)_{\rm PS} \times SU(2)_L \times SU(2)_R \,, \tag{3.1}$$

from which the name of Techni-Pati-Salam (TPS) model [66]. The next two questions involve the choices of fermions in the TPS model, which can accommodate for both the chiral SM fermions and the non-chiral hyper-fermions, as well as the choice of scalars, which are responsible for breaking the TPS group down to the SM plus HC gauge symmetries.

2 .2 Fermion embedding

In the TPS model, both SM fermions and hyper-fermions need to be embedded into representations of the TPS group. As we will see, the multiplicity and quantum numbers for the hyper-fermions are determined by this choice, thus while we use M8 as a template model, the details of the IR dynamics will not necessarily be the same. To indicate the representations, we will use the following notations:

$$\{\mathbf{d}_{\rm PS},\ \mathbf{d}_L,\ \mathbf{d}_R\} \Rightarrow \mathcal{G}_{\rm TPS} \,, \tag{3.2}$$

where $\mathbf{d}_X$ indicates the dimension of the representation under the TPS group X, while for the IR quantum numbers we omit the $SU(2)_L$ (as it remains unbroken all the way from the UV to the IR) and use

$$(d_4,\ d_3)_Y \Rightarrow (Sp(4)_{\rm HC}, SU(3)_c)_{U(1)_Y} \,. \tag{3.3}$$

Details on how the IR gauge groups are embedded in the TPS one in the UV will be presented in the next subsection.

Firstly, for the SM fermions we follow the hint from Pati-Salam [76] and we embedded them in a fundamental, Ω, and anti-fundamental, Υ, of $SU(8)_{\rm PS}$, as follows:

$$\Omega = \{\mathbf{8},\ \mathbf{2},\ \mathbf{1}\} = \begin{pmatrix} L \\ q_L \\ l_L \end{pmatrix} , \tag{3.4}$$

$$\Upsilon = \{\bar{\mathbf{8}},\ \mathbf{1},\ \mathbf{2}\} = \begin{pmatrix} U_d & D_u \\ d_R^c & u_R^c \\ e_R^c & \nu_R^c \end{pmatrix} ; \tag{3.5}$$

where all spinors are left-handed Weyl, and the two columns in Eq. (3.5) explicitly show the two components of the $SU(2)_R$ doublet. The rows follow the $SU(8)_{\rm PS}$ structure, where we embed the IR gauge groups in the following block-diagonal form:

$$SU(8)_{PS} \Rightarrow \left(\begin{array}{c|c|c} Sp(4)_{\rm HC} & & \\ \hline & SU(3)_c & \\ \hline & & \end{array} \right) . \tag{3.6}$$

One set of Ω and Υ, therefore, contains a complete SM generation

$$\begin{gathered} q_L = (1,3)_{1/6} ,\ \ t_R^c = (1,\bar{3})_{-2/3} ,\ \ b_R^c = (1,\bar{3})_{1/3} , \\ l_L = (1,1)_{-1/2} ,\ \ e_R^c = (1,1)_1 ,\ \ \nu_R^c = (1,1)_0 , \end{gathered} \tag{3.7}$$

including a right-handed neutrino, and the 4 hyper-fermions that generate the pNGB Higgs as a bound state (as in M8)

$$L = (4,1)_0 ,\ \ U_d = (4,1)_{1/2} ,\ \ D_u = (4,1)_{-1/2} . \tag{3.8}$$

Secondly, we need to embed the hyper-fermions in the two-index antisymmetric of $Sp(4)_{\rm HC}$ into the TPS gauge symmetry. The minimal way is to employ antisymmetric representations of $SU(8)_{\rm PS}$: we find convenient and minimal to use the 4-index one, which is a real representation. Other possibilities are discussed in Appendix A .1. The new fermion decomposes as

$$\Xi = \{\mathbf{70},\ \mathbf{1},\ \mathbf{1}\} = \begin{pmatrix} U_t & \chi & \rho & \eta & \omega \\ D_b & \tilde{\chi} & \tilde{\rho} & \tilde{\eta} & \tilde{\omega} \end{pmatrix} , \tag{3.9}$$

where the top row corresponds to fields belonging to a **35** of $SU(7)_{\rm EHC}$ and the ones in the bottom row to the conjugate representation. Thus, fields in the same column have conjugate quantum numbers. The components have the following quantum numbers:

$$\begin{gathered} U_t = (4,1)_{-1/2} ,\ \ \chi = (5,3)_{-1/3} ,\ \ \eta = (4,\bar{3})_{-1/6} , \\ \omega = (1,3)_{-1/3} ,\ \ \rho = (1,1)_0 . \end{gathered} \tag{3.10}$$

	Breaking Pattern	
	Ψ–Θ path	Δ path
PS breaking	$SU(8)_{\rm PS} \times SU(2)_R \to SU(7)_{\rm EHC} \times U(1)_E$	
EHC breaking	$SU(7)_{\rm EHC} \to SU(4)_{\rm CHC} \times SU(3)_c \times U(1)_X$	$SU(7)_{\rm EHC} \times U(1)_E \to SU(4)_{\rm CHC} \times SU(3)_c \times U(1)_Y$
CHC breaking	$SU(4)_{\rm CHC} \times U(1)_E \times U(1)_X \to Sp(4)_{\rm HC} \times U(1)_Y$	$SU(4)_{\rm CHC} \to Sp(4)_{\rm HC}$

Table 3.1: Gauge symmetry breaking steps from the UV TPS theory down to the IR HC composite Higgs model. The two paths correspond to two different ways to give VEVs to the scalar fields.

We see that the hyper-fermions in the antisymmetric of $Sp(4)_{\rm HC}$ have hypercharge $-1/3$, which does not match the one of M8. As we will see, however, this model set-up allows to construct top partners at low energy. Furthermore, the multiplet Ξ contains two hyperfermions, U_t and D_b, with quantum numbers matching D_u and U_d in Υ, and a set of hyper-fermions carrying QCD charges, $\eta/\tilde{\eta}$. The multiplet also contains fermions that are not charged under the HC group: a vector-like partner of the right-handed bottom, $\omega/\tilde{\omega}$, and a singlet $\rho/\tilde{\rho}$. All these components may play a role in giving masses to the SM fermions, as we will discuss in the next section.

For now, this should be considered a minimal set of TPS fermions that contain the key players for a correct IR dynamics. The interesting point to remark now is that the TPS embedding fixes the quantum numbers of the hyperfermions and their multiplicity: a set of Ω, Υ and Ξ contains 12 Weyl spinors in the fundamental and 6 Weyl spinors in the antisymmetric of the HC group. Additional HC-singlets are also predicted. As already mentioned, alternative choices are presented in Appendix A .1.

2 .3 Scalar sector and TPS symmetry breaking

Various scalar multiplets can accommodate the needed breaking steps between the UV TPS theory and the IR model. We identified two paths that are of interest for phenomenology, summarized in Table 3.1, as we will detail in this subsection. We first remark that, besides the gauge symmetry breaking, scalar fields also play the crucial role of generating masses for the hyper-fermions and mediating PC4F interactions for the SM fermions, and we will see them in action in the next two sections. Here, we limit ourselves to discuss the gauge symmetry breaking patterns.

The breaking of $SU(8)_{\rm PS}$, and splitting of the leptons from quarks/hyper-fermions, can be done in a similar way to the standard Pati-Salam model by introducing

$$\Phi = \{\mathbf{8},\ \mathbf{1},\ \mathbf{2}\}\,. \tag{3.11}$$

Once it develops a VEV, which can be aligned as follows[1]

$$\langle\Phi\rangle = \frac{v_{\rm PS}^{\Phi}}{\sqrt{2}}\begin{pmatrix} 0 & 0 \\ \vdots & \vdots \\ 0 & \\ 1 & 0 \end{pmatrix}, \tag{3.12}$$

it will break $SU(8)_{\rm PS} \times SU(2)_R \to SU(7)_{\rm EHC} \times U(1)_E$ [77]. The unbroken $U(1)_E$ charge can be expressed as

$$Q_E = T_R^3 + \frac{2}{\sqrt{7}} T_{\rm PS}^8 \,, \tag{3.13}$$

where T_R^3 is the diagonal generator of $SU(2)_R$ and

$$T_{\rm PS}^8 = \frac{1}{4\sqrt{7}}\begin{pmatrix} 1_{7\times 7} & \\ & -7 \end{pmatrix}. \tag{3.14}$$

The fermion multiplets introduced above decompose as

$$\Omega \;\Rightarrow\; [7,\ 2]_{1/14} \oplus [1,\ 2]_{-1/2}\,, \tag{3.15}$$
$$\Upsilon \;\Rightarrow\; [\overline{7},\ 1]_{-1/14\pm 1/2} \oplus [1,\ 1]_{1/2\pm 1/2}\,, \tag{3.16}$$
$$\Xi \;\Rightarrow\; [35,\ 1]_{-2/7} \oplus [\overline{35},\ 1]_{2/7}\,, \tag{3.17}$$

where $[SU(7)_{\rm EHC},\ SU(2)_L]_{Q_E}$.

The further breaking down to the IR model can follow two paths, which we discuss below.

The Ψ–Θ path

The first path requires the following scalar multiplets:

$$\Psi \;=\; \{\mathbf{63},\ \mathbf{1},\ \mathbf{1}\}\,, \tag{3.18}$$
$$\Theta \;=\; \{\mathbf{28},\ \mathbf{1},\ \mathbf{1}\}\,. \tag{3.19}$$

The adjoint Ψ is assumed to develop a VEV proportional to [77, 78]

$$\langle\Psi\rangle = \frac{v_{\rm EHC}^{\Psi}}{4}\begin{pmatrix} 1_{4\times 4} & \\ & -1_{4\times 4} \end{pmatrix}, \tag{3.20}$$

which, once combined with the Φ VEV [79,80], breaks $SU(7)_{\rm EHC} \to SU(4)_{\rm CHC} \times SU(3)_c \times U(1)_X$. The group $SU(4)_{\rm CHC}$, which we dub complex-HC, contains $Sp(4)_{\rm HC}$, and the would-be hyper-fermions transform as complex representations under the CHC group (see Appendix A .1 for more details). The unbroken $U(1)_X$ charge corresponds to a diagonal generator of $SU(7)_{\rm EHC}$ that can be expressed in terms of $SU(8)_{\rm PS}$ as

$$Q_X = \frac{1}{42}\begin{pmatrix} 3_{4\times 4} & & \\ & -4_{3\times 3} & \\ & & 0 \end{pmatrix}. \tag{3.21}$$

[1] The two columns correspond to components of $SU(2)_R$.

Details about the decomposition of fermion, gauge and scalar multiplets after this step are reported in Appendix A .1.

The gauge couplings are matched to the TPS ones as follows:

$$g_{\rm CHC} = g_c = g_{\rm PS}\,, \tag{3.22}$$

$$g_E = \frac{2\sqrt{7}g_R g_{\rm PS}}{\sqrt{4g_R^2+7g_{\rm PS}^2}}\,, \tag{3.23}$$

$$g_X = \sqrt{\frac{21}{2}}g_{\rm PS}\,. \tag{3.24}$$

The breaking pattern will also produce massive gauge bosons, among which the most interesting ones are

$$C_\mu = (4,1)_{1/2}\,,\quad D_\mu = (1,3)_{2/3}\,,\quad E_\mu = (4,3)_{1/6}\,, \tag{3.25}$$

where the first two form a fundamental of $SU(7)_{\rm EHC}$. As we will see, E_μ and C_μ play an important role in mediating PC4F operators, while D_μ generates four-fermion interactions between quarks and leptons, like in the standard Pati-Salam. Their masses are given by:

$$\begin{gathered} M_E^2 = \tfrac{g_{\rm PS}^2}{4}(v_{\rm EHC}^\Psi)^2\,,\quad M_C^2 = \tfrac{g_{\rm PS}^2}{4}(v_{\rm EHC}^\Psi + v_{\rm PS}^\Phi)^2\,, \\ M_D^2 = \tfrac{g_{\rm PS}^2}{4}(v_{\rm PS}^\Phi)^2\,, \end{gathered} \tag{3.26}$$

where we remark that $M_C > M_E$. For completeness, the spectrum also contains one neutral and one charged singlet deriving from the breaking of $SU(2)_R$, with masses

$$M_{W_R^\pm}^2 = \frac{g_R^2}{4}(v_{\rm PS}^\Phi)^2\,,\quad M_{Z_\Psi}^2 = \frac{4g_R^2+7g_{\rm PS}^2}{16}(v_{\rm PS}^\Phi)^2\,. \tag{3.27}$$

The next step consists in breaking the CHC group down to $Sp(4)_{\rm HC}$, so that the hyper-fermions can transform under a pseudo-real representation of the HC group. We will pragmatically assume that this breaking may occur at any energy between $\Lambda_{\rm PS}$ and $\Lambda_{\rm HC}$. Some phenomenological consideration on the relevance of this scale will be presented in the next subsection. To achieve this step, we need a field transforming as a two-index antisymmetric of $SU(4)_{\rm CHC}$, which is naturally contained in Θ, also carrying charges $Q_E = Q_X = 1/7$. A VEV in this component, would also break $U(1)_E \times U(1)_X \to U(1)_Y$, with

$$Y = Q_E - Q_X\,, \tag{3.28}$$

and gauge coupling matching

$$g_Y = \frac{g_E g_X}{\sqrt{g_E^2+g_X^2}}\,,\quad g_{\rm HC} = g_{\rm CHC}\,. \tag{3.29}$$

The spectrum will now contain two additional gauge bosons, a singlet and $H_\Theta^\mu = (5,1)_0$, with masses

$$M_{H_\Theta}^2 = \frac{g_{\rm CHC}^2}{4}(v_{\rm CHC}^\Theta)^2\,,\quad M_{Z_\Theta}^2 = \frac{g_E^2+g_X^2}{4}(v_{\rm CHC}^\Theta)^2\,. \tag{3.30}$$

The Δ path

A second possible path can be achieved by use of a three-index antisymmetric representation

$$\Delta = \{\mathbf{56},\ \mathbf{1},\ \mathbf{2}\}\,, \tag{3.31}$$

whose VEV can break $SU(8) \to SU(3) \times SU(5)$ [81, 82]. As this VEV also break $U(1)_E$, it needs to transform as an $SU(2)_R$ doublet, with the VEV aligned with the $T_R^3 = -1/2$ component in order to preserve the hypercharge. Thus, together with the Φ VEV, Δ can break $SU(7)_{\rm EHC} \times U(1)_E \to SU(4)_{\rm CHC} \times SU(3)_c \times U(1)_Y$.

The matching of the gauge couplings read

$$g_{\rm CHC} = g_c = g_{\rm PS}\,, \tag{3.32}$$

$$g_Y = \frac{g_R g_{\rm PS}}{\sqrt{g_R^2 + g_R^2 \frac{5}{21} + g_{\rm PS}^2 \frac{16}{7}}}\,. \tag{3.33}$$

The spectrum of massive gauge bosons will now read

$$\begin{aligned} M_E^2 = \tfrac{g_{\rm PS}^2}{4}(v_{\rm EHC}^{\Delta})^2\,,\ \ M_C^2 = \tfrac{g_{\rm PS}^2}{4}(v_{\rm PS}^{\Phi})^2\,, \\ M_D^2 = \tfrac{g_{\rm PS}^2}{4}(v_{\rm PS}^{\Phi} + v_{\rm EHC}^{\Delta})^2\,,\ \ M_{W_R^{\pm}}^2 = \tfrac{g_{\rm R}^2}{4}(v_{\rm PS}^{\Phi} + v_{\rm EHC}^{\Delta})^2\,; \end{aligned} \tag{3.34}$$

plus two massive singlets. We note that $M_C > M_E$ if $v_{\rm PS}^{\Phi} > v_{\rm EHC}^{\Delta}$.

Furthermore, the $T_R^3 = 1/2$ component of Δ contains a component transforming as the two-index antisymmetric of $SU(4)_{\rm CHC}$ with zero hypercharge, thus it can be used to break the CHC symmetry with a VEV $v_{\rm CHC}^{\Delta} < v_{\rm EHC}^{\Delta}$. This breaking will simply leave one massive gauge boson, $H_{\Delta}^{\mu} = (5,1)_0$, with mass

$$M_{H_\Delta}^2 = \frac{g_{\rm CHC}^2}{4}(v_{\rm CHC}^{\Delta})^2\,. \tag{3.35}$$

2 .4 Hypercolor dynamics

A key ingredient for any composite Higgs model with top partial compositeness is the presence of a near-conformal "walking" dynamics above the condensation scale $\Lambda_{\rm HC}$. This may ensure that the hyper-baryons that couple to the top develop a large anomalous dimensions, which in turn can enhance the top PC couplings at low energy. For this mechanism to have any hope to work, the theory in the walking phase should lie as close as possible to the lower edge of the conformal window, thus being in a strongly coupled regime. Unfortunately, estimating the location of the conformal edge in terms of the fermion multiplicities is subject to many uncertainties, due to the strong coupling. In the following, we will adopt two methods developed in the literature: the Pica-Sannino (PS) all order beta function [83], and the Schwinger-Dyson (SD) equation approach [84]. The former is based on a conjectured all-order beta function that depends on the mass anomalous dimensions of the fermions charged under the running gauge coupling. In the conformal window, the beta function should vanish, while the mass anomalous dimensions

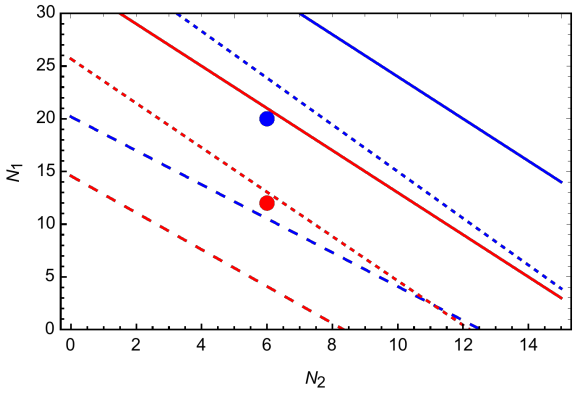

Figure 3.2: Conformal window as a function of the number of Weyl spinors in the fundamental (N_1) and antisymmetric (N_2) for $Sp(4)_{\rm HC}$ (red) and $SU(4)_{\rm CHC}$ (blue). The solid line indicates where asymptotic freedom is lost, while the dashed and dotted lines indicate the expected lower edge using the PS or SD methods, respectively.

are expected to be of order unity. Thus, this provides enough constraints to fix the number of fermions, leading to

$$11C_2(G) - \sum_r T(r)n_r \left(3 + \frac{7}{11}\frac{C_2(G)}{C_2(r)}\right) = 0\,, \tag{3.36}$$

where C_2 is the Casimir and T the dynkin index of the representation (G indicates the adjoint), while n_r is the number of Weyl fermions in the representation r. The SD method uses the ladder approximation in the gap equation to determine the critical value of the gauge coupling where chiral symmetry is broken. This can be compared to the zero of the beta function, which first appears at two loops, leading to

$$\alpha^* = -\frac{4\pi\beta_0}{\beta_1} = \frac{\pi}{3C_2(r)}\,. \tag{3.37}$$

As we have two different representations, we will consider the one whose anomalous dimension reaches unity first, i.e. the antisymmetric. A more sophisticated method, based on a scheme-independent determination of the mass anomalous dimension, has been recently proposed in [85] and gives results somewhat in between the ones obtained by the SD and PS methods.

We first apply these methods to a $Sp(4)_{\rm HC}$ theory [86] with N_1 Weyl spinors in the fundamental and N_2 Weyl spinors in the antisymmetric. The result is shown in Fig. 3.2 by the red lines, where the dashed (dotted) correspond to the PS (SD) method. In solid we show the line above which asymptotic freedom is lost. This case is relevant for the TPS model when the CHC breaking occurs at high scale, i.e. before the onset of the walking phase. The model we presented in this section contains $N_2 = 6$ degrees of freedom in the antisymmetric representation, coming from the Ξ multiplet. For $N_2 = 6$, the PC method gives the lower edge starting at $N_1 = 5$, while for SD it starts at $N_1 = 13$ (while asymptotic freedom is lost for $N_1 = 21$). To compare with a realistic scenario, we recall

that one SM generation ($\Omega + \Upsilon$) plus a Ξ contains $N_1 = 12$, which is in between the two results (C.f., red dot in Fig. 3.2), and very close to the boundary according to the SD method. The method from [85] gives $N_1 = 10$. Thus, the model has good chances of being close to the edge and develop large anomalous dimensions. We anticipate that extending to 3 generations would minimally require to add a flavor index to Ω and Υ, raising the number of fundamental hyper-fermions to $N_1 = 20$, which is well too close to the edge of asymptotic freedom loss, where the theory becomes weakly coupled. This simple analysis shows that the hyper-fermions associated to the light generations should not be light, feature that we will exploit in the next sections.

It is also interesting to consider the case where the CHC symmetry is only broken at low energies, after the model enters the walking phase. As the hyper-fermions contained in Ω and Υ inherit the chiral structure of the SM fermions, they cannot acquire a mass before CHC is broken. Thus, the minimal model with three generations will have $N_1 = 20$. The case of $SU(4)_{\text{CHC}}$ [87] is shown in Fig. 3.2 in blue, with the same conventions as above: the conformal window edge is expected at $N_1 = 11$ with the PS method, and $N_1 = 23$ with SD (while the asymptotic freedom loss occurs at $N_1 = 32$) The minimal model, represented by the blue dot, is again close to the SD lower edge of the conformal window. The case with low scale CHC breaking is therefore also interesting. However, it can only occur if a mechanism that generates a large hierarchy between the VEVs of various scalars is understood. In the following we will focus on the case of high scale CHC breaking, leaving the low scale case for further investigation.

The theory we consider in the following, therefore, features the $Sp(4)_{\text{HC}}$ dynamics in a walking regime between Λ_{HC} and Λ_F. As a further consistency check, as many fermions are present in this wide energy range, we checked that the running of the SM gauge couplings, g_3 for QCD, g_2 for $SU(2)_L$ and g_Y for hypercharge do not develop a Landau pole before the Λ_{PU} scale. We thus used `PyR@TE` [88, 89] to compute the running where only one generation of hyper-fermions is included (i.e., $N_1 = 12$). The two-loop running is shown in Fig. 3.3, proving that the gauge couplings remain under control. These results are mainly qualitative, as the contribution of the HC gauge coupling, which is strong, has not been included. There might be concern that $g_3 \sim 1$ is too perturbative around $\sim 10^{16}$ GeV where it unifies with $SU(4)_{CHC}$, so that the resulting $Sp(4)_{HC}$ coupling might spend unacceptably long RG time in the perturbative regime. However, the ignored HC correction might alter the evolution of g_3 so that $SU(4)_{CHC}$ and $SU(3)_C$ unify at some semi-perturbative value, which we will assume. Also, above the PU scale, the two $SU(2)$ gauge couplings keep growing as their beta function has lost asymptotic freedom: including 3 generation of Ω and Υ, each has 3×8 Weyl spinors. However, this may be a minor issue, because the Planck scale is close to Λ_{PU} by construction, where quantum gravity effects should start to be relevant and may tame the growth of the gauge couplings [90].

To determine whether the desired unification occurs and whether the associated SM gauge couplings avoid hitting a Landau pole at relatively low scales, it is necessary to compute the HC correction to their RG evolution. This problem is inherently non-perturbative and there is no mature computational framework that has been employed to address such problems. One potential route, based on solid field theory principles, is conformal perturbation theory (C.f. Section 2 of Ref. [91] and references therein). Compared to ordinary

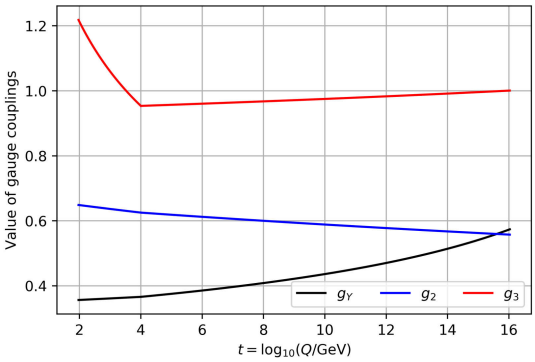

Figure 3.3: Perturbative evolution of SM gauge couplings. Two-loop effects from SM gauge interactions are taken into account, while HC corrections are not included.

Field	Spin	$SU(8)_{\text{PS}}$	$SU(2)_L$	$SU(2)_R$	Q_G
Φ	0	**8**	**1**	**2**	q
Θ	0	**28**	**1**	**1**	$2q$
Δ	0	**56**	**1**	**2**	q
Ψ	0	**63**	**1**	**1**	0
N	1/2	**1**	**1**	**1**	0
Ω	1/2	**8**	**2**	**1**	q
Υ	1/2	$\overline{\mathbf{8}}$	**1**	**2**	$-q$
Ξ	1/2	**70**	**1**	**1**	0

Table 3.2: Scalar and (left-handed Weyl) fermion field content. The last column indicates the global $U(1)_G$ charges, with $q \neq 0$ being an arbitrary normalization factor.

perturbation theory, new terms in the beta functions of the couplings emerge that depend on the CFT data (i.e., coefficients of three-point functions) associated with the conformal fixed point. If one can obtain the CFT data from non-perturbative methods, such as lattice computations, then one can solve the renormalization group equation with the modified beta functions and determine more realistically the evolution of SM gauge couplings.

3 Techni-Pati-Salam for the Third Family

In this section, we will first construct a model that provides masses for one generation of SM fermions, namely the third one, as this exercise allows to better illustrate the main properties of the model. Extension to 3 generations will be presented in the next section. The minimal field content is listed in Table 3.2. We add all the scalars discussed in the previous section in order to keep open both paths of symmetry breaking and also, as we will see, because they all play a crucial role in generating SM fermion masses.

3 .1 Lagrangian and gauge-mediated PC4F Operators

The complete Lagrangian of the model, including only renormalizable operators, can be decomposed as

$$\mathcal{L}_{\text{TPS}^3} = \mathcal{L}_G + \mathcal{L}_F + \mathcal{L}_S + \mathcal{L}_Y + \mathcal{L}_V \,, \tag{3.38}$$

where $\mathcal{L}_G$, $\mathcal{L}_F$ and $\mathcal{L}_S$ denote the kinetic terms for gauge, fermion and scalar fields respectively (including gauge interactions), $\mathcal{L}_Y$ contains the fermion bare mass terms and Yukawa interactions, while $\mathcal{L}_V = -V(\Phi, \Theta, \Delta, \Psi)$ is the scalar potential term. For our purposes, the most relevant part is $\mathcal{L}_Y$, which is given explicitly by:

$$\begin{aligned}\mathcal{L}_Y = &-\frac{1}{2}\mu_N NN - \frac{1}{2}\mu_\Xi \Xi\Xi - \frac{1}{2}\lambda_\Psi \Xi\Psi\Xi - (\lambda_\Phi \Upsilon\Phi N \\ &+\lambda_{\Theta L}\Omega\Theta^*\Omega + \lambda_{\Theta R}\Upsilon\Theta\Upsilon + \lambda_\Delta \Upsilon\Delta^*\Xi + \text{h.c.}) \,,\end{aligned} \tag{3.39}$$

where the first three terms are self-hermitian. In principle, the Yukawas λ_i (except λ_Ψ) are complex parameters, however one can use arbitrary phase redefinitions of the fermion and scalar fields to make all of them real, without loss of generality. At this stage, therefore, physical phases can only be contained in the scalar potential $\mathcal{L}_V$. The interaction terms in $\mathcal{L}_Y$ (including the kinetic terms) also leave a global $U(1)_G$ unbroken, with charges defined in Table 3.2. Explicit $U(1)_G$-breaking terms may appear in the scalar potential. We assume minimizing the scalar potential leads to the desired VEV configuration that break the PS, EHC and CHC groups (see discussion in Sec. 2 .3).

The gauge couplings relevant for generating PC4F operators involve only 2 of the massive gauge bosons, deriving from the PS and EHC breaking: $E_\mu = (\mathbf{4}, \mathbf{3})_{1/6}$ and $C_\mu = (\mathbf{4}, \mathbf{1})_{1/2}$. Their couplings read [2]

$$\mathcal{L}_F \supset \frac{g_{\text{PS}}}{\sqrt{2}}\, C_\mu J_C^\mu + \frac{g_{\text{EHC}}}{\sqrt{2}}\, E_\mu J_E^\mu + \text{h.c.} \,, \tag{3.40}$$

where g_{PS} and g_{EHC} are the gauge couplings of $SU(8)_{\text{PS}}$ and $SU(7)_{\text{EHC}}$ respectively, with $g_{\text{EHC}} \approx g_{\text{PS}}$ if the breaking of the two symmetries is happening at closeby scales. The two currents read:

$$\begin{aligned}J_E^\mu = &\bar{q}_L\bar{\sigma}^\mu L^3 - \bar{D}_u^3\bar{\sigma}^\mu t_R^c - \bar{U}_d^3\bar{\sigma}^\mu b_R^c + \frac{1}{2}\left(\bar{\chi}\bar{\sigma}^\mu U_t - \bar{D}_b\bar{\sigma}^\mu\tilde{\chi}\right) - (\bar{\eta}\bar{\sigma}^\mu\chi - \bar{\tilde{\chi}}\bar{\sigma}^\mu\tilde{\eta}) \\ &- (\bar{\eta}\bar{\sigma}^\mu\omega - \bar{\tilde{\omega}}\bar{\sigma}^\mu\tilde{\eta}) + \frac{1}{2}\left(\rho\bar{\sigma}^\mu\eta - \bar{\tilde{\eta}}\bar{\sigma}^\mu\tilde{\rho}\right) + \frac{1}{2}\left(\bar{\omega}\bar{\sigma}^\mu U_t - \bar{D}_b\bar{\sigma}^\mu\tilde{\omega}\right) \,,\end{aligned} \tag{3.41}$$

$$J_C^\mu = \bar{L}^3\bar{\sigma}^\mu l_L - \bar{\nu}_{\tau R}^c\bar{\sigma}^\mu D_u^3 - \bar{\tau}_R^c\bar{\sigma}^\mu U_d^3 - \frac{1}{2}\left(\bar{\tilde{\eta}}\bar{\sigma}^\mu\chi + \bar{\tilde{\chi}}\bar{\sigma}^\mu\eta\right) - \frac{1}{2}\left(\bar{\tilde{\eta}}\bar{\sigma}^\mu\omega + \bar{\tilde{\omega}}\bar{\sigma}^\mu\eta\right) - \frac{1}{6}\left(\bar{\tilde{\rho}}\bar{\sigma}U_t + \bar{D}_b\bar{\sigma}\rho\right) \,. \tag{3.42}$$

[2] According to our normalization and sign convention, the covariant derivative of a fermion ψ_i in the fundamental of $SU(8)_{PS}$ is written as $D_\mu\psi_i = \partial_\mu\psi_i - i\frac{g_{PS}}{\sqrt{2}}W_{\mu i}^j\psi_j$ with i, j being $SU(8)$ indices. The same convention is used for $SU(7)_{EHC}$.

	1 SM field							0 SM field						
φ_i	$(\mathbf{4},\mathbf{1})_{-\frac{1}{2}}$	$(\mathbf{4},\mathbf{3})_{\frac{1}{6}}$	$(\mathbf{4},\mathbf{3})_{-\frac{5}{6}}$	$(\mathbf{5},\mathbf{1})_{0}$	$(\mathbf{5},\mathbf{1})_{-1}$	$(\mathbf{5},\mathbf{3})_{\frac{2}{3}}$	$(\mathbf{5},\mathbf{3})_{-\frac{1}{3}}$	$(\mathbf{4},\mathbf{1})_{\frac{1}{2}}$	$(\mathbf{4},\mathbf{3})_{\frac{1}{6}}$	$(\mathbf{4},\mathbf{3})_{-\frac{5}{6}}$	$(\mathbf{5},\mathbf{1})_{0}$	$(\mathbf{5},\mathbf{1})_{-1}$	$(\mathbf{5},\mathbf{3})_{\frac{2}{3}}$	$(\mathbf{5},\mathbf{3})_{-\frac{1}{3}}$
$\Omega\Theta^*\Omega$	$(L^3 l_L)$	$(L^3 q_L)$	-	-	-	-	-	-	-	-	$(L^3 L^3)$	-	-	-
$\Upsilon\Theta\Upsilon$	$(U_d^3 \nu_R^c)$ $(D_u^3 \tau_R^c)$	$(U_d^3 t_R^c)$ $(D_u^3 b_R^c)$	- -	- -	- -	- -	- -	- -	- -	- -	$(U_d^3 D_u^3)$	- -	- -	- -
$\Xi\Psi\Xi$	-	-	-	-	-	-	-	$(\chi\eta)$ $(\tilde{\chi}\tilde{\eta})$	(χD_b) $(U_t\tilde{\chi})$ $(\eta\tilde{\chi})$ $(\chi\tilde{\eta})$	-	$(U_t D_b)$ $(\eta\tilde{\eta})$	-	-	-
$\Upsilon\Delta^*\Xi$	$(U_t\nu_R^c)$ $(U_t\tau_R^c)$ $(\tilde{\eta}t_R^c)$ $(\tilde{\eta}b_R^c)$	$(D_b t_R^c)$ (ηb_R^c) $(\eta\nu_R^c)$	$(D_b b_R^c)$ (ηt_R^c) $(\eta\tau_R^c)$	(χb_R^c)	(χt_R^c)	$(\tilde{\chi} b_R^c)$ $(\chi\tau_R^c)$	$(\tilde{\chi} t_R^c)$ $(\chi\nu_R^c)$	-	(χU_d^3) $(\tilde{\chi} D_u^3)$	(χD_u^3) $(\tilde{\chi} U_d^3)$	$(U_t U_d^3)$	$(U_t D_u^3)$	$(\tilde{\eta} U_d^3)$	$(\tilde{\eta} D_u^3)$

Table 3.3: Scalar mediators φ_i (quantum numbers listed in the top row), with the fermion bilinears they couple with. The rows correspond to different Yukawa interactions from $\mathcal{L}_Y$. The fermion bilinears in red couple to the conjugate scalar, φ_i^*.

By integrating out the two vector mediators, we obtain the following four fermion operators, linear in the SM fields:

$$\mathcal{L}_{\text{PC4F}} \supset -\frac{g_{\text{EHC}}^2}{2M_E^2}\left(\bar{L}^3\bar{\sigma}^\mu q_L - \bar{t}_R^c\bar{\sigma}^\mu D_u^3 - \bar{b}_R^c\bar{\sigma}^\mu U_d^3\right)\left(\frac{1}{2}\bar{\chi}\bar{\sigma}_\mu U_t - \frac{1}{2}\bar{D}_b\bar{\sigma}_\mu\tilde{\chi} - \bar{\eta}\bar{\sigma}_\mu\chi + \bar{\tilde{\chi}}\bar{\sigma}_\mu\tilde{\eta}\right)$$
$$-\frac{g_{\text{PS}}^2}{2M_C^2}\left(\bar{L}^3\bar{\sigma}^\mu l_L - \bar{\nu}_{\tau R}^c\bar{\sigma}^\mu D_u^3 - \bar{\tau}_R^c\bar{\sigma}^\mu U_d^3\right)\left(-\frac{1}{2}\bar{\chi}\bar{\sigma}_\mu\tilde{\eta} - \frac{1}{2}\bar{\eta}\bar{\sigma}_\mu\tilde{\chi}\right). \quad (3.43)$$

The interesting property of Eq. (3.43) is that all quark operators are mediated by $E_\mu = (\mathbf{4},\mathbf{3})_{1/6}$, which becomes massive from the EHC breaking, while all lepton operators are mediated by $C_\mu = (\mathbf{4},\mathbf{1})_{1/2}$, which becomes massive from the PS breaking. The mass hierarchy between leptons and quarks could, therefore, be explained by a hierarchy in the masses of the mediators if $M_C > M_E$ (see Sec. 2 .3). Furthermore, lepton operators always involve the QCD-colored hyper-fermions η–$\tilde{\eta}$, while the quark ones also involve the QCD-singlets U_t and D_b.

It is remarkable that our PUPC approach allows to generate appropriate PC4F operators for all SM quarks from gauge interactions, however there is no distinction between fermions in the same weak isospin multiplet. In other words, the gauge interactions themselves cannot distinguish between top-bottom, nor between tau-neutrino. Such mass splittings, which need violation of $SU(2)_R$, naturally receive contributions in our model: from scalar mediated PC4F operators, from the masses of the involved hyper-fermions, and, in the case of the neutrino, from mixing with the singlet N via λ_Φ. These effects are discussed in the following sub-sections.

3 .2 Scalar mediated PC4F operators

The Yukawa couplings in $\mathcal{L}_Y$, Eq. (3.39), allow for many scalar components to mediate PC4F operators. All the relevant combinations are listed in Table 3.3, where we have identified 7 distinct mediators, whose quantum numbers are listed in the top row. The rows

correspond to different Yukawa couplings, while the left block "1 SM field" contains fermion bilinears containing one SM field and the right one "0 SM field" bilinears involves only hyper-fermions. The PC4F operators can thus be constructed by coupling one fermion bilinear from the left block with one from the right block, if they have matching quantum numbers. If they belong to different Yukawa couplings, the resulting operator can only be generated if the components in the two scalar multiplets mix. As an example, the mediators $\varphi_4 = (\mathbf{5},\mathbf{1})_0$ and $\varphi_5 = (\mathbf{5},\mathbf{1})_{-1}$, components of Δ, will generate the following PC4F operators for right-handed top and bottom:

$$\mathcal{L}_{\text{PC4F}} \supset -\frac{\lambda_\Delta^2}{M_{\varphi_4}^2} c_4 \, (\overline{U}_t \overline{U}_d^3)(\chi b_R^c) - \frac{\lambda_\Delta^2}{M_{\varphi_5}^2} c_5 \, (\overline{U}_t \overline{D}_u^3)(\chi t_R^c) \,, \tag{3.44}$$

where $c_{4,5}$ are group theory factors. This example illustrates how a mass splitting between top and bottom could arise if the above couplings are dominant, and there exist a significant mass difference between the two scalar mediators. Scalar-mediated PC4F operators are subject to a larger degree of arbitrariness compared to vector-mediated PC4F operators, because their strengths are determined by the non-universal Yukawa couplings, and masses and mixing of scalar components controlled by details of the scalar potential. Nevertheless, they are also generated automatically from the renormalizable Lagrangian, rather than being put in by hand.

The main ingredients that determine the relevance of scalar mediated PC4F operators are the following:

- the masses and mixing pattern of the scalars.

- the size of the Yukawa couplings. As we will see in the next section, the masses of the hyper-fermions also depend on some of these Yukawas. To keep some hyper-fermions light, therefore, a number of Yukawas need to be small, thus also being ineffective in generating sizable PC4F operators.

In the next 3 subsections, we will discuss the impact of the Yukawa couplings on the hyper-fermion masses, and list the concrete ways the model allows to generate the top-bottom mass hierarchy and small neutrino masses.

3 .3 Hyper-fermion masses

Hyper-fermion masses play an important role in determining the properties of the model. Firstly, the low-energy global symmetry pattern is determined by the number of hyper-fermions that are lighter than the hypercolor condensation scale $\Lambda_{\text{HC}} \sim 10$ TeV. Secondly, whether the HC dynamics enters a strongly-coupled near-conformal regime above Λ_{HC} depends on the additional hyper-fermions that have a mass between Λ_{HC} and Λ_{EHC}, as discussed in Sec. 2 .4. Thirdly, the mass of the hyper-fermions participating in the PC4F operators determines the masses of the corresponding SM fermions: assuming that the dominant contribution is coming from local insertions of the PC4F operators, the SM fermion mass is proportional to the corresponding Fourier-transformed two-point hyper-baryon correlator at zero momentum [92]. When one of the participating hyper-fermions

is heavier than $\Lambda_{\rm HC}$, the correlator is expected to be suppressed by some power of the hyper-fermion mass, as it can be analyzed via the Shifman-Vainshtein-Zakharov (SVZ) expansion [93, 94].

Let's start the discussion with the hyper-fermions χ–$\tilde{\chi}$ and η–$\tilde{\eta}$: they enter in all PC4F operators for quarks and leptons, thus they cannot be too heavy. In particular, as all quark operators, both from gauge and scalar mediation, contain χ or $\tilde{\chi}$, while all fermion operators contain η or $\tilde{\eta}$, in order to obtain a large enough top and tau masses it would be optimal to have $M_\chi \leq \Lambda_{\rm HC}$ and $M_\eta \leq \mathcal{O}(10) \times \Lambda_{\rm HC}$. Furthermore, a hierarchy $M_\chi < M_\eta$ could explain why leptons are lighter than quarks. These hyper-fermion masses receive contributions only from the Ξ mass term and from the Yukawa λ_Ψ via the Ψ VEV, resulting in the following terms

$$\begin{aligned}\mathcal{L}_Y \supset & -\mu_0 U_t D_b - (\mu_0 - 5\mu_1)(\tilde{\chi}\chi + \tilde{\omega}\omega) \\ & - (\mu_0 + 2\mu_1)\tilde{\eta}\eta - \mu_0 \tilde{\rho}\rho + \text{h.c.}\end{aligned} \tag{3.45}$$

where

$$\mu_0 \propto \mu_\Xi\,, \qquad \mu_1 \propto \lambda_\Psi v^\Psi_{\rm EHC}\,. \tag{3.46}$$

Note that, as expected, μ_0 is a universal term for all components of Ξ, while μ_1 only contributes to a sub-set of them. Thus, we can identify

$$M_\chi = |\mu_0 - 5\mu_1|\,, \qquad M_\eta = |\mu_0 + 2\mu_1|\,, \tag{3.47}$$

while the masses of the other components receive additional contributions via mixing, as we will discuss below. The desired hierarchy $M_\chi < M_\eta$ is thus achieved for $0 < \mu_1 < \frac{2}{3}\mu_0$, where we have assumed $\mu_0 > 0$ without loss of generality. The value of the parameter μ_0, which contributes to the mass of the singlet ρ–$\tilde{\rho}$ and of the hyper-fermions U_t–D_b, is related to the two masses by the inequality

$$\mu_0 \leq \frac{2}{7} M_\chi + \frac{5}{7} M_\eta\,, \tag{3.48}$$

implying that is tends to be smaller than the two masses. An important lesson we can take from this analysis is that, barring fine cancellations, $\mu_0, \mu_1 \ll \Lambda_{EHC}$, which implies that the Yukawa λ_Ψ needs to be very small. This is technically natural, however it has an important consequence on the scalar mediated PC4F operators: the ones stemming from $\Xi\Psi\Xi$ (see Table 3.3) are highly suppressed.

We can now discuss the masses of the QCD-singlet hyper-fermions, L^3, D^3_u, U^3_d, U_t and D_b, which are relevant for generating the composite Higgs at low energy. The pNGB Higgs, in fact, is a bound state of L^3 and one of the weak iso-singlets: this implies that one needs L^3 and one set of the iso-singlets to be much lighter that $\Lambda_{\rm HC}$. While the Ξ components U_t–D_b receive a mass from Eq. (3.45), the other hyper-fermions receive a mass via the Θ-VEV as follows:

$$\mathcal{L}_Y \supset -\mu_L L^3 L^3 - \mu_R U^3_d D^3_u\,, \tag{3.49}$$

where

$$\mu_L = \lambda_{\Theta L} v^\Theta_{\rm CHC}\,, \qquad \mu_R = \lambda_{\Theta R} v^\Theta_{\rm CHC}\,. \tag{3.50}$$

For the iso-doublet, this is the only contribution to the mass, so that $M_L = \mu_L$. To keep this mass small, there are three possibilities: a) $\lambda_{\Theta L} \ll 1$ and $v^{\Theta}_{\rm CHC} \gg \Lambda_{\rm HC}$, thus the scalar-mediated PC4F operators cannot receive contributions from $\Omega\Theta^*\Omega$; b) $\lambda_{\Theta L} \lesssim 1$ and $v^{\Theta}_{\rm CHC} \geq \Lambda_{\rm HC}$; c) $v^{\Theta}_{\rm CHC} = 0$. In the last two cases the Yukawa could give sizable contributions to scalar-mediated PC4F operators. In the case of the iso-singlets, mixing terms are also generated in the presence of VEVs for Δ, in the form

$$\begin{aligned}\mathcal{L}_Y \supset & -\mu_{\Delta 1}\left(D_u^3 D_b - \nu_{\tau R}^c \rho\right) \\ & - \mu_{\Delta 2}\left(U_d^3 U_t + \sqrt{2} b_R^c \omega\right) + \text{h.c.}\end{aligned} \tag{3.51}$$

where

$$\mu_{\Delta 1} = \lambda_\Delta v^{\Delta}_{\rm EHC}\,, \qquad \mu_{\Delta 2} = \lambda_\Delta v^{\Delta}_{\rm CHC}\,. \tag{3.52}$$

Note that these two terms also induce a mixing of ρ with the neutrinos, and of ω with the right-handed bottom. We will come back to their effect in the next two subsections. In the hyper-fermion sector, this leads to the following mass matrix:

$$\mathcal{L}_Y \supset -\begin{pmatrix} U_d^3 & D_b \end{pmatrix} \begin{pmatrix} \mu_R & \mu_{\Delta 2} \\ \mu_{\Delta 1} & \mu_0 \end{pmatrix} \begin{pmatrix} D_u^3 \\ U_t \end{pmatrix} + \text{h.c.}\,, \tag{3.53}$$

which has eigenvalues

$$\begin{aligned} M^2_{R1,2} &= \frac{1}{2}\left(\tilde{\mu}^2 \mp \sqrt{\tilde{\mu}^4 - 4(\mu_0\mu_R - \mu_{\Delta 1}\mu_{\Delta 2})^2}\right)\,, \\ &\text{with}\;\; \tilde{\mu}^2 = \mu_0^2 + \mu_R^2 + \mu_{\Delta 1}^2 + \mu_{\Delta 2}^2\,. \end{aligned} \tag{3.54}$$

We see that one can achieve at least one small mass eigenvalue if either all μ's are small, or

$$2(\mu_0\mu_R - \mu_{\Delta 1}\mu_{\Delta 2}) \ll \tilde{\mu}^2\,. \tag{3.55}$$

Seen the constraints on μ_0 coming from the χ and η masses, the latter condition may be achieved for

$$\begin{aligned} \text{a)} \quad & \mu_R \ll \mu_0\,, \;\; \mu_{\Delta 1}\mu_{\Delta 2} \ll \mu_0^2\,, \\ & \Rightarrow M_{R1} \approx \left|\mu_R - \frac{\mu_{\Delta 1}\mu_{\Delta 2}}{\mu_0}\right|\,, \;\; M_{R2} \approx \mu_0\,; \end{aligned} \tag{3.56}$$

or

$$\begin{aligned} \text{b)} \quad & \mu_0 \ll \mu_R\,, \;\; \mu_{\Delta 1}\mu_{\Delta 2} \ll \mu_R^2\,, \\ & \Rightarrow M_{R1} \approx \left|\mu_0 - \frac{\mu_{\Delta 1}\mu_{\Delta 2}}{\mu_R}\right|\,, \;\; M_{R2} \approx \mu_R\,. \end{aligned} \tag{3.57}$$

In the latter case, if $\mu_R \geq \Lambda_{\rm HC}$, one could have that only one mass eigenstate is below the condensation scale, while in the former typically both are light. One can see, therefore,

that the masses have a crucial impact on the low energy dynamics of the theory by influencing the global coset that determines the properties of the composite Higgs:

$$M_{R2} \geq \Lambda_{\rm HC} \Leftrightarrow \frac{SU(4)}{Sp(4)} \quad [95, 96]\,,$$
$$M_{R2} \ll \Lambda_{\rm HC} \Leftrightarrow \frac{SU(6)}{Sp(6)} \quad [97]\,.$$

We also remark that, keeping $\mu_{\Delta 1}\mu_{\Delta 2}$ small would imply either $\lambda_\Delta \ll 1$, or a large hierarchy between the VEVs, $v^\Delta_{\rm CHC} \ll v^\Delta_{\rm EHC}$, with the extreme case $v^\Delta_{\rm CHC} = 0$. These various possibilities have an important impact on the scalar PC4F sector, by determining which terms can be sizable and which ones are always suppressed. The implications for the masses of leptons and quarks will be discussed in the following two subsections.

We recall that the patterns of hyper-fermion masses depend crucially on the pattern of VEVs that break the TPS group down to the low energy theory. In this discussion we work under the assumption that the desired vacuum misalignment and EWSB can be achieved, leaving a detailed study of the vacuum misalignment mechanism to future work [98].

To conclude, we would like to recap the main findings in two special cases of VEV patterns, following the discussion in Sec. 2 .3.

A) $\langle\Delta\rangle = 0$. In this case, the EHC breaking is due to $v^\Psi_{\rm EHC}$, while $v^\Theta_{\rm CHC}$ breaks $SU(4)_{\rm CHC}$ down to $Sp(4)_{\rm HC}$. The mixing terms between iso-singlet hyper-fermions vanish, so that we have a simple mass pattern:

$$M_L = \mu_L\,, \quad M_{R1} = \min\{\mu_R, \mu_0\}\,,$$
$$M_{R2} = \max\{\mu_R, \mu_0\}\,. \tag{3.58}$$

Furthermore, the HC-singlets ω and ρ do not mix and have masses

$$M_\omega = M_\chi\,, \quad M_\rho = \mu_0\,. \tag{3.59}$$

The only large Yukawa is therefore λ_Δ, which is responsible for generating scalar PC4F operators (one could also have sizable $\lambda_{\Theta L/R}$ if $v^\Theta_{\rm CHC} \approx \Lambda_{\rm HC}$). Note that keeping M_χ below $\Lambda_{\rm HC}$ requires small μ_1, where the hierarchy $M_\chi < M_\eta$ can be kept for $0 < \mu_1 < 2/3\ \mu_0$.

B) $\langle\Theta\rangle = \langle\Psi\rangle = 0$. In this case, both EHC and CHC breaking is due to VEVs of the field Δ. As $\mu_1 = \mu_L = \mu_R = 0$, we have

$$M_\chi = M_\eta = \mu_0\,, \quad M_L = 0\,, \tag{3.60}$$

while the iso-singlet masses are given by Eq.(3.57) with $\mu_R = 0$. At least one light eigenstate can be achieved by keeping the mixing terms small, thus requiring $\lambda_\Delta \ll 1$ (and the corresponding Yukawa ineffective in generating scalar PC4F operators).

3 .4 Top-Bottom Mass Splitting

The SM features a large hierarchy between top and bottom masses, with $m_t/m_b \sim 60$ at the weak scale. In the TPS model, the top-bottom mass splitting must be traced back to spontaneous $SU(2)_R$-breaking. We identified three effects that may explain this feature, which we analyse in detail below.

Firstly, we noted that gauge mediators as well as scalar mediators from the $\Upsilon\Theta\Upsilon$ Yukawa cannot be used as they contain both b_R^c and t_R^c. However, scalar-mediated PC4F operators constructed from $\Upsilon\Delta\Xi$ involve mediators that differ in type and properties for t_R^c and b_R^c, as it can be seen in Table 3.3. Thus, a split between top and bottom can simply arise from a difference in mass between the two mediators. One example shown in Eq. (3.44) involves $\varphi_4 = (\mathbf{5},\mathbf{1})_0$ and $\varphi_5 = (\mathbf{5},\mathbf{1})_{-1}$. Another example involves $\varphi_2 = (\mathbf{4},\mathbf{3})_{1/6}$ and $\varphi_3 = (\mathbf{4},\mathbf{3})_{-5/6}$. In both cases, the scalar mass difference breaks $SU(2)_R$, and a sizable coefficient can arise from a large λ_Δ, allowed for vanishing Δ VEV. [3] Another source of mass split lies in the fact that the quantum number $(\mathbf{5},\mathbf{1})_0$ has more ways of pairing compared to $(\mathbf{5},\mathbf{1})_{-1}$ since it also appears in Yukawa terms other than $\Upsilon\Delta\Xi$. Note this is not incompatible with the fact that the Yukawa Lagrangian explicitly preserves $SU(2)_R$ which is a gauge symmetry. The reason is that the required mixing between scalar components with quantum number $(\mathbf{5},\mathbf{1})_0$ can only occur if there exists spontaneous $SU(2)_R$-breaking from the scalar potential. Let us also note that this mechanism does not lead to a prediction of the top-bottom mass splitting, nor a prediction of which quark is heavier, because these properties sensitively depend on details of the scalar potential.

Secondly, a differentiation of top and bottom may come from the mixing in the iso-singlet hyper-fermion sector, given by Eq. (3.53). This opens the possibility that the top has a larger coupling to the lighter mass eigenstate, while the bottom dominantly couples to the heavier one, thus having its mass suppressed. To be more specific, we can analyse the case of dominant gauge mediation: from Eq. (3.41) we see that t_R^c couples to D_u^3, while b_R^c to U_d^3. As the mixing angles for the pairs D_u^3–U_t and U_d^3–D_b are different if $\mu_{\Delta 1} \neq \mu_{\Delta 2}$, one can easily generate hierarchical mixing angles. For instance, for $\mu_R = 0$ (achieved if $\langle\Theta\rangle = 0$) the mixing relevant for the top is proportional to $\mu_{\Delta 2}$, while the one for the bottom to $\mu_{\Delta 1}$. As

$$\frac{\mu_{\Delta 1}}{\mu_{\Delta 2}} \propto \frac{v^{\Delta}_{\text{EHC}}}{v^{\Delta}_{\text{CHC}}} > 1\,, \tag{3.61}$$

a larger mixing angle for the bottom is assured. Another interesting possibility is that both iso-singlet hyper-fermions remain light, in which case the theory features two Higgs doublets in the IR, and the mass hierarchy may be due to the distribution of the EW VEV on the two doublets [99], as in traditional 2HDM [100].

Thirdly, the most interesting mechanism sprouts from the mixing between b_R^c and ω, see Eq. (3.51). As no such term exists for the top quark, this mixing leads to a suppression of the bottom mass. The complete mass term reads

$$\mathcal{L}_Y \supset -\omega\left((\mu_0 - 5\mu_1)\tilde{\omega} + \sqrt{2}\mu_{\Delta 2} b_R^c\right) + \text{h.c.} \tag{3.62}$$

[3] In a less minimal model, this effect could also arise in presence of multiple Δ-multiplets.

Thus we can define mass eigenstates as

$$B_L = \omega\,,\;\; B_R^c = \cos\alpha_b\;\tilde{\omega} + \sin\alpha_b\;b_R^c\,,$$
$$\tilde{b}_R^c = \cos\alpha_b\;b_R^c - \sin\alpha_b\;\tilde{\omega}\,, \tag{3.63}$$

where

$$\tan\alpha_b = \text{sign}(\mu_0 - 5\mu_1)\;\frac{\sqrt{2}\mu_{\Delta 2}}{M_\chi}\,, \tag{3.64}$$

$$M_B = \sqrt{M_\chi^2 + 2\mu_{\Delta 2}^2} \geq M_\chi\,, \tag{3.65}$$

while $\tilde{b}_R^c$ can be identified with the (massless) right-handed bottom. In the case of gauge mediation, the current in Eq. (3.41) can be re-written as

$$J_E^\mu \supset \left(-\cos(\alpha_b)\bar{U}_d^3 - \frac{1}{2}\sin(\alpha_b)\bar{D}_b\right)\bar{\sigma}^\mu\tilde{b}_R^c + \ldots \tag{3.66}$$

Combined with the mixing between U_d^3–D_b, this could lead to a suppressed coupling of the right-handed bottom to the PC4F operators.

It is also instructive to study a case where an effective mass term for the bottom is induced in the form $-\mu_b b_L b_R^c$. The mixing with ω will therefore appear as:

$$\mathcal{L}_{b\omega} = -\begin{pmatrix} b_L & \omega \end{pmatrix}\begin{pmatrix} m_{11} & 0 \\ m_{21} & m_{22} \end{pmatrix}\begin{pmatrix} b_R^c \\ \tilde{\omega} \end{pmatrix} + \text{h.c.} \tag{3.67}$$

with

$$m_{22} = \mu_0 - 5\mu_1\,, \quad m_{21} = \sqrt{2}\mu_u^3\,, \quad m_{11} = \mu_b\,. \tag{3.68}$$

A small bottom mass can be achieved if and only if

$$4|m_{11}m_{22}| \ll (m_{11}^2 + m_{21}^2 + m_{22}^2)\,, \tag{3.69}$$

condition that is compatible with having μ_b smaller than the other mass terms. Within the approximation in Eq. (3.69), for small μ_b, we obtain

$$\frac{m_b}{\mu_b} \approx \frac{|\mu_0 - 5\mu_1|}{\sqrt{(\mu_0 - 5\mu_1)^2 + 2\mu_{\Delta 2}^2}}\,, \tag{3.70}$$

$$M_B \approx \sqrt{(\mu_0 - 5\mu_1)^2 + 2\mu_{\Delta 2}^2}\,. \tag{3.71}$$

The suppression of the bottom mass with respect to μ_b is thus related to the ratio of masses

$$\frac{m_b}{\mu_b} \approx \frac{M_\chi}{M_B}\,, \tag{3.72}$$

which is again compatible with the requirement of a light χ. Assuming that $m_b \lesssim \mu_b \lesssim m_t$, i.e. that the top mass is the largest mass generated by partial compositeness, we obtain the following range for M_B:

$$M_\chi \lesssim M_B \lesssim \frac{m_t}{m_b} \times M_\chi \lesssim \frac{m_t}{m_b} \times \Lambda_{\rm HC}\,, \tag{3.73}$$

which in turn implies

$$|\sqrt{2}\mu_{\Delta 2}| \lesssim \frac{m_t}{m_b} \times \Lambda_{\rm HC}\,. \tag{3.74}$$

Namely, $|\mu_{\Delta 2}|$ cannot be too large, otherwise it leads to over-suppression of the bottom mass. It is also interesting to note the presence of a vector-like bottom quark B, with charge 1/3, which is predicted to be heavier than the hyper-fermion χ: however, it cannot be much heavier, thus its mass will stay in the multi-TeV range and B should be discoverable at future high energy colliders.

Finally let us note that when we evolve the PC4F operators from high scale to low scale, radiative corrections due to hypercharge interaction do not respect $SU(2)_R$ and thus may also contribute to the top-bottom mass splitting. However, the effect is expected to be small. A naive estimate of the relative correction gives

$$\frac{g_Y^2}{(4\pi)^2} \ln \frac{\Lambda_{EHC}}{v_{EW}} \approx 0.05\,, \tag{3.75}$$

where $\Lambda_{EHC} \gtrsim 10^{16}$ GeV denotes the EHC breaking scale, $v_{EW} \approx 246$ GeV and g_Y is the hypercharge coupling constant. So we only expect correction at $\mathcal{O}(10\%)$, which is far from explaining the complete top-bottom mass splitting.

3 .5 Lepton Masses

As it can be inferred from Eq. (3.43) and Table 3.3, the τ lepton mass can be generated via several gauge and scalar-mediated PC4F operators. The model also naturally contains mechanisms that can explain why leptons are lighter than quarks. From gauge mediation, we saw that lepton PC4Fs are generated by a different mediator then the quark ones, with a mass that is naturally larger as it is associated to the breaking of the PS symmetry. If the dominant effect is due to scalar mediators, the masses of the scalars can be arranged in order to suppress more the lepton operators. In both cases, we also observed that lepton operators always involve the hyper-fermion η: if $M_\eta > M_\chi$, therefore, the leptons will be lighter as their mass is more suppressed. It is, therefore, relatively easy to explain the lightness of the tau with respect to the top.

For neutrinos, the situation is more critical, as they are many orders of magnitude lighter than the corresponding charged leptons. If we only consider the effects of PC4F operators, it is possible to generate a neutrino mass that is different (and suppressed) relative to the charged lepton mass, however it is hard to generate such a large difference just using the mediator spectra. One possibility could be to rely on the anomalous dimension of the operator associated to neutrinos.

To make the situation easier, in analogy with the Pati-Salam model, we introduced a singlet fermion N [101]. The Yukawa Lagrangian contains the terms $-\mu_N NN - \lambda_\Phi \Upsilon \Phi N +$ h.c., the latter of which generates a mixing between N and the right-handed neutrino $\nu^c_{\tau R}$ once the scalar Φ generates the PS-breaking VEV. This mixing can be used to implement an inverse see-saw mechanism in the model [102]. To illustrate how this works, we will assume that a large Dirac mass is generated for the neutrinos, in the form $-\mu_\nu\ \nu_L \nu^c_R +$h.c., where $\mu_\nu \approx m_\tau$. The singlet ρ also enters in the game via the mixing in Eq. (3.51). All in all, the relevant mass matrix reads:

$$\mathcal{L}_\nu = -\frac{1}{2}\begin{pmatrix}\nu_L & \nu^c_R & N & \rho & \tilde{\rho}\end{pmatrix}\begin{pmatrix}0 & \mu_\nu & 0 & 0 & 0\\ \mu_\nu & 0 & \mu_\Phi & -\mu_{\Delta 1} & 0\\ 0 & \mu_\Phi & \mu_N & 0 & 0\\ 0 & -\mu_{\Delta 1} & 0 & 0 & \mu_0\\ 0 & 0 & 0 & \mu_0 & 0\end{pmatrix}\begin{pmatrix}\nu_L\\ \nu^c_R\\ N\\ \rho\\ \tilde{\rho}\end{pmatrix} + \text{h.c.} \tag{3.76}$$

where

$$\mu_\Phi \propto \lambda_\Phi v^\Phi_{\rm PS}\,. \tag{3.77}$$

As explained in the previous sections, we expect $\mu_{\Delta 1}$ to be relatively small compared to the scalar VEV scales (it could even vanish in the vacuum with vanishing Δ VEV), thus we can work in the approximation where ρ decouples from the rest. The upper 3×3 block, therefore, exhibits the inverse seesaw form discussed in Ref. [102], allowing for a small neutrino mass for $\mu_N \ll \mu_\Phi \approx v^\Phi_{\rm PS}$. Other scenarios giving realistic neutrino spectra may also be possible.

3 .6 Operator Classification

In any composite Higgs model with fermion partial compositeness, the onset of a near-conformal dynamics above the condensation scale is crucial in order to generate an enhanced coupling of the top quark fields. In the TPS model, the transition between the conformal and confined phases can be traced back to some of the hyper-fermions acquiring a mass of the order of $\Lambda_{\rm HC}$. Thus, the global symmetries in the two phases are not the same. Identifying the operators that couple to the top fields (and to other SM fermions) is crucial in a twofold way: on the one hand, to be able to check if a sufficient anomalous dimension is generated in the conformal phase; on the other hand, to identify the hyper-baryons that mix with the SM fermions at low energy. The latter has important consequences for the low energy phenomenology of the model [38], and the eventual collider signatures.

We will approach this analysis in the following way:

- In the conformal window, we identify the operators in terms of the global symmetry $G_{\rm CFT}$, and match them to the PC4F operators. This allow us to identify the global symmetry properties of each SM fermion partner. The anomalous dimensions need to be computed on the lattice.

Field	quantum numbers	mass	collective names	
L	$(\mathbf{4},\mathbf{1},\mathbf{2})_0$	$M_L \ll \Lambda_{\rm HC}$	ψ_l^i [4]	ψ^α [12]
U_1	$(\mathbf{4},\mathbf{1},\mathbf{1})_{1/2}$	$M_{R1} \ll \Lambda_{\rm HC}$		
D_1	$(\mathbf{4},\mathbf{1},\mathbf{1})_{-1/2}$	$M_{R1} \ll \Lambda_{\rm HC}$		
U_2	$(\mathbf{4},\mathbf{1},\mathbf{1})_{1/2}$	M_{R2}	ψ_h^j [8]	
D_2	$(\mathbf{4},\mathbf{1},\mathbf{1})_{-1/2}$	M_{R2}		
η	$(\mathbf{4},\bar{\mathbf{3}},\mathbf{1})_{-1/6}$	$M_\eta > \Lambda_{\rm HC}$		
$\tilde{\eta}$	$(\mathbf{4},\mathbf{3},\mathbf{1})_{1/6}$	$M_\eta > \Lambda_{\rm HC}$		
χ	$(\mathbf{5},\mathbf{3},\mathbf{1})_{-1/3}$	$M_\chi \lesssim \Lambda_{\rm HC}$		χ^k [6]
$\tilde{\chi}$	$(\mathbf{5},\bar{\mathbf{3}},\mathbf{1})_{1/3}$	$M_\chi \lesssim \Lambda_{\rm HC}$		

Table 3.4: Example of "light" hyper-fermions in the minimal model, classified in terms of their $(Sp(4)_{\rm HC},\ SU(3)_c,\ SU(2)_L)_{U(1)_Y}$ quantum numbers. The number of Weyl flavors is indicated in square brackets in the "collective names" column.

- At $\Lambda_{\rm HC}$, some heavy fermions can be integrated out, and the low energy theory can be characterized in terms of "light" degrees of freedom, with a global symmetry G/H. The SM fermions can now be embedded into representations of G, while baryons (i.e., spin-1/2 resonances with a definite mass) are matched to the respective operators and classified in terms of the unbroken symmetry H.

- The low energy effective theory can thus be constructed in terms of the light degrees of freedom, including light baryon resonances [37, 38, 103].

We recall that some fermions, like leptons, may couple to baryons containing a "heavy" fermion, i.e. a hyper-fermion with a mass larger than $\Lambda_{\rm HC}$. In such cases, techniques like HQET [104, 105], developed to study bound states containing one bottom or charm quark in QCD, can be deployed.

In the following we outline the analysis of operator classification according to their transformation properties under the global symmetry. We simply focus on partners of the left-handed top-bottom doublet, while the analysis for the remaining quark and lepton partners can be carried out in a similar manner. The relevant hyper-fermions, with their quantum numbers and collective notations are listed in Table 3.4. The iso-singlet hyper-fermions are indicated in terms of the mass eigenstates, $U_{1,2} \leftrightarrow \{U_d^3, D_b\}$ and $D_{1,2} \leftrightarrow \{D_u^3, U_t\}$, of the mass matrix in Eq. (3.53). For simplicity, we consider that only 4 hyper-fermions in the fundamental of $Sp(4)_{\rm HC}$ are light, togheter with χ, thus they constitute the "light" degrees-of-freedom (the other two iso-singlets may also be light, without changing qualitatively the discussion). The others have masses of the order of $\Lambda_{\rm HC}$.

In the regime where the hypercolor theory exhibits its strongly-coupled near-conformal dynamics, all hyper-fermions listed in Table 3.4 are active degrees of freedom. The global symmetry of the composite sector is then

$$G_{\rm CFT} = SU(12)_\psi \times SU(6)_\chi \times U(1)\,, \tag{3.78}$$

where $N_\psi = 12$ and $N_\chi = 6$ count the Weyl spinors in the two species, and $U(1)$ is the anomaly-free abelian symmetry, with charges $q_\psi = -q_\chi = 1$. The spin-1/2 hyper-baryon

operators can be constructed with two spinors of specie ψ and one χ. As to the contraction of spinor indices, here we note that hyper-baryon operators can be further grouped into two types: $\langle XYZ\rangle$ and $\langle X\bar{Y}\bar{Z}\rangle$, where X, Y, Z are three generic Weyl fermions of the hypercolor group. [4] It is understood that $\langle XYZ\rangle$ contains two irreducible Lorentz representations $(0, 1/2)$ and $(0, 1/2)'$, while $\langle X\bar{Y}\bar{Z}\rangle$ contains only one Lorentz representation $(0, 1/2)''$ [106]. Note that we focus here on left-handed operators, while right-handed ones can be constructed by replacing each spinor with its charge-conjugate. Hyper-baryon operators with definite transformation properties under the global symmetry group can be constructed schematically as follows:

$$\mathcal{O}_S = \frac{1}{2}\langle(\psi^i_\alpha\psi^j_\beta + \psi^j_\alpha\psi^i_\beta)\chi^k_\beta\rangle = (\mathbf{S},\mathbf{F})_1, \tag{3.79}$$

$$\mathcal{O}_A = \frac{1}{2}\langle(\psi^i_\alpha\psi^j_\beta - \psi^j_\alpha\psi^i_\beta)\chi^k_\beta\rangle = (\mathbf{A},\mathbf{F})_1, \tag{3.80}$$

$$\mathcal{O}_{A'} = \langle\psi^i_\beta\psi^j_\beta\chi^k_\alpha\rangle = (\mathbf{A},\mathbf{F})_1, \tag{3.81}$$

$$\mathcal{O}_{\bar{A}} = \langle\bar{\psi}^i_{\dot\beta}\bar{\psi}^j_{\dot\beta}\chi^k_\alpha\rangle = (\bar{\mathbf{A}},\mathbf{F})_{-3}, \tag{3.82}$$

$$\mathcal{O}_{Adj} = \langle\bar{\psi}^i_{\dot\beta}\bar{\chi}^k_{\dot\beta}\psi^j_\alpha\rangle = (\mathbf{Adj},\bar{\mathbf{F}})_1, \tag{3.83}$$

$$\mathcal{O}_0 = \langle\bar{\psi}^l_{\dot\beta}\bar{\chi}^k_{\dot\beta}\psi^l_\alpha\rangle = (\mathbf{1},\bar{\mathbf{F}})_1; \tag{3.84}$$

where $\alpha, \beta, \dot\alpha, \dot\beta$ are spinorial indices and repeated β are contracted with the usual anti-symmetric tensor, while i, j, l represent indices of $SU(12)_\psi$ and k of $SU(6)_\chi$. The notation $(\mathbf{S},\mathbf{F})_1$ means the operator transforms in the two-index symmetric representation of $SU(12)_\psi$, fundamental representation of $SU(N)_\chi$ and carries a $U(1)$ charge equal to $2q_\psi+q_\chi = 1$. The meaning of the remaining quantum number notations is self-explanatory. Note also that $\mathcal{O}_A$ and $\mathcal{O}_{A'}$ are the two irreducible Lorentz representations one can build for this type of hyper-baryon operators, while the symmetric $\mathcal{O}_S$ can only be constructed with one. The anomalous dimensions of these operators must be computed on the lattice: yet, as they only depend on the spin and hypercolor structures, we can derive some interesting relations. First, $\gamma_A = \gamma_S$ and $\gamma_{Adj} = \gamma_0$. Furthermore, $\mathcal{O}_A$ and $\mathcal{O}_{A'}$ mix as they belong to the same type and have the same charges under the global symmetry [106].

To match the PC4F operators to the above conformal hyper-baryons, we need to find the correspondence between all 3-fermion operators that may couple to the SM fields and the operators build above. Below we give an explicit example for the left-handed quark iso-doublet, with the other cases being straightforward. All the possibilities are thus listed

[4] We recall that the bar indicates the charge conjugate (right-handed) spinor.

below:

$$q_L \Rightarrow Q_R^C \rightarrow \begin{cases} \left[Q_R^C\right]^1_{S/A/A'} = \langle L D_1 \tilde{\chi}\rangle \subset \mathcal{O}_{S/A/A'}\,, \\ \left[Q_R^C\right]^2_{S/A/A'} = \langle L D_2 \tilde{\chi}\rangle \subset \mathcal{O}_{S/A/A'}\,, \\ \left[Q_R^C\right]^3_{S/A/A'} = \langle L \tilde{\eta} \chi\rangle \subset \mathcal{O}_{S/A/A'}\,, \\ \left[Q_R^C\right]^1_{\bar{A}} = \langle \bar{L} \bar{U}_1 \tilde{\chi}\rangle \subset \mathcal{O}_{\bar{A}}\,, \\ \left[Q_R^C\right]^2_{\bar{A}} = \langle \bar{L} \bar{U}_2 \tilde{\chi}\rangle \subset \mathcal{O}_{\bar{A}}\,, \\ \left[Q_R^C\right]^3_{\bar{A}} = \langle \bar{L} \bar{\eta} \chi\rangle \subset \mathcal{O}_{\bar{A}}\,, \\ \left[Q_R^C\right]^1_{Adj} = \langle \bar{L} D_1 \bar{\chi}\rangle \subset \mathcal{O}_{Adj}\,, \\ \left[Q_R^C\right]^2_{Adj} = \langle \bar{L} D_2 \bar{\chi}\rangle \subset \mathcal{O}_{Adj}\,, \\ \left[Q_R^C\right]^3_{Adj} = \langle \bar{L} \tilde{\eta} \bar{\tilde{\chi}}\rangle \subset \mathcal{O}_{Adj}\,, \\ \left[Q_R^C\right]^4_{Adj} = \langle L \bar{U}_1 \bar{\chi}\rangle \subset \mathcal{O}_{Adj}\,, \\ \left[Q_R^C\right]^5_{Adj} = \langle L \bar{U}_2 \bar{\chi}\rangle \subset \mathcal{O}_{Adj}\,, \\ \left[Q_R^C\right]^6_{Adj} = \langle L \bar{\eta} \bar{\tilde{\chi}}\rangle \subset \mathcal{O}_{Adj}\,. \end{cases} \tag{3.85}$$

Note the SM gauge quantum numbers should all match. The superscript index labels different components inside the same multiplet of the global symmetries that can potentially couple to q_L: this shows that hyper-baryon operators in the symmetric or antisymmetric have 3 possible ways, while in the adjoint there are 6. As mentioned above, the HC dynamics can only mix the two operators $\mathcal{O}_A$ and $\mathcal{O}_{A'}$, however it will not generate mixing between the various components inside each operator which couple to the SM fields. This is due to the fact that they are protected by the global symmetries. On the other hand, some mixing may be generated by the SM gauge symmetries: this is the case, for instance, for operators containing $D_{1,2}$ and $U_{1,2}$, as they have exactly the same quantum numbers. Others cannot mix: for example, we do not expect a mixing between $\left[Q_R^C\right]^3_{\bar{A}}$ and $\left[Q_R^C\right]^{1,2}_{\bar{A}}$, as the former contain the QCD-charged η while the latter contains QCD-neutral iso-singlets.

Vector-mediated PC4F operators associated with q_L can then be classified as

$$\begin{aligned} &\frac{1}{M_V^2} q_L \left[c_1\ \bar{L}\bar{\eta}\chi + c_2^i\ \bar{L}\bar{U}_i\tilde{\chi} + c_3^j\ \bar{L}\bar{\chi}D_j + c_4\ \bar{L}\bar{\tilde{\chi}}\tilde{\eta}\right] \\ &= \frac{1}{M_V^2} q_L \Bigg[c_1 \left[Q_R^C\right]^3_{\bar{A}} + c_2^1 \left[Q_R^C\right]^1_{\bar{A}} + c_2^2 \left[Q_R^C\right]^2_{\bar{A}} \\ &+ c_3^1 \left[Q_R^C\right]^1_{Adj} + c_3^2 \left[Q_R^C\right]^2_{Adj} + c_4 \left[Q_R^C\right]^3_{Adj} \Bigg], \end{aligned} \tag{3.86}$$

where the c_i's are calculable dimension-less coefficients. Note that $c_2^{1,2}$ and $c_3^{1,2}$ are related to each other by rotation angles from Eq. (3.53), as they stem from operators containing D_b and U_t respectively. For gauge-mediated PC4F operators, therefore, only $\mathcal{O}_{\bar{A}}$ and $\mathcal{O}_{Adj}$ are relevant. The anomalous dimensions have been computed perturbatively at one loop

order in Ref. [106], yielding:

$$\begin{aligned}\gamma_{\bar{A}} &= -\frac{3g_{\rm HC}^2}{16\pi^2}\left(2C_2(R_\psi) - C_2(R_\chi)\right) = -\frac{1}{2}\frac{3g_{\rm HC}^2}{16\pi^2}\,,\\ \gamma_{Adj} &= -\frac{3g_{\rm HC}^2}{16\pi^2}\left(C_2(R_\chi)\right) = -2\frac{3g_{\rm HC}^2}{16\pi^2}\,.\end{aligned} \tag{3.87}$$

While these results have limited validity, they seem to suggest the correct sign and that $|\gamma_{Adj}| > |\gamma_{\bar{A}}|$, so that the adjoint would lead to larger enhancement.

Once the theory flows down to energies $\sim \Lambda_{\rm HC}$, the heavy hyper-fermions in Table 3.4 can be integrated out, and the theory with only light flavors condenses and generates dynamically a mass gap. The global symmetry is thus:

$$\frac{G}{H} = \frac{SU(4)_\psi \times SU(6)_\chi \times U(1)}{Sp(4)_\psi \times SO(6)_\chi}\,, \tag{3.88}$$

where the $U(1)$ charges are $q'_\psi = -3q'_\chi = 1$. We can now build operators containing two light flavors in the same way as in Eqs. (3.79)–(3.84), except for the the different $U(1)$ charges:

$$\begin{gathered}\mathcal{O}^{ll}_S = (\mathbf{S},\mathbf{F})_{5/3},\;\; \mathcal{O}^{ll}_{A/A'} = (\mathbf{A},\mathbf{F})_{5/3},\;\; \mathcal{O}^{ll}_{\bar{A}} = (\bar{\mathbf{A}},\mathbf{F})_{-7/3},\\ \mathcal{O}^{ll}_{Adj} = (\mathbf{Adj},\bar{\mathbf{F}})_{1/3},\;\; \mathcal{O}^{ll}_0 = (\mathbf{1},\bar{\mathbf{F}})_{1/3},\end{gathered} \tag{3.89}$$

where the quantum numbers in parenthesis correspond to the global symmetry G. Operators containing one heavy flavor are also relevant, and they can be classified as:

$$\mathcal{O}^{lh}_{FF/FF'} = \langle\psi^l\psi^h\chi\rangle = (\mathbf{F},\mathbf{F})_{2/3}\,, \tag{3.90}$$

$$\mathcal{O}^{lh}_{F\bar{F}} = \langle\psi^l\bar{\psi}^h\bar{\chi}\rangle = (\mathbf{F},\bar{\mathbf{F}})_{4/3}\,, \tag{3.91}$$

$$\mathcal{O}^{lh}_{\bar{F}F} = \langle\bar{\psi}^l\bar{\psi}^h\chi\rangle = (\bar{\mathbf{F}},\mathbf{F})_{-4/3}\,, \tag{3.92}$$

$$\mathcal{O}^{lh}_{\bar{F}\bar{F}} = \langle\bar{\psi}^l\psi^h\bar{\chi}\rangle = (\bar{\mathbf{F}},\bar{\mathbf{F}})_{-2/3}\,. \tag{3.93}$$

The matching of the possible PC4F couplings from Eq. (3.85) also changes: focusing for simplicity on the example of the adjoint components in Eq. (3.86), we see

$$[Q^C_R]^1_{Adj} \subset \mathcal{O}^{ll}_{Adj}\,, \quad [Q^C_R]^{2,3}_{Adj} \subset \mathcal{O}^{lh}_{\bar{F}\bar{F}}\,. \tag{3.94}$$

This matching allows to construct spurions that encode the SM spinor q_L, and can be used to construct the low energy effective Lagrangian [37]. As a final step, the operators above should be matched to the baryon resonances, which have definite masses. They can be classified in terms of the unbroken symmetry H. For instance,

$$\mathcal{O}^{ll}_{Adj} \to \mathcal{B}^{jj}_{[A,F]} + \mathcal{B}^{jj}_{[S,F]}\,, \tag{3.95}$$

where the subscript denotes the representation under $H = [Sp(4), SO(6)]$. Note that the same hyperbaryon resonance also overlap with the other operators, as they share the same quantum numbers under the unbroken symmetry H, but with different structure functions [52]:

$$\mathcal{O}^{ll}_S \to \mathcal{B}^{jj}_{[S,F]}\,, \;\; \mathcal{O}^{ll}_{A,A',\bar{A}} \to \mathcal{B}^{jj}_{[A,F]}\,. \tag{3.96}$$

1st Family	2nd Family	3rd Family
N^1	N^2	N^3
$\Omega^1 = \left(\begin{pmatrix} L_u^1 \\ u_L^1 \\ \nu_L^1 \end{pmatrix} \begin{pmatrix} L_d^1 \\ d_L^1 \\ e_L^1 \end{pmatrix}\right)$	$\Omega^2 = \left(\begin{pmatrix} L_u^2 \\ u_L^2 \\ \nu_L^2 \end{pmatrix} \begin{pmatrix} L_d^2 \\ d_L^2 \\ e_L^2 \end{pmatrix}\right)$	$\Omega^3 = \left(\begin{pmatrix} L_u^3 \\ u_L^3 \\ \nu_L^3 \end{pmatrix} \begin{pmatrix} L_d^3 \\ d_L^3 \\ e_L^3 \end{pmatrix}\right)$
$\Upsilon^1 = \left(\begin{pmatrix} U_d^1 \\ d_R^{1c} \\ e_R^{1c} \end{pmatrix} \begin{pmatrix} D_u^1 \\ u_R^{1c} \\ \nu_R^{1c} \end{pmatrix}\right)$	$\Upsilon^2 = \left(\begin{pmatrix} U_d^2 \\ d_R^{2c} \\ e_R^{2c} \end{pmatrix} \begin{pmatrix} D_u^2 \\ u_R^{2c} \\ \nu_R^{2c} \end{pmatrix}\right)$	$\Upsilon^3 = \left(\begin{pmatrix} U_d^3 \\ d_R^{3c} \\ e_R^{3c} \end{pmatrix} \begin{pmatrix} D_u^3 \\ u_R^{3c} \\ \nu_R^{3c} \end{pmatrix}\right)$
$\Xi = \left(\begin{bmatrix} U_t \\ \chi \\ \eta \\ \omega \\ \rho \end{bmatrix} \begin{bmatrix} D_b \\ \tilde{\chi} \\ \tilde{\eta} \\ \tilde{\omega} \\ \tilde{\rho} \end{bmatrix}\right)$		

Table 3.5: Extension of the TPS fermion sector to three families. For Ω^a and Υ^a, the two columns correspond to the $SU(2)_{L/R}$ components while the rows are connected by the $SU(8)_{\rm PS}$ symmetry. For Ξ, the two columns correspond to the **35** and $\bar{\mathbf{35}}$ components of the multiplet under $SU(7)_{\rm EHC}$.

In this case, the most relevant resonance will be determined by the spectrum. In the case of operators containing one heavy flavor, they all overlap with the same baryon, namely

$$\mathcal{O}_X^{lh} \to \mathcal{B}_{[F,F]}^{lh}\,, \tag{3.97}$$

where hyper-baryon operators containing different heavy flavors, U_2/D_2, $\eta/\tilde{\eta}$, should be considered as different states. Also the corresponding baryon resonance will have a mass larger than that of the $\mathcal{B}^{ll}$ states, and proportional to the mass of the heavy flavour, M_{R2} or M_η.

4 Three family model

A realistic composite Higgs model must not only account for EWSB within the dynamics of the pNGBs and generate masses for the third family SM fermions, but also be able to generate masses of the first and second family SM fermions and non-trivial mixing matrices. So far, the issue of flavor physics in composite models has been discussed only in the context of effective field descriptions, for both quarks [67–69, 107] and leptons [70, 108, 109], or in extra dimensional holographic descriptions [110–112]. Models with a microscopic description of the composite dynamics [73,74] do not go beyond the generation of the top mass. In particular, in Ref. [68] a model was proposed where two scales are identified: a light one where the physics relevant for the top quark resides with light top partners, and a larger scale where masses for the light generations and flavor mixing are generated. This approach has been pushed forward in Ref. [69], where a multi-scale

scenario is discussed where each SM fermion has a partner at a different mass scale. Our PUPC approach offers the unique opportunity to explore in detail the origin of flavor physics and fermion masses in a composite Higgs scenario: while in previous approaches the couplings relevant for flavor physics were added as effective operators, without any possible attempt to investigate the physics that sources them, in the PUPC approach they can be clearly associated to either gauge or scalar couplings. They can, therefore, be considered fundamental by all means. As we will demonstrate in this section, this has important consequences for the low energy physics. In this section we will, therefore, describe how to expand the TPS model to give mass to first and second generation.

The first obvious step consists in adding new fermions containing the first and second family SM fermions, in terms of TPS gauge multiplets. The simplest option is to introduce two more copies of Ω and Υ, see Eqs (3.4) and (3.5). A priori, there is no need to introduce more copies of the Ξ field since it does not contain SM fermions. The sterile fermion N is also extended to three families. In Table 3.5 we summarize in detail the fermion multiplets and their components. We want to remark the introduction of two additional copies of the hyper-fermions L, U_d and D_u, which come along the SM fermions. Thus, the total number of hyper-fermions in the fundamental of $Sp(4)_{\rm HC}$ becomes $N_\psi = 20$, which is too much in order to keep the theory inside a near-conformal phase below the TPS symmetry breaking, as discussed in Sec. 2 .4. This observation already suggests that the hyper-fermions associated to the first two generations should be heavy, with a mass close to the TPS symmetry breaking scale. [5]

The next step consists in extending the Lagrangian to the three family case: adding family indices to Eq. (3.39), we obtain

$$\begin{aligned}\mathcal{L}_Y = &-\frac{1}{2}\mu_N^a N^a N^a - \frac{1}{2}\mu_\Xi \Xi\Xi - \frac{1}{2}\lambda_\Psi \Xi\Psi\Xi - \big(\lambda_\Phi^{ab}\Upsilon^a \Phi N^b \\ &+\lambda_{\Theta L}^a \Omega^a \Theta^* \Omega^a + \lambda_{\Theta R}^a \Upsilon^a \Theta \Upsilon^a + \lambda_\Delta^a \Upsilon^a \Delta^* \Xi + \text{h.c.}\big)\,,\end{aligned} \tag{3.98}$$

where, without loss of generality, we have used the $U(3)$ flavor symmetry of the fields N^a, Ω^a and Υ^a to diagonalize the matrices μ_N and $\lambda_{\Theta L/R}$. We can already remark that the only terms that connect different flavors are λ_Φ^{ab}, which characterizes the mixing between right-handed and sterile neutrinos, and λ_Δ^a, which introduces couplings between the right-handed SM fermions and the hyper-fermions contained in Ξ.

As discussed in the previous section, masses for the hyper-fermions in Ω^a and Υ^a are generated by the Yukawas $\lambda_{\Theta L/R}$ upon Θ developing its CHC-breaking VEV. Thus, in order to preserve a wide walking window, we need

$$v_{\rm CHC}^\Theta \gg \Lambda_{\rm HC}\,, \quad \lambda_{\Theta L/R}^{1,2} \sim \mathcal{O}(1)\,, \quad \lambda_{\Theta L/R}^3 \ll 1\,. \tag{3.99}$$

The latter comes from the need to keep the hyper-fermions of the third generation light, as discussed in the previous section. Note that this necessary set-up already allows us to rule out the scenario of Ref. [69] in the TPS framework: as partners of the light generations can only contain the hyper-fermions $L^{1,2}$, $U_d^{1,2}$ and $D_u^{1,2}$, it is not possible to generate

[5] The only way to keep all the hyper-fermions light is to break the CHC symmetry at low energy, close to $\Lambda_{\rm HC}$, so that the conformal window is generated by the $SU(4)_{\rm CHC}$ dynamics, C.f. Sec. 2 .4.

hierarchical masses for them without spoiling the walking in the near-conformal window (this would lead to an excessive suppression of the top mass).

In the remainder of this section we will focus on the symmetry breaking pattern involving VEVs for the scalar multiplets Φ, Ψ and Θ, because it allows to preserve baryon number, as we will discuss later.

4 .1 Scenarios for EWSB with flavor

In the previous section, the composite Higgs was associated with the hyper-fermions of the third family and the ones contained in Ξ, which need to remain relatively light. As we have shown, it is also necessary to keep the hyper-fermions of the light generations very heavy. To discuss light generation masses, we need to first explore how they can couple to the source of EWSB. We envision three potential scenarios:

1. Private Higgs scenario: it may be possible that each family receives the EWSB from a bound state of the hyper-fermions of the same generation. This scenario has some similarities with the private Higgs proposed in Ref. [113]. As we will explain below, this case should be discarded.

2. Flavorful Partial Compositeness: light generation may be connected to their own partners, i.e. spin-1/2 resonances from the hyper-barion operators of 1st and 2nd generation. As we mentioned, the need for a walking window implies that the light generation partners should have a fairly large mass, close to the CHC breaking scale $v^{\Theta}_{\rm CHC}$. Unless this scale can be pushed to relatively low values, this scenario seems unlikely because the masses would be excessively suppressed.

3. Flavored couplings: the remaining scenario consist in generating couplings for all SM fermions to the hyper-fermions of the third generation. The flavor structure is thus embedded in the couplings. As we will see, this scenario requires an extension of the scalar sector as compared to the minimal model of Sec. 3 .

To better understand why the scenario 1 should be discarded, we need to closely investigate the global symmetries of the TPS model extended to three generations. Firstly, for each family, we may introduce a discrete $\mathbb{Z}_2$ symmetry that we name $\mathbb{Z}_{L,p}$ (p being the family index), under which all components of the Ω^p field are odd, while all other fields are even (including Ω^q, $q \neq p$). Secondly, for each family, we may introduce a global $SU(2)_{L,p}$ symmetry, which is the simultaneous $SU(2)_L$ rotation of all components in Ω^p (while Ω^q with $q \neq p$ are untouched). In the minimal model with a single Θ field, charaterized by the Yukawa terms in Eq. (3.98), all the $\mathbb{Z}_{L,p}$'s are explicitly preserved by the complete Lagrangian of the TPS model, while the $SU(2)_{L,p}$'s are only broken due to the $SU(2)_L$ gauging.

The mass terms of the SM fermions in the generation p necessarily break both $\mathbb{Z}_p$ and $SU(2)_{L,p}$, or in other words the private Higgses H^p are charged under these symmetries. In scenario 1, we implicitly assume that these symmetries are broken spontaneously, leading to the presence of 3 sets of pNGBs due to the breaking of the global $SU(2)_{L,p}$ symmetries. While one set constitutes the exact Goldstones of the $W^{\pm}$ and Z bosons,

the others will acquire a mass via the explicit breaking due to the $SU(2)_L$ gauging, and independent of the mass of the hyper-fermions. This seems to be in contradiction with the decoupling condition [114, 115], which dictates that heavy particles should be decoupled from IR physics. The existence of a massless Goldstone boson composed of superheavy constituents certainly contradicts the decoupling condition. Note also that a theorem by Vafa and Witten [116] states that "non-chiral" global symmetries cannot be spontaneously broken. Strictly speaking, the TPS model is not a vector-like theory, even though an $SU(2)_{L,p}$ invariant mass for L^p can be written, so that this theorem cannot be directly applied. Yet, the argument above suggests that the EWSB must be associated only with light hyper-fermions, i.e. the third generation ones and the ones contained in Ξ, as we studied in the previous section.

Another possibility is that the EWSB is communicated to the heavy hyper-fermions via explicit breaking, like loops of the $SU(2)_L$ gauge bosons. However, the breaking would be suppressed by the mass of the heavy hyper-fermions, $\sim v_{\rm SM}^2/v_{\rm CHC}^{\Theta}$. Unless the CHC breaking scale is low, this possibility is excluded in the same way as scenario 2.

4 .2 Second Family masses, and the rank of the mass matrix

In the orginal work proposing Partial Compositeness [46], D.B.Kaplan realized that, although at high energy three families with the most general flavor structure are included, the fermion mass matrix obtained at low energy may turn out to be of rank 1, as its entries can be expressed as

$$m_{ab} = \kappa_a \tilde{\kappa}_b \,, \tag{3.100}$$

where $a, b = 1, 2, 3$ are family indices. Thus, to generate masses for the first and second families he introduced mechanisms other than PC. In the TPS model we should also check that the rank of the mass matrix is enough to give mass to all generations. For each SM fermion f, the mass matrix can be schematically written as

$$M_f = \begin{pmatrix} < O_{L1} O_{R1} > & < O_{L1} O_{R2} > & < O_{L1} O_{R3} > \\ < O_{L2} O_{R1} > & < O_{L2} O_{R2} > & < O_{L2} O_{R3} > \\ < O_{L3} O_{R1} > & < O_{L3} O_{R2} > & < O_{L3} O_{R3} > \end{pmatrix} , \tag{3.101}$$

where $O_{L/Ra}$, with $a = 1, 2, 3$, are the sum of hyper-baryon operators that couple to the SM fermion fields f_{Li}, f_{Rj}, while $< ... >$ denotes the Fourier-transformed correlator at zero external momenta.

Eq. (3.101), which connects the fermion mass matrix and the hyper-baryon correlator matrix, requires some technical explanations. In the one family case, the relation between the generated fermion mass and the corresponding two-point hyper-baryon correlator can be derived by matching the functional derivatives of the generating functional obtained in the low-energy effective theory (described in terms of pNGBs and external elementary fields) and the UV description of the model [92]. Here we simply generalize the formula to the three family case. Since the low-energy effective theory is valid up to $\Lambda_{\rm HC}$, the matching must be done at low-energy as well. To compute the fermion mass matrix M_f, therefore, the operators O_{Li}, O_{Rj} that appear in Eq. (3.101) should be viewed as

renormalized operators defined at $\sim \Lambda_{\rm HC}$. The running and mixing effects, together with all effects of original couplings and integrating out mediators, have been taken into account in the definition of these operators.

We note that one PC4F operator can be mediated by multiple vector and scalar mediators. In the scalar mediator part there can be complicated mixing which affects the mass eigenvalues and Yukawa couplings of the scalar components. Nevertheless, as long as we go below the scale of the lightest mediator mass, all PC four-fermion interactions can be incorporated into local effective PC4F operators, regardless of the origin and properties of the mediators. Moreover, let us note that, mediator masses and mixings are certainly family-independent, and one side of the mediator must be connected to two hyper-fermions which is also described by a family-independent coupling. The family-dependence only comes in at the other side where a scalar mediator is connected to one SM fermion and one hyper-fermion, and is only embodied in one proportionality factor at tree-level.

Complication may arise due to the hierarchical hyper-fermion masses. When the theory is evolved from UV to IR, in principle we should integrate out heavy hyper-fermions when we go below the corresponding mass thresholds. However, if this is done for all hyper-fermions heavier than $\Lambda_{\rm HC}$, Eq. (3.101) may be invalid since some contributions other than hyper-baryon correlators are ignored. On the other hand, the form of Eq. (3.101) is convenient for the analysis of its rank. Our strategy will be as follows. We subdivide all hyper-fermions heavier than $\Lambda_{\rm HC}$ into two types. The first type includes those hyper-fermions that are so heavy that their effect on SM fermion mass generation can be safely ignored. This is the case for hyper-fermions in the first and second families, which are assumed to have superheavy masses $\sim v^{\Theta}_{\rm CHC}$. The second type includes those hyper-fermions that have a mass close to $\Lambda_{\rm HC}$, like η and $\tilde{\eta}$, as their effect on SM fermion mass generation cannot be ignored. We will simply integrate out hyper-fermions of the first type, but retain hyper-fermions of the second type when we perform the matching to obtain Eq. (3.101). In this manner the convenience of Eq. (3.101) is retained. Of course if concrete calculations are to be carried out, we need be extremely careful about how the correlators involving heavy hyper-fermions are computed. However in the following analysis we are not bothered with such complication since we are only concerned with the rank of M_f.

Now, one of the elementary property of the correlator $< O_{La} O_{Rb} >$ is that it is linear with respect to the participating operators O_{La} and O_{Rb}. This sounds trivial but it turns out to be crucial for the model building. For example, suppose the participating hyper-baryon operators have the structure

$$O_{La} = y_{La} O_L, \quad O_{Rb} = y_{Rb} O_R \,, \tag{3.102}$$

where O_L, O_R are fermionic operators, and $y_{L/Ra}$ are arbitrary coefficients, then we immediately realize the resulting mass matrix will have entries like Eq. (3.100), which means its rank is 1 and will not be able to give masses to all three families.

What is the situation for the TPS model described so far? Firstly, we note that gauge-mediation can only be effective for third generation, as it only couples components inside the same multiplet. Scalar mediation, on the other hand, is sensitive to the details of the Yukawa interactions in Eq. (3.98). The couplings of the left-handed doublets, contained in

Ω^p, are only generated by the Yukawa $\lambda^a_{\Theta L}$, which is diagonal. This implies that only the third generation SM fermions can couple to the light hyper-fermions, and furthermore, $\lambda^3_{\Theta L} \ll 1$. Thus, the left-handed operators will have the form:

$$O_{La} = \delta_{a3} O_L \,, \tag{3.103}$$

leading to rank-1 mass matrix. To mend this problem, we can extend the minimal model by adding a second Θ scalar and a second Ψ scalar. We can further use a rotation symmetry between the two to cast the VEVs on the first, Θ_1 and Ψ_1, while the second ones, Θ_2 and Ψ_2, have a large mass. The Yukawa Lagrangian now contains two copies of the couplings, as listed below:

$$\mathcal{L}_Y \supset -\left(\lambda^{kab}_{\Theta L} \Omega^a \Theta^*_k \Omega^b + \lambda^{kab}_{\Theta R} \Upsilon^a \Theta_k \Upsilon^b + \text{h.c.}\right) - \frac{1}{2} \lambda^k_\Psi \Xi \Psi_k \Xi \,. \tag{3.104}$$

We can again use $U(3)$ flavor rotations to cast $\lambda^{1ab}_{\Theta L/R}$ into a diagonal form, so that the mass matrices for the hyper-fermions generated by the Θ_1 VEV are diagonal. Note that $\lambda^{1ab}_{\Theta L/R}$ entries need to fulfil the condition in Eq. (3.99), while all the entries in $\lambda^{2ab}_{\Theta L/R}$ can be sizeable. Similarly, we can have $\lambda^1_\Psi \ll 1$ and $\lambda^2_\Psi \sim \mathcal{O}(1)$. From Table 3.3, we see that PC4F operators for q_L and l_L can be generated by the scalar components φ_2 and φ_1 respectively, via mixing between Θ^2 and Ψ^2. In both cases, one additional operator is generated, in the form

$$O'_{La} = \lambda^{2a3}_{\Theta L} \lambda^2_\Psi \mathcal{O}_{L,\varphi} \,, \tag{3.105}$$

which, once added to the one from vector mediation, gives rank-2 to the mass matrix, thus allowing for the second generation masses.

We finally remark that for right-handed fermions, there are already at least 3 channels: the gauge mediation for third generation, the $\lambda^{2a3}_{\Theta R} \lambda^2_\Psi$ combination, and the combination from the λ_Δ Yukawa, which can generate at least 3 independent baryonic operators. In addition, we recall that from Table 3.3 the right-handed fermions appear in more mediator channels than the left-handed ones. The limitation in the rank of the mass matrix, therefore, uniquely arises from the left-handed sector.

4 .3 First family masses

So far, the first generation of SM fermions remains massless. Adding further Θ scalar multiplets does not help: while one can introduce additional flavor structures, they will only appear in a linear combination to the low energy lagrangian, once the mediators are integrated out. In other words, the form of the operator in Eq. (3.105) remains unchanged, with $\lambda^{2a3}_{\Theta L}$ replaced by a linear combination of Yukawa couplings.

A possible solution to this problem consists in introducing a new scalar field Δ_L, transforming as a **56** under $SU(8)_{PS}$, doublet under $SU(2)_L$ and singlet under $SU(2)_R$, and a new Yukawa coupling:

$$\mathcal{L}_Y \supset -\lambda^a_{\Delta L} \Omega^a \Delta_L \Xi + \text{h.c.} \tag{3.106}$$

3-family TPS model						
Field	Spin	$SU(8)_{\rm PS}$	$SU(2)_L$	$SU(2)_R$	Q_G	#
Φ	0	**8**	**1**	**2**	q	1
Θ	0	**28**	**1**	**1**	$2q$	2
Δ	0	**56**	**1**	**2**	q	1
Δ_L	0	**56**	**2**	**1**	$-q$	1
Ψ	0	**63**	**1**	**1**	0	2
N	1/2	**1**	**1**	**1**	0	3
Ω	1/2	**8**	**2**	**1**	q	3
Υ	1/2	$\bar{\mathbf{8}}$	**1**	**2**	$-q$	3
Ξ	1/2	**70**	**1**	**1**	0	1

Table 3.6: Minimal scalar and (left-handed Weyl) fermion field content in the TPS model that accounts for three families. The last column indicates the minimal number of fields needed.

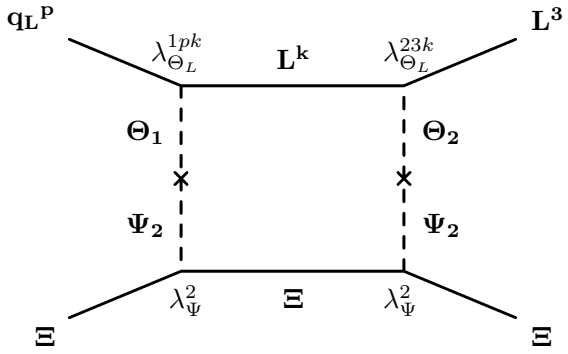

Figure 3.4: Loop-induced PC4F operators as an explanation for the 1st family fermion masses.

As Δ_L is not allowed to develop a VEV, $\lambda^a_{\Delta L}$ can be sizable and generate a new set of operators for the left-handed doublets, in the form:

$$O''_{La} = \lambda^a_{\Delta L}\lambda^3_{\Delta L}\mathcal{O}_{L,\Delta}\,, \tag{3.107}$$

thus elevating the mass matrix rank to the desired 3. As the flavor structures in the left and right-handed sectors are independent, this allows to generate the needed flavor mixing and non trivial CKM and PMNS mixing matrices. CP violating phases can be traced back either to physical phases in the Yukawas or in phases developed by the hyper-baryon correlators. In Table 3.6 we summarize the complete field content of the 3-generation model.

Another possible solution, which does not require introducing Δ_L, is to consider loop-induced PC4F operators. This mechanism relies on the fact that the couplings to the superheavy hyper-fermions can be transmitted to the light hyper-fermions via loops of the Yukawa couplings. As an example, in Fig. 3.4 we show schematically a loop generating a

Global charges			
Fields	B	L	H
SM quarks	$1/3$	0	0
SM leptons	0	1	0
L^p	0	0	$1/2$
U_d^p, D_u^p	0	0	$-1/2$
U_t	$-1/2$	$1/2$	$1/2$
χ, ω	$-1/6$	$1/2$	0
η	$1/6$	$1/2$	$-1/2$
ρ	$1/2$	$1/2$	-1
N^p	0	0	0
$v_{\rm PS}^{\Phi}$	0	1	0
$v_{\rm EHC}^{\Psi}$	0	0	0
$v_{\rm CHC}^{\Theta}$	0	0	1
$v_{\rm EHC}^{\Delta}$	$1/2$	$-1/2$	-1
$v_{\rm CHC}^{\Delta}$	$-1/2$	$1/2$	0

Table 3.7: Global charges B, L and H for the fermions in the TPS model. We also list the charges of the scalar VEVs, to highlight which symmetries are broken.

coupling for the left-handed quarks q_L. This would generate a new coupling of the form:

$$O''_{La} = (\lambda^2_{\Psi})^2 \lambda^{1aa}_{\Theta L} (\lambda^{2a3}_{\Theta L})^{\dagger} \mathcal{O}_{L,\rm loop}\,. \tag{3.108}$$

Because of the insertion of $\lambda^{1aa}_{\Theta L}$ (for which $a = 1, 2$ have large entries, see Eq. (3.99)), this operator has a different flavour structure than O'_{La} in Eq. (3.105), thus raising the rank of the mass matrix to 3, and generating masses for the first generation.

4 .4 Baryon Number conservation and Dark Matter

In all models where quarks and leptons are unified in a single multiplet, proton decay, or any other process violating lepton L and baryon B numbers, is a potential threat. Proton and neutron decay experiments, in fact, can constrain the scale of violation to very high values, $\sim 10^{15\div 16}$ GeV. The Pati-Salam model [76] is known to have neutron-antineutron oscillation instead of proton decay [117, 118]. The reason is that, although there exist gauge bosons that connect quarks and leptons, such transition preserves baryon number. The baryon number violation then depends on the detail of the scalar sector.

In the TPS model, it is possible to define both ordinary baryon and lepton numbers and a hyperbaryon number H. We normalize B and L like in the SM, while we assign H number $\pm 1/2$ to the hyper-fermions in the Ω^p and Υ^p multiplets (see top block in Table 3.7). If we only focus on the gauge and Yukawa terms, we realize that B, L and H can be consistently assigned to all the fermion components, as shown in the second block of Table 3.7. This can be easily understood by looking at the $U(1)$'s contained in the TPS gauge group: in fact, two combinations of B, L and H are contained in two (broken) generators of $SU(8)_{\rm PS}$ (while the unbroken hypercharge is defined as a linear combination

of $B-L$ inside $SU(8)_{\rm PS}$ and the diagonal generator of $SU(2)_R$). Finally, the remaining combination corresponds to the global $U(1)_G$ defined in Table 3.6, with

$$Q_G = 2H + 3B + L\,, \tag{3.109}$$

which yields $q=1$. The survival of these symmetries is therefore linked to the breaking of the gauge symmetries: in the bottom two blocks of Table 3.7, we report the charges of the VEVs contained in the scalar sector of the theory. We see that the VEV breaking the $SU(8)_{\rm PS}$ gauge symmetry also violates L (recall that this VEV generates the mixing between the right-handed neutrinos and the singlets N). The CHC breaking VEV in Θ breaks H (and generates masses for the hyper-fermions in the Ω^p and Υ^p multiplets). Thus, if the breaking is due only to VEVs in Φ, Ψ and Θ, B remains unbroken. Note also that all the Goldstone bosons associated to the two broken symmetries are eaten by the massive gauge bosons, thus no light scalar remains. In this section, we will focus on the B-preserving scenario, while the B-violating case (due to the VEVs in Δ) will be discussed in the next subsection. Note finally that no explicit $U(1)_G$ breaking should be present in the scalar sector.

The main consequence of this scenario, which we shall call B-preserving vacuum, is that proton and neutron decays are forbidden, thus avoiding the strong bounds deriving from experiments. [6] The price to pay is that mixing between the Ξ-components and other fermions are turned off, so that many interesting effects discussed in Sec. 3 , like the b^c_R–$\tilde{\omega}$ mixing, are forbidden. This vacuum, however, also enjoys the presence of fermions with exotic B-charges, which therefore cannot decay back into SM states. The lightest of the Ξ-components, therefore, can play the role of Dark Matter candidate. Of course, if the lightest state is charged under $Sp(4)_{\rm HC}$, the Dark Matter candidate can be a meson containing one such hyper-fermion.

The mass spectrum of the Ξ components in the B-preserving vacuum has been discussed in Sec. 3 .3: here we simply recall that

$$M_\omega = M_\chi \ = |\mu_0 - 5\mu_1|, \ \ M_\rho = \mu_0\ , \tag{3.110}$$

and the two iso-singlet hyper-fermions have the same mass as ρ, while $M_\eta = |\mu_0 + 2\mu_1|$ is correlated with the other two. As ω does not carry HC charges, it is crucial that it is not the lightest state. Furthermore, as η is the only hyper-fermion in the fundamental of $Sp(4)_{\rm HC}$ that carries QCD color charges, mesons containing a single η or $\tilde{\eta}$ are not good Dark Matter candidates. In the following, with the aim of presenting a qualilative discussion of the typical dark matter phenomenology, let us consider the case in which $\rho, \tilde{\rho}$ act as the dark matter candidate, with the typical parameter space for masses characterized by

$$M_\rho < M_\omega = M_\chi\,, \text{and } M_\rho < M_\eta \tag{3.111}$$

This configuration occurs in the light and dark green areas in Fig.3.5 in the μ_0–μ_1 parameter space. The light green wedge also features $M_\chi < M_\eta$, which could explain the

[6] Nevertheless, we will consider that the breaking of the symmetries occurs at high scale, in order to keep the scalar sector "natural", i.e. avoiding a large hierarchy between elementary scalar masses and the Planck scale.

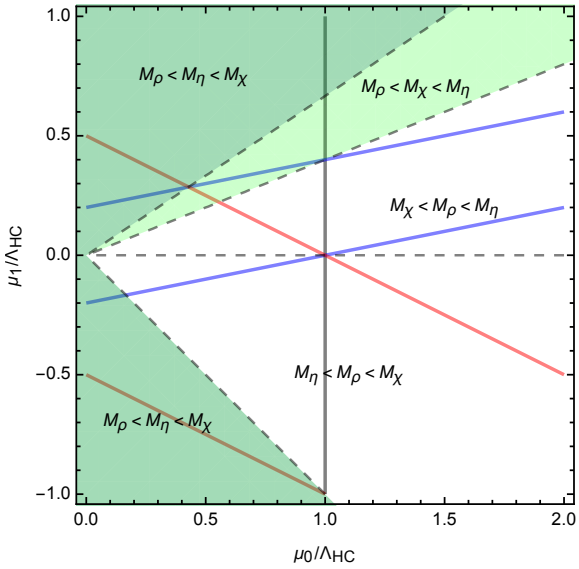

Figure 3.5: Mass hierarchy between ρ, χ/ω and η in the μ_0–μ_1 parameter space. The green regions are favourable for Dark Matter. The solid lines give, as a reference, the boundaries of the regions where $M_\rho < \Lambda_{\rm HC}$ (gray), $M_\chi = M_\omega < \Lambda_{\rm HC}$ (blue) and $M_\eta < \Lambda_{\rm HC}$ (red).

lightness of leptons with respect to quarks in the same generation, C.f. Sec. 3 .5. As a final comment, bound states of U_t–D_b, if they receive a negative contribution to their mass from the binding energy, may also be lighter than ρ and play the role of composite Dark Matter candidate. We also checked that all states with exotic B charges can decay into ρ: for instance, $\omega \to \tilde{\rho} + t + \tau^-$, $\langle L_u^3 \eta \rangle \to \rho + \bar{b}$, and so on. These may be very interesting final states to look for at the LHC or at future high energy hadron colliders.

A detailed study of the Dark Matter phenomenology of ρ goes beyond the scope of this manuscript, and we leave it for further exploration. Yet, the most interesting property of this Dark Matter candidate is that it is stable thanks to the ordinary baryon numbers. Its relic density can, therefore, be linked to that of the ordinary baryons under some simple assumptions: a) a baryon or lepton asymmetry is generated at scales well above the EWSB scale (for instance, via leptogenesis [119]); b) the EW phase transition is strong. Both conditions can be attained in the TPS model: the former via the presence of the heavy sterile neutrinos N, the latter thanks to the presence of additional light pNGBs accompanying the Higgs [120, 121]. At the EW phase transition, therefore, the lepton or baryon asymmetries will be re-shuffled between the various active degrees of freedom in thermal equilibrium. The number of Ξ-components in the baryon asymmetry can then be computed following the procedure delineated in Ref. [122] (see also Refs [123, 124]). In our case, the ρ and ω are in thermal equilibrium thanks to the couplings to PC4F operators, which are enhanced at low energy by the anomalous dimensions, as it can be inferred, for instance, from the gauge-mediation currents in Eqs (3.41) and (3.42). More details on this calculation, and the assumptions adopted, are reported in the Appendix A .2. The final result is that the ratio of Dark Matter and baryon densities can be written

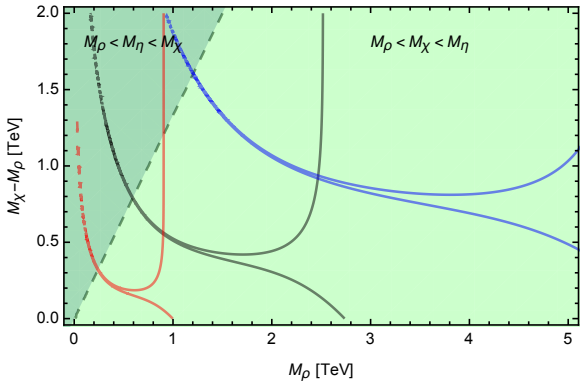

Figure 3.6: Points saturating the DM relic density in the M_ρ vs. $M_\chi - M_\rho$ parameter space. The solid lines correspond to $T_* = 246$ GeV (black), $T_* = 100$ GeV (red) and $T_* = 500$ GeV (blue).

as

$$\frac{\Omega_{\rm DM}}{\Omega_b} = \frac{M_\rho}{m_N} \left| 2\sigma_D - 2\sigma_\eta - 5\sigma_\chi - \sigma_\omega \right| , \tag{3.112}$$

where σ_X is a Boltzmann suppression factor which depends on the mass of the particle X and the critical temperature T_* of the EW phase transition, defined in Eq. (3.136).

In Fig. 3.6 we show the numerical result in the parameter region where ρ is the lightest Ξ-component, focusing on the $\mu_1 > 0$ region (C.f. Fig. 3.5). We expressed the mass parameters $\mu_{0,1}$ in terms of M_ρ and the mass difference $M_\chi - M_\rho$, where the dashed line corresponds to $M_\eta = M_\chi$ boundary. The black line corresponds to points saturating the Planck measurement [125] for $T_* = v_{\rm SM} = 246$ GeV, showing that the ρ mass is typically between 2.5÷3 TeV, except for a funnel region where cancellations between the Boltzmann factors occur. We also show results for $T_* = 100$ GeV (red) and $T_* = 500$ GeV (blue), showing how the ρ mass can be lowered or enhanced. While these results are qualitative, they provide a reliable indication of the typical mass range for the components of the Ξ multiplet, which also have consequences for the low energy properties of the composite theory. We see that the region with the mass hierarchy $M_\rho < M_\chi < M_\eta$, relevant in explaining the lightness of lepton masses, seems particularly favourable for this kind of Dark Matter candidate.

4 .5 Baryon Number Violation

Baryon number violation can occur in the TPS model in two ways: either via explicit interactions in the scalar potential, or via spontaneous breaking due to scalar VEVs.

As a example of the former, let's consider the following quartic coupling:

$$\mathcal{L}_V \supset -\lambda_{4\Theta}\, \epsilon_{ijklmnop} \Theta^{ij*} \Theta^{kl*} \Theta^{mn*} \Theta^{op*} + \text{c.c.} \tag{3.113}$$

where $i, \ldots, p$ are $SU(8)_{\rm PS}$ indices. This terms explicitly violates $U(1)_G$, thus it leads to baryon number violation. If we examine the decomposition of Θ at the HC level, we may identify two scalars with quantum numbers $\theta = (\mathbf{1}, \mathbf{3})_{-1/3}$ and $\bar{\theta} = (\mathbf{1}, \bar{\mathbf{3}})_{1/3}$, which

coincides with the quantum number of one type of scalar leptoquark that can mediate proton decay [126]. However, while θ has $B_\theta = 1/3$ and $L_\theta = 1$, $\bar{\theta}$ has $B_{\bar{\theta}} = 2/3$ and $L_{\bar{\theta}} = 0$. Thus, the former behaves like a lepto-quark, while the latter as a di-quark:

$$\theta \to u + e^- \,, \quad \bar{\theta} \to u + d \,. \tag{3.114}$$

The coupling in Eq. (3.113), after Θ acquires a VEV, will however generate a mass mixing in the form $\lambda_{4\Theta}(v^{\Theta}_{\rm CHC})^2\theta\bar{\theta}$, thus allowing the standard proton decay operator

$$\frac{1}{M_\theta^2}(ud)(ue^-) \,. \tag{3.115}$$

This kind of processes would require that the mass of these scalars is very large, $M_\theta \approx 10^{15\div 16}$ GeV.

The source of spontaneous B-violation is due to VEV(s) for the scalar multiplet Δ, as shown in the bottom block of Table 3.7. This scenario has several interesting features, linked to mixing between the Ξ components and other fermions and hyper-fermions, as discussed in Sec. 3 . However, it may also generate dangerous B violating effects. One example is the presence of B-violating PC4F operators, mediated by scalars mixing Δ with other multiplets, as shown in Table 3.3. Such effects, while suppressed by a large scalar mass, may be enhanced at low energy by the anomalous running in the conformal phase, thus leaving sizeable traces at low energy. It may, therefore, not be enough to push the scalar masses and symmetry breaking scales above the proton decay limits.

4 .6 Final remarks

We have found that the TPS model can accommodate for masses and flavor mixing between the three SM generations, once it is suitably extended as shown in Table 3.6. The model can preserve baryon number, B, if the symmetry breaking is due to VEVs for Φ, Ψ and Θ^1, while some couplings in the scalar potential are forbidden. This scenario also entails a candidate for Dark Matter, protected by a semi-integer baryon number.

One remarkable consequence of the TPS construction is that it fixes many essential properties of the model in the IR, i.e. in the confined phase. Besides the choice for the HC gauge group, this goes into the number of light hyper-fermions and their EW quantum numbers. For instance, we found that the low energy model resembles M8 of [47], except for the hypercharge of χ (which is $-1/3$ in the TPS model, instead of $2/3$ [73, 74]). This difference implies that the low energy model suffers from corrections to the bottom couplings to the Z boson [127], with strong bounds on the masses of the baryons as a consequence.

Furthermore, a detailed study of the low energy dynamics is crucial to establish the viability of the model in view of unwanted flavor and CP violation. This analysis is made more difficult by the ignorance of the dynamics in the walking phase, which can only be studied on the lattice: although the flavor scale is superheavy ($\Lambda_F \sim 10^{16}$ GeV), flavor-violation is incorporated into local PC4F operators whose effects are preserved down to $\Lambda_{HC} \sim 10$ TeV due to large anomalous dimensions of certain hyperbaryon operators. The flavor-violating couplings are introduced due to the need to generate masses for the first

and second family SM fermions, so we expect flavor violation is suppressed by light SM fermion Yukawas. However, it is known such suppression is not enough to be compatible with experimental bounds [38]. CP-violating couplings are also needed to generate the phase of CKM matrix in order to account for CP-violation phenomena in the quark sector. However, unwanted CP-violation may result in observables like electron electric dipole moment (EDM). Recent electron EDM results [128] lead to strong constraint on the compositeness scale: $f \gtrsim 100$ TeV where f is the Goldstone decay constant [129]. In the low-energy effective theory, introducing certain flavor symmetries may help relax the constraint [67, 70]. It could be tricky (if possible) to implement such symmetries in a UV-complete model like TPS, without affecting generating realistic masses and mixing of SM fermions. We therefore leave this issue for future study [98].

5 Summary and Outlook

That EWSB may originate from condensation in a new sector of strong dynamics is an attractive idea. Compared to the SM Higgs sector, which is parametrized via an elementary scalar field, it may naturally provide deeper insights into the possible origin of the EWSB and its connection to fermion mass generation. With the discovery of a 125 GeV Higgs-like particle and the need to accommodate the large top quark mass, it is then compelling to combine the idea of a pNGB Higgs and fermion partial compositeness in order to achieve natural and realistic models of EWSB based on strong dynamics.

In underlying gauge-fermion realisations, PC is realized via four-fermion operators built out of one SM fermion and three hyper-fermions charged under the new confining HC gauge group. In this work, we propose the first complete model, valid up to the Planck scale, that can generate the necessary four fermion operators (PC4F) in a model that has all the necessary features to provide a realistic low energy dynamics. This construction is based on the PUPC framework [66], where the HC and SM gauge symmetries are partially unified. When the larger gauge group undergoes spontaneous symmetry breaking, the resulting massive gauge bosons (and massive scalars) act as mediators for the PC4F operators.

Realizing the PUPC framework in practice, however, is highly non-trivial due to the many theoretical and phenomenological requirements. We found that the simplest model is based on an $SU(8)_{\rm PS}\times SU(2)_L\times SU(2)_R$ (TPS) gauge group, which breaks to an $Sp(4)_{\rm HC}$ and the SM gauge groups at a high scale $\Lambda_{\rm PU}\approx 10^{16}$ GeV. A minimal anomaly-free set of fermions can embed both the SM fermions and hyper-fermions needed to generate PC at low energy. Furthermore, we add suitable scalar fields at high scale (thus being natural) that play the roles of breaking the gauge group, generate PC4F operators via Yukawa couplings, and give masses to some hyper-fermions. The last feature is crucial in order to generate a walking dynamics between the UV unified phase and the IR confined one. We demonstrated that a renormalizable gauge-Yukawa theory based on the TPS gauge group automatically contains all the ingredients necessary to achieve the above goals. Thus, by a higher level unification we naturally achieve a tighter theoretical structure which gives deeper insight of the origin of fermion PC and mass generation.

In this work we have shown how the TPS model can generate masses for the three

generations of SM fermions, with non-trivial mixing among them, while preserving all the attractive features of composite pNGB Higgs models. We identify several mechanisms that can explain the mass split between the various SM fermions (i.e., leptons versus quarks, bottom versus top) and the lightness of neutrinos via an inverse see-saw mechanism that arises naturally in this construction. Finally, the walking phase can be achieved by giving appropriate masses to the hyper-fermions appearing in the model. We pointed out that accidental $U(1)$ symmetries corresponding to the hyperbaryon number, the baryon number and the lepton number have important and interesting phenomenological consequences. In our TPS construction it is possible to preserve baryon number, thus avoiding strong constraints from proton and neutron decays, with the bonus feature of obtaining a Dark Matter candidate thanks to the presence of semi-integer baryon number neutral states. Under certain circumstances, the relic density can be linked to the baryon asymmetry, leading to typical masses for the Dark Matter candidate in the few TeV range.

While in this work we have proven the feasibility of the PUPC framework, via the explicit TPS realization, this work should be considered as a stepping stone to further investigate the phenomenology of the TPS model. The main points that need further investigations are:

- We have identified the minimal scalar sector and the phenomenologically relevant symmetry breaking patterns, due to scalar VEVs that are proven to exist in the literature. It is, nevertheless, necessary to check if the desired VEV patterns can be realized in the scalar potential of the complete model.

- The presence of a walking phase, where the theory approaches an IR conformal fixed point, is crucial for the realization of flavor physics in this model. While estimates seem to support the presence of such a phase in the TPS model, only lattice calculations can verify this non-perturbatively. Remarkably, in the TPS model both the gauge symmetry and the fermion properties are specified. Furthermore, calculating the anomalous dimensions of the hyper-baryon operators in this phase is crucial to understand the flavour structure at low energy.

- We have shown that the model can generate the needed flavor structures of the SM. A more detailed analysis is needed, however, to check if unwanted CP and flavor violating effects survive at low energy, which should face the strong experimental bounds. This analysis can be done in a reliable way only after lattice input is provided, in the form of anomalous dimensions in the walking phase to study the enhancement of flavor violating effects at low energy, and the spectrum of the baryons below the condensation scale.

- Finally, the running of the gauge couplings should be studied in detail, in order to check the consistency of partial unification, where the QCD and HC ones are the most relevant. This task is daring due to the fact that the HC dynamics is strong over many decades of energy, thus non-perturbative techniques are needed.

Although we do not attempt to solve these issues in the present work, we hope that our model-building effort can provide new perspectives for understanding and evaluating

the pNGB Higgs and PC ideas, and motivate the community to investigate the related problems and the lattice community to explore uncharted territories that are crucial for our quest for mass generation.

A Appendix

A .1 Field Decompositions

To match the TPS theory in the UV with the composite Higgs model in the IR, it is important to understand the decomposition of the TPS multiplets at various steps of the gauge symmetry breaking path. To this end, in this appendix we will provide for the reader all the necessary information, following the steps:

$$SU(8)_{\rm PS} \times SU(2)_R \to SU(7)_{\rm EHC} \times U(1)_E \to SU(4)_{\rm CHC} \times U(1)_Y \,, \tag{3.116}$$

where we omitted the $SU(2)_L$ gauge as it remains unbroken all the way down to the compositeness scale. Also, we recall that the additional $U(1)_X$ charges, relevant for the Ψ–Θ path, can be recovered as $Q_X = Q_E - Y$. Also, the $SU(4)_{\rm CHC}$ representations can be easily matched to the $Sp(4)_{\rm HC}$ ones as follows:

$$\mathbf{15}_{\rm CHC} \to \mathbf{10}_{\rm HC} \oplus \mathbf{5}_{\rm HC} \,, \quad \mathbf{6}_{\rm CHC} \to \mathbf{5}_{\rm HC} \oplus \mathbf{1}_{\rm HC} \,, \quad \mathbf{4/\bar{4}}_{\rm CHC} \to \mathbf{4}_{\rm HC} \,. \tag{3.117}$$

To distinguish the components at various steps, we will use the following notation:

$$\{\mathbf{56},\mathbf{2}\} \Rightarrow \{SU(8)_{PS}, SU(2)_R)\}, \quad \mathbf{21}_{1/7} \Rightarrow SU(7)_{EHC,U(1)_E}, \quad [\mathbf{1},\bar{\mathbf{3}}]_{1/3} \Rightarrow [SU(4)_{CHC}, SU(3)_C]_{U(1)_Y}. \tag{3.118}$$

The decomposition of the $SU(2)_L$ and $SU(2)_R$ gauge bosons being rather straightforward, we will omit them and report the gauge multiplet of $SU(8)_{PS}$:

$$\{\mathbf{63},\mathbf{1}\} = \left\{ \begin{array}{rcl} \mathbf{1}_0 & = & [\mathbf{1},\mathbf{1}]_0 \\ \mathbf{7}_{4/7} & = & [\mathbf{1},\mathbf{3}]_{2/3} \oplus [\mathbf{4},\mathbf{1}]_{1/2} \\ \bar{\mathbf{7}}_{-4/7} & = & [\mathbf{1},\bar{\mathbf{3}}]_{-2/3} \oplus [\bar{\mathbf{4}},\mathbf{1}]_{-1/2} \\ \mathbf{48}_0 & = & [\mathbf{1},\mathbf{1}]_0 \oplus [\mathbf{4},\bar{\mathbf{3}}]_{-1/6} \oplus [\bar{\mathbf{4}},\mathbf{3}]_{1/6} \oplus [\mathbf{1},\mathbf{8}]_0 \oplus [\mathbf{15},\mathbf{1}]_0 \end{array} \right. \tag{3.119}$$

For the scalar fields used in the model building, we have:

$$\Phi = \{\mathbf{8},\mathbf{2}\} = \left\{ \begin{array}{rcl} \mathbf{1}_0 & = & [\mathbf{1},\mathbf{1}]_0 \\ \mathbf{1}_{-1} & = & [\mathbf{1},\mathbf{1}]_{-1} \\ \mathbf{7}_{4/7} & = & [\mathbf{1},\mathbf{3}]_{2/3} \oplus [\mathbf{4},\mathbf{1}]_{1/2} \\ \mathbf{7}_{-3/7} & = & [\mathbf{1},\mathbf{3}]_{-1/3} \oplus [\mathbf{4},\mathbf{1}]_{-1/2} \end{array} \right. \tag{3.120}$$

$$\Theta = \{\mathbf{28},\mathbf{1}\} = \left\{ \begin{array}{rcl} \mathbf{7}_{-3/7} & = & [\mathbf{1},\mathbf{3}]_{-1/3} \oplus [\mathbf{4},\mathbf{1}]_{-1/2} \\ \mathbf{21}_{1/7} & = & [\mathbf{1},\bar{\mathbf{3}}]_{1/3} \oplus [\mathbf{4},\mathbf{3}]_{1/6} \oplus [\mathbf{6},\mathbf{1}]_0 \end{array} \right. \tag{3.121}$$

$$\Delta = \{\mathbf{56},\mathbf{2}\} = \left\{ \begin{array}{rcl} \mathbf{21}_{1/7} & = & [\mathbf{1},\bar{\mathbf{3}}]_{1/3} \oplus [\mathbf{4},\mathbf{3}]_{1/6} \oplus [\mathbf{6},\mathbf{1}]_0 \\ \mathbf{21}_{-6/7} & = & [\mathbf{1},\bar{\mathbf{3}}]_{-2/3} \oplus [\mathbf{4},\mathbf{3}]_{-5/6} \oplus [\mathbf{6},\mathbf{1}]_{-1} \\ \mathbf{35}_{5/7} & = & [\mathbf{1},\mathbf{1}]_1 \oplus [\bar{\mathbf{4}},\mathbf{1}]_{1/2} \oplus [\mathbf{4},\bar{\mathbf{3}}]_{5/6} \oplus [\mathbf{6},\mathbf{3}]_{2/3} \\ \mathbf{35}_{-2/7} & = & [\mathbf{1},\mathbf{1}]_0 \oplus [\bar{\mathbf{4}},\mathbf{1}]_{-1/2} \oplus [\mathbf{4},\bar{\mathbf{3}}]_{-1/6} \oplus [\mathbf{6},\mathbf{3}]_{-1/3} \end{array} \right. \tag{3.122}$$

$$\Delta_L = \{\mathbf{56},\mathbf{1}\} = \left\{ \begin{array}{rcl} \mathbf{21}_{-5/14} & = & [\mathbf{1},\bar{\mathbf{3}}]_{-1/6} \oplus [\mathbf{4},\mathbf{3}]_{-1/3} \oplus [\mathbf{6},\mathbf{1}]_{-1/2} \\ \mathbf{35}_{3/14} & = & [\mathbf{1},\mathbf{1}]_{1/2} \oplus [\bar{\mathbf{4}},\mathbf{1}]_0 \oplus [\mathbf{4},\bar{\mathbf{3}}]_{1/3} \oplus [\mathbf{6},\mathbf{3}]_{1/6} \end{array} \right. \tag{3.123}$$

while for the adjoint $\Psi = \{\mathbf{63},\mathbf{1}\}$ the same decomposition as for the $SU(8)_{\rm PS}$ gauge bosons applies.

For the fermion multiplets used in the main text, we obtain

$$\Omega = \{\mathbf{8},\mathbf{1}\} \;=\; \begin{cases} \mathbf{1}_{-1/2} &= [\mathbf{1},\mathbf{1}]_{-1/2} \\ \mathbf{7}_{-3/7} &= [\mathbf{1},\mathbf{3}]_{1/6} \oplus [\mathbf{4},\mathbf{1}]_{0} \end{cases} \tag{3.124}$$

$$\Upsilon = \{\mathbf{8},\mathbf{2}\} \;=\; \begin{cases} \mathbf{1}_{0} &= [\mathbf{1},\mathbf{1}]_{0} \\ \mathbf{1}_{-1} &= [\mathbf{1},\mathbf{1}]_{-1} \\ \mathbf{7}_{4/7} &= [\mathbf{1},\mathbf{3}]_{2/3} \oplus [\mathbf{4},\mathbf{1}]_{1/2} \\ \mathbf{7}_{-3/7} &= [\mathbf{1},\mathbf{3}]_{-1/3} \oplus [\mathbf{4},\mathbf{1}]_{-1/2} \end{cases} \tag{3.125}$$

$$\Xi = \{\mathbf{70},\mathbf{1}\} \;=\; \begin{cases} \mathbf{35}_{-2/7} &= [\mathbf{1},\mathbf{1}]_{0} \oplus [\bar{\mathbf{4}},\mathbf{1}]_{-1/2} \oplus [\mathbf{4},\bar{\mathbf{3}}]_{-1/6} \oplus [\mathbf{6},\mathbf{3}]_{-1/3} \\ \bar{\mathbf{35}}_{2/7} &= [\mathbf{1},\mathbf{1}]_{0} \oplus [\mathbf{4},\mathbf{1}]_{1/2} \oplus [\bar{\mathbf{4}},\mathbf{3}]_{1/6} \oplus [\mathbf{6},\bar{\mathbf{3}}]_{1/3} \end{cases} \tag{3.126}$$

In principle, the multiplet Ξ could be replaced by other anti-symmetric representations of $SU(8)_{\rm PS}$. We will briefly discuss the alternatives below.

2-index case

The fermion multiplet Ξ coule be replaced by a two-index anti-symmetric Γ_2, and its conjugate $\bar{\Gamma}_2$, decomposing as

$$\Gamma_2 = \{\mathbf{28},\mathbf{1}\} \;=\; \begin{cases} \mathbf{7}_{-3/7} &= [\mathbf{1},\mathbf{3}]_{-1/3} \oplus [\mathbf{4},\mathbf{1}]_{-1/2} \\ \mathbf{21}_{1/7} &= [\mathbf{1},\bar{\mathbf{3}}]_{1/3} \oplus [\mathbf{4},\mathbf{3}]_{1/6} \oplus [\mathbf{6},\mathbf{1}]_{0} \end{cases} \tag{3.127}$$

$$\bar{\Gamma}_2 = \{\bar{\mathbf{28}},\mathbf{1}\} \;=\; \begin{cases} \bar{\mathbf{7}}_{3/7} &= [\mathbf{1},\bar{\mathbf{3}}]_{1/3} \oplus [\bar{\mathbf{4}},\mathbf{1}]_{1/2} \\ \bar{\mathbf{21}}_{-1/7} &= [\mathbf{1},\mathbf{3}]_{-1/3} \oplus [\bar{\mathbf{4}},\bar{\mathbf{3}}]_{-1/6} \oplus [\mathbf{6},\mathbf{1}]_{0} \end{cases} \tag{3.128}$$

Comparing with Eq. (3.126), we see that both contain iso-singlet hyper-fermions D_b and U_t, QCD-colored hyper-fermions η–$\tilde{\eta}$, while the new fermions contain two copies of the bottom partners ω–$\tilde{\omega}$. The main difference stands in the χ-sector: for this choice, the χ has no QCD-colour charges. Thus, all the hyper-baryons coupling to quarks must contain η or $\tilde{\eta}$, contrary to what we found in the TPS model with Ξ. Note also that the Yukawa couplings with Γ_2 would be different from the ones involving Ξ.

3-index case

Another alternative consists in using 3-index anti-symmetric representations, which will have the same decomposition as the scalars Δ and Δ_L. In particular, we see from Eq. (3.123) that a singlet of the $SU(2)_{L/R}$ would contain a neutral iso-singlet hyper-fermion and a color-triplet with charge 1/6, which is necessarily stable. To avoid this issue, the minimal option would be to promote the fermion Γ_3 to a doublet of $SU(2)_R$, thus having the same decomposition as Δ:

$$\Gamma_3 = \{\mathbf{56},\mathbf{2}\} \;=\; \begin{cases} \mathbf{21}_{1/7} &= [\mathbf{1},\bar{\mathbf{3}}]_{1/3} \oplus [\mathbf{4},\mathbf{3}]_{1/6} \oplus [\mathbf{6},\mathbf{1}]_{0} \\ \mathbf{21}_{-6/7} &= [\mathbf{1},\bar{\mathbf{3}}]_{-2/3} \oplus [\mathbf{4},\mathbf{3}]_{-5/6} \oplus [\mathbf{6},\mathbf{1}]_{-1} \\ \mathbf{35}_{5/7} &= [\mathbf{1},\mathbf{1}]_{1} \oplus [\bar{\mathbf{4}},\mathbf{1}]_{1/2} \oplus [\mathbf{4},\bar{\mathbf{3}}]_{5/6} \oplus [\mathbf{6},\mathbf{3}]_{2/3} \\ \mathbf{35}_{-2/7} &= [\mathbf{1},\mathbf{1}]_{0} \oplus [\bar{\mathbf{4}},\mathbf{1}]_{-1/2} \oplus [\mathbf{4},\bar{\mathbf{3}}]_{-1/6} \oplus [\mathbf{6},\mathbf{3}]_{-1/3} \end{cases} \tag{3.129}$$

$$\bar{\Gamma}_3 = \{\bar{\mathbf{56}},\mathbf{2}\} \;=\; \begin{cases} \bar{\mathbf{21}}_{-1/7} &= [\mathbf{1},\mathbf{3}]_{-1/3} \oplus [\bar{\mathbf{4}},\bar{\mathbf{3}}]_{-1/6} \oplus [\mathbf{6},\mathbf{1}]_{0} \\ \bar{\mathbf{21}}_{6/7} &= [\mathbf{1},\mathbf{3}]_{2/3} \oplus [\bar{\mathbf{4}},\bar{\mathbf{3}}]_{5/6} \oplus [\mathbf{6},\mathbf{1}]_{1} \\ \bar{\mathbf{35}}_{-5/7} &= [\mathbf{1},\mathbf{1}]_{-1} \oplus [\mathbf{4},\mathbf{1}]_{-1/2} \oplus [\bar{\mathbf{4}},\mathbf{3}]_{-5/6} \oplus [\mathbf{6},\bar{\mathbf{3}}]_{-2/3} \\ \bar{\mathbf{35}}_{2/7} &= [\mathbf{1},\mathbf{1}]_{0} \oplus [\mathbf{4},\mathbf{1}]_{1/2} \oplus [\bar{\mathbf{4}},\mathbf{3}]_{1/6} \oplus [\mathbf{6},\bar{\mathbf{3}}]_{1/3} \end{cases} \tag{3.130}$$

SM + standard hyper-fermions						exotic B fermions					
		Q	T_L^3	B	n_f			Q	T_L^3	B	n_f
t_L	μ_{t_L}	$2/3$	$1/2$	$1/3$	9	U_t	$-\mu_D$	$-1/2$	0	$-1/2$	4
b_L	μ_{b_L}	$-1/3$	$-1/2$	$1/3$	9	D_b	μ_D	$1/2$	0	$1/2$	4
t_R^c	$-\mu_{t_R}$	$-2/3$	0	$-1/3$	9	χ	μ_χ	$-1/3$	0	$-1/6$	15
b_R^c	$-\mu_{b_R}$	$1/3$	0	$-1/3$	9	$\tilde{\chi}$	$-\mu_\chi$	$1/3$	0	$1/6$	15
ν_L	μ_{ν_L}	0	$1/2$	0	3	η	μ_η	$-1/6$	0	$1/6$	12
τ_L	μ_{τ_L}	-1	$-1/2$	0	3	$\tilde{\eta}$	$-\mu_\eta$	$1/6$	0	$-1/6$	12
τ_R^c	$-\mu_{\tau_R}$	1	0	0	3	ω	μ_ω	$-1/3$	0	$-1/6$	3
ν_R^c	$-\nu_{\nu_R}$	0	0	0	3	$\tilde{\omega}$	$-\mu_\omega$	$1/3$	0	$1/6$	3
L_u^3	μ_L	$1/2$	$1/2$	0	4	ρ	μ_ρ	0	0	$1/2$	1
L_d^3	$-\mu_L$	$-1/2$	$-1/2$	0	4	$\tilde{\rho}$	μ_ρ	0	0	$-1/2$	1
U_d^3	μ_U	$1/2$	0	0	4						
D_u^3	$-\mu_U$	$-1/2$	0	0	4						

Table 3.8: Weyl fermions participating to the EW phase transition; n_f indicates the degrees of freedom of each spinor.

The main drawback of this choice is that is contains a much larger number of hyper-fermions, thus seriously endangering the presence of a walking dynamics in the IR, C.f. sec. 2 .4.

A .2 Dark Matter relic density calculation

To compute how the baryon number generated above $\Lambda_{\rm HC}$ is transferred to the SM and to the fermions with fractional baryon number (components of Ξ), we consider only the states that have a mass below or around $\Lambda_{\rm HC}$. The fermions are listed in Table 3.8, with their electric charge Q, their weak iso-spin T_L^3, their baryon number B, and the multiplicity (which counts the gauge degrees of freedom). We already imposed the relation between the chemical potentials deriving from the hyper-fermion masses.

We shall also consider the $W^\pm$ gauge boson, for which we choose chemical potential μ_W associated to W^- (and $-\mu_W$ for W^+). The EW interactions within the iso-doublets require:

$$\mu_{b_L} = \mu_{t_L} + \mu_W\,, \quad \mu_{\tau_L} = \mu_{\nu_L} + \mu_W\,, \quad \mu_L = -\frac{1}{2}\mu_W\,. \tag{3.131}$$

To take into account the HC dynamics, which replaces the Higgs sector of the SM, we include in the counting of degrees of freedom the hyper-fermions themselves. This is a rough approximation, as the EW phase transition may occur below the condensation scale, where it would be more appropriate to consider bound states. Nevertheless, as we want to obtain a rough estimate of the Dark Matter mass, to simplify the analysis we will stay within this approximation.

Additional relations between the chemical potentials derive from the PC4F operators that survive at low energy due to the large anomalous dimension enhancement. To simplify the analysis, again, we will only consider gauge-mediated PC4F operators. Looking at the

expression of the currents in Eqs (3.41) and (3.42), we see that the Ξ-components ρ and ω also participate to PC. Thus, considering the PC4F operators is equivalent to imposing the equality of the chemical potentials of the various components of the currents, namely for J^μ_E:

$$-\mu_{t_L}+\mu_L = \mu_U-\mu_{t_R} = -\mu_U-\mu_{b_R} = -\mu_\chi-\mu_D = -\mu_\eta+\mu_\chi = -\mu_\eta+\mu_\omega = -\mu_\rho+\mu_\eta = -\mu_\omega-\mu_D\,; \tag{3.132}$$

while for J^μ_C:

$$\mu_L + \mu_{\tau_L} = \mu_{\nu_R} - \mu_U = \mu_{\tau_R} + \mu_U = \mu_\eta + \mu_\chi = \mu_\eta + \mu_\omega = \mu_\rho - \mu_D\,. \tag{3.133}$$

The relations above allow to determine all the chemical potentials but 4.

A phase transition of the 1st order is characterized by the vanishing of the total electric charge and iso-spin, given by

$$Q_{\rm tot} = 9\left[\frac{2}{3}(\mu_{t_L}+\mu_{t_R}) - \frac{1}{3}(\mu_{b_L}+\mu_{b_R})\right] + 3\left[-(\mu_{\tau_L}+\mu_{\tau_R})\right] + 4\left[\frac{1}{2}\mu_L 2\sigma_L + \frac{1}{2}\mu_U 2\sigma_U + \frac{1}{2}\mu_D 2\sigma_D\right] + 15\left(-\frac{1}{3}\mu_\chi\right)2\sigma_\chi + 12\left(-\frac{1}{6}\mu_\eta\right)2\sigma_\eta + 3\left(-\frac{1}{3}\mu_\omega\right)2\sigma_\omega + 4(-\mu_W)\,, \tag{3.134}$$

$$T^3_{\rm tot} = \frac{1}{2}\left[9(\mu_{t_L}-\mu_{b_L}) + 3(\mu_{\nu_L}-\mu_{\tau_R}) + 4\mu_L 2\sigma_L\right] - 4\mu_W\,, \tag{3.135}$$

where we have introduced the statistical factor for fermions

$$\sigma_X = \frac{3}{2\pi^2}\int_0^\infty dx\; x^2 \cosh^{-2}\left(\frac{1}{2}\sqrt{x^2+z^2}\right)\,, \qquad z = \frac{m_X}{T}\,, \tag{3.136}$$

T being the temperature. The conditions $Q_{\rm tot} = 0$ and $T^3_{\rm tot} = 0$, together with the EW Sphaleron condition

$$\mu_{t_L} + 2\mu_{b_L} + \mu_{\nu_L} = 0\,, \tag{3.137}$$

allow to fix all chemical potentials as a function of one.

Finally, the baryon number density in the SM quarks (which corresponds after the EW phase transition to the net baryon number density in the Universe), can be expressed as

$$n_b^{\rm SM} = -\frac{12(3+\sigma_U)}{6+3\sigma_D+\sigma_\eta+5\sigma_\chi+\sigma_\omega}\mu_U\,, \tag{3.138}$$

while the total number density of fermions in the ξ–components is

$$n_\Xi = -\frac{12(3+\sigma_U)(2\sigma_D-2\sigma_\eta-5\sigma_\chi-\sigma_\omega)}{6+3\sigma_D+\sigma_\eta+5\sigma_\chi+\sigma_\omega}\mu_U = (2\sigma_D-2\sigma_\eta-5\sigma_\chi-\sigma_\omega)n_b^{\rm SM}\,. \tag{3.139}$$

Finally, we can express the relic density of Dark Matter, divided by the baryon density, as

$$\frac{\Omega_{\rm DM}}{\Omega_b} = \frac{M_\rho}{m_N}\left|\frac{n_\Xi}{n_b^{\rm SM}}\right| = |2\sigma_D-2\sigma_\eta-5\sigma_\chi-\sigma_\omega|\frac{M_\rho}{m_N} = 5.36\,, \tag{3.140}$$

where $m_N \approx 1$ GeV is the nucleon mass, and the numerical value comes from the Planck 2018 measurement [125]. The equation above can be used to determine the mass of the Dark Matter, M_ρ, as a function of the temperature of the EW phase transition (which enters in the expressions for the σ-functions).

Chapter 4

The Large N for Multiple Representation

The more the merrier.

In another attempt to UV complete CHM, we took to our advantage the huge number of fermions, which are necessary to generate masses to all the SM fields. Indeed, the resulting number of flavor N can be used to expand the β-functions of the different couplings of the theory in powers of N, instead of the traditional perturbation theory. This technique offers a complete different UV behaviour and is the main subject of this chapter. It can be seen as an introductory chapter, laying the differents formula needed for the study of a specific model proposed in Chapter 5.

1 Introduction

The expansion in large number of fermionic matter fields, N_f, has been used to study the dynamical properties of gauge theories. In particular, the gauge beta function, relevant for the renormalisation group equation (RGE) of the gauge coupling and the mass anomalous dimension have been computed for both abelian [130, 131] and non abelian [132] theories. Some information about higher-order terms is also available [133–135]. An important property of this expansion is that the first order is scheme independent, as discussed in [136–138]. More recently, this technique has been reused to show that gauge theories in the large-N_f limit may feature a non-trivial, interacting Ultra-Violet (UV) fixed point [139] (see also [140]). This observation is very important in understanding the dynamics of gauge theories, as the presence of an UV fixed point would allow to understand large-N_f gauge theories as fundamental, in the Wilsonian sense [141, 142]. This effort falls in the larger quest for asymptotic freedom, first identified by S.Weinberg for quantum gravity [143] and later discovered by F.Sannino and D.Litim for perturbative gauge-Yukawa theories [144].

The presence of a fixed point is linked to the fact that the first order in the large-N_f expansion has a negative pole at a given value of the gauge coupling, thus cancelling

the positive leading term when the gauge coupling grows near the singular value. This conclusion has been recently challenged in Ref. [145], where the resummation was reorganised thanks to non-perturbative information obtained from critical exponents. The result shows that a singularity in the leading large-N_f critical exponent does not necessarily imply a singularity in the beta function, however without excluding the presence of an UV fixed point. Preliminary results from large-N_f lattice studies also remain inconclusive [146]. Thus, at the moment the presence of a physical UV fixed point cannot be excluded. This phenomenon has been applied in various contexts, from attempts to define a safe Standard Model [147–152], to Grand Unification [153, 154], Dark Matter [155, 156] and a variety of New Physics scenarios [157–159]. In composite Higgs models with fermion partial compositeness [157], two irreps are needed to form spin-1/2 bound states that couple to the elementary quark and lepton fields.

The basic formulae for large-N_f resummation are known [160] for a simple gauge group $\mathcal{G}$, while an extension to semi-simple groups $\mathcal{G} = \times_\alpha \mathcal{G}_\alpha$ can be found in Ref. [161]. In all cases, the large multiplicity fermions belong to a single irreducible representation (irrep) R_f of the gauge groups. In this note, we generalise the resummation to cases with a large multiplicity of fermions in multiple irreps of the gauge groups. We find that the pole structure is preserved, revealing that its presence is intrinsically linked to the non-abelian structure of the gauge group. This result is in agreement with the presence of the UV safety for non-abelian gauge groups and not for abelian ones. The latter was already in question due to the fact that the mass anomalous dimension diverges near the pole [139]. Our results are also relevant to understand the dynamical properties of some class of models, like gauge theories with a large number of chiral families, and composite Higgs models with top partial compositeness [157].

The paper is organised as follows: in Sec. 2 we review the main results useful for large-N_f resummation, while presenting the results in a different form that can be applied to the case of multiple irreps. In Sec. 3 we present general formulae for the new case, before applying the results to physically interesting theories in Sec. 4 . We offer our conclusion in Sec. 5 .

2 Basic resummation results

In this section we will give a pedagogical introduction to the basic results for the large-N_f beta-function calculation, following Ref. [161]. We will however change some definitions, which will be useful to better understand the origin of the singularity and to extend the calculation to multiple irrep cases in the next section.

Let us consider a gauge-fermion theory with one species of Dirac fermions, Ψ, in the irrep R of a simple gauge group $\mathcal{G}$ (with gauge coupling constant g). To compute the β-function we need to calculate the radiative corrections to the 2-point function of the gauge boson propagator. For large number of fermions, the leading contribution to the beta function comes from the one loop fermion contribution:

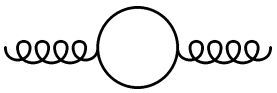

$$= K \times \int \frac{\mathrm{d}^4 k}{4\pi^2} \frac{\mathrm{Tr}\left[\gamma^\mu \left(\not{k} - \not{p}\right) \gamma^\nu \not{k}\right]}{(p-k)^2 k^2}\,, \tag{4.1}$$

where we have defined an effective gauge coupling K, which takes into account the large fermion multiplicity as

$$K = \frac{g^2}{4\pi^2} N_f \; T(R)\,, \tag{4.2}$$

where $T(R)$ is the index of the fermion irrep R. K can be considered as the effective coupling controlling the perturbative expansion, thus the one-loop contribution can be counted at $\mathcal{O}(N_f^0)$. This also allows to define a chain of fermion bubbles, which are all contributing at $\mathcal{O}(N_f^0)$, as shown in Fig. 4.1.

Figure 4.1: Example of *bubble-chain* of length 5.

Two-loop corrections to the diagram in Eq. (4.1) correspond to attaching a gauge propagator to the fermion loop: as no additional N_f multiplicity is added, this diagram will effectively contribute to order K^2/N_f, thus providing next-to-leading order terms. Now, replacing the simple gauge propagator with a *bubble-chain*, will not increase the $1/N_f$ order. In fact, the leading term is simply given by the resummation of the *bubble-chain* in the gauge propagator, as shown in the first two diagrams in Fig. 4.2. For a non-abelian theory, there are also contributions coming from gauge boson self-interactions: in this case, even the one-loop result is suppressed by $1/N_f$ and should be considered at next-to-leading order. As before, the resummed results stem from dressing the gauge propagators with the *bubble-chain*, as exemplified in the third diagram in Fig. 4.2.

For each type of diagram $\mathbf{X}$, we can write the amplitude in the form $\delta^{ab} p^2 \Delta_{\mu\nu}(p)\, \Pi_{\mathbf{X}}^{(n)}(p)$, where $\Delta_{\mu\nu}(p) = \eta_{\mu\nu} - p_\mu p_\nu / p^2$. Here n corresponds to the length of the *bubble-chain* in $\mathbf{A}$ and $\mathbf{B}$, while for $\mathbf{C}$ it's the total length of the two *bubble-chains*. A simple calculation gives:

$$\Pi_{\mathbf{A}}^{(n)}(p) = N_f g^4 \; T(R) \; C(R) \; \frac{K^n}{(4\pi^2)^2} A_{\mathbf{A}}^{(n)}(p)\,, \tag{4.3}$$

$$\Pi_{\mathbf{B}}^{(n)}(p) = N_f g^4 \; T(R) \; C(R) \; \left(1 - \frac{1}{2}\frac{C(G)}{C(R)}\right) \; \frac{K^n}{(4\pi^2)^2} A_{\mathbf{B}}^{(n)}(p)\,, \tag{4.4}$$

$$\Pi_{\mathbf{C}}^{(n)}(p) = g^2 \; C(G) \; \frac{K^n}{(4\pi^2)} A_{\mathbf{C}}^{(n)}(p)\,, \tag{4.5}$$

where $C(R)$ the Casimir of the irrep R and $C(G)$ of the adjoint. The functions $A_{\mathbf{X}}^{(n)}$ are integrals of the loop momentum and contain the information needed to compute

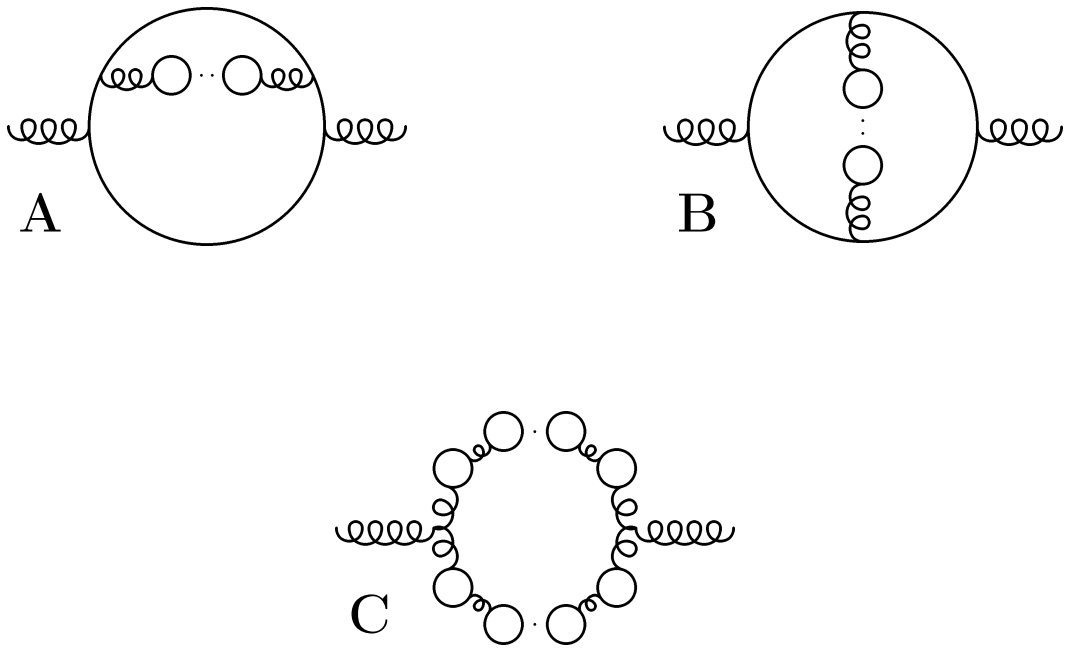

Figure 4.2: Next-to-leading order diagrams. **C** is one representative of the diagrams containing gauge boson self-interactions.

the leading order, however we need to take into account all the n-long *bubble-chains* to extract the contribution to the β-function. The beauty of the large-N_f expansion stands in the fact that this resummation can be done, and the ϵ-dependence of the loop in dimensional regularisation can be converted in a dependence on K of the resummed result (see Ref. [131] and the appendix of Ref. [161] for the proof).

To compute the evolution of the coupling we need to sum up all the diagrams: the total contribution thus reads

$$\Pi = \sum_n 2\Pi_{\mathbf{A}}^{(n)} + \Pi_{\mathbf{B}}^{(n)} + \Pi_{\mathbf{C}}^{(n)} = \frac{K}{N_f T(R)} C(G) \sum_n K^n A_{\mathbf{C}}^{(n)}(p) + \frac{K^2}{N_f T(R)} C(R) \sum_n K^n \left[2\, A_{\mathbf{A}}^{(n)}(p) + \left(1 - \frac{1}{2}\frac{C(G)}{C(R)}\right) A_{\mathbf{B}}^{(n)}(p) \right], \quad (4.6)$$

where the factor of 2 comes from the two possible insertions of the *bubble-chain* in the diagram **A**. Upon closer inspection to the above formula, we can reorganise the sum as

follows:

$$\Pi = \frac{K}{N_f T(R)} \sum_n \left\{ C(R)\ K^n \underbrace{\left[2A_{\mathbf{A}}^{(n-1)} + A_{\mathbf{B}}^{(n-1)}\right]}_{(*)} + C(G)\ K^{n-1} \underbrace{\left[A_{\mathbf{C}}^{(n-1)} - K A_{\mathbf{B}}^{(n-1)}/2\right]}_{(**)} \right\} . \tag{4.7}$$

The combination $(*)$ encodes the contribution to the beta function for an abelian gauge group (for which $C(G) = 0$ and $C(R) \to Q_f^2$) and was computed originally in Ref. [131], while the combination $(**)$ encodes the effect of the non-abelian dynamics. After resummation, we define two functions corresponding to the two combinations as follows

$$\beta(K) = \frac{2K^2}{3}\left[1 + \frac{C(G)}{N_f T(R)}\left\{\frac{-11}{4} + H(K)\right\} + \frac{C(R)}{N_f T(R)} F(K)\right] , \tag{4.8}$$

where $F(K)$ stems from $(*)$ and $H(K)$ from $(**)$. Note that the $-11/4$ term isolates the 1-loop contribution of gauge couplings, which is of order $1/N_f$, wile the 1 corresponds to the one-loop contribution of the fermions. Thus, in our definition, the functions $F(K)$ and $H(K)$ explicitly contain only the resummed higher-loop contribution. They are defined as [1]:

$$F(K) = \frac{3}{4}\int_0^K \mathrm{d}x\ \tilde{F}\left(0, \frac{2}{3}x\right) , \qquad H(K) = \frac{3}{4}\int_0^K \mathrm{d}x\ \tilde{F}\left(0, \frac{2}{3}x\right)\ \tilde{G}\left(0, \frac{1}{3}x\right) ; \tag{4.9}$$

with

$$\tilde{F}(0,\epsilon) = \frac{(1-\epsilon)\left(1-\frac{\epsilon}{3}\right)\left(1+\frac{\epsilon}{2}\right)\Gamma(4-\epsilon)}{3\Gamma^2\left(2-\frac{\epsilon}{2}\right)\Gamma\left(3-\frac{\epsilon}{2}\right)\Gamma\left(1+\frac{\epsilon}{2}\right)} , \tag{4.10}$$

$$\tilde{G}(0,\epsilon) = \frac{20 - 43\epsilon + 32\epsilon^2 - 14\epsilon^3 + 4\epsilon^4}{4(2\epsilon-1)(2\epsilon-3)(1-\epsilon^2)} . \tag{4.11}$$

The function $F(K)$ has a singularity at $K^* = 15/2$: this specifically arises from the singularity in the factor $\Gamma(4-\epsilon)$ in the loop integral $\tilde{F}(0,\epsilon)$. This term is relevant for abelian gauge groups. Instead, $H(K)$ has a singularity at $K^* = 3$, which stems from the $(1-\epsilon^2)$ factor in the denominator of $\tilde{G}(0,\epsilon)$. Thus, the presence of a pole at $K = 3$ for non-abelian gauge theories is to be traced back to the non-abelian nature of the gauge bosons. It has been observed in Ref. [161] that the mass anomalous dimension is finite in $K^* = 3$, while it diverges at $K^* = 15/2$, thus supporting the presence of an UV fixed point for the non-abelian gauge only. Furthermore, preliminary results for the $1/N_f^2$ contribution to the abelian β-function show that a discontinuity in $K^* = 3$ emerges. Both observations seem to support the idea that the non-abelian fixed point may be physical,

[1] The functions F and G we define are related to the F_1 and H_1 functions of Ref. [161] as

$$F_1 = F , \qquad H_1 = F_1 + \frac{C(G)}{C(R)}\left(-\frac{11}{4} + H\right) .$$

while the abelian one is more arguable. In the remainder of this work, we will therefore focus on non-abelian gauge symmetries.

The resummation has been extended to semi-simple gauge groups in Ref. [161], and we will review the main results here. We consider a gauge group $\mathcal{G} = \times_\alpha \mathcal{G}_\alpha$, with gauge couplings g_α, and n_f fermions in the irrep $R_f = \times_\alpha R_\alpha$. Instead of defining a single effective N_f as in Ref. [161], we find more convenient to define a fermion number N_α for each gauge group, as this will allow us to easily generalise the result to multiple irreps. We will consider that each fermion number, defined as

$$N_\alpha = n_f \Pi_{\beta\neq\alpha} d(R_\beta)\,, \tag{4.12}$$

is of the same order for all gauge groups, i.e. $N_\alpha = \mathcal{O}(N_f)$. Similarly, we define effective gauge couplings as follows:

$$K_\alpha = \frac{g_\alpha^2}{4\pi^2} N_\alpha\,. \tag{4.13}$$

The only new ingredient in the case of semi-simple gauge groups is that the gauge couplings contribute to each other's β-function. As gauge bosons of different groups do not interact with each other, the leading order in N_f stems from diagrams of type **A** and **B**, where the gauge boson in the *bubble-chain* is different from the external ones, as shown in Fig. 4.3. The amplitudes can be written as:

$$\Pi^{(n)}_{\mathbf{A'/B'}}(p) = g_\alpha^2 T(R_\alpha) \sum_{\beta\neq\alpha} g_\beta^2 C(R_\beta) d(R_\beta) \Pi_{\gamma\neq\alpha,\beta} d(R_\gamma)\; n_f\; \frac{K_\beta^n}{(4\pi^2)^2} A^{(n)}_{\mathbf{A/B}}(p)\,, \tag{4.14}$$

where the integral functions are the same as before. Using $d(R_\beta)\Pi_{\gamma\neq\alpha,\beta} d(R_\gamma)\; n_f = N_\beta$, the total contribution can be written as:

$$\Pi = \frac{K_\alpha}{N_\alpha} \sum_{\beta\neq\alpha} \frac{C(R_\beta)}{T(R_\beta)}\; K_\beta^{n+1} \left(2A^{(n)}_{\mathbf{A}}(p) + A^{(n)}_{\mathbf{B}}(p)\right)\,, \tag{4.15}$$

where we recognise the function also appearing in the abelian case.

Finally, the β-function for K_α can be written as

$$\beta(K_\alpha) = \frac{2K_\alpha^2}{3}\left[1 + \frac{C(G_\alpha)}{N_\alpha T(R_\alpha)}\left\{-\frac{11}{4} + H(K_\alpha)\right\} + \sum_\beta \frac{C(R_\beta)}{N_\alpha T(R_\beta)} F(K_\beta)\right]\,. \tag{4.16}$$

If we only consider non-abelian gauge groups, the second term, which includes the mixed contributions, will always remain finite and small as $K_\beta < 3$. Thus, the presence of an UV fixed point only comes from the first term, i.e. from the non-abelian nature of each gauge factor in the semi-simple group.

In order to offer a direct comparison with the results in the next section, we can also redefine the fermion multiplicities by absorbing the index of the irrep:

$$\tilde{N}_\alpha = N_\alpha T(R_\alpha)\,, \quad K_\alpha = \frac{g_\alpha^2}{4\pi^2}\tilde{N}_\alpha\,, \tag{4.17}$$

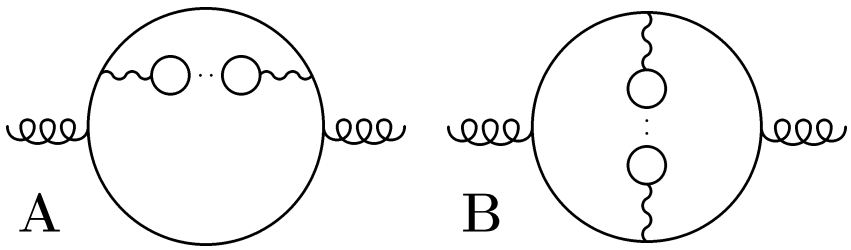

A' **B'**

Figure 4.3: Next-to-leading order diagrams for the mixed contributions, where the gauge bosons in the *bubble-chain* and on the external legs belong to different gauge groups.

with the β-function given by

$$\beta(K_\alpha) = \frac{2K_\alpha^2}{3}\left[1 + \frac{C(G_\alpha)}{\tilde{N}_\alpha}\left\{-\frac{11}{4} + H(K_\alpha)\right\} + \frac{1}{\tilde{N}_\alpha}\sum_\beta \frac{C(R_\beta)T(R_\alpha)}{T(R_\beta)}F(K_\beta)\right] . \quad (4.18)$$

In the above form, the β-function can be easily extended to cases with a large multiplicity of multiple irreps, as we will show in the coming section.

3 Extension to multiple irreps

We are now ready to extend the resummation formulae to cases with large numbers of multiple irreps. We will first start with a simple gauge group, and then generalise to semi-simple groups.

3 .1 Simple Gauge Group

We start with the case of a simple gauge group $\mathcal{G}$ with n_i fermions Ψ_i in different irreps R_i. In such a case, the leading order contribution is given by the one-loop diagram below, where we sum over all the fermion species:

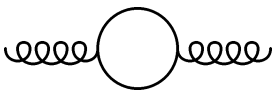

$$= \frac{g^2}{4\pi^2}\sum_i T\left(R_i\right) n_i \times \int \frac{\mathrm{d}^4 k}{4\pi^2} \frac{\mathrm{Tr}\left[\gamma^\mu \left(\not{k} - \not{p}\right)\gamma^\nu \not{k}\right]}{\left(p-k\right)^2 k^2} . \quad (4.19)$$

Following Eq. (4.1), we can define an effective gauge coupling as follows:

$$K = \frac{g^2}{4\pi^2}N , \qquad N = \sum_i n_i T(R_i) , \quad (4.20)$$

where it is evident why we absorbed the index of the irrep in the definition of the fermion multiplicity. Interestingly, a large N can now be due also by the contribution of irreps with large index.

The next-to-leading order in $1/N$ is given by the same diagrams **A**, **B** and **C** in Fig. 4.2, yielding:

$$\Pi^{(n)}_{\mathbf{A}}(p) = g^4 \sum_i T(R_i)\, C(R_i) n_i \frac{K^n}{(4\pi^2)^2} A^{(n)}_{\mathbf{A}}(p)\,, \tag{4.21}$$

$$\Pi^{(n)}_{\mathbf{B}}(p) = g^4 \sum_i T(R_i)\, C(R_i) \left(1 - \frac{1}{2}\frac{C(G)}{C(R_i)}\right) n_i \frac{K^n}{(4\pi^2)^2} A^{(n)}_{\mathbf{B}}(p)\,, \tag{4.22}$$

$$\Pi^{(n)}_{\mathbf{C}}(p) = g^2\, C(G) \frac{K^n}{(4\pi^2)} A^{(n)}_{\mathbf{C}}(p)\,. \tag{4.23}$$

It's crucial to note that the loop factors do not depend on the irrep of the fermions. Furthermore, a sum on the fermion species can be introduced in the third contribution by inserting

$$\Pi^{(n)}_{\mathbf{C}}(p) = g^2 \sum_i \frac{n_i T(R_i)}{N} C(G) \frac{K^n}{(4\pi^2)} A^{(n)}_{\mathbf{C}}(p)\,. \tag{4.24}$$

The total result can thus be written as:

$$\sum_n 2\Pi^{(n)}_{\mathbf{A}} + \Pi^{(n)}_{\mathbf{B}} + \Pi^{(n)}_{\mathbf{C}} = \frac{K}{N}\sum_i \left\{ \sum_n \frac{n_i T(R_i) C(R_i)}{N} K^n \left[2A^{(n-1)}_{\mathbf{A}}(p) + A^{(n-1)}_{\mathbf{B}}(p)\right] + \sum_n \frac{n_i T(R_i) C(G)}{N}\, K^{n-1} \left[A^{(n-1)}_{\mathbf{C}}(p) - K A^{(n-1)}_{\mathbf{B}}(p)/2\right] \right\}. \tag{4.25}$$

We can now identify again the sums leading to the abelian $F(K)$ and non-abelian $H(K)$ functions, defined in Eq. (4.9). The β-function can thus be expressed as

$$\beta(K) = \frac{2K^2}{3}\left[1 + \frac{C(G)}{N}\left\{\frac{-11}{4} + H(K)\right\} + \frac{1}{N}\left(\sum_i \frac{T(R_i)\, C(R_i)\, n_i}{N}\right) F(K)\right]. \tag{4.26}$$

The coefficient in front of $F(K)$ evaluates to an $\mathcal{O}(1)$ number as it sums the degrees of freedom of the fermions weighted by the Casimirs, thus the second term is genuinely an $\mathcal{O}(1/N)$ contribution. Nevertheless, we see that for non-abelian gauge groups, the singularity driving the UV fixed point is the same as in the case of a single large-multiplicity irrep. Note how this result compares to Eq. (4.18).

This result proves that models with multiple irreps have the same dynamics as models with a single irrep in the large-N_f limit.

3 .2 Semi-simple Gauge Group

We now consider the most general case of a semi-simple gauge group $\mathcal{G} = \times_\alpha \mathcal{G}_\alpha$ with n_i fermions Ψ_i in the irrep $R_i = \times_\alpha R_{i\alpha}$. Combining the definitions in the previous sections,

we can define a fermion multiplicity for each gauge group as follows:

$$N_\alpha = \sum_i n_i \ (\Pi_{\beta\neq\alpha} d(R_{i\beta})) \ T(R_{i\alpha}) \,, \qquad K_\alpha = \frac{g_\alpha^2}{4\pi^2} N_\alpha \,. \tag{4.27}$$

It is convenient to define effective fermion multiplicities that count the multiplicity of fermion specie Ψ_i relative to one or two gauge groups respectively:

$$\tilde{n}_{i\alpha} = n_i \ (\Pi_{\beta\neq\alpha} d(R_{i\beta})) \ , \quad \tilde{n}_{i\alpha\beta} = n_i \ (\Pi_{\gamma\neq\alpha,\beta} d(R_{i\gamma})) \ , \tag{4.28}$$

so that $N_\alpha = \sum_i \tilde{n}_{i\alpha} T(R_\alpha)$.

The generalisation of the β-function is now straightforward, starting from Eqs (4.18) and (4.26):

$$\beta(K_\alpha) = \frac{2K_\alpha^2}{3} \left[1 + \frac{C(G_\alpha)}{N_\alpha} \left\{ -\frac{11}{4} + H(K) \right\} + \right.$$
$$\left. \frac{1}{N_\alpha} \left\{ \sum_i \frac{\tilde{n}_{i\alpha} T(R_{i\alpha}) C(R_{i\alpha})}{N_\alpha} F(K_\alpha) + \sum_{\beta\neq\alpha} \sum_i \frac{\tilde{n}_{i\alpha\beta} T(R_{i\alpha}) C(R_{i\beta})}{N_\beta} F(K_\beta) \right\} \right] \,. \tag{4.29}$$

The above result confirms that the UV dynamics of the theory is fully determined by the non-abelian structure, as the additional terms proportional to $F(K)$ remain finite for $K < 3$ in the case of non-abelian gauge groups. We also note that, as in the simple case, the β-function and thus its pole are scheme independent (see proof in Appendix A .2).

For completeness and reference, in Appendix A .1 we provide the β-functions for Yukawa couplings from Ref [161], adapted to our formalism and extended to the case of multiple irreps. As we will show in Appendix A .2, they maintain the scheme independence property of the first order in the expansion.

4 Application to chiral gauge theories: generalised Georgi-Glashow and Bars-Yankielowicz models

Chiral gauge theories have received substantial attention in the literature, especially when asymptotically free because of the interesting low energy dynamics [162–165]. The simplest incarnations consist of two different species of fermions, whose multiplicities are chosen to cancel the gauge anomaly. Theories of this class can be constructed on a simple SU(N_c) gauge group, with one fermion in the symmetric or anti-symmetric irrep and a suitable number of conjugate fundamental to cancel the gauge anomaly. They go under the names of Bars-Yankielowicz (BY) [166] and generalised Georgi-Glashow (GG) [167] theories. Their low energy dynamics is still not fully understood in the asymptotic free case with small number of chiral families [168, 169]: indications of the possible allowed phases have been inferred by use of the mininization of degrees of freedom [164, 165], or the recent idea of generalized anomalies [170, 171].

In this work we are interested in the limit of large number of fermions, so that we will consider a case with n_g chiral generations. The fermion content of the two template theories thus consists of:

$$\text{BY} \;\Rightarrow\; R_1 = \square\square \;\; [n_g]\,, \qquad R_2 = \overline{\square} \;\; [(N+4)n_g]\,; \tag{4.30}$$

$$\text{GG} \;\Rightarrow\; R_1 = \begin{array}{|c|}\hline\;\;\\\hline\;\;\\\hline\end{array} \;\; [n_g]\,, \qquad R_2 = \overline{\square} \;\; [(N-4)n_g]\,. \tag{4.31}$$

Following Eq. (4.20), we can define the following fermion multiplicity:

$$N_{\text{BY/GG}} = n_g \frac{N \pm 3}{2}\,, \tag{4.32}$$

which is large when n_g is large. Thus, the β-functions from Eq. (4.26) read

$$\beta(K)_{\text{BY/GG}} = \frac{2K^2}{3}\left[1 + \frac{2N}{n_g(N\pm 3)}\left\{-\frac{11}{4} + H(K)\right\} + \frac{1}{n_g}\frac{3N^2 \pm N - 4}{2N(N\pm 3)}F(K)\right]\,, \tag{4.33}$$

where the large-n_g expansion is evident, and we recall that $N \geq 3$ for BY and $N \geq 5$ for GG. The UV dynamics of the theories, therefore, is determined by the $H(K)$ dependence, which produces an attractive fixed point for $K^* = 3$, corresponding to

$$\frac{g_*^2}{4\pi} = \frac{6\pi}{n_g(N\pm 3)}\,. \tag{4.34}$$

We now investigate the UV properties of the BY and GG models with an additional Yukawa coupling. For this purpose, we focus of the simplest possibility: besides the two fermions Ψ_{R1} and Ψ_{R2}, we extend the models by a scalar ϕ in the anti-fundamental representation. This allows to include a Yukawa interaction and a quartic coupling, as follows:

$$\mathcal{L} \supset -y\;\phi_a\;\Psi_{bR2}\;\Psi^{ab}{}_{R1} - \lambda\;\phi^{*a}\phi^{*b}\phi_a\phi_b + \text{h.c.}\,, \tag{4.35}$$

where a, b are gauge indices, and we omit the flavor index. The general formulae for the beta function for the new couplings can be found in Appendix A .1. They can be simplified under the assumption that the gauge coupling approached quickly its fixed point, so that we can replace $K = 3$. For the two models, we find:

$$\beta\,(y)_{\text{BY/GG}} = y^3\;\frac{3N+1}{32\pi^2} - y\;\frac{7N^2 \pm 4N - 1}{8n_g(N\pm 3)N} \tag{4.36}$$

$$\beta\,(\lambda)_{\text{BY/GG}} = \lambda^2\frac{2N+5}{16\pi^2} + \lambda\;\left(\frac{y^2N}{4\pi^2} - \frac{N^2-1}{n_gN(N\pm 3)}\right) - \left(\frac{y^4N}{4\pi^2} + \frac{(N^2-1)(N^2-2)c_\lambda}{{n_g}^2(N\pm 3)^2N}\right)\,, \tag{4.37}$$

where $c_\lambda = 192$ is a numerical coefficient stemming from the gauge fixed point. The Yukawa beta function features a flow from an IR fixed point at

$$\frac{y_{\text{IR}}^2}{4\pi^2} = \frac{7N^2 \pm 4N - 1}{N(N\pm 3)(3N+1)n_g}\,, \tag{4.38}$$

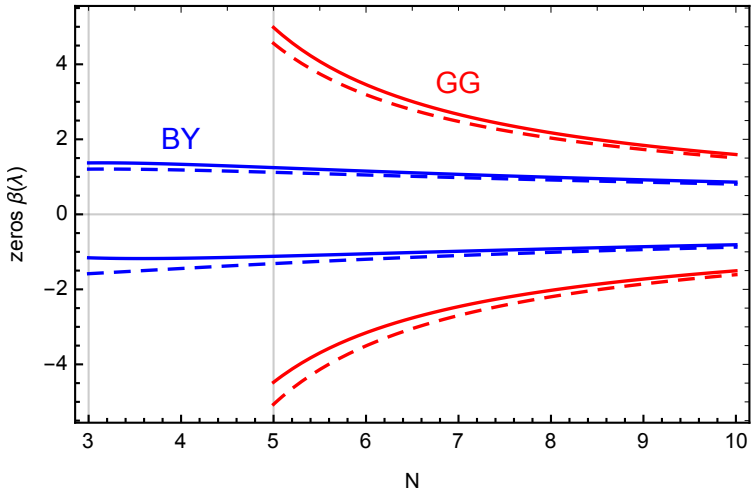

Figure 4.4: Zeros of $\beta(\lambda)$ as a function of N for BY (blue) and GG (red) models. The solid lines correspond to $y = y_{\rm UV} = 0$, while the dashed ones to $y = y_{\rm IR}$. The numerical values correspond to $n_g = 10N$, however other choices can be easily inferred knowing that the zeros scale as $\lambda^* \sim n_g^{-1}$.

to a free UV fixed point $y_{\rm UV} = 0$.

From the quartic coupling beta function, we can see that there always exist two real zeros for any value of y. Numerical values are shown in Fig. 4.4 for $n_g = 10\ N$. These results can be generalised to any value of n_g knowing that the zeros scale as $\lambda^* \sim n_g^{-1}$ (as $y^2_{\rm IR} \sim n_g^{-1}$). Thus, for values below the positive zero, $\lambda < \lambda^*_+$, the couplings will flow in the UV towards the negative zero, $\lambda_{\rm UV} = \lambda^*_-$. The plot also shows that the running is not very sensitive to the value of the Yukawa coupling.

This analysis shows that chiral gauge theories as the BY and GG models, even when enriched with a scalar field, can feature a completely UV safe behaviour. The fact that the quartic coupling flows towards a negative value at high energy, though, may signal an instability in the scalar potential.

5 Conclusions

Large-N_f resummation has proven a useful tool to study the UV dynamics of gauge theories with large multiplicity of fermions. This has lead to the conjecture of the emergence of an attractive interacting fixed point in the UV, which is due to the presence of a pole in the resummed leading order in the beta function. In this note, we extended the standard formalism to include cases with multiple fermion representations. We showed that the pole can be traced back to the intrinsic non-abelian nature of the gauge group, independently on the specific representations of the fermions. Thus, we support the conjecture for non-abelian gauge groups.

As a consequence, the pole, and the UV fixed point, are also found in theories with multiple representations. We apply these results to the simplest cases of chiral gauge theories, based on SU(N_c) gauge groups. As long as a large-enough number of chiral

families are added, the theories develop an UV safe dynamics. As an example with physical interest, we study extended Grand Unified Theories, where a large number of fermions may be allowed below the symmetry breaking scale. We show, in one specific example based on SU(9) without supersymmetry, that the mass of such fermions can be split from the symmetry breaking scale arbitrarily, because the low energy SU(5) GUT flows towards a UV fixed point. Thus, the onset of SU(9) can be delayed to arbitrarily large energies.

A Appendix

A .1 Large-N_f β-functions for Yukawa and quartic couplings

For completeness, we will list here the resummed β-functions for Yukawa couplings [172] from Ref. [161], adapted to the notation we use in this paper, and to the case with multiple fermion irreps. We complete the model by adding a scalar field ϕ^A in the irrep $R_\phi = \times_\alpha R_{\phi\alpha}$, where A is a generic gauge index for the scalar irrep. The new Lagrangian interactions read:

$$\mathcal{L} \supset -y_{A\mathsf{bc}}\, \phi^A\, \Psi_i^{\mathsf{b}}\, \Psi_j^{\mathsf{c}} - \lambda_{CD}^{AB}\, \phi^{*,A}\phi^{*,B}\phi_C\phi_D + \text{h.c.}\,, \tag{4.39}$$

where b and c are gauge indices of the fermion irreps, and it is understood that the scalar gauge quantum numbers allow for the Yukawa coupling to be gauge-invariant. First we note that the scalar will contribute to the gauge β-function with a $1/N_f$ term

$$\Delta\beta(K_\alpha)|_{\text{scalar}} \supset \frac{2K_\alpha^2}{3}\frac{T\left(R_{\phi\,\alpha}\right)}{4N_\alpha}\,, \tag{4.40}$$

which corresponds to the one-loop result.

We recall that consistency of the expansion requires that the Yukawa and quartic couplings shall scale in a give way with N_f, as follows:

$$y^2 \sim \lambda \sim \frac{1}{N_f}\,. \tag{4.41}$$

This counting ensures that the non-gauge contribution to the beta function at one loop counts $1/N_f$ in the expansion. The β-function for the Yukawa coupling reads:

$$\begin{aligned}\beta\left(y_{A\mathsf{bc}}\right) =& \frac{1}{32\pi^2}\left[\left(y_D y^{*,D} y_A\right)_{\mathsf{bc}} + \left(y_A y^{*,D} y_D\right)_{\mathsf{bc}} + 2\text{Tr}\left[y_A y^{*,D}\right] y_{D\mathsf{bc}}\right] \\ & - y_{A\mathsf{bc}} \sum_\alpha \frac{3K_\alpha}{4N_\alpha} H_0\left(\frac{2K_\alpha}{3}\right)\left[C\left(R_{i\,\alpha}\right) + C\left(R_{j\,\alpha}\right) + \frac{K_\alpha}{6}C\left(R_{\phi\,\alpha}\right)\right]\,,\end{aligned}$$

where the traces and contractions are intended for the fermion gauge indices, and

$$H_0(x) = \frac{\left(1-\frac{x}{3}\right)\Gamma\left(4-x\right)}{3\Gamma^2\left(2-\frac{x}{2}\right)\Gamma\left(3-\frac{x}{2}\right)\Gamma\left(1+\frac{x}{2}\right)}\,. \tag{4.42}$$

We recall that H_0 is a smooth function up to $K = 15/2$, where a pole is developed. Thus, for non-abelian semi-simple groups, the gauge contribution to the Yukawa running remains finite. If it dominates over the contribution of the pure Yukawa term, the coupling will flow towards a non-interactive fixed point (asymptotic free). If there is another yukawa y', mix contributions will play a role in the running as $\beta(y) \supset\sim yy'^2$. Thus we get the same behaviour.

For the quartic coupling we obtain the following β-function:

$$\begin{aligned}\beta\left(\lambda^{AB}{}_{CD}\right) =& \frac{1}{16\pi^2}\left[2\lambda^{AE}{}_{CF}\lambda^{BF}{}_{DE} + 2\lambda^{AE}{}_{DF}\lambda^{BF}{}_{CE} + \lambda^{AB}{}_{EF}\lambda^{EF}{}_{CD}\right] \\ &+ \frac{1}{4\pi^2}\mathrm{Tr}\left[y_D y^{*,E}\right]\lambda^{AB}{}_{CE} - \frac{1}{4\pi^2}\mathrm{Tr}\left[y^A y^*_C y^B y^*_D + y^A y^*_D y^B y^*_C\right] \\ &- \lambda^{AB}{}_{CD}\sum_\alpha \frac{3}{N_\alpha} C\left(R_{\phi\,\alpha}\right) K_\alpha H_0\left(\frac{2K_\alpha}{3}\right) \\ &+ 48\pi^2 \sum_{\alpha<\beta} \frac{B^{AB}_{\alpha,\beta\,CD}}{N_\alpha N_\beta}\frac{K_\alpha K_\beta}{K_\alpha - K_\beta}\left[K_\alpha(1-\frac{K_\alpha}{6})H_0\left(\frac{2K_\alpha}{3}\right) - K_\beta(1-\frac{K_\beta}{6})H_0\left(\frac{2K_\beta}{3}\right)\right] \\ &+ 24\pi^2 \sum_\alpha \frac{A^{AB}_{\alpha\;CD}}{N_\alpha^2}K_\alpha^2\left[(1-\frac{K_\alpha}{3})H_0\left(\frac{2K_\alpha}{3}\right) + K_\alpha(1-\frac{K_\alpha}{6})\frac{\partial}{\partial K_\alpha}H_0\left(\frac{2K_\alpha}{3}\right)\right],\end{aligned} \tag{4.43}$$

where the tensors A and B are defined as:

$$A^{AB}_{\alpha\;CD} = \frac{1}{8}\left[\{T^a_{R_{\phi\,\alpha}}, T^b_{R_{\phi\,\alpha}}\}^A_C\{T^a_{R_{\phi\,\alpha}}, T^b_{R_{\phi\,\alpha}}\}^B_D + \{T^a_{R_{\phi\,\alpha}}, T^b_{R_{\phi\,\alpha}}\}^A_D\{T^a_{R_{\phi\,\alpha}}, T^b_{R_{\phi\,\alpha}}\}^B_C\right] \tag{4.44}$$

$$B^{AB}_{\alpha,\beta\,CD} = \frac{1}{2}\left[\left(T^a_{R_{\phi\,\alpha}}T^b_{R_{\phi\,\beta}}\right)^A_C\left(T^a_{R_{\phi\,\alpha}}T^b_{R_{\phi\,\beta}}\right)^B_D + \left(T^a_{R_{\phi\,\alpha}}T^b_{R_{\phi\,\beta}}\right)^A_D\left(T^a_{R_{\phi\,\alpha}}T^b_{R_{\phi\,\beta}}\right)^B_C\right] \tag{4.45}$$

A .2 Scheme Transformations

In this section we prove the scheme independence of all the β-functions above. For that purpose first we recall that a scheme transformation will map a gauge coupling $\alpha = \frac{g^2}{4\pi^2}$ to a new one $\alpha' = \frac{g'^2}{4\pi^2}$. This mapping must be inversible and as mentioned in [136] [137] [138] can be parametrized as:

$$\alpha = \alpha'\mathcal{F}(\alpha') \tag{4.46}$$

$$\mathcal{F}(\alpha') = 1 + t_1\alpha' + t_2\alpha'^2 + \dots \tag{4.47}$$

Thus if we do a scheme transformation only for the gauge groupe $\mathcal{G}_\alpha$ we obtain:

$$K_\alpha = K'_\alpha\mathcal{F}(K'_\alpha/N_\alpha) \tag{4.48}$$

$$= K'_\alpha(1 + t_1K'_\alpha/N_\alpha + t_2K'^2_\alpha/N^2_\alpha + \dots) \tag{4.49}$$

This feeds the gauge β-function in two ways. First the β-function of $\mathcal{G}_\alpha$ is already known to be scheme invariant as explain in [136] [137] [138]. We note that the contribution from the other gauge group is unchanged. Secondly, for the other β-functions, the contribution from K_a enters through functions that are already at order 1 in N. Changing the scheme push to expand those functions using (4.49). But the expansion is in higher power in N_α. Thus at first order all the β-function here are scheme independent.

Chapter 5

The Safe Composite

We need more men.

Sansa Stark, Game of Thrones.

1 Introduction

The ultra-violet (UV) behaviour is crucial for a quantum field theory (QFT) to be predictive and fundamental up to high scales [141, 142]. The presence of fixed points in the renormalisation group evolution of gauge and non-gauge couplings plays a central role in this. The Large N formalism exhibits at first order such a safe scenario that can be used in favor of stability. However the class of models of interest will also have a non attractive feature, a large multiplicity of fermion matter fields, as it can be seen in the attempts to build a safe extension of the Standard Model [149, 150]. Whilst this possibility is not ruled out experimentally, postulating the presence of tens of new massive fermions at the multi-TeV scale for the sole purpose of changing the UV behaviour of the theory contradicts the principle of minimality [1]. In this work we want to point out a class of theories where the presence of large multiplicities of heavy fermions is required for another crucial reason: the generation of masses for all Standard Model fermions in models of composite Higgs with partial compositeness. In these models, minimality requires that there exists one composite operator for each chiral fermionic field in the Standard Model. To generate such a spectrum of operators, an underlying theory needs to contain a large number of preons, the fundamental degrees of freedom that constitute the composite objects. Furthermore, considerations related to the hierarchy problem lead to postulating fermionic preons.

A classification of underlying theories based on gauge-fermion interactions can be found in Ref. [74]. The main constraint on this model building effort is precisely the requirement that the theory shall remain confining at low energies [173]. This limits the

[1] Quantum gravity effects may also be able to drive the Standard Model interactions to a safe UV, see for instance Ref. [90].

number of underlying fermions to the ones responsible for giving mass to the top quark only. This problem is absent in theories with scalar fields [55] at the price of reintroducing the hierarchy problem related to elementary scalar masses. In any case, these theories remain underlying descriptions of the composite Higgs dynamics of top partial compositeness, but far from being true UV completions. In fact, the origin of the light fermion masses as well as the source for the couplings generating the partial compositeness remain absent. Our goal is therefore to take a decisive step towards addressing these issues and being able to construct a genuine UV complete theory that can be trusted at arbitrarily high energies, at least up to the Planck scale. In this perspective, providing a Dark Matter candidate becomes a key ingredient.

In this work we present a new paradigm that allows to define composite Higgs models with underlying fermions up to arbitrary high energies. The large number of fermions needed to give mass to all standard quarks and leptons drives the theory to a complete UV interacting fixed point. The fermions associated with the two light generations are supposed to have a large mass, thus explaining the lightness of their partners compared to the electroweak scale. Once integrated out, the remaining degrees of freedom drive the confining gauge interaction towards an Infra-Red (IR) fixed point [174]. The resulting conformal window, similar in nature to walking Technicolor [175, 176], allows to further split the scale of the heavy fermions where flavour effects also arise, from the condensation and electroweak scales. The exit from the IR fixed point can be driven by integrating out a subset of the remaining light fermions, leaving one of the models of Ref. [74] at low scale. In this framework, fundamental scalar fields can also be added in a natural way [2], as long as their masses are close to the mass of the heaviest fermions [177], and they can be responsible for generating the needed four-fermion interactions. The low-energy flavour mixing of the SM can therefore be traced back to high-scale Yukawa couplings of scalars that, as we will show, are charged under the confining strong interactions. A Dark Matter candidate can be easily included in this class of theories [178–180]. The new scenario we discuss here, therefore, allows to define composite models that can in principle be as predictive as supersymmetric extensions of the Standard Model.

This chapter is organised as follows: after introducing the general set-up in Sec. 2 , we describe in Sec. 3 how two underlying models of top partial compositeness with Dark Matter can be extended to UV safety. In Sec. 4 we introduce the scalar sector at high energy, responsible for generating the flavour couplings. In Sec. 5 we embed the two models in a Pati-Salam unification framework, thus eliminating the $U(1)$ problem. Finally, in Sec. 6 we analyse the phenomenology of the Dark Matter candidate, before offering our conclusions in Sec. 7 .

ψ irrep	coset	pNGBs	pNGB EW charges	models	$\mathcal{G}_{\rm HC}$
pseudo-real	SU(4)/Sp(4)	5	$2_{\pm 1/2} \oplus 1_0$	M8-M9	Sp(4), SO(11)
real	SU(5)/SO(5)	14	$2_{\pm 1/2} \oplus 3_{\pm 1} \oplus 3_0 \oplus 1_0$	M1-M7	SU(4), Sp(4), SO(7), SO(9), SO(10)
complex	$\mathrm{SU}(4)^2/\mathrm{SU}(4)$	15	$2 \times 2_{\pm 1/2} \oplus 3_0$	M10-M12	SO(10), SU(4), SU(5)
			$\oplus 1_{\pm 1} \oplus 2 \times 1_0$	MV	SU(3)

Table 5.1: Minimal cosets with a pNGB Higgs doublet arising from an underlying gauge-fermion theory. The fourth column shows the $\mathrm{SU}(2)_L$ *irrep*, with the hypercharge as subscript. The last two columns show some properties of the explicit models, with the nomenclature M1-M12 from Ref. [47], and MV being the model from Ref. [75].

2 Choosing the model

The CHM we shall consider are the twelve selected models proposed in [47] along the paradigm of PC. We thus deal with two representations of the HC group $\mathcal{G}_{\rm HC}$ represented by the species ψ and χ as they were introduced in the precedent chapters. Furthermore, we recall that the spin-1/2 bound states entering in partial compositeness arise as chimera baryons [181] made of both species of fermions, in the two alternative forms

$$\mathcal{B} = \langle \psi\psi\chi \rangle \quad \text{or} \quad \langle \psi\chi\chi \rangle \,. \tag{5.1}$$

The low energy models we consider here, and their key features, are listed in Table 5.1.

To define a genuine UV completion for these models, the issue of Dark Matter cannot be avoided. The simplest possibility is that one of the additional pNGBs may be stable. The minimal case is offered by the coset $\mathrm{SU}(4)_L \times \mathrm{SU}(4)_R/\mathrm{SU}(4)$ [178, 182], which can be obtained in models M10-12, and the models of Refs [55, 75]. In fact, the other two minimal cosets do not feature a stable pNGB because of the Wess-Zumino-Witten topological term. They could feature a DM candidate only if extended. As it was shown in Ref. [182], in the EW sector there is a unique $\mathbb{Z}_2$ parity that is conserved by the fermion condensate (if custodial symmetry is preserved) and by the EW gauging, as well as being anomaly free: it is defined in terms of charge conjugation in the ψ sector plus a flavour rotation in the SU(4) flavour space. If the top couplings also respect this parity, the pNGB spectrum will contain several odd scalars, in particular a doublet and a triplet of $\mathrm{SU}(2)_L$ plus a neutral and a charged singlet. Such states mix, and the lightest neutral one plays the role of Dark Matter candidate (see Ref. [182] for more details on the pNGB structure).

To extend the Dark $\mathbb{Z}_2$ parity in the case of partial compositeness, we need to make sure that the composite operator $\mathcal{B}$ that mixes with the top has well-defined transformation properties and contains even states with the same quantum numbers as the top quark fields. As the Dark parity contains charge conjugation in the ψ-sector (but not χ), it is

[2]Note that the protection in this safe model is against modifications of the UV running of gauge couplings due, for instance, to the presence of Landau poles. This is the case for the hypercharge coupling in the SM. We do not address here the corrections coming from the Planck scale, which can only be treated once a consistent theory of gravity is integrated with the model.

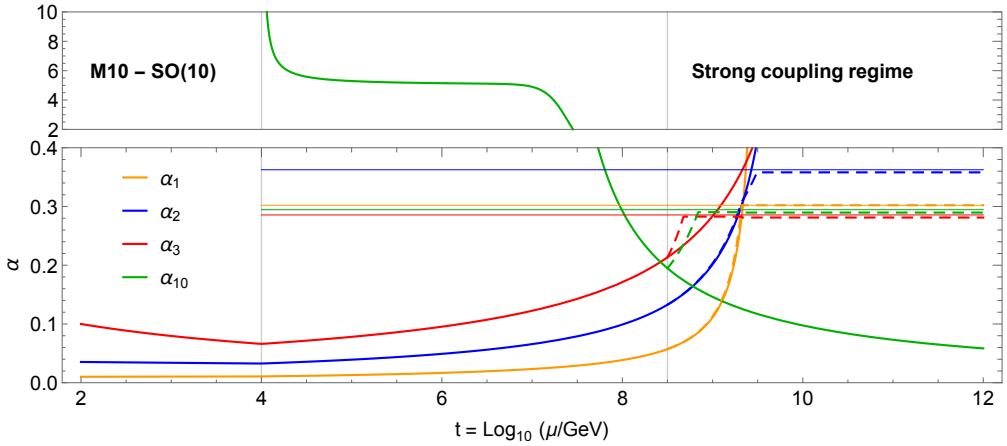

Figure 5.1: Renormalisation group running of the gauge couplings α_i for model M10, $\mathcal{G}_{\rm HC} = {\rm SO}(10)$. The dashed lines show the effect of the large-N_f resummation above $\Lambda_{\rm Fl} = 10^{8.5}$ GeV. The upper panel shows a cartoon of the running at strong coupling.

crucial that the bound state contains two ψ's: this simple fact rules out the case with HC-charged scalars of Ref. [55]. Furthermore, the ψ-bilinear in $\mathcal{B}$ needs to be in a real *irrep* of $\mathcal{G}_{\rm HC}$ (ruling out M12 and the model of Ref. [75]). We are therefore left with the models M10 and M11, based on ${\rm SO}(10)_{\rm HC}$ and ${\rm SO}(6)_{\rm HC} \equiv {\rm SU}(4)_{\rm HC}$ respectively, with ψ_i in the spinorial (**Sp**) *irrep* and χ_j in the fundamental (**F**). For the top partners, there remains two choices that preserve the Dark parity: case a) a bi-fundamental of ${\rm SU}(4)_L \times {\rm SU}(4)_R$, which decomposes into a symmetric and an anti-symmetric of the unbroken SU(4); case b) a pair of symmetric *irreps*. As we will see in Section 6 , only case a) leads to a feasible low energy model.

3 A fundamental theory with UV safety and Dark Matter

In the following, we will focus on M10 and M11: they only differ in the HC group, ${\rm SO}(10)_{\rm HC}$ versus ${\rm SO}(6)_{\rm HC}$. The low-energy fermion content [74] consists of 4 EW-charged ψ's and a QCD-coloured triplet of χ's, as shown in the upper block of Table 5.2. These fermions characterise the composite states below the condensation scale $\Lambda_{\rm HC}$, including the Higgs, the Dark Matter candidate and the top partners.

To complete the model, we will extend it by adding one appropriate χ for each standard fermion that acquires mass via the Higgs mechanism, as shown in the remaining two blocks of Table 5.2. We add the partners for the bottom quark and tau lepton at a scale close to $\Lambda_{\rm HC}$, *i.e.* 5 additional χ-flavours. This is enough to push the theory into the conformal window (more details in A .1): right above the condensation scale, therefore, the strong sector flows into a conformal phase where the gauge coupling remains strong and slowly walking. This phase may ensure that the operators that mix to the light generations

	$SO(\mathcal{N})_{HC}$	$SU(3)_c$	$SU(2)_L$	$U(1)_Y$	mass
ψ_Q	**Sp**	1	2	0	~ 0
ψ_U	**Sp**	1	1	1/2	
ψ_D	**Sp**	1	1	$-1/2$	
χ_u^3	**F**	3	1	2/3	
χ_d^3	**F**	3	1	$-1/3$	$\sim \Lambda_{HC}$
χ_l^3		1	2	$-1/2$	
$\chi_u^{1,2}$	**F**	3	1	2/3	Λ_{Fl} ($\gg \Lambda_{HC}$)
$\chi_d^{1,2}$		3	1	$-1/3$	
$\chi_l^{1,2}$		1	2	$-1/2$	

Table 5.2: Fermion content of the extended M10 ($\mathcal{N} = 10$) and M11 ($\mathcal{N} = 6$) - all fermions are Dirac spinors.

acquire a largish anomalous dimension, allowing to sufficiently decouple the scale where they are introduced. The χ fermions associated to the light generations are, in fact, introduced at a scale $\Lambda_{Fl} \gg \Lambda_{HC}$, where flavour effects are also generated. Above Λ_{Fl}, the number of fermions is such that the running of all gauge couplings are not asymptotically free any more. The lepton partners, χ_l^i, are chosen to be doublets of $SU(2)_L$ for two reasons: on the one hand, their presence will assure that the $SU(2)_L$ gauge coupling also runs into safety; on the other hand, the quantum numbers are such that chimera baryons containing χ_l^i also feature a neutral singlet, i.e. right-handed neutrinos, thus allowing to generate neutrino masses. We will first study how the gauge couplings of these theories may flow to a UV safe fixed point.

Our set up differs from the ones considered in the literature (see Ref. [139]) in the fact that we have different sets of fermions participating to the running of the four gauge couplings. Furthermore, for the $SO(\mathcal{N})$ group, there are two different irreps that need to be taken into account [183]. For these reasons, we define the large-N_f gauge couplings as follows:

$$K_i \equiv N_i \frac{\alpha_i}{\pi}\,, \quad N_i = \sum_f n_f T(r_f)\,; \tag{5.2}$$

with $i = 1, 2, 3, \mathcal{N}$ labelling the four gauge groups (for U(1), replace $T(r_f) \to Y_f^2$). As there are many fermions in different *irreps* of the gauge groups, in our case we cannot define a unique N_f valid for all gauge coupling running, but rather we need to define a different multiplicity N_i for each group. We will assume that formally they are all of the same order. For the extended models in Table 5.2, we find the multiplicity factors listed in Table 5.3. For the running of the $SO(\mathcal{N})$ gauge coupling, as there are two different

irreps that contribute, we follow the results in Ref. [183]:

$$\frac{B_i^{(1)}}{N_f} = \frac{C_2(G_i)}{N_i}\left(-\frac{11}{4} + G_1(K_i)\right) + \sum_{j=1}^{\mathcal{N}} \frac{c_{i,j}}{N_j} F_1(K_j)\,, \tag{5.3}$$

where the functions F_1 and G_1 are defined in A .2, and $C_2(G_i)$ is the Casimir of the adjoint of the i–th gauge group (for the abelian case, $C_2(G_1) = 0$). Note that the $-11/4$ term corresponds to the one loop contribution of gauge bosons. The coefficients $c_{i,j}$ are all positive, and their values can be found in A .2.

	$\mathrm{SO}(\mathcal{N})_{\mathrm{HC}}$	M10	M11
$N_{\mathcal{N}}$	$24 + 2^{\frac{\mathcal{N}-4}{2}}$	32	26
N_3	$3(\mathcal{N}+1)$	33	21
N_2	$3 + \frac{3}{2}\mathcal{N} + 2^{\frac{\mathcal{N}-4}{2}}$	26	14
N_1	$5 + \frac{13}{2}\mathcal{N} + 2^{\frac{\mathcal{N}-4}{2}}$	78	46

Table 5.3: Multiplicity factors for the resummation of the four gauge couplings above Λ_{Fl}. The numerical values in the last two columns refer to M10 ($\mathcal{N} = 10$) and M11 ($\mathcal{N} = 6$).

A key property of the above result is that the function $G_1(K)$, relevant for non-abelian gauge couplings, has a pole at negative values for $K = 3$, while $F_1(K)$ has a negative pole at $K_1 = 15/2$, while the resummation fails for coupling values above the pole. This feature, thus, acts as a barrier for the evolution of the respective coupling towards the UV, hinting at the presence of an interacting UV fixed point [139]. In other words, if the value of the coupling at the threshold Λ_{Fl} is below the pole, the evolution towards the UV will stop at that value where the beta function vanishes and the theory approaches a fixed point. We, therefore, expect the UV fixed point to arise at $K_i = 3$ for non-abelian groups, and $K_1 = 15/2$ for the abelian one. The condition for the model to have a UV safe fixed point for all gauge couplings is that their value is below the pole, i.e.

$$\alpha_i < \frac{3\pi}{N_i} \;\text{ for }\; i \neq 1\,, \quad \text{and} \;\; \alpha_1 < \frac{15\pi}{2N_1}\,. \tag{5.4}$$

The above conditions provide an upper bound on Λ_{Fl} due to the fact that some of the gauge couplings increase towards the UV above Λ_{HC}. On the other hand, an indirect lower bound derives from flavour physics, which gives $\Lambda_{\mathrm{Fl}} > 10^5$ TeV for generic flavour violating effects.

In Fig. 5.1 we show the running of the 4 gauge couplings above the EW scale for the model M10, assuming $\Lambda_{\mathrm{HC}} = 10$ TeV (solid lines). While the SO(10) gauge coupling α_{10} is asymptotically free, the other three run into a Landau pole below 10^{10} GeV. Furthermore, it is the QCD coupling α_3 that crosses the UV-safe threshold first, thus setting the maximum allowed value of Λ_{Fl} right below 10^9 GeV. In the numerical example, we added the complete set of fermions at a scale $\Lambda_{\mathrm{Fl}} = 10^{8.5}$ GeV: the modified running is plotted

in dashed lines, clearly showing how the gauge couplings approach the UV fixed values. Note that they are a bit below the predicted ones: this is due to the backreaction of the U(1) pole on the running of the non-abelian couplings, due to the fact that $F_1(K_1)$ in Eq. (5.3) also has a pole at the fixed point. In the upper panel we illustrate the running of α_{10} in the strong coupling regime, which features a walking region between 10^4 and 10^7 GeV. This part of the plot, being non-perturbative, can only be confirmed by lattice calculations along the lines of Refs [50, 181, 184, 185]. These results show that the model M10 allows for a narrow mass window where the fermions at $\Lambda_{\rm Fl}$ can be added, squeezed between the flavour bounds and the limit from UV safety.

A similar analysis can be done for the model M11, based on $\mathcal{G}_{\rm HC} = {\rm SO}(6)$: in this case, it is the U(1) coupling α_1 that crosses the threshold first at a scale around 10^{13} GeV, while the α_2 and α_3 run much slower. This model can therefore allow for a larger flavour scale, and a wider walking window for α_6.

The models we have studied here, however, are not truly UV complete, because the dynamics generating the partial compositeness four-fermion interactions is not included. In the following sections we will discuss how scalar mediators can do the job.

4 High-scale scalar mediation, and the U(1) problem

	${\rm SO}(\mathcal{N})_{\rm HC}$	${\rm SU}(3)_c$	${\rm SU}(2)_L$	${\rm U}(1)_Y$	mass
ϕ_q^a	$\mathbf{Sp}$	3	1	1/6	$\sim \Lambda_{\rm Fl}$
$\bar{\phi}_q^a$	$\overline{\mathbf{Sp}}$				
ϕ_l^a	$\mathbf{Sp}$	1	1	$-1/2$	$\sim \Lambda_{\rm Fl}$
$\bar{\phi}_l^a$	$\overline{\mathbf{Sp}}$				

Table 5.4: Scalar mediators for lepton and quark partial compositeness.

The four-fermion interactions responsible for the partial compositeness couplings at low energy can be generated via scalar mediation. This is acceptable in this class of models because scalar masses are "natural" if they are close to the largest fermion mass in the model [177], namely $m_\phi \approx \Lambda_{\rm Fl}$. The only additional condition would be to check that all new couplings in the scalar sector, i.e. Yukawas and quartic couplings, also run to a UV safe fixed point. In this and in the next sections we will address this question.

Firstly, in order to preserve the Dark $\mathbb{Z}_2$, it is necessary to add pairs of scalar fields that have the same quantum numbers under the SM gauge symmetries, while they are in conjugate $\mathbf{Sp}$ and $\overline{\mathbf{Sp}}$ irreps of the strong ${\rm SO}(\mathcal{N})$. One minimal set of mediators is shown in Table 5.4, where $a = 1, 2, 3$ is an index running over the SM generations. These four

fields allow to add the following Yukawa couplings above $\Lambda_{\rm Fl}$:

$$\begin{aligned}\mathcal{L}_{\rm Yuk,q} \;=\; & \big\{\lambda_q^{ab}\;\phi_q^{b,*}[q_L^a]_l[\psi_Q]_l + \lambda_u^{ab}\phi_q^{b,*}[u_R^a]_r[\psi_D]_r + \\ & \lambda_d^{ab}\phi_q^{b,*}[d_R^a]_r[\psi_U]_r + \\ & \xi_{ur}^{ab}\;\phi_q^a[\chi_u^b]_l^c[\psi_U]_r + \xi_{ul}^{ab}\;\phi_q^a[\chi_u^b]_r^c[\psi_U]_l + \\ & \xi_{dr}^{ab}\;\phi_q^a[\chi_d^b]_l^c[\psi_D]_r + \xi_{dl}^{ab}\;\phi_q^a[\chi_d^b]_r^c[\psi_D]_l + \\ & \bar\lambda_q^{ab}\;\overline{\phi}_q^{b,*}[q_L^a]_l[\psi_Q]_r^c + \bar\lambda_u^{ab}\overline{\phi}_q^{b,*}[u_R^a]_r[\psi_U]_l^c + \\ & \bar\lambda_d^{ab}\overline{\phi}_q^{b,*}[d_R^a]_r[\psi_D]_l^c + \\ & \bar\xi_{ur}^{ab}\;\overline{\phi}_q^a[\chi_u^b]_l^c[\psi_D]_l^c + \bar\xi_{ul}^{ab}\;\overline{\phi}_q^a[\chi_u^b]_r^c[\psi_D]_r^c + \\ & \bar\xi_{dr}^{ab}\;\overline{\phi}_q^a[\chi_d^b]_l^c[\psi_U]_l^c + \bar\xi_{dl}^{ab}\;\overline{\phi}_q^a[\chi_d^b]_r^c[\psi_U]_r^c\Big\} + h.c.,\end{aligned} \tag{5.5}$$

and

$$\begin{aligned}\mathcal{L}_{\rm Yuk,l} \;=\; & \Big\{\lambda_l^{ab}\;\phi_l^{b,*}[l_L^a]_l[\psi_Q]_l + \lambda_e^{ab}\phi_l^{b,*}[e_R^a]_r[\psi_U]_r + \\ & \lambda_\nu^{ab}\phi_l^{b,*}[\nu_R^a]_r[\psi_D]_r + \\ & \xi_{er}^{ab}\;\phi_l^a[\chi_l^b]_l^c[\psi_Q]_r + \xi_{el}^{ab}\;\phi_l^a[\chi_l^b]_r^c[\psi_Q]_l + \\ & \bar\lambda_l^{ab}\;\overline{\phi}_l^{b,*}[l_L^a]_l[\psi_Q]_r^c + \bar\lambda_e^{ab}\overline{\phi}_l^{b,*}[e_R^a]_r[\psi_D]_l^c + \\ & \bar\lambda_\nu^{ab}\overline{\phi}_l^{b,*}[\nu_R^a]_r[\psi_U]_l^c + \\ & \bar\xi_{er}^{ab}\;\overline{\phi}_l^a[\chi_l^b]_l^c[\psi_Q]_l^c + \bar\xi_{el}^{ab}\;\overline{\phi}_l^a[\chi_l^b]_r^c[\psi_Q]_r^c\Big\} + h.c.;\end{aligned} \tag{5.6}$$

where a sum over the SM flavour indices is left understood, the subscripts $[.]_{l/r}$ indicate respectively the left and right-handed chiralities, and the superscript $[.]^c$ the charge-conjugation. The Dark parity is preserved as long as $\lambda = \bar\lambda$ and $\xi = \bar\xi$: as we will see this condition is renormalisation evolution invariant, thus it is preserved at all scales once it is imposed at $\mu = \Lambda_{\rm Fl}$. We also need to impose that the two scalars have the same mass. Once they are integrated out, they generate appropriate four-fermion interactions for all SM fermions. As an example, for the top (up-type quarks), among others:

$$\begin{aligned}\mathcal{L}_{\Lambda_{\rm Fl}} =& \frac{\kappa_q^{ab}}{\Lambda_{\rm Fl}^2}\Big([q_L^a]_l\cdot[\psi_Q]_l[\chi_u^b]_l^c\cdot[\psi_U]_r + [q_L^a]_l\cdot[\psi_Q]_r^c[\chi_u^b]_l^c\cdot[\psi_D]_l^c\Big) \\ & + \frac{\kappa_u^{ab}}{\Lambda_{\rm Fl}^2}\Big([u_R^a]_r\cdot[\psi_D]_r[\chi_u^b]_r^c\cdot[\psi_U]_l + [u_R^a]_r\cdot[\psi_U]_l^c[\chi_u^b]_r^c\cdot[\psi_D]_r^c\Big),\end{aligned} \tag{5.7}$$

with

$$\frac{\kappa_q^{ab}}{\Lambda_{\rm Fl}^2} = \lambda_q^{ac}[m_\phi^2]_{cd}^{-1}\xi_{u_l}^{db}\,, \quad \frac{\kappa_u^{ab}}{\Lambda_{\rm Fl}^2} = \lambda_u^{ab}[m_\phi^2]_{cd}^{-1}\xi_{u_r}^{db}\,. \tag{5.8}$$

The mediators and Yukawa couplings have been selected such that the four-fermion interactions in Eq. (5.7) generate a coupling of the top fields to a composite baryon in the *irrep* $(\mathbf{4},\mathbf{4})\oplus(\bar{\mathbf{4}},\bar{\mathbf{4}})$ of the global symmetry $\mathrm{SU}(4)_L\times SU(4)_R$, which we will use in Section 6 for the Dark Matter study.

The contribution of the scalars above $\Lambda_{\rm Fl}$ will not affect significantly the running of the gauge couplings. The running of the Yukawa couplings above $\Lambda_{\rm Fl}$ follows the calculations done in Ref. [161]: it has been observed that the dominant contribution is due to the U(1) gauge coupling once it has approached its fixed point, as the contribution to the Yukawa beta function has a pole at the same position. For all Yukawas y_i, the beta function can, therefore, be approximated by

$$\beta(y_i) \approx -y_i \frac{15}{16\pi^2 N_1}(2d_{y_i,1} + 15d'_{y_i,1}) \frac{1}{\frac{15}{2} - K_1}\,, \tag{5.9}$$

where K_1 is exponentially close (from below) to 15/2, and

$$d_{y_i,1} = Y_\phi^2 + 2Y_{f1}Y_{f2}\,, \quad d'_{y_i,1} = \frac{(Y_{f1} - Y_{f2})^2}{6}\,, \tag{5.10}$$

with Y_x being the hypercharges of the scalar and fermions in the Yukawa coupling y_i. Thus, if

$$X_{y_i} = 2d_{y_i,1} + 15d'_{y_i,1} > 0\,, \tag{5.11}$$

the Yukawa coupling y_i runs to zero in the UV. In our model, we find the values in Table 5.5, which show that all the Yukawa couplings in Eqs (5.5) and (5.6) are asymptotically free.

y_i	$d_{y_i,1}$	$d'_{y_i,1}$	X_{y_i}
$\lambda_q,\ \bar{\lambda}_q$	1/36	1/216	1/16
$\lambda_u,\ \xi_{ur},\ \xi_{ul},$ $\bar{\lambda}_u,\ \bar{\xi}_{ur},\ \bar{\xi}_{ul}$	−23/36	49/216	17/16
$\lambda_d,\ \xi_{dr},\ \xi_{dl},$ $\bar{\lambda}_d,\ \bar{\xi}_{dr},\ \bar{\xi}_{dl}$	−11/36	25/216	9/16
$\lambda_l,\ \lambda_\nu,\ \bar{\lambda}_l,\ \bar{\lambda}_\nu$	1/4	1/24	9/16
$\lambda_e,\ \xi_{er},\ \xi_{el},$ $\bar{\lambda}_e,\ \bar{\xi}_{er},\ \bar{\xi}_{el}$	−3/4	3/8	33/16

Table 5.5: Beta function coefficients for the Yukawas in Eqs (5.5) and (5.6).

While the U(1) fixed point drives the Yukawas to be asymptotically free, it is well established that it has a dangerous effect on scalar quartic couplings, which are driven to a Landau pole [161]. We can address this issue by partly unifying the U(1) into a non abelian gauge group, and our model offers an elegant path via a Pati-Salam structure, as discussed in the next section.

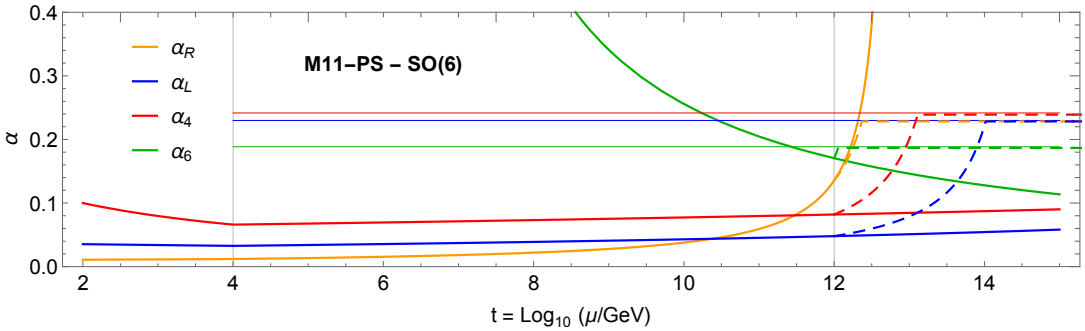

Figure 5.2: Renormalisation group running of the gauge couplings α_i for model M11-PS, $\mathcal{G}_{\rm HC} = {\rm SO}(6)$. The dashed lines show the effect of the large-N_f resummation above $\Lambda_{\rm Fl} = 10^{12}$ GeV.

5 Pati-Salam UV-safe completion.

To remove the destabilising effect of the U(1) pole on scalar quartic couplings, we can embed the model above $\Lambda_{\rm Fl}$ into a Pati-Salam [76] partial unification for the SM interactions [153]. The new models, that we dub M10-PS and M11-PS, feature the field content in Table 5.6. The Pati-Salam gauge group, ${\rm SU}(4) \times SU(2)_L \times {\rm SU}(2)_R$ is broken by a scalar field $\varphi_{\rm PS}$, with a vacuum expectation value of the order of $\Lambda_{\rm Fl}$. To study the UV properties of this model, we can calculate the beta functions following the same procedure highlighted in Section 3 , with the important difference that the contribution of other gauge couplings remains negligible due to the absence of an abelian group. The new N_i are given in Table 5.7: they are substantially larger than the corresponding ones in the previous models, indicating lower values for the UV fixed points. This is potentially dangerous, as the upper limit on $\Lambda_{\rm Fl}$ will tend to decrease.

In Fig. 5.2 we show the running of the Pati-Salam gauge couplings in the model M11-PS [3]: the first coupling to pass the safe threshold is α_R, at an energy scale slightly lower than that for M11. In the numerical example, we fixed $\Lambda_{\rm Fl} = 10^{12}$ GeV, where the field content of M11-PS is added. Besides the difference in scales, the approach to the UV fixed point is similar, also showing the same fixed point for the two SU(2)'s thanks to the left-right symmetry of the model. For M10-PS, we find that the maximum allowed value for $\Lambda_{\rm Fl}$ is slightly above 10^7 GeV, thus generating potential conflict with flavour bounds and also leaving too small space for the IR walking window. These results show that M11-PS is favoured.

We can now study the safety of the Yukawa couplings, which can be written in the

[3] The usual matching applies:

$$\alpha_4 = \alpha_3\,, \quad \alpha_L = \alpha_2\,, \quad \alpha_R = \frac{3\alpha_1\alpha_3}{3\alpha_3 - 2\alpha_1}\,.$$

	$\mathrm{SO}(\mathcal{N})_{\mathrm{HC}}$	$\mathrm{SU}(4)$	$\mathrm{SU}(2)_L$	$\mathrm{SU}(2)_R$	
ω_L^a	**1**	4	2	1	$q_L^a,\ l_L^a$
ω_R^a	**1**	4	1	2	$u_R^a,\ d_R^a,$ $e_L^a,\ \nu_R^a$
Ψ_L	**Sp**	1	2	1	ψ_Q
Ψ_R	**Sp**	1	1	2	$\psi_U,\ \psi_D$
Ξ_R^a	**F**	4	1	2	$\chi_u^a,\ \chi_d^a$
Ξ_L^a	**F**	4	2	1	χ_l^a
Φ^a	**Sp**	4	1	1	$\phi_q^a,\ \phi_l^a$
$\overline{\Phi}^a$	$\overline{\mathbf{Sp}}$	4	1	1	$\overline{\phi}_q^a,\ \overline{\phi}_l^a$
φ_{PS}	**1**	4	1	2	–

Table 5.6: Fermion content of the Pati-Salam extended M10-PS ($\mathcal{N}=10$) and M11-PS ($\mathcal{N}=6$) - all fermions ω, Ψ and Ξ are Dirac spinors.

	$\mathrm{SO}(\mathcal{N})_{\mathrm{HC}}$	M10-PS	M11-PS
$N_{\mathcal{N}}$	$48+2^{\frac{\mathcal{N}-4}{2}}$	56	50
N_4	$3(2\mathcal{N}+1)$	63	39
$N_L=N_R$	$3+6\mathcal{N}+2^{\frac{\mathcal{N}-4}{2}}$	71	41

Table 5.7: Multiplicity factors for the gauge couplings in the Pati-Salam UV completions.

Pati-Salam unified models as

$$\begin{aligned}\mathcal{L}_{\mathrm{Yuk,PS}} \quad = \quad & \big\{\gamma_L^{ab}\ \Phi^{b,*}[\omega_L^a]_l[\Psi_L]_l+\gamma_R^{ab}\Phi^{b,*}[\omega_R]_r[\Psi_R]_r+\\ & \zeta_{Rr}^{ab}\ \Phi^a[\Xi_R^b]_l^c[\Psi_R]_r+\zeta_{Rl}^{ab}\ \Phi^a[\Xi_R^b]_r^c[\Psi_R]_l+\\ & \zeta_{Lr}^{ab}\ \Phi^a[\Xi_L^b]_l^c[\Psi_L]_r+\zeta_{Ll}^{ab}\ \Phi^a[\Xi_L^b]_r^c[\Psi_L]_l+\\ & \bar{\gamma}_L^{ab}\ \overline{\Phi}^{b,*}[\omega_L^a]_l[\Psi_L]_r^c+\bar{\gamma}_R^{ab}\overline{\Phi}^{b,*}[\omega_R]_r[\Psi_R]_l^c+\\ & \bar{\zeta}_{Rr}^{ab}\ \overline{\Phi}^a[\Xi_R^b]_l^c[\Psi_R]_l^c+\bar{\zeta}_{Rl}^{ab}\ \overline{\Phi}^a[\Xi_R^b]_r^c[\Psi_R]_r^c+\\ & \bar{\zeta}_{Lr}^{ab}\ \overline{\Phi}^a[\Xi_L^b]_l^c[\Psi_L]_l^c+\bar{\zeta}_{Ll}^{ab}\ \overline{\Phi}^a[\Xi_L^b]_r^c[\Psi_L]_r^c\big\}\\ & +h.c.. \end{aligned} \tag{5.12}$$

In absence of U(1) couplings, the contribution of Yukawas and gauge couplings can be

comparable. The beta function can be written as [161, 183]

$$(\beta_y)_{aij} = \frac{1}{32\pi^2}\Big\{(y_b \cdot y^{\dagger,b} \cdot y_a)_{ij} + (y_a \cdot y^{\dagger,b} \cdot y_b)_{ij} + 2\mathrm{Tr}[y_a \cdot y^{\dagger,b}]y_{bij}\Big\} - \frac{3}{2}y_{aij}\sum_\alpha \frac{K_\alpha}{N_\alpha}H_0(K_\alpha)\times \left(\frac{C_2(f_1)+C_2(f_2)}{2} + \frac{C_2(\Phi)}{12}K_\alpha\right), \quad (5.13)$$

where α indicates the sum over the 4 gauge groups, and C_2 are the Casimirs of the irreps of the two fermions and scalar under each gauge group. The function H_0 remains finite up to $K < 15/2$, thus the gauge contribution remains small up to the UV fixed points, reached for $K_\alpha = 3$ (where $H_0(3) = 1/9$). The beta function, after the gauge couplings have reached the fixed points, thus reads

$$\beta(y_k) = \frac{y_k}{32\pi^2}\sum_p d_{kp}y_p^2 - C_{y_k}y_k\,, \quad (5.14)$$

where $d_{kp} > 0$ and order 1. Thus all Yukawas run to zero as long as $C_{y_k} > 0$ and y_k is small enough at $\Lambda_{\rm Fl}$ that the beta functions are negative. We find that the C_{y_k} are the same for all the γ-type ($\bar{\gamma}$) and ζ-type ($\bar{\zeta}$) Yukawas in Eq. (5.12), with

$$\begin{aligned} &C_\gamma = 0.046\,, \quad C_\zeta = 0.066\,, \quad \text{for M10-PS}\,; \\ &C_\gamma = 0.028\,, \quad C_\zeta = 0.040\,, \quad \text{for M11-PS}\,. \end{aligned} \quad (5.15)$$

As they are all positive and one order of magnitude larger than the factor $\frac{1}{32\pi^2}$, the Yukawas are asymptotically free in both models with values of $\mathcal{O}(1)$ allowed at $\Lambda_{\rm Fl}$.

6 Dark Matter phenomenology

The low energy physics of the two models, M10 and M11, can be described by the same effective field theory as they have the same global symmetries. The only distinction, besides the value of the low energy constants, can be traced in the properties of the pNGBs associated to the global U(1) symmetries broken by the condensates [47, 189]. The Dark Matter sector is similar to that of the model in Ref. [182]: the odd pNGBs consist of a triplet of $\mathrm{SU}(2)_L$, an inert Higgs doublet and charged and neutral singlets (forming a triplet of the custodial $\mathrm{SU}(2)_R$). However, the pNGB potential generated by the top interactions is very different, as here we use partial compositeness to generate the top mass, while in Ref. [182] bilinear Yukawa-like interactions are considered. Thus, mass spectra and couplings are different from those in the model of Ref. [182]. In this work we explicitly computed loops of the top and top partners after imposing the maximal symmetry [190] to keep the loops calculable and finite.

The nature of the lightest neutral stable scalar crucially depends on the masses of the preons: here we assume that the ψ_U and ψ_D have a common mass m_R in order to

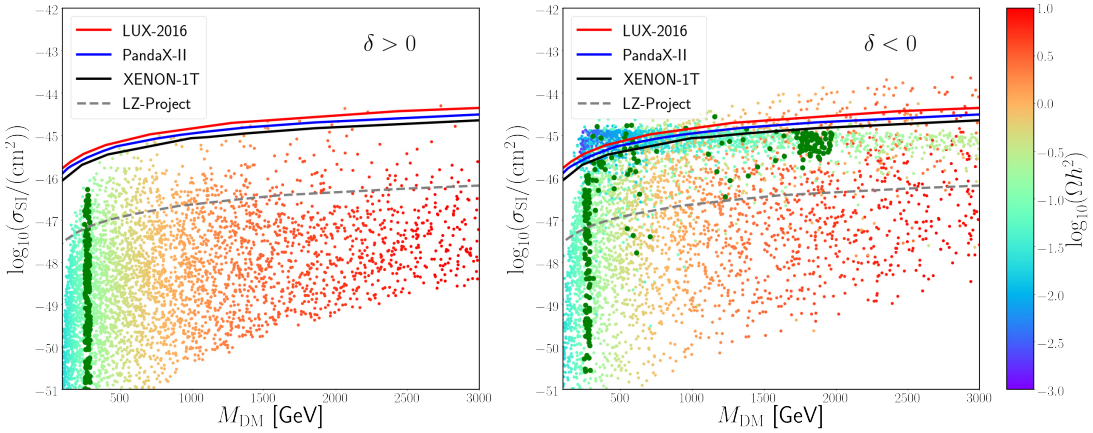

Figure 5.3: Direct detection constraints [186–188] for $\delta > 0$ (left) and $\delta < 0$ (right). The colour encodes the relic density for each parameter point, which is used to rescale the spin-independent cross section $\sigma_{\rm SI}$. The dark green points saturate the measured relic density value, with points having warmer colour being excluded by over-density.

preserve the global custodial $\mathrm{SU}(2)_R$, while the mass of ψ_Q is m_L. The crucial parameter is thus the mass difference $\delta \equiv (m_L - m_R)/(m_L + m_R)$. For $\delta < 0$, the lightest neutral stable scalar mostly coincides with the $\mathrm{SU}(2)_L$ triplet, while for $\delta > 0$ it has maximal overlap with the singlets. For $\delta \sim 0$, maximal mixing with the doublet is active. This mixing pattern determines the annihilation rates of the Dark Matter candidate, which is dominated by the final states in two EW gauge bosons and two tops. The annihilation cross section is thus larger for $\delta < 0$, leading to larger allowed Dark Matter masses.

To study a concrete example, we computed the top and gauge boson loop potential, considering case a), where the top partners transform in the anti-symmetric of the unbroken SU(4), as embedded in the bi-fundamental (see A .3 for more details). We constrain the parameter space by fixing the masses of the top (173 GeV) and Higgs (125 GeV) at the minimum of the potential. We then scan the remaining parameter space and compute relic abundance and spin-independent cross section off nuclei by using the `micrOMEGAs` [191] package. For the misalignment angle, $\sin\theta = \frac{v}{f}$, we probe values between 0.0003 and 0.3. Here, $v = 246$ GeV is the SM Higgs vacuum expectation value, $f \sim \frac{\Lambda_{\rm HC}}{4\pi}$ the decay constant of the composite Higgs, and the Dark Matter mass is proportional to f. In Fig. 5.3 we show the results of our scan in the plane of the Dark Matter mass versus the cross section rescaled by the actual relic abundance. In this way, all points can be compared to the Direct Detection exclusion, shown by the solid black, blue and red lines. Points that saturate the relic abundance within 10σ are highlighted in dark green. We see that the model can explain the Dark Matter abundance without being excluded for $M_{\rm DM} \approx 260$ GeV, while larger values up to $1.5 \sim 2$ TeV are allowed for $\delta < 0$. The region at DM masses close to 260 GeV is dominated by co-annihilation with the the next-to-lightest odd state ($\phi_1^\pm$) due to the small mass splitting. The fixed value of the DM mass stems from the dominance of the annihilation process $\phi_1^+\phi_1^- \to \gamma\gamma$ via gauge interactions: thus, the relic density highly depends on the masses. Note also that the larger Dark Matter masses will be probed by future direct detection experiments. We remark that those

masses have reasonable values compared to the typical compositeness scale at the TeV. While in the $\delta > 0$ case, being the DM dominantly a singlet, indirect detection constraints can be neglected, in the $\delta < 0$ case they might be relevant [179, 192]. However, we have checked that the current bounds are very weak and not competitive with direct detection.

We also performed a similar scan for top partners in case b), finding that all points saturating the relic density are excluded by direct detection. Having demonstrated that a feasible Dark Matter candidate is present in the model, we leave a detailed study of the low energy phenomenology of these models for future work.

7 Conclusions and Outlook

We have presented a new paradigm that allows to define composite Higgs models with partial compositeness for the top quark up to arbitrarily high scales. For the first time, we can endow composite models with predictivity power. Based on gauge-fermion underlying descriptions of the low energy physics, we use the need for a large multiplicity of fermions, related to the large number of fermions and generations in the Standard Model, to predict the presence of UV safe fixed points for the complete theory.

We apply this paradigm to models that also feature a composite scalar Dark Matter candidate. We show that the gauge couplings, which include the coupling of the confining group $\mathrm{SO}(10)_{\mathrm{HC}}$ (for M10) or $\mathrm{SO}(6)_{\mathrm{HC}}$ (for M11), can develop a UV interacting fixed point while also allowing for an IR conformal window and a sufficient hierarchy between the scale of flavour physics generation and the EW scale. Furthermore, a Dark Matter candidate is predicted in a consistent mass ballpark, which can also saturate the relic abundance while evading direct detection bounds.

In the paradigm we propose, the four fermion interactions corresponding to partial compositeness for the Standard Model fermions are generated by scalar mediators with a mass close to Λ_{Fl}, i.e. the scale where the theory approaches the UV fixed point. We showed that the Yukawa couplings run to zero in the UV, thus not spoiling the safety of the model. The well known instability on the scalar quartic couplings can be cured by embedding the model in a Pati-Salam envelope above Λ_{Fl}. We have shown that the two models, M10-PS and M11-PS, also feature an interacting fixed point for the gauge couplings, and asymptotically free Yukawas, while M11-PS based on $\mathrm{SO}(6)_{\mathrm{HC}}$ is preferred due to the higher flavour scale. This also leaves open the possibility that the four-fermion interactions are generated by vector mediators, *à la* Extended Technicolor. We leave the investigation of this point for further work.

A Appendix

A .1 Conformal window

To estimate if the model below $\Lambda_{\rm Fl}$ is inside the IR conformal window, we will utilise the Schwinger-Dyson rainbow approximation [193, 194] and the beta-function at two loops to estimate the position of the fixed point. Following Ref. [84], the beta functions read:

$$\begin{aligned} \beta_0 &= \frac{11}{3}C_2(\mathbf{G}) - \frac{4}{3}\sum_{i=\psi,\chi} T(r_i)n_i\,, \\ \beta_1 &= \frac{34}{3}C_2^2(\mathbf{G}) - \frac{4}{3}\sum_{i=\psi,\chi} \left[5C_2(\mathbf{G}) + 3C_2(r_i)\right] T(r_i)n_i\,, \end{aligned} \tag{5.16}$$

where $\mathbf{G}$ indicates the adjoint representation. The IR fixed point, if existent, is characterised by the gauge coupling:

$$\alpha^* = -4\pi\frac{\beta_0}{\beta_1}\,, \tag{5.17}$$

assuming that $\beta_1 < 0$ (and $\beta_0 > 0$ as the theory is asymptotically free). In the rainbow approximation, we can calculate the value of the gauge coupling where the condensate of the two species become critical: as the theory flows from an UV free point, the critical value is given by the smallest value of the two condensates:

$$\alpha_c = \min\left\{\frac{\pi}{3C_2(r_i)}\right\}\,. \tag{5.18}$$

Equating $\alpha_c \equiv \alpha^*$ determines the lower edge of the conformal window. For the two models M10 and M11, fixing $n_\psi = 4$, we can find the range of n_χ leading to a theory inside the IR conformal window:

$$\text{SO}(10) \;\Rightarrow\; 4 < n_\chi < 14\,, \tag{5.19}$$

$$\text{SO}(6) \;\Rightarrow\; 6 < n_\chi < 9\,, \tag{5.20}$$

where the upper edge is determined by the loss of asymptotic freedom. The models in Table 5.2 have $n_\chi = 8$ below $\Lambda_{\rm Fl}$, thus they are expected to be well inside the conformal window.

As large anomalous dimensions are needed to enhance the top partial compositeness in particular, it may be needed to push the theory closer to the lower edge, where the coupling is stronger. In M10, for instance, one could push the mass of χ_d^3 close to $\Lambda_{\rm Fl}$ in order to have $n_\chi = 5$ (while the bottom mass could be generated by the chimera baryons containing χ_u^3). For M11, one could replace χ_l^3 with an $\text{SU}(2)_L$ singlet with hypercharge -1, thus leading to $n_\chi = 7$: this will marginally affect the running above $\Lambda_{\rm Fl}$, while only two neutrino masses can be generated (i.e., predicting one massless neutrino).

An alternative method to determine the conformal window, proposed in Ref. [87], is based on an all-order beta function conjecture, and it would lead to a lower edge for the conformal window, leading to $n_\chi > 3$ for both models.

A .2 Resummation

The functions appearing in the gauge coupling running are defined as [183]:

$$\begin{aligned} G_1(K) &= \frac{3}{4}\int_0^K dx\ \tilde{F}(0,\frac{2}{3}x)\ \tilde{g}(\frac{1}{3}x)\,, \\ F_1(K) &= \frac{3}{4}\int_0^K dx\ \tilde{F}(0,\frac{2}{3}x)\,, \end{aligned} \tag{5.21}$$

where

$$\begin{aligned} \tilde{F}(0,y) &= \frac{(1-y)(1-\frac{y}{3})(1+\frac{y}{2})\Gamma(4-y)}{3\Gamma^2(2-\frac{y}{2})\Gamma(3-\frac{y}{2})\Gamma(1+\frac{y}{2})}\,, \\ \tilde{g}(y) &= \frac{20-43y+32y^2-14y^3+4y^4}{4(2y-1)(2y-3)(1-y^2)}\,. \end{aligned}$$

We remark that the pole in $K = 15/2$ comes from the $\Gamma(4-y)$–factor in $\tilde{F}$, which diverges for $y \to 5$, while the pole in $K = 3$ for $G_1(K)$ comes from the factor $(1-y^2)$ at the denominator of $\tilde{g}$. We remind the reader that $F_1(K)$ corresponds to the resummation for abelian gauge groups [131], and it encodes 2-loop diagrams with fermion bubbles inserted in the gauge propagators. On the other hand, $G_1(K)$ includes the contribution of 2-loop diagrams involving the triliner gauge boson self coupling [132,160], with fermion bubble insertions. It is useful to connect our definitions with the function H_1 defined in Ref. [161]:

$$H_1 = \frac{C_2(\mathbf{G})}{C_2(R_f)}\left(-\frac{11}{4}+G_1\right)+F_1\,. \tag{5.22}$$

For the UV completions of the models M10 and M11, we find:

$$c_{\mathcal{N},\mathcal{N}} = C_2(\mathbf{F}) = \frac{\mathcal{N}-1}{2}\,, \tag{5.23}$$

$$c_{\mathcal{N},3} = 24\frac{T(\mathbf{F})}{N_{\mathcal{N}}}\,, \tag{5.24}$$

$$c_{\mathcal{N},2} = \frac{3T(\mathbf{F})}{2N_{\mathcal{N}}}\left(3+\frac{T(\mathbf{Sp})}{T(\mathbf{F})}\right)\,, \tag{5.25}$$

$$c_{\mathcal{N},1} = \frac{T(\mathbf{F})}{N_{\mathcal{N}}}\left(\frac{13}{2}+\frac{T(\mathbf{Sp})}{2T(\mathbf{F})}\right)\,, \tag{5.26}$$

$$c_{3,\mathcal{N}} = 3\frac{T(\mathbf{F})d(\mathbf{G})}{N_3}\,, \tag{5.27}$$

$$c_{3,3} = \frac{4}{3}\,, \tag{5.28}$$

$$c_{3,2} = \frac{9}{8N_3}\,, \tag{5.29}$$

$$c_{3,1} = \frac{1}{N_3}\left(\frac{5}{6}d(\mathbf{F})+\frac{11}{24}\right)\,, \tag{5.30}$$

$$c_{2,\mathcal{N}} = \frac{T(\mathbf{F})d(\mathbf{G})}{N_2}\left(\frac{3}{2}+\frac{T(\mathbf{Sp})}{2T(\mathbf{F})}\right), \tag{5.31}$$

$$c_{2,3} = \frac{3}{N_2}, \tag{5.32}$$

$$c_{2,2} = \frac{3}{4}, \tag{5.33}$$

$$c_{2,1} = \frac{1}{N_2}\left(\frac{3}{8}d(\mathbf{F})+\frac{1}{4}\right), \tag{5.34}$$

$$c_{1,\mathcal{N}} = \frac{T(\mathbf{F})d(\mathbf{G})}{N_1}\left(\frac{13}{2}+\frac{T(\mathbf{Sp})}{2T(\mathbf{F})}\right), \tag{5.35}$$

$$c_{1,3} = \frac{1}{N_1}\left(\frac{20}{3}d(\mathbf{F})+\frac{11}{3}\right), \tag{5.36}$$

$$c_{1,2} = \frac{1}{N_1}\left(\frac{9}{8}d(\mathbf{F})+\frac{3}{4}\right), \tag{5.37}$$

$$c_{1,1} = \frac{1}{N_1}\left(\frac{163}{72}d(\mathbf{F})+\frac{1}{8}d(\mathbf{Sp})+\frac{95}{36}\right). \tag{5.38}$$

The group theory factors appearing in the above expressions refer to the SO($\mathcal{N}$) irreps, and are equal to

$$\begin{array}{lll} d(\mathbf{G})=\frac{\mathcal{N}(\mathcal{N}-1)}{2}, & d(\mathbf{F})=\mathcal{N}, & d(\mathbf{Sp})=2^{\frac{\mathcal{N}-2}{2}}, \\ T(\mathbf{G})=\mathcal{N}-2, & T(\mathbf{F})=1, & T(\mathbf{Sp})=2^{\frac{\mathcal{N}-8}{2}}, \\ C_2(\mathbf{G})=\mathcal{N}-2, & C_2(\mathbf{F})=\frac{\mathcal{N}-1}{2}, & C_2(\mathbf{Sp})=\frac{\mathcal{N}(\mathcal{N}-1)}{16}. \end{array}$$

Numerically, for M10 we find:

$$c_{i,j}^{M10} = \begin{pmatrix} 4.5 & 0.75 & 0.234 & 0.234 \\ 4.09 & 1.33 & 0.068 & 0.266 \\ 4.33 & 0.115 & 0.75 & 0.154 \\ 4.33 & 0.90 & 0.154 & 0.350 \end{pmatrix}; \tag{5.39}$$

while for M11:

$$c_{i,j}^{M11} = \begin{pmatrix} 2.5 & 0.923 & 0.202 & 0.260 \\ 2.14 & 1.33 & 0.107 & 0.260 \\ 1.88 & 0.214 & 0.75 & 0.179 \\ 2.20 & 0.949 & 0.163 & 0.364 \end{pmatrix}; \tag{5.40}$$

where $i,j = \mathcal{N}, 3, 2, 1$.

A .3 Top partners

For partial compositeness, based on the UV completions in Table 5.2, we are considering the case where composite top partners transform in the antisymmetric representations 6 and $\bar{6}$ under unbroken subgroup SU(4) of the global symmetry $\mathrm{SU}(4)_L \times \mathrm{SU}(4)_R$. In order to preserve the Dark parity in the theory, we shall include both representations in a symmetric way. To write the proper mixing terms, the elementary top quark fields need to be embedded in the above representations, by way of the following spurions:

$$
\begin{aligned}
\psi_{q_L}^{u,6} &= \frac{1}{\sqrt{2}} \begin{pmatrix} 0 & 0 & 0 & t_L \\ 0 & 0 & 0 & b_L \\ 0 & 0 & 0 & 0 \\ -t_L & -b_L & 0 & 0 \end{pmatrix}, \\
\psi_{q_L}^{d,6} &= \frac{1}{\sqrt{2}} \begin{pmatrix} 0 & 0 & t_L & 0 \\ 0 & 0 & b_L & 0 \\ -t_L & -b_L & 0 & 0 \\ 0 & 0 & 0 & 0 \end{pmatrix}, \\
\psi_{q_L}^{u,\bar{6}} &= \frac{1}{\sqrt{2}} \begin{pmatrix} 0 & 0 & -b_L & 0 \\ 0 & 0 & t_L & 0 \\ b_L & -t_L & 0 & 0 \\ 0 & 0 & 0 & 0 \end{pmatrix}, \\
\psi_{q_L}^{d,\bar{6}} &= \frac{1}{\sqrt{2}} \begin{pmatrix} 0 & 0 & 0 & b_L \\ 0 & 0 & 0 & -t_L \\ 0 & 0 & 0 & 0 \\ -b_L & t_L & 0 & 0 \end{pmatrix}, \\
\psi_{t_R}^{6(\bar{6})} &= \frac{1}{\sqrt{2}} \begin{pmatrix} 0 & t_R & 0 & 0 \\ -t_R & 0 & 0 & 0 \\ 0 & 0 & 0 & 0 \\ 0 & 0 & 0 & 0 \end{pmatrix}, \\
\psi_{b_R}^{6(\bar{6})} &= \frac{1}{\sqrt{2}} \begin{pmatrix} 0 & b_R & 0 & 0 \\ -b_R & 0 & 0 & 0 \\ 0 & 0 & 0 & 0 \\ 0 & 0 & 0 & 0 \end{pmatrix}.
\end{aligned}
\tag{5.41}
$$

The transformation properties of these spurions are

$$\begin{aligned}
\psi^{u/d,6}_{q_L} &\to L\psi^{u/d,6}_{q_L}L^T,\\
\psi^{u/d,\bar{6}}_{q_L} &\to R^*\psi^{u/d,\bar{6}}_{q_L}R^\dagger,\\
\psi^{6}_{t_R/b_R} &\to L\psi^{6}_{t_R/b_R}L^T,\\
\psi^{\bar{6}}_{t_R/b_R} &\to R^*\psi^{\bar{6}}_{t_R/b_R}R^\dagger,
\end{aligned} \tag{5.42}$$

where L (R) is an element of the global symmetry $\mathrm{SU}(4)_L$ ($\mathrm{SU}(4)_R$).

At low energies, the partial compositeness Lagrangian can be written as

$$\begin{aligned}
\mathcal{L} = {}& \epsilon^{u,6}_L f\mathrm{Tr}[\bar{\psi}^{u,6}_{q_L}U\mathcal{B}^{u,6}_{q_L}U^T] + \epsilon^{u,\bar{6}}_L f\mathrm{Tr}[\bar{\psi}^{u,\bar{6}}_{q_L}U^T\mathcal{B}^{u,\bar{6}}_{q_L}U]\\
&+ \epsilon^{d,6}_L f\mathrm{Tr}[\bar{\psi}^{d,6}_{q_L}U\mathcal{B}^{d,6}_{q_L}U^T] + \epsilon^{d,\bar{6}}_L f\mathrm{Tr}[\bar{\psi}^{d,\bar{6}}_{q_L}U^T\mathcal{B}^{d,\bar{6}}_{q_L}U]\\
&+ \epsilon^{u,6}_R f\mathrm{Tr}[\bar{\psi}^{6}_{t_R}U\mathcal{B}^{6}_{t_R}U^T] + \epsilon^{u,\bar{6}}_R f\mathrm{Tr}[\bar{\psi}^{\bar{6}}_{t_R}U^T\mathcal{B}^{\bar{6}}_{t_R}U]\\
&+ \epsilon^{d,6}_R f\mathrm{Tr}[\bar{\psi}^{6}_{b_R}U\mathcal{B}^{6}_{b_R}U^T] + \epsilon^{d,\bar{6}}_R f\mathrm{Tr}[\bar{\psi}^{\bar{6}}_{b_R}U^T\mathcal{B}^{\bar{6}}_{b_R}U]\\
&+ M^u_{6\bar{6}}\mathrm{Tr}[\bar{\mathcal{B}}^{u,6}_{q_L}\mathcal{B}^{\bar{6}\prime}_{t_R}] + M^u_{\bar{6}6}\mathrm{Tr}[\bar{\mathcal{B}}^{u,\bar{6}}_{q_L}\mathcal{B}^{6\prime}_{t_R}]\\
&+ M^d_{6\bar{6}}\mathrm{Tr}[\bar{\mathcal{B}}^{d,6}_{q_L}\mathcal{B}^{\bar{6}\prime}_{b_R}] + M^d_{\bar{6}6}\mathrm{Tr}[\bar{\mathcal{B}}^{d,\bar{6}}_{q_L}\mathcal{B}^{6\prime}_{b_R}] + h.c.
\end{aligned} \tag{5.43}$$

where the $\mathcal{B}$'s are the corresponding top partners, $\mathcal{B}'_{ij} = \epsilon_{ijkl}\mathcal{B}_{kl}$ and U is the usual non-linear sigma field, which transforms under the global symmetry as

$$U \to LUh^\dagger\,, \quad U \to hUR^\dagger\,, \tag{5.44}$$

where h is an element of the unbroken group $\mathrm{SU}(4)$. In order to preserve the Dark parity, the following conditions must be satisfied:

$$\begin{aligned}
\epsilon^{u,6}_L = -\epsilon^{u,\bar{6}}_L \equiv \epsilon^u_L, \quad \epsilon^{d,6}_L = -\epsilon^{d,\bar{6}}_L \equiv \epsilon^d_L,\\
\epsilon^{u,6}_R = \epsilon^{u,\bar{6}}_R \equiv \epsilon^u_R, \quad \epsilon^{d,6}_R = \epsilon^{d,\bar{6}}_R \equiv \epsilon^d_R,\\
M^u_{6\bar{6}} = M^u_{\bar{6}6} \equiv M^u_\Delta, \quad M^d_{6\bar{6}} = M^d_{\bar{6}6} \equiv M^d_\Delta.
\end{aligned} \tag{5.45}$$

It is straightforward to verify that the underlying Lagrangian is invariant under the DM parity with the following transformations:

$$\begin{aligned}
&\psi^6_X \leftrightarrow -P_B(\psi^{\bar{6}}_X)P_B^\dagger = \psi^6_X\,,\\
&\mathcal{B}^6_X \leftrightarrow P_B\mathcal{B}^{\bar{6}}_X P_B^\dagger\,, \quad U \to P_B U^T P_B^\dagger\,;
\end{aligned} \tag{5.46}$$

where P_B is the Dark parity transformation defined in [182]:

$$P_B = \begin{pmatrix} \sigma_2 & 0 \\ 0 & -\sigma_2 \end{pmatrix}.$$

The scalar potential has a similar form to the one used in [178, 182], with the fermion-induced potential replaced by the one induced by loops of the above partial compositeness Lagrangian. The full potential has been coded into `FeynRules` [195], and then interfaced to `micrOMEGAs` [196]. The latter tool is then used to calculate the DM relic density as well as the scattering cross-sections for direct and indirect detection.

Chapter 6

Surprise

Quoi de neuf docteur?

Bugs Bunny.

During the last year of my thesis I have been offered an incredible opportunity to join a collaboration of physicists on a Covid-19 project. The main subject is the study of a virus spread, from a macroscopic point of view like in European countries or equivalently US states. The recent events speak for themselves to motivate the need for predictions.

This project has been a very daring task, and one which is somewhat removed from theoretical physics, but as rich and interesting as any particle physics project. It has taken lot of time, and I find it deserves to form a part of my thesis. For this reason I would like to present, very briefly, the progress on this subject and the work I have been doing.

The first part of this project consisted of a review on the different diffusion models at our disposal. Historically there were:

- Compartmental Models: A population of N individuals is divided into categories, the Susceptible $S(t)$ (part of the population that could be infected at time t), the Infectious $I(t)$ (number of infected, that can pass the disease to susceptible) and the Removed $R(t)$ (people that have been infected but are now removed because they healed or died). This is one of the simplest models, one could add more categories and complexity. The time evolution is deduced from the SIR equations:

$$\frac{\mathrm{d}S(t)}{\mathrm{d}t} = -\frac{\gamma}{N} I(t)S(t) \tag{6.1}$$

$$\frac{\mathrm{d}I(t)}{\mathrm{d}t} = \frac{\gamma}{N} I(t)S(t) - \epsilon I(t) \tag{6.2}$$

$$\frac{\mathrm{d}R(t)}{\mathrm{d}t} = \epsilon I(t) \tag{6.3}$$

  with γ and ϵ corresponding respectively to the infection rate and the recovery rate. Depending on the initial values of S, I and R and on the specified γ and ϵ, the

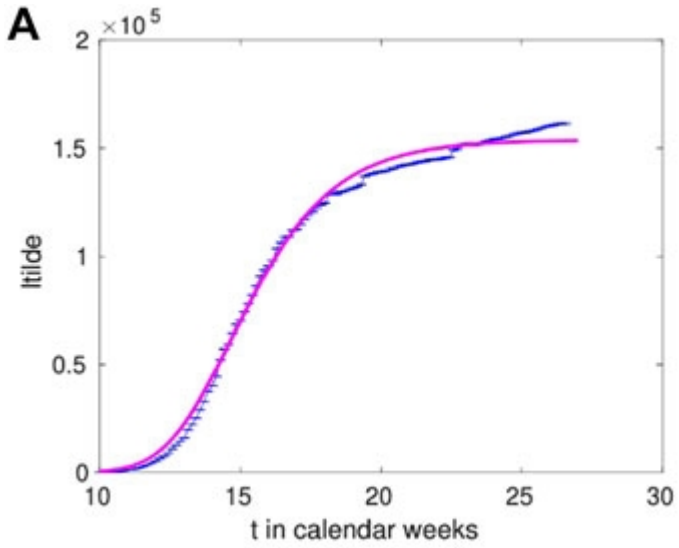

Figure 6.1: Fit of the eRG on the real data of France

dynamics will encode a disease that dies off, or that spreads up to a certain fraction of the population in a single wave before disappearing.

- The Lattice Simulation: The population is represented as a lattice and can be classified into any one of the three states defined above, Suceptible, Infectious or Recovered. At each time step the states of the lattice sites are modified according to stochastic rules, the propability of being infected (similar to γ from the SIR) and the probability of being removed (similar to ϵ). The different dynamics produced are very close to the predictions of the Compartmental Models.

- Percolation Field Theory. Like the Lattice simulations, it is based on discretized time and population. In this theory, processes similar to the rules of the Lattice are quantified in the Field Theory language leading to an Action being obtained.

Recently a new approach has been proposed by M. Della Morte, D. Orlando and F. Sannino called the epidemiological Renormalization Group (eRG). In this approach, the time derivative of the cumulative number of infected is viewed as a beta-function of the renormalization group framework. This has proven to be a very precise and effective way to fit the real data, as it can be seen in Figure 6.1 (from [197])

To illustrate those approaches to the reader, Figure 6.2 (from [198]) compares the evolution of the cumulative number of infected in a Lattice simulation. The time evolution is very similar to the analytic SIR model as well as the asymptotic number of infected. In Figure 6.3 (from [198]) we show that in the limit where far away sites are in contact, the SIR and the lattice lead to identical predictions for the same value of γ and ϵ. To be more precise, in the lattice we defined the coordination number, it corresponds to a radius, in lattice spacing units, indicating the scope of the infected over the suceptible. By increasing this value up to the size of the total grid, we observe Figure 6.3 a convergence of the SIR and the Lattice.

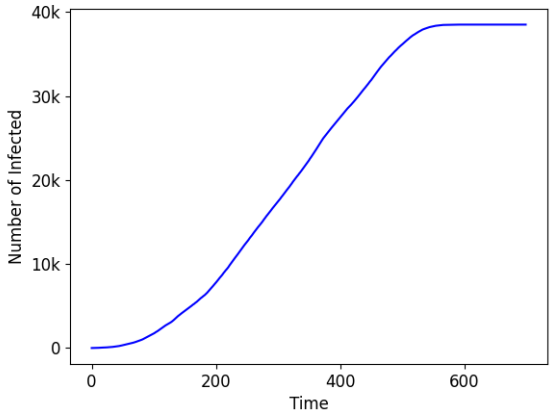

Figure 6.2: Evolution of the number of Infected, in a Lattice of size 200×200. The value of γ and ϵ have been respectively fixed to 0.7 and 0.1

In the review [198] we show how the critical behaviour of the Lattice simulations can be explained in the language of Field Theory and especially in the framework of Percolation Field Theory. An extended review is then proposed on Comportamental Models, offering a variety of dynamics, up to near time-invariance. The latter is an intrisic property of the eRG approach which is shown to be a SIR model with time dependent coefficient.

After we proposed our review, it became apparent that the propagation in countries moved in a succession of waves, and the virus started to mutate. The recent Covid-19 data confirmed this new features. Thus we investigated how these two phenomena were related. This has been challenging for two reasons: firstly, the usual models failed to explain and predict the muliple waves, and secondly the mutation had to be understood. Indeed, biologists define a variant through the phylogenetic tree, where they sequence the genome of the viruses collected to identify which virus descends from which virus like a family tree. When it is observed that a specific genomic sequence is repeatedly collected, the related branch of the tree will therefore correspond to a new variant, or variant of concern. We decided to study the spread of each variant; however, at that time the data we had access to was not fully analyzed and so variants were not specifically defined. We knew that the third wave in the UK was mainly coming from the so-called British variant, but other than that the impact of variants was hard to capture. However, we had access to a large bank of data from GISAID Initiative (https://www.gisaid.org/), which include a collection of DNA sequences (and the date of sample), but also certain encoded protein sequences. Thus we utilised this data to define our own variant!

For this purpose we used Machine Learning, specifically the hierarchical clustering alogrithm, to build groups of sequences, our own variants or clusters. The idea was to regroup the viruses according to the Spike protein sequencing, since because this protein connects to the human cells, it should play a key role in the propagation of the virus. To do this analysis it was necessary to compare sequences for which we chose the Levenshtein measure. Considering two lists of characters (i.e. two sequences), this measure computes the minimal number of operations (deletion, substitution and insertion) needed

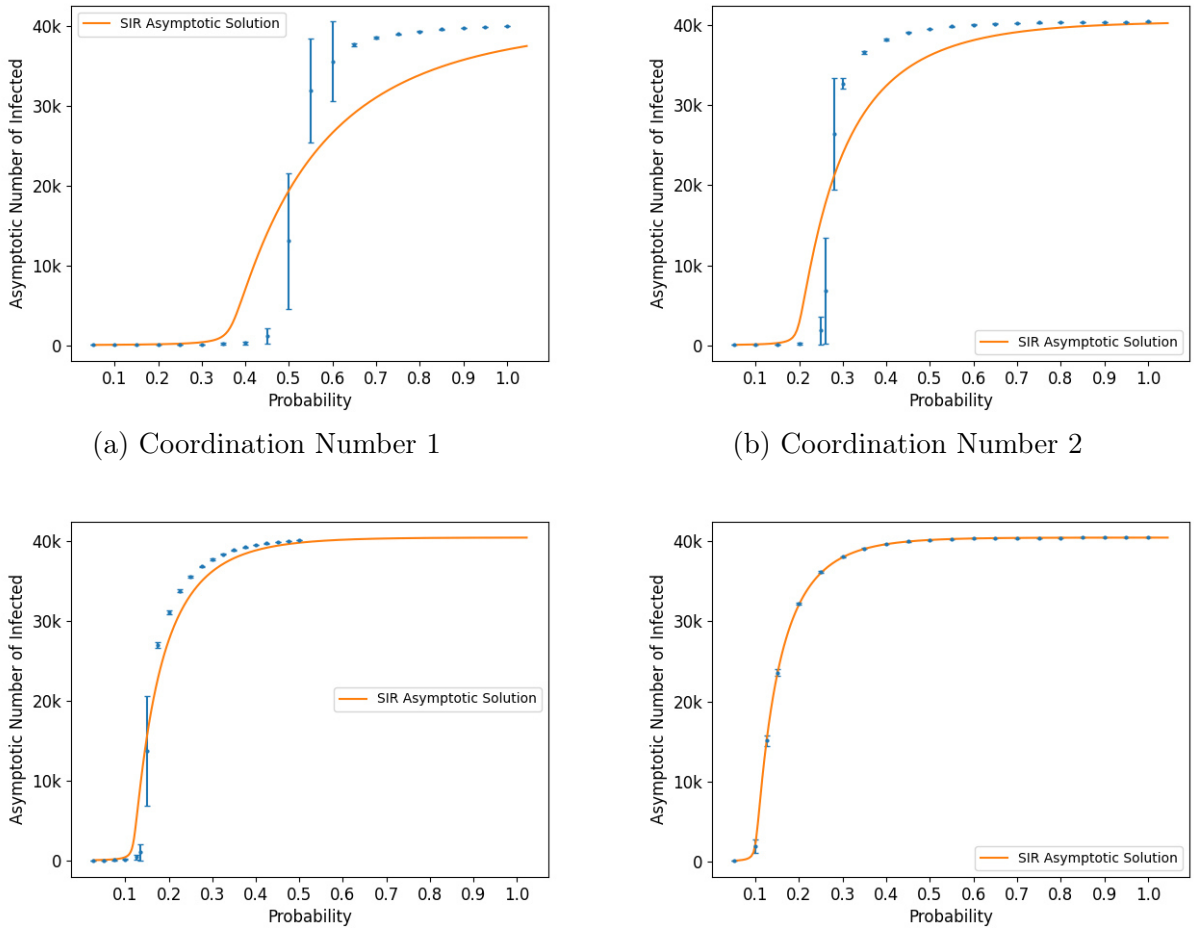

(a) Coordination Number 1

(b) Coordination Number 2

(c) Coordination Number 5

(d) Coordination Number 50

Figure 6.3: Evolution of the final number of infected cases as a function of the infection probability for different coordination radii r, compared to the asymptotic solution of the SIR model. The optimal factor found for the cases (a),(b),(c) and (d) are respectively: $\rho = 0.27,\ 0.42,\ 0.50,\ 0.99$.

to transform one to the other. This is a very naive approach, as we consider that, all of these operations are equally weighted. However, it is known that biologically speaking, some of them are enhanced during the multiplication process of a virus, while others are very rare. Regardless, it seems to be a good starting point. Once we had obtained the distances between each of the pairs of sequences from a given country, we input them as an argument to the Machine Learning algorithm. The result is a tree of proximity relating the closer sequences (see Figure 6.4). To finally obtain clusters we need to define a cut, in the form of a maximal distance allowed between the sequence to be in the same group. This is well illustrated by a horizontal cut of the tree in Figure 6.4 . The cut branches indentify our desired groups. In each of those clusters we select only the one that corresponds to a relevant number of infected (colored in the tree). It is worth noting

that those groups were built only by their related sequences and the obtained clusters are unrelated to the number of times each protein has been sequences and also to the temporal collection of it, even if we have access to that information.

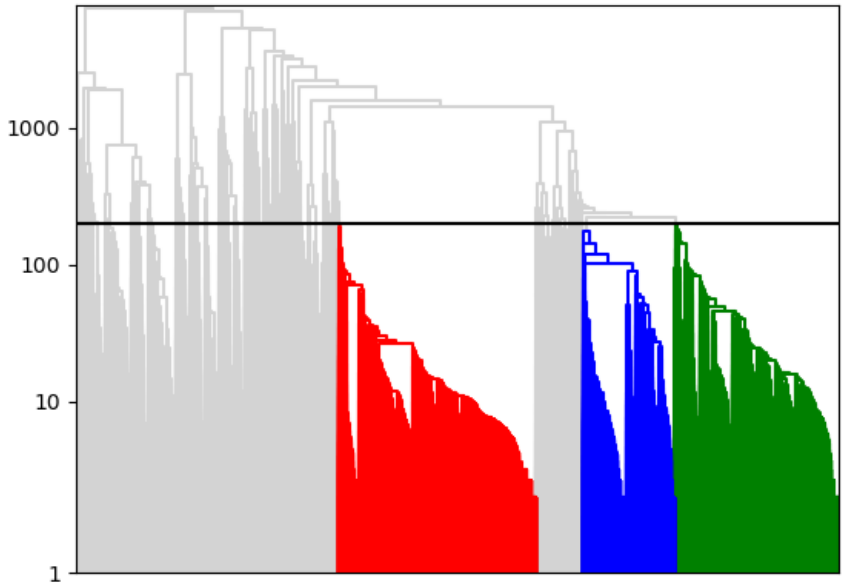

Figure 6.4: The tree of proximity. The y axis represents the distance between branches. The green, blue and red branches are the relevant clusters coming from the horizontal cut ($\sim$ 200 in units of the Levenshtein distance)

Nonetheless we can now try to plot the evolution of the number of infected for our relevant groups. Based on the sequences we have, we can compute the evolution of the frequency of each groups. In countries like England, where they do a lot of sequencing, this frequency should be relevant and multiplying it by the total number of new cases should give a good indication of the global evolution of those groups. Figure 6.5 illustrates the case of England, and as it is evident that each wave appears to be dominated by a single group! Unfortunately this kind of analysis cannot be repeated in all the countries, as many are limited by the low sequencing they do.

As a final discussion of the covid project I would like to mention that these Machine Learning results were confirmed by biologists analysis, as is clear from the British variant curve in Figure 6.5. This curve can is extracted from the raw data of GISAID by matching the sequences with the specific mutations of the British variant defined by biologists, and it matches very closely our cluster 3! Covid analysis is a competitive world, but nevertheless we obtained similar clusters based on a very naive approach and focusing only on the Spike protein. This points toward the importance of that protein in the spreading mechanism. The clustering programmes written are our own, thus simplying future analysis in deeper studies of the impact of mutation on the spread of viruses such as Covid.

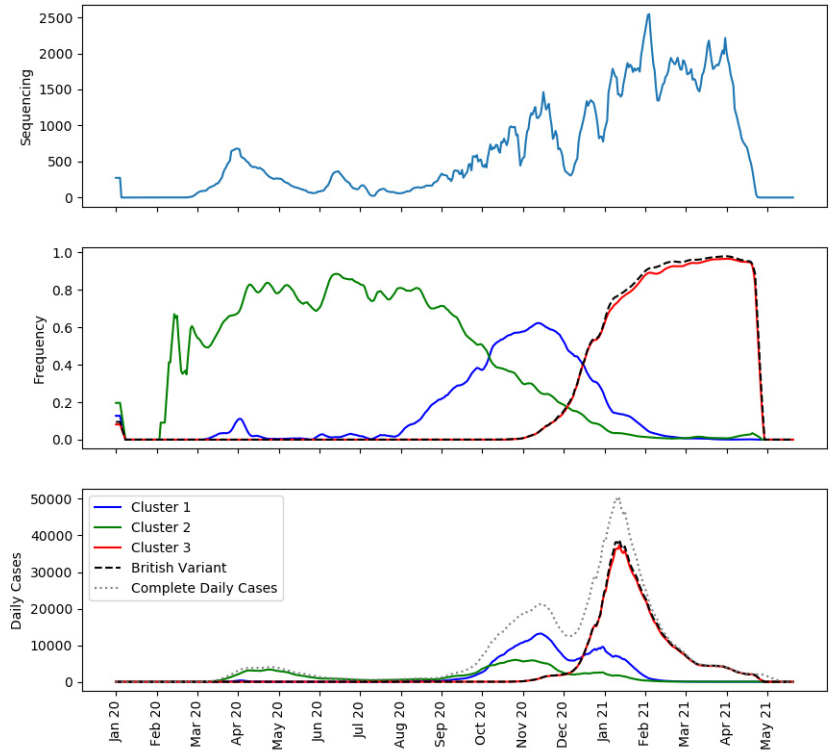

Figure 6.5: Time evolution of the different clusters in England. The upper panel shows the number of sequencing by day. The middle graph represents the frequency of each cluster and the frequency of the british variant. The last plot is the frequency multiply by the number of cases. In the last panel we also display in dashes the new infected.

Conclusion

It is time to conclude those three years of work. The main projects have already been concluded but here I would like to emphasize on some points.

Composite Higgs Models are an alternative as viable as many BSM extension, I particulary have in mind SUSY. Why should one study CHM? At the end it is a matter of taste. Personally I have been seduced by this approach and the fact that QCD already realized in nature a similar scenario.

This subject has been a door through the world of particle physics, and future investigations. CHM are well study from an EFT point of view, however this work shows that only specific models survive our attempts for UV Completion. In the same spirit, Lattice simulations could select some particular models, whatever the direction is. Criteria, wheter they discard or open a road, they always add a piece to the puzzle and that is what is needed.

The fact is that it is really hard to describe those strong interacting theory. For example, in QCD the origin of the spin of the proton is still under investigation! It is a common effort, from the lattice side and formal research that we could settle the place of a new strong sector.

Questionning another side of CHM could also point toward a particular direction. Here we mainly put our efforts to explain the EWSB and the origin of the mass, but a recent study on the $g-2$ muon anomaly points toward a TC scenario rather than a CH. In this perspective one could study Leptogenesis inside the TPS model, the result could be surprising! Flavor consraints also play an important role. Still it is very hard to follow the tensions of the different observables for the whole set of CHM. Maybe one day, (with the help of the recent programs and algorithms), that could be done, and it will be fantastic to have an overview.

I am excited to keep working in all of those directions, but also to read, understand and use what others are going to propose in the near future.

Bibliography

[1] S. L. Glashow, "Partial Symmetries of Weak Interactions," Nucl. Phys., vol. 22, pp. 579–588, 1961.

[2] S. Weinberg, "A Model of Leptons," Phys. Rev. Lett., vol. 19, pp. 1264–1266, 1967.

[3] A. Salam, "Weak and Electromagnetic Interactions," Conf. Proc., vol. C680519, pp. 367–377, 1968.

[4] G. Aad et al., "Observation of a new particle in the search for the Standard Model Higgs boson with the ATLAS detector at the LHC," Phys. Lett., vol. B716, pp. 1–29, 2012.

[5] S. Chatrchyan et al., "Observation of a New Boson at a Mass of 125 GeV with the CMS Experiment at the LHC," Phys. Lett., vol. B716, pp. 30–61, 2012.

[6] R. Barbieri, A. Pomarol, R. Rattazzi, and A. Strumia, "Electroweak symmetry breaking after LEP-1 and LEP-2," Nucl. Phys., vol. B703, pp. 127–146, 2004.

[7] F. Englert and R. Brout, "Broken Symmetry and the Mass of Gauge Vector Mesons," Phys. Rev. Lett., vol. 13, pp. 321–323, 1964.

[8] P. W. Higgs, "Broken symmetries, massless particles and gauge fields," Phys. Lett., vol. 12, pp. 132–133, 1964.

[9] P. W. Higgs, "Broken Symmetries and the Masses of Gauge Bosons," Phys. Rev. Lett., vol. 13, pp. 508–509, 1964.

[10] G. S. Guralnik, C. R. Hagen, and T. W. B. Kibble, "Global Conservation Laws and Massless Particles," Phys. Rev. Lett., vol. 13, pp. 585–587, 1964.

[11] G. Aad et al., "Measurements of the Higgs boson production and decay rates and constraints on its couplings from a combined ATLAS and CMS analysis of the LHC pp collision data at $\sqrt{s} = 7$ and 8 TeV," JHEP, vol. 08, p. 045, 2016.

[12] M. Cepeda et al., Report from Working Group 2: Higgs Physics at the HL-LHC and HE-LHC, vol. 7, pp. 221–584. 12 2019.

[13] E. Fermi, "Trends to a Theory of beta Radiation. (In Italian)," Nuovo Cim., vol. 11, pp. 1–19, 1934.

[14] G. Arnison et al., "Experimental Observation of Isolated Large Transverse Energy Electrons with Associated Missing Energy at $\sqrt{s} = 540$ GeV," Phys. Lett. B, vol. 122, pp. 103–116, 1983.

[15] H. Yukawa, "On the Interaction of Elementary Particles I," Proc. Phys. Math. Soc. Jap., vol. 17, pp. 48–57, 1935.

[16] J. R. Oppenheimer et al., "Strange particles and weak interactions," in 7th Annual Rochester Conference on High energy nuclear physics, 1957.

[17] S. Sakata, "On a Composite Model for the New Particles," Prog. Theor. Phys., vol. 16, pp. 686–688, 1956.

[18] M. Gell-Mann, "The Eightfold Way: A Theory of strong interaction symmetry," 3 1961.

[19] V. E. Barnes et al., "Observation of a Hyperon with Strangeness Minus Three," Phys. Rev. Lett., vol. 12, pp. 204–206, 1964.

[20] G. Zweig, "Origins of the Quark Model," CaltechAUTHORS, vol. 68-805, 1980.

[21] D. J. Gross and F. Wilczek, "Asymptotically Free Gauge Theories - I," Phys. Rev. D, vol. 8, pp. 3633–3652, 1973.

[22] H. D. Politzer, "Reliable Perturbative Results for Strong Interactions?," Phys. Rev. Lett., vol. 30, pp. 1346–1349, 1973. [,274(1973)].

[23] J. R. Ellis, M. K. Gaillard, and G. G. Ross, "Search for Gluons in e+ e- Annihilation," Nucl. Phys. B, vol. 111, p. 253, 1976. [Erratum: Nucl.Phys.B 130, 516 (1977)].

[24] E. C. G. Sudarshan and R. e. Marshak, "Chirality invariance and the universal Fermi interaction," Phys. Rev., vol. 109, pp. 1860–1860, 1958.

[25] R. P. Feynman and M. Gell-Mann, "Theory of Fermi interaction," Phys. Rev., vol. 109, pp. 193–198, 1958.

[26] C. S. Wu, E. Ambler, R. W. Hayward, D. D. Hoppes, and R. P. Hudson, "Experimental Test of Parity Conservation in β Decay," Phys. Rev., vol. 105, pp. 1413–1414, 1957.

[27] S. L. Glashow, J. Iliopoulos, and L. Maiani, "Weak Interactions with Lepton-Hadron Symmetry," Phys. Rev. D, vol. 2, pp. 1285–1292, 1970.

[28] J. J. Aubert et al., "Experimental Observation of a Heavy Particle J," Phys. Rev. Lett., vol. 33, pp. 1404–1406, 1974.

[29] J. E. Augustin et al., "Discovery of a Narrow Resonance in e^+e^- Annihilation," Phys. Rev. Lett., vol. 33, pp. 1406–1408, 1974.

[30] M. D. Schwartz, Quantum Field Theory and the Standard Model. Cambridge University Press, 3 2014.

[31] R. Contino, "The Higgs as a Composite Nambu-Goldstone Boson," in Physics of the large and the small, TASI 09, proceedings of the Theoretical Advanced Study I pp. 235–306, 2011.

[32] M. Kobayashi and T. Maskawa, "CP Violation in the Renormalizable Theory of Weak Interaction," Prog. Theor. Phys., vol. 49, pp. 652–657, 1973.

[33] S. Weinberg, "Implications of Dynamical Symmetry Breaking," Phys. Rev., vol. D13, pp. 974–996, 1976. [Addendum: Phys. Rev.D19,1277(1979)].

[34] L. Susskind, "Dynamics of Spontaneous Symmetry Breaking in the Weinberg-Salam Theory," Phys. Rev. D, vol. 20, pp. 2619–2625, 1979.

[35] E. Eichten and K. D. Lane, "Dynamical Breaking of Weak Interaction Symmetries," Phys. Lett., vol. 90B, pp. 125–130, 1980.

[36] D. B. Kaplan and H. Georgi, "SU(2) x U(1) Breaking by Vacuum Misalignment," Phys. Lett., vol. 136B, pp. 183–186, 1984.

[37] D. Marzocca, M. Serone, and J. Shu, "General Composite Higgs Models," JHEP, vol. 08, p. 013, 2012.

[38] G. Panico and A. Wulzer, "The Composite Nambu-Goldstone Higgs," Lect. Notes Phys., vol. 913, pp. pp.1–316, 2016.

[39] G. Cacciapaglia, C. Pica, and F. Sannino, "Fundamental Composite Dynamics: A Review," 2020.

[40] S. Coleman, J. Wess, and B. Zumino, "Structure of phenomenological lagrangians. i," Phys. Rev., vol. 177, pp. 2239–2247, Jan 1969.

[41] C. G. Callan, S. Coleman, J. Wess, and B. Zumino, "Structure of phenomenological lagrangians. ii," Phys. Rev., vol. 177, pp. 2247–2250, Jan 1969.

[42] P. P. Stangl, Direct Constraints, Flavor Physics, and Flavor Anomalies in Composite Higgs M PhD thesis, Munich, Tech. U., 2018.

[43] R. Lewis, C. Pica, and F. Sannino, "Light Asymmetric Dark Matter on the Lattice: SU(2) Technicolor with Two Fundamental Flavors," Phys. Rev. D, vol. 85, p. 014504, 2012.

[44] A. Hietanen, R. Lewis, C. Pica, and F. Sannino, "Composite Goldstone Dark Matter: Experimental Predictions from the Lattice," JHEP, vol. 12, p. 130, 2014.

[45] A. Hietanen, R. Lewis, C. Pica, and F. Sannino, "Fundamental Composite Higgs Dynamics on the Lattice: SU(2) with Two Flavors," JHEP, vol. 07, p. 116, 2014.

[46] D. B. Kaplan, "Flavor at SSC energies: A New mechanism for dynamically generated fermion masses," Nucl. Phys., vol. B365, pp. 259–278, 1991.

[47] A. Belyaev, G. Cacciapaglia, H. Cai, G. Ferretti, T. Flacke, A. Parolini, and H. Serôdio, "Di-boson signatures as Standard Candles for Partial Compositeness," JHEP, vol. 01, p. 094, 2017. [Erratum: JHEP12,088(2017)].

[48] H. S. Fukano and F. Sannino, "Conformal Window of Gauge Theories with Four-Fermion Interactions and Ideal Walking," Phys. Rev. D, vol. 82, p. 035021, 2010.

[49] T. DeGrand, "Lattice tests of beyond Standard Model dynamics," Rev. Mod. Phys., vol. 88, p. 015001, 2016.

[50] E. Bennett, D. K. Hong, J.-W. Lee, C. J. D. Lin, B. Lucini, M. Piai, and D. Vadacchino, "Sp(4) gauge theory on the lattice: towards SU(4)/Sp(4) composite Higgs (and beyond)," JHEP, vol. 03, p. 185, 2018.

[51] V. Ayyar, T. Degrand, D. C. Hackett, W. I. Jay, E. T. Neil, Y. Shamir, and B. Svetitsky, "Baryon spectrum of SU(4) composite Higgs theory with two distinct fermion representations," Phys. Rev., vol. D97, no. 11, p. 114505, 2018.

[52] V. Ayyar, T. DeGrand, D. C. Hackett, W. I. Jay, E. T. Neil, Y. Shamir, and B. Svetitsky, "Partial compositeness and baryon matrix elements on the lattice," Phys. Rev., vol. D99, no. 9, p. 094502, 2019.

[53] Bennett, D. K. Hong, J.-W. Lee, C. J. D. Lin, B. Lucini, M. Piai, and D. Vadacchino, "Sp(4) gauge theories on the lattice: $N_f = 2$ dynamical fundamental fermions," 2019.

[54] A. Hasenfratz, C. Rebbi, and O. Witzel, "Large scale separation and resonances within LHC range from a prototype BSM model," Phys. Lett., vol. B773, pp. 86–90, 2017.

[55] F. Sannino, A. Strumia, A. Tesi, and E. Vigiani, "Fundamental partial compositeness," JHEP, vol. 11, p. 029, 2016.

[56] G. Cacciapaglia, H. Gertov, F. Sannino, and A. E. Thomsen, "Minimal Fundamental Partial Compositeness," Phys. Rev., vol. D98, no. 1, p. 015006, 2018.

[57] F. Sannino, P. Stangl, D. M. Straub, and A. E. Thomsen, "Flavor Physics and Flavor Anomalies in Minimal Fundamental Partial Compositeness," Phys. Rev., vol. D97, no. 11, p. 115046, 2018.

[58] S. Samuel, "Bosonic Technicolor," Nucl. Phys., vol. B347, pp. 625–650, 1990.

[59] J. Galloway, A. L. Kagan, and A. Martin, "A UV complete partially composite-pNGB Higgs," Phys. Rev., vol. D95, no. 3, p. 035038, 2017.

[60] A. Agugliaro, O. Antipin, D. Becciolini, S. De Curtis, and M. Redi, "UV complete composite Higgs models," Phys. Rev., vol. D95, no. 3, p. 035019, 2017.

[61] S. Dimopoulos and L. Susskind, "Mass Without Scalars," vol. 2, pp. 930–930, 1979.

[62] C. T. Hill and E. H. Simmons, "Strong dynamics and electroweak symmetry breaking," Phys. Rept., vol. 381, pp. 235–402, 2003. [Erratum: Phys. Rept.390,553(2004)].

[63] T. Appelquist and R. Shrock, "Dynamical symmetry breaking of extended gauge symmetries," Phys. Rev. Lett., vol. 90, p. 201801, 2003.

[64] T. Appelquist, M. Piai, and R. Shrock, "Fermion masses and mixing in extended technicolor models," Phys. Rev., vol. D69, p. 015002, 2004.

[65] T. Appelquist, N. D. Christensen, M. Piai, and R. Shrock, "Flavor-changing processes in extended technicolor," Phys. Rev., vol. D70, p. 093010, 2004.

[66] G. Cacciapaglia, S. Vatani, and C. Zhang, "Composite Higgs Meets Planck Scale: Partial Compositeness from Partial Unification," 2019.

[67] O. Matsedonskyi, "On Flavour and Naturalness of Composite Higgs Models," JHEP, vol. 02, p. 154, 2015.

[68] G. Cacciapaglia, H. Cai, T. Flacke, S. J. Lee, A. Parolini, and H. Serôdio, "Anarchic Yukawas and top partial compositeness: the flavour of a successful marriage," JHEP, vol. 06, p. 085, 2015.

[69] G. Panico and A. Pomarol, "Flavor hierarchies from dynamical scales," JHEP, vol. 07, p. 097, 2016.

[70] M. Frigerio, M. Nardecchia, J. Serra, and L. Vecchi, "The Bearable Compositeness of Leptons," JHEP, vol. 10, p. 017, 2018.

[71] N. Cabibbo, "Unitary Symmetry and Leptonic Decays," Phys. Rev. Lett., vol. 10, pp. 531–533, 1963.

[72] Z. Maki, M. Nakagawa, and S. Sakata, "Remarks on the unified model of elementary particles," Prog. Theor. Phys., vol. 28, pp. 870–880, 1962.

[73] J. Barnard, T. Gherghetta, and T. S. Ray, "UV descriptions of composite Higgs models without elementary scalars," JHEP, vol. 02, p. 002, 2014.

[74] G. Ferretti and D. Karateev, "Fermionic UV completions of Composite Higgs models," JHEP, vol. 03, p. 077, 2014.

[75] L. Vecchi, "A dangerous irrelevant UV-completion of the composite Higgs," JHEP, vol. 02, p. 094, 2017.

[76] J. C. Pati and A. Salam, "Lepton Number as the Fourth Color," Phys. Rev., vol. D10, pp. 275–289, 1974. [Erratum: Phys. Rev.D11,703(1975)].

[77] L.-F. Li, "Group Theory of the Spontaneously Broken Gauge Symmetries," Phys. Rev. D, vol. 9, pp. 1723–1739, 1974.

[78] V. Elias, S. Eliezer, and A. Swift, "Comment on 'Group Theory of the Spontaneously Broken Gauge Symmetries'," Phys. Rev. D, vol. 12, p. 3356, 1975.

[79] F. Buccella, H. Ruegg, and C. A. Savoy, "Spontaneous Symmetry Breaking of SU(n)," Nucl. Phys. B, vol. 169, pp. 68–76, 1980.

[80] H. Ruegg, "Extremas of SU(N) Higgs Potentials and Symmetry Breaking Pattern," Phys. Rev. D, vol. 22, p. 2040, 1980.

[81] C. Cummins and R. King, "SYMMETRY BREAKING PATTERNS FOR THIRD RANK TOTALLY ANTISYMMETRIC TENSOR REPRESENTATIONS OF UNITARY GROUPS," J. Phys. A, vol. 17, pp. L627–L633, 1984.

[82] S. L. Adler, "$SU(n)$ symmetry breaking by rank three and rank two antisymmetric tensor scalars," Phys. Lett. B, vol. 744, pp. 380–384, 2015.

[83] C. Pica and F. Sannino, "Beta Function and Anomalous Dimensions," Phys. Rev., vol. D83, p. 116001, 2011.

[84] F. Sannino, "Conformal Dynamics for TeV Physics and Cosmology," Acta Phys. Polon., vol. B40, pp. 3533–3743, 2009.

[85] B. S. Kim, D. K. Hong, and J.-W. Lee, "Into the conformal window: Multirepresentation gauge theories," Phys. Rev. D, vol. 101, no. 5, p. 056008, 2020.

[86] F. Sannino, "Conformal Windows of SP(2N) and SO(N) Gauge Theories," Phys. Rev., vol. D79, p. 096007, 2009.

[87] T. A. Ryttov and F. Sannino, "Conformal House," Int. J. Mod. Phys., vol. A25, pp. 4603–4621, 2010.

[88] F. Lyonnet, I. Schienbein, F. Staub, and A. Wingerter, "PyR@TE: Renormalization Group Equations for General Gauge Theories," Comput. Phys. Commun., vol. 185, pp. 1130–1152, 2014.

[89] F. Lyonnet and I. Schienbein, "PyR@TE 2: A Python tool for computing RGEs at two-loop," Comput. Phys. Commun., vol. 213, pp. 181–196, 2017.

[90] A. Eichhorn, "An asymptotically safe guide to quantum gravity and matter," Front. Astron. Space Sci., vol. 5, p. 47, 2019.

[91] V. Bashmakov, M. Bertolini, and H. Raj, "On non-supersymmetric conformal manifolds: field theory and holography," JHEP, vol. 11, p. 167, 2017.

[92] M. Golterman and Y. Shamir, "Top quark induced effective potential in a composite Higgs model," Phys. Rev., vol. D91, no. 9, p. 094506, 2015.

[93] M. A. Shifman, A. I. Vainshtein, and V. I. Zakharov, "QCD and Resonance Physics. Theoretical Foundations," Nucl. Phys., vol. B147, pp. 385–447, 1979.

[94] M. A. Shifman, A. I. Vainshtein, and V. I. Zakharov, "QCD and Resonance Physics: Applications," Nucl. Phys., vol. B147, pp. 448–518, 1979.

[95] J. Galloway, J. A. Evans, M. A. Luty, and R. A. Tacchi, "Minimal Conformal Technicolor and Precision Electroweak Tests," JHEP, vol. 10, p. 086, 2010.

[96] G. Cacciapaglia and F. Sannino, "Fundamental Composite (Goldstone) Higgs Dynamics," JHEP, vol. 04, p. 111, 2014.

[97] C. Cai, G. Cacciapaglia, and H.-H. Zhang, "Vacuum alignment in a composite 2HDM," 2018.

[98] G. Cacciapaglia, S. Vatani, and C. Zhang. in preparation.

[99] M. Rosenlyst and C. T. Hill, "Natural Top-Bottom Mass Hierarchy in Composite Higgs Models," Phys. Rev. D, vol. 101, p. 095027, 2020.

[100] G. C. Branco, P. M. Ferreira, L. Lavoura, M. N. Rebelo, M. Sher, and J. P. Silva, "Theory and phenomenology of two-Higgs-doublet models," Phys. Rept., vol. 516, pp. 1–102, 2012.

[101] R. Volkas, "Prospects for mass unification at low-energy scales," Phys. Rev. D, vol. 53, pp. 2681–2698, 1996.

[102] A. Abada and M. Lucente, "Looking for the minimal inverse seesaw realisation," Nucl. Phys., vol. B885, pp. 651–678, 2014.

[103] H.-L. Li, L.-X. Xu, J.-H. Yu, and S.-H. Zhu, "EFTs meet Higgs Nonlinearity, Compositeness and (Neutral) Naturalness," JHEP, vol. 09, p. 010, 2019.

[104] E. Eichten and B. R. Hill, "An Effective Field Theory for the Calculation of Matrix Elements Involving Heavy Quarks," Phys. Lett. B, vol. 234, pp. 511–516, 1990.

[105] H. Georgi, "An Effective Field Theory for Heavy Quarks at Low-energies," Phys. Lett. B, vol. 240, pp. 447–450, 1990.

[106] D. Buarque Franzosi and G. Ferretti, "Anomalous dimensions of potential top-partners," SciPost Phys., vol. 7, p. 027, 2019.

[107] K. Agashe and R. Contino, "Composite Higgs-Mediated FCNC," Phys. Rev. D, vol. 80, p. 075016, 2009.

[108] A. Carmona and F. Goertz, "Custodial Leptons and Higgs Decays," JHEP, vol. 04, p. 163, 2013.

[109] A. Carmona and F. Goertz, "Lepton Flavor and Nonuniversality from Minimal Composite Higgs Setups," Phys. Rev. Lett., vol. 116, no. 25, p. 251801, 2016.

[110] G. Cacciapaglia, C. Csaki, J. Galloway, G. Marandella, J. Terning, and A. Weiler, "A GIM Mechanism from Extra Dimensions," JHEP, vol. 04, p. 006, 2008.

[111] A. Fitzpatrick, G. Perez, and L. Randall, "Flavor anarchy in a Randall-Sundrum model with 5D minimal flavor violation and a low Kaluza-Klein scale," Phys. Rev. Lett., vol. 100, p. 171604, 2008.

[112] C. Csaki, A. Falkowski, and A. Weiler, "The Flavor of the Composite Pseudo-Goldstone Higgs," JHEP, vol. 09, p. 008, 2008.

[113] R. A. Porto and A. Zee, "The Private Higgs," Phys. Lett. B, vol. 666, pp. 491–495, 2008.

[114] J. Preskill and S. Weinberg, "'Decoupling' constraints on massless composite particles," Phys. Rev., vol. D24, p. 1059, 1981.

[115] S. Weinberg, The quantum theory of fields. Vol. 2: Modern applications. Cambridge University Press, 2013.

[116] C. Vafa and E. Witten, "Restrictions on Symmetry Breaking in Vector-Like Gauge Theories," Nucl. Phys., vol. B234, pp. 173–188, 1984.

[117] R. N. Mohapatra and R. E. Marshak, "Local B-L Symmetry of Electroweak Interactions, Majorana Neutrinos and Neutron Oscillations," Phys. Rev. Lett., vol. 44, pp. 1316–1319, 1980. [Erratum: Phys. Rev. Lett.44,1643(1980)].

[118] L. Di Luzio, Aspects of symmetry breaking in Grand Unified Theories. PhD thesis, SISSA, Trieste, 2011.

[119] S. Davidson, E. Nardi, and Y. Nir, "Leptogenesis," Phys. Rept., vol. 466, pp. 105–177, 2008.

[120] L. Bian, Y. Wu, and K.-P. Xie, "Electroweak phase transition with composite Higgs models: calculability, gravitational waves and collider searches," JHEP, vol. 12, p. 028, 2019.

[121] S. De Curtis, L. Delle Rose, and G. Panico, "Composite Dynamics in the Early Universe," JHEP, vol. 12, p. 149, 2019.

[122] J. A. Harvey and M. S. Turner, "Cosmological baryon and lepton number in the presence of electroweak fermion number violation," Phys. Rev. D, vol. 42, pp. 3344–3349, 1990.

[123] S. B. Gudnason, C. Kouvaris, and F. Sannino, "Dark Matter from new Technicolor Theories," Phys. Rev., vol. D74, p. 095008, 2006.

[124] T. A. Ryttov and F. Sannino, "Ultra Minimal Technicolor and its Dark Matter TIMP," Phys. Rev. D, vol. 78, p. 115010, 2008.

[125] N. Aghanim et al., "Planck 2018 results. VI. Cosmological parameters," 7 2018.

[126] I. Dorsner, S. Fajfer, A. Greljo, J. F. Kamenik, and N. Kosnik, "Physics of leptoquarks in precision experiments and at particle colliders," Phys. Rept., vol. 641, pp. 1–68, 2016.

[127] K. Agashe, R. Contino, L. Da Rold, and A. Pomarol, "A Custodial symmetry for $Zb\bar{b}$," Phys. Lett. B, vol. 641, pp. 62–66, 2006.

[128] V. Andreev et al., "Improved limit on the electric dipole moment of the electron," Nature, vol. 562, no. 7727, pp. 355–360, 2018.

[129] G. Panico, A. Pomarol, and M. Riembau, "EFT approach to the electron Electric Dipole Moment at the two-loop level," JHEP, vol. 04, p. 090, 2019.

[130] D. Espriu, A. Palanques-Mestre, P. Pascual, and R. Tarrach, "The γ Function in the $1/N_f$ Expansion," Z. Phys., vol. C13, p. 153, 1982.

[131] A. Palanques-Mestre and P. Pascual, "The $1/N_f$ Expansion of the γ and Beta Functions in QED," Commun. Math. Phys., vol. 95, p. 277, 1984.

[132] J. A. Gracey, "The QCD Beta function at O(1/N(f))," Phys. Lett., vol. B373, pp. 178–184, 1996.

[133] M. Ciuchini, S. E. Derkachov, J. A. Gracey, and A. N. Manashov, "Quark mass anomalous dimension at O(1/N(f)**2) in QCD," Phys. Lett., vol. B458, pp. 117–126, 1999.

[134] M. Ciuchini, S. E. Derkachov, J. A. Gracey, and A. N. Manashov, "Computation of quark mass anomalous dimension at O(1 / N**2(f)) in quantum chromodynamics," Nucl. Phys., vol. B579, pp. 56–100, 2000.

[135] N. A. Dondi, G. V. Dunne, M. Reichert, and F. Sannino, "Towards the QED beta function and renormalons at $1/N_f^2$ and $1/N_f^3$," 2020.

[136] T. A. Ryttov and R. Shrock, "Scheme transformations in the vicinity of an infrared fixed point," Physical Review D, vol. 86, Sep 2012.

[137] T. A. Ryttov and R. Shrock, "Analysis of scheme transformations in the vicinity of an infrared fixed point," Physical Review D, vol. 86, Oct 2012.

[138] R. Shrock, "Study of possible ultraviolet zero of the beta function in gauge theories with many fermions," Physical Review D, vol. 89, Feb 2014.

[139] O. Antipin and F. Sannino, "Conformal Window 2.0: The large N_f safe story," Phys. Rev., vol. D97, no. 11, p. 116007, 2018.

[140] R. Shrock, "Study of Possible Ultraviolet Zero of the Beta Function in Gauge Theories with Many Fermions," Phys. Rev. D, vol. 89, no. 4, p. 045019, 2014.

[141] K. G. Wilson, "Renormalization group and critical phenomena. 1. Renormalization group and the Kadanoff scaling picture," Phys. Rev., vol. B4, pp. 3174–3183, 1971.

[142] K. G. Wilson, "Renormalization group and critical phenomena. 2. Phase space cell analysis of critical behavior," Phys. Rev., vol. B4, pp. 3184–3205, 1971.

[143] S. Weinberg, "Ultraviolet divergences in quantum theories of gravitation," in General Relativity: An Einstein Centenary Survey, pp. 790–831, 1980.

[144] D. F. Litim and F. Sannino, "Asymptotic safety guaranteed," JHEP, vol. 12, p. 178, 2014.

[145] T. Alanne, S. Blasi, and N. A. Dondi, "Critical Look at β -Function Singularities at Large N," Phys. Rev. Lett., vol. 123, no. 13, p. 131602, 2019.

[146] V. Leino, T. Rindlisbacher, K. Rummukainen, F. Sannino, and K. Tuominen, "Safety versus triviality on the lattice," 8 2019.

[147] A. D. Bond, G. Hiller, K. Kowalska, and D. F. Litim, "Directions for model building from asymptotic safety," JHEP, vol. 08, p. 004, 2017.

[148] S. Abel and F. Sannino, "Framework for an asymptotically safe Standard Model via dynamical breaking," Phys. Rev., vol. D96, no. 5, p. 055021, 2017.

[149] R. Mann, J. Meffe, F. Sannino, T. Steele, Z.-W. Wang, and C. Zhang, "Asymptotically Safe Standard Model via Vectorlike Fermions," Phys. Rev. Lett., vol. 119, no. 26, p. 261802, 2017.

[150] G. M. Pelaggi, A. D. Plascencia, A. Salvio, F. Sannino, J. Smirnov, and A. Strumia, "Asymptotically Safe Standard Model Extensions?," Phys. Rev., vol. D97, no. 9, p. 095013, 2018.

[151] S. Abel, E. Mølgaard, and F. Sannino, "Complete asymptotically safe embedding of the standard model," Phys. Rev., vol. D99, no. 3, p. 035030, 2019.

[152] K. Kowalska, A. Bond, G. Hiller, and D. Litim, "Towards an asymptotically safe completion of the Standard Model," PoS, vol. EPS-HEP2017, p. 542, 2017.

[153] E. Molinaro, F. Sannino, and Z. W. Wang, "Asymptotically safe Pati-Salam theory," Phys. Rev., vol. D98, no. 11, p. 115007, 2018.

[154] Z.-W. Wang, A. Al Balushi, R. Mann, and H.-M. Jiang, "Safe Trinification," Phys. Rev. D, vol. 99, no. 11, p. 115017, 2019.

[155] F. Sannino and I. M. Shoemaker, "Asymptotically Safe Dark Matter," Phys. Rev. D, vol. 92, no. 4, p. 043518, 2015.

[156] C. Cai and H.-H. Zhang, "Minimal asymptotically safe dark matter," Phys. Lett. B, vol. 798, p. 134947, 2019.

[157] G. Cacciapaglia, S. Vatani, T. Ma, and Y. Wu, "Towards a fundamental safe theory of composite Higgs and Dark Matter," 2018.

[158] F. Sannino, J. Smirnov, and Z.-W. Wang, "Asymptotically safe clockwork mechanism," Phys. Rev., vol. D100, no. 7, p. 075009, 2019.

[159] T. A. Ryttov and K. Tuominen, "Safe Glueballs and Baryons," JHEP, vol. 04, p. 173, 2019.

[160] B. Holdom, "Large N flavor beta-functions: a recap," Phys. Lett., vol. B694, pp. 74–79, 2011.

[161] O. Antipin, N. A. Dondi, F. Sannino, A. E. Thomsen, and Z.-W. Wang, "Gauge-Yukawa theories: Beta functions at large N_f," Phys. Rev., vol. D98, no. 1, p. 016003, 2018.

[162] S. Raby, S. Dimopoulos, and L. Susskind, "Tumbling Gauge Theories," Nucl. Phys. B, vol. 169, pp. 373–383, 1980.

[163] H. Georgi, L. J. Hall, and M. B. Wise, "Remarks on Mass Hierarchies From Tumbling Gauge Theories," Phys. Lett. B, vol. 102, p. 315, 1981. [Erratum: Phys.Lett.B 104, 499 (1981)].

[164] T. Appelquist, Z.-y. Duan, and F. Sannino, "Phases of chiral gauge theories," Phys. Rev. D, vol. 61, p. 125009, 2000.

[165] T. Appelquist and R. Shrock, "Ultraviolet to infrared evolution of chiral gauge theories," Phys. Rev. D, vol. 88, p. 105012, 2013.

[166] I. Bars and S. Yankielowicz, "Composite Quarks and Leptons as Solutions of Anomaly Constraints," Phys. Lett., vol. 101B, pp. 159–165, 1981.

[167] T. Appelquist, A. G. Cohen, M. Schmaltz, and R. Shrock, "New constraints on chiral gauge theories," Phys. Lett., vol. B459, pp. 235–241, 1999.

[168] S. Bolognesi and K. Konishi, "Dynamics and symmetries in chiral $SU(N)$ gauge theories," Phys. Rev. D, vol. 100, no. 11, p. 114008, 2019.

[169] S. Bolognesi, K. Konishi, and M. Shifman, "Patterns of symmetry breaking in chiral QCD," Phys. Rev. D, vol. 97, no. 9, p. 094007, 2018.

[170] S. Bolognesi, K. Konishi, and A. Luzio, "Dynamics from symmetries in chiral $SU(N)$ gauge theories," JHEP, vol. 09, p. 001, 2020.

[171] S. Bolognesi, K. Konishi, and A. Luzio, "Probing the dynamics of chiral SU(N) gauge theories via generalized anomalies," 1 2021.

[172] K. Kowalska and E. M. Sessolo, "Gauge contribution to the $1/N_f$ expansion of the Yukawa coupling beta function," JHEP, vol. 04, p. 027, 2018.

[173] G. Ferretti, "Gauge theories of Partial Compositeness: Scenarios for Run-II of the LHC," JHEP, vol. 06, p. 107, 2016.

[174] T. Banks and A. Zaks, "On the Phase Structure of Vector-Like Gauge Theories with Massless Fermions," Nucl. Phys., vol. B196, pp. 189–204, 1982.

[175] B. Holdom, "Raising the Sideways Scale," Phys. Rev., vol. D24, p. 1441, 1981.

[176] K. Yamawaki, M. Bando, and K.-i. Matumoto, "Scale Invariant Technicolor Model and a Technidilaton," Phys. Rev. Lett., vol. 56, p. 1335, 1986.

[177] G. M. Pelaggi, F. Sannino, A. Strumia, and E. Vigiani, "Naturalness of asymptotically safe Higgs," Front.in Phys., vol. 5, p. 49, 2017.

[178] Y. Wu, T. Ma, B. Zhang, and G. Cacciapaglia, "Composite Dark Matter and Higgs," JHEP, vol. 11, p. 058, 2017.

[179] G. Ballesteros, A. Carmona, and M. Chala, "Exceptional Composite Dark Matter," Eur. Phys. J., vol. C77, no. 7, p. 468, 2017.

[180] R. Balkin, M. Ruhdorfer, E. Salvioni, and A. Weiler, "Charged Composite Scalar Dark Matter," JHEP, vol. 11, p. 094, 2017.

[181] V. Ayyar, T. DeGrand, M. Golterman, D. C. Hackett, W. I. Jay, E. T. Neil, Y. Shamir, and B. Svetitsky, "Spectroscopy of SU(4) composite Higgs theory with two distinct fermion representations," Phys. Rev., vol. D97, no. 7, p. 074505, 2018.

[182] T. Ma and G. Cacciapaglia, "Fundamental Composite 2HDM: SU(N) with 4 flavours," JHEP, vol. 03, p. 211, 2016.

[183] G. Cacciapaglia and S. Vatani, "Large N_f for multiple representations," 5 2020.

[184] J.-W. Lee, Bennett, D. K. Hong, C. J. D. Lin, B. Lucini, M. Piai, and D. Vadacchino, "Progress in the lattice simulations of Sp(2N) gauge theories," PoS, vol. LATTICE2018, p. 192, 2018.

[185] O. Witzel, A. Hasenfratz, and C. Rebbi, "Composite Higgs from mass-split models," in 13th Conference on the Intersections of Particle and Nuclear Physics (CIPANP 2018) Palm Sprin 2018.

[186] X. Cui et al., "Dark Matter Results From 54-Ton-Day Exposure of PandaX-II Experiment," Phys. Rev. Lett., vol. 119, no. 18, p. 181302, 2017.

[187] D. S. Akerib et al., "Results from a search for dark matter in the complete LUX exposure," Phys. Rev. Lett., vol. 118, no. 2, p. 021303, 2017.

[188] E. Aprile et al., "Dark Matter Search Results from a One Ton-Year Exposure of XENON1T," Phys. Rev. Lett., vol. 121, no. 11, p. 111302, 2018.

[189] G. Cacciapaglia, G. Ferretti, T. Flacke, and H. Serôdio, "Light scalars in composite Higgs models," Front.in Phys., vol. 7, p. 22, 2019.

[190] C. Csaki, T. Ma, and J. Shu, "Maximally Symmetric Composite Higgs Models," Phys. Rev. Lett., vol. 119, no. 13, p. 131803, 2017.

[191] G. Belanger, F. Boudjema, A. Pukhov, and A. Semenov, "micrOMEGAs3: A program for calculating dark matter observables," Comput. Phys. Commun., vol. 185, pp. 960–985, 2014.

[192] M. Cirelli, A. Strumia, and M. Tamburini, "Cosmology and astrophysics of minimal dark matter," Nuclear Physics B, vol. 787, p. 152–175, Dec 2007.

[193] T. Maskawa and H. Nakajima, "Spontaneous Symmetry Breaking in Vector-Gluon Model," Prog. Theor. Phys., vol. 52, pp. 1326–1354, 1974.

[194] R. Fukuda and T. Kugo, "Schwinger-Dyson Equation for Massless Vector Theory and Absence of Fermion Pole," Nucl. Phys., vol. B117, pp. 250–264, 1976.

[195] A. Alloul, N. D. Christensen, C. Degrande, C. Duhr, and B. Fuks, "FeynRules 2.0 - A complete toolbox for tree-level phenomenology," Comput. Phys. Commun., vol. 185, pp. 2250–2300, 2014.

[196] D. Barducci, G. Belanger, J. Bernon, F. Boudjema, J. Da Silva, S. Kraml, U. Laa, and A. Pukhov, "Collider limits on new physics within micrOMEGAs_4.3," Comput. Phys. Commun., vol. 222, pp. 327–338, 2018.

[197] M. Della Morte and F. Sannino, "Renormalization group approach to pandemics as a time-dependent sir model," Frontiers in Physics, vol. 8, Jan 2021.

[198] G. Cacciapaglia, C. Cot, M. Della Morte, S. Hohenegger, F. Sannino, and S. Vatani, "The field theoretical ABC of epidemic dynamics," 1 2021.